A comparative study between Fe@Cu core-shell nanoparticles with iron and copper nanoparticles synthesized using a bioflocculant: characterization, industrial application and biosafety

University of Zululand

PhD Thesis

By

Nkosinathi Goodman Dlamini

Student number: 201100021

Thesis submitted in fulfilment of the requirements for the degree of

Doctor of philosophy (Microbiology)

Faculty of Science and Agriculture

Department of Biochemistry and Microbiology

University of Zululand

Private Bag x1001

KwaDlangezwa

3886

Supervisor: Prof A .K. Basson

Co-supervisors: Prof V.S.R. Rajasekhar Pullabhotla and Mr. J.S.E. Shandu

DECLARATION

I acknowledge that I have read and understood the University's policies and rules applicable to postgraduate research, and I certify that I have, to the best of my knowledge and belief, complied with their requirements.

I declare that this thesis, save for the supervisory guidance received, is the product of my own work and effort. I have, to the best of my knowledge and belief, acknowledged all sources of information in line with normal academic conventions.
I further certify that the thesis research is original, and that the material to be submitted for examination has not been submitted, either in whole or in part, for a degree at this or any other university.

I have subjected this document to the University‘s text-matching and/or similarity-checking procedures and I consider it to be free of any form of plagiarism.

---------- ----------
Mr. N.G. Dlamini Date

---------- ----------
Prof A.K. Basson Date

---------- ----------
Prof V.S.R. Rajasekhar Pullabhotla Date

ACKNOWLEDGEMENTS

I dedicate this work to God Almighty for His unconditional love and mercy through Jesus Christ the Lord. This work is dedicated to my family and friends, especial to Miss ND Qumbisa for showing me support and love throughout the time of my study. Thanks to the staff of the Department of Biochemistry and Microbiology at the University of Zululand for providing me with the platform to conduct this research. I would also like to express my deepest gratitude to the following special people without whom this work could not have been completed:

My indebtedness goes to Prof Basson for his thorough supervision, support and for all the knowledge gained through his guidance. For the record, I learnt a lot from him since I started tertiary education. The passion and love he has for Microbiology made me love the discipline. Prof Basson influenced my life in a special way, he always had words of wisdom and encouragement that kept me going even when then the going was getting tough. Most importantly, Prof Basson believes in my capabilities, which is something very essential to me. He has always been there for me whenever I needed him and encouraged me to finish on record time.

My sincere gratitude goes to Prof V.S.R. Rajasekhar Pullabhotla to learn from him to be where I am today. Prof Raj has helped me to develop in research in a tremendous way, whenever I faced any difficulties or challenges in my research, was there to offer assistance. He became more than a supervisor to me; he always pushes me to succeed as a researcher but also in my career. The love he has for his student is amazing; through him, I have learnt the significance of publishing research papers and is always supporting me to do more for that I would always be grateful to him. In addition, whenever I needed help from outside the department in which I am registered, he always made sure that I am assisted promptly so that I do not get delay in my work, even when I needed assistance outside UNIZULU. He would always make sure he goes an extra mile for me to get help from UKZN through his associates and for that, I would always be indebted to him.

Mr. J.S.E Shandu, Mr. Z.G Ntombela and Dr Maliehe for their supervision, concrete support and their endless efforts to see to it that this research has been fulfilled as planned. I am extending my gratitude to my TEAM Bioflocculation group. I am also grateful to colleagues at Unizulu Teaching Learning Centre (TLC) staff of the Writing Centre, specially thanks to Dr J Mkhize and Dr M Sibuqashe for always encouraging me.

The author acknowledges the full support of the University of Zululand Research and Innovation Committee, Thendele Coal Mine and Mining Qualification Authority. I would like to acknowledge the Council for Scientific and Industrial Research (CSIR, South Africa) for the financial assistance in the form of the Ph.D. Lastly; I extend my sincere gratitude to UKZN for allowing us to conduct some of the experiments in their institution.

Special thanks to my family members at Pongola Kwa-Shoba for all the support I received and would like to express my gratitude to Jordan Evangelical Church for spiritual upliftment more especially Pastor S.E Simelane and his wife Mrs. M.O Simelane. These people are recognized according to the hierarchy which is based on the age where respect must be given. My mom Mrs. Z.N Dlamini, my two sisters, my only brother and all my nephews and nieces I am grateful family and will always love you.

ABBREVIATIONS

ANOVA	One-way Analysis Of Variance
BOD	Biological Oxygen Demand
BSA	Bovine serum albumin
COD	Chemical oxygen demand
CuNPs	Copper nanoparticles
CSNs	Core-shell nanoparticles
FA	Flocculation activity
$FeCl_3$	Iron chloride/ ferric chloride
FeNPs	Iron nanoparticles
Fe@Cu core-shell	Iron copper core-shell nanoparticles
FT-IR	Fourier transform infrared spectroscopy
g	Gram
HEK 293	Normal cells
hr	hour
hrs	hours
INT	*P-iodonitrotetrazodium* violet
L	Litre
MBC	minimal bactericidal concentration
MCF7	canceral cells
mg	milligram
MIC	minimal inhibitory concentration
min	minutes
mL	Millilitre

Mn^{2+}	Manganese(II) ion or Manganous ion
nm	Nanometer
NO^{3-}	Nitrate ion
OD	Optical density
RE	Removal efficiency
rpm	Revolutions per minute
SD	Standard deviation
SEM	Scanning electron microscope
SPR	Plasmon resonance spectra
Td	Degradation temperature
TGA	Thermo gravimetric analysis
TEM	Transmission electron microscope
UV	Ultraviolet
V	Volume
*T*d	Degradation temperature
V	Volume
Wt	Weight
WEF	Water Environment Federation
WHO	World Health Organisation
XRD	X-ray Diffraction

RESEARCH OUTPUT

Published manuscripts

- **Dlamini, N.G**.; Basson, A.K.; Pullabhotla, V.S.R. Optimization and Application of Bioflocculant Passivated Copper Nanoparticles in the Wastewater Treatment. *Int. J. Environ. Res. Public Health*.
- **Dlamini, N.G**.; Basson, A.K.; Pullabhotla, V.S.R.R. Biosynthesis and characterization of copper nanoparticles using a bioflocculant extracted from Alcaligenes faecalis HCB2. *Adv. Sci. Eng. Med.*
- **Dlamini, N.G**.; Basson, A. K.; Shandu, J. S. E.; Mavuso, S. S.; Pullabhotla., V. S. R. Biosynthesis, Characterization, and Application of Iron Nanoparticles: in Dye Removal and as Antimicrobial Agent. *Water, Air, & Soil Pollution*.
- **Dlamini, N.G**.; Basson, A.K.; Pullabhotla, V.S.R. Biosynthesis of bioflocculant passivated copper nanoparticles, characterization and application. *Physics and Chemistry of the Earth.*
- **Dlamini, N.G**.; Basson, A.K.; Pullabhotla, V.S.R.R. Green Synthesis of Iron Nanoparticles by a Polysaccharide Bioflocculant from Marine *Alcaligenes faecalis* sp. and Characterization. *Adv. Sci. Eng. Med.*
- **Dlamini, N.G**.; Basson, A.K.; Shandu, J.S.E; Pullabhotla, V.S.R.R. Optimization of Fe@Cu core-shell nanoparticles synthesis, characterization and application in dye removal and wastewater treatment. *Catalysts.*
- **Dlamini, N.G**.; Basson, A.K.; Pullabhotla, V.S.R.R. Wastewater treatment by a polymeric bioflocculant and iron nanoparticles synthesized from a bioflocculant. *Polymer*.
- **Dlamini, N.G**.; Basson, A.K.; Pullabhotla, V.S.R.R. A comparative study between bimetallic iron@copper nanoparticles with iron and copper nanoparticles synthesized using a bioflocculant: their applications and biosafety. *Processes.*

Conference and Journal submitted manuscripts

- Biosynthesis of bioflocculant passivated copper nanoparticles, characterization and application. Conference paper: 19th WaterNet/WARFSA/GWPSA Symposium – Livingstone Zambia 2018.

- Application and biosafety of the Fe@Cu core-shell nanoparticles. Conference paper: 4th Interdisciplinary Research and Innovation Conference 2019— Durban Hilton hotel.

Table of Contents

List of Figures

List of Tables

ABSTRACT

Nanotechnology addresses numerous environmental problems such as wastewater treatment. Ground water, surface water and wastewater that is contaminated by toxic organic, inorganic solutes and pathogenic microorganisms can now be treated through the application of nanotechnology. This thesis focuses mainly on the synthesis of single metallic and core-shell metallic nanoparticles using a greener approach and application of these materials in the wastewater treatment. Characterization of the as-synthesised materials (FeNPs, CuNPs and Fe@Cu core-shell) was achieved with the analytical techniques such as Fourier Transform-Infrared spectroscopy (FT-IR), Thermogravimetric analysis (TGA), Scanning Electron Microscopy (SEM), Transmission Electron Microscopy (TEM), X-Ray Diffraction (XRD) and UV-Vis spectroscopy (UV-Vis).

The as-synthesised iron nanoparticles (FeNPs) revealed a spherical morphology and elements such as oxygen and iron contributed 65.25 % Wt% with oxygen having 47.94 followed by iron with 17.31% through TEM and SEM-EDX analysis. The X-ray diffractograms reveals the broad peaks that are observed between 2θ ~ 24°, 29°, 30° and 35°. The presence of hydroxyl (–OH) and amine ($–NH_2$) groups were shown by FT-IR spectroscopy studies. The highest flocculation activity (FA) was achieved at a dosage of 0.4 mg/mL. The iron nanoparticles were found as pH stable as their flocculation activity was 77 and 93 % at pH 3 and 11 respectively. These nanoparticles flocculate best in the presence of cations and are thermostable as the flocculation activity was above 88% at 100 °C. Moreover, the as-synthesized FeNPs showed to possess no antimicrobial activity and the removal efficiency of dyes was very poor in the absence of cation. With the addition of 2mL, 1% Mg^{2+}, the removal of methylene orange improved from 45% to 58% in 5 minutes.

The transmission electron microscopy analysis of as-synthesised copper nanoparticles (CuNPs) showed close to spherical shapes with an average particle size of ~53 nm. Energy dispersive X-ray spectroscopy analysis confirmed the presence of the Cu nanoparticles and also the other elements such as O, C, P, Ca, Cl, Na, K, Mg, and S originated from the bioflocculant. FT-IR results showed the presence of the –OH and $–NH_2$ functional groups. The highest flocculation activity (96%) was achieved with the lowest concentration (0.2 mg/mL) of copper nanoparticles and the least 80% was attained at 1 mg/mL. The CuNPs showed a maximum flocculation activity of 96% without the addition of the cation and worked best at all pH ranges of acidic, neutral, and alkaline regions with an optimal FA at pH 7 (96%). Furthermore, the as-

synthesised copper nanoparticles were found to be thermostable with 91% FA at 100 °C. The synthesized copper nanoparticles are also high in removal efficiency of staining dyes, such as safranin (92%), carbol fuchsine (94%), malachite green (97%), and methylene blue (85%). The high removal efficiency of nutrients such as phosphate and total nitrogen in both domestic wastewater and Mzingazi river water was observed. In comparison to ciprofloxacin, CuNPs revealed some remarkable properties, as they are able to kill both the Gram-positive and Gram-negative microorganisms.

In the optimization of Fe@Cu core-shell nanoparticles; to enhance best concentration for core-shell formation, different ratios of iron to copper were prepared. Sample 1 (S1) contained 1:3 iron to copper (Fe 25% - Cu 75%), sample 2 (S2) contained 1:1 iron to copper (Fe 50% - Cu 50%) and third sample (S3) contained 3:1 iron to copper (Fe 75% - Cu 25%). The flocculation activity was above 98% at a dosage of 0.2 mg/mL for all the samples and flocculate well at acidic, alkaline and neutral pH conditions. Sample 3 showed to be thermostable with flocculation activity above 90% and both sample 2 and 1 were also thermostable, but the flocculation decreased to 87 at 100 ℃. All three samples revealed some remarkable properties for staining dye removal as the removal efficiency was above 89% for all dyes tested. The synthesized core-shell nanoparticles could remove nutrients such as total nitrogen and phosphate in both domestic wastewater and Mzingazi river water. Furthermore, high removal efficiency for COD and BOD was also observed.

The Fe@Cu core-shell nanoparticles possess antimicrobial activity against both Gram-positive and Gram-negative microorganisms. The Minimal Inhibitory Concentration (MIC) and Bactericidal Minimal Concentration (MBC) was observed at a lower concentration of 1.563 mg/mL. Cell viability against HEK 293 and MCF7 was high at the lower concentration with the increase in concentration the decrease in cell viability was observed. The high removal efficiency (RE) of COD, BOD, total nitrogen and phosphate was observed in all wastewater samples examined. The removal efficiency of the dyes was found to be above 93% for all dye samples.

***Keywords**:* Bioflocculant, Copper nanoparticles, Characterization, Fe@Cu core-shell nanoparticles, Iron nanoparticles, Removal efficiency

Chapter 1 General introduction

1.1 Introduction

Water pollution constitutes to about 80% of infections in developing world and about a billion people have no clean water facility (Tiwari et al., 2008). Water borne diseases and cancer which is caused by effluents from industries is a major cause for high death rate in developing countries (Tiwari et al., 2008). The city of Johannesburg is famous in South Africa for production of gold. Ground water in gold mine surroundings was found to be acidified and heavily contaminated as the results of pyrite oxidation (FeS_2). This poses a health risk to people who consume the water without further purification (Naicker et al., 2003). The search for a new, low cost and effective antimicrobial agents due to an increase in antibiotic resistance by emerging microorganisms and the ever increasing health cost (Ashajyothi et al., 2016). Nanoparticle with antimicrobial activity function can be viewed as a promising alternative. Certain nanoparticles (copper, iron, and gold nanoparticles) exhibit the activity towards broad spectrum (Singhal et al., 2011).

Effluents discharged without proper treatment creates potential risk in the environment and leads to ecosystem breakdown (Rebah and Siddeeg, 2017). Wastewater treatment process consist of sequences which is the combination of physical (ion exchange, adsorption, membrane technologies etc.), chemical (chemical oxidation, coagulation, electrochemical treatments, etc.) and biological (sequential batch reactor and biofilter). Though these methods have shown a huge potential to remove pollutants in water, some disadvantages have been noted as well. For instance, the use of synthetic flocculants such as acrylamides have been reported to be neurotoxic (Rebah and Siddeeg, 2017). Moreover, addition of chemicals into water may resulting into new unknown products with unknown health hazards. Contrarily, bioflocculant synthesized nanoparticles are said to have eco-friendly nature and have little to no environmental effect. However, high production cost and low efficiencies are blockages in their commercialisation. Core-shell nanoparticles possess enhanced functionalities due to compatible relationship between the core and the shell (Kaur et al., 2018). In addition to that core-shell nanoparticles could be recyclable. Several dyes which are discharged to water in industrial effluents are carcinogenic in nature, such as vat, indigo and azo (Fonovich, 2013). For this reason, it is essential to minimise the hazards caused by treating and removing these dyes from water bodies. Nanoparticles application in dye degradation or removal is reported to have high efficiency, and is of view as the promising method (Majdalawieh et al., 2014).

1.2 Background of the study

Copper (Cu) is crucial in living organisms and plays a vital role in the function of proteins as the trace element. Nonetheless, the transport of copper into the cells is tightly controlled due to its redox activity. Due to the antimicrobial activity, conductivity of fluids and polymers and various other applications, cu-containing nanoparticles are used in various industries (Karlsson et al., 2013). Iron nanoparticles have proven to be relatively effective catalyst for a wide variety of environmental contaminants such as chlorinated organic compounds and metal ions (Mukherjee et al., 2016). Iron nanoparticles can reduce halogenated hydrocarbons such as ethylene, benzene and chlorinated methane to nonthreatening hydrocarbons (Mukherjee et al., 2016). Moreover, nano-size iron particles are versatile remediation material due to their high reactivity in water and excellent electron donating properties. Biodegradation of azo dyes is very resistant and not easy due to the azo bond they possess, iron is known to reduce the azo bond to compound which can be treated biologically in the environment (Fan et al., 2009).

Core-shell are compounds with one material acting as the core while the other material act as a shell. The ability to function over a wide range of pH and temperatures are some of the properties of core-shell nanoparticles. These nanoparticles also possesses magnetic conductivity and antimicrobial activity (Zaimy et al., 2016). Finally, ability to absorb pollutants from wastewater, enhanced biocompatibility and economic validation for large scale production are some of valued attributes for core-shell nanoparticles (Zaimy et al., 2016).

There are various categories of nanoparticles (NPs) depending on their size, chemical properties and morphology (Khan et al., 2017). Based on physical and chemical characteristics, NPs can be classified as: carbon-base NPs this include two major classes (carbon nanotubes and fullerenes). Fullerenes are materials that are made of globular hallow cage. Notable commercial interest has been created by these class NPs due to their structure, electron affinity, high strength, electrical conductivity, and versatility (Astefanei et al., 2015). They are also commercially applicable in industries as fillers (Beik et al., 2016). These class of nanomaterials possesses arranged structures of carbon (pentagonal and hexagonal).

Metallic NPs results purely from metal precursors. These class of NPs possesses unique optoelectrical properties due to well-known localized surface Plasmon resonance (LSPR) features. Alkali and noble metals NPs i.e. Ag, Au and Cu have a visible zone with a broad absorption band (Dreaden et al., 2012). Advanced optical properties have found metal NPs

numerous applications in several research areas. Use of gold nanoparticles (AuNPs) on sample coating for SEM image enhancement is one of the important applications (Rieter et al., 2006).

Non-metallic inorganic solids are called ceramic nanoparticles and their synthesis is achieved via heat and successive cooling. They can be found in porous or hollow forms, amorphous, dense and polycrystalline (Leong et al., 2015). Great attention has been given to this class of nanoparticles due to their applicable ability in photocatalysis, catalysis, image applications and photo degradation of dyes (Thomas et al., 2015).

Another class of nanomaterial is semiconductors. These conductors possess metals and non-metals properties and have several applications (Saravanan et al., 2013). Semiconductors are efficiently used in water splitting applications, due to their suitable band-gap and band-edge position (Hisatomi et al., 2014). Polymer nanoparticles (PNP) are normally organic based and exist as nano-spheres or nano-capsular mostly (Khan et al., 2017).

1.3 Problem statement

Nearly a billion people have no facilities of potable water and approximately 80% of infections in developing countries are a result of unclean water (Tiwari et al., 2008). South Africa is a water scarce country, and the demand for water is in excess of natural water availability in several river basins. This is owed to inconsistence rainfall patterns and different climatic regimes and high evaporation rates across the country (Ziervogel et al., 2014). With the rise and proliferation of multiple drug resistant microorganisms, and with the unending rise of health care cost, the focus of researchers is to develop new, low cost and effective antimicrobial agents (Ashajyothi et al., 2016). There are many factors, which can result in microorganisms being resistant to antibiotics, with the misuse of antibiotics the main reason. Numerous approaches have been used for core shell synthesis for the treatment of antibiotic resistant microorganisms. However, the problem persist. Some of the approaches involve the use of chemicals, which have been found to be detrimental to the environment. The use of biological entity such as bioflocculant from microorganism for the treatment of water, dye degradation is of view as a promising solution to water pollution. Furthermore, new antimicrobial compounds are needed to combat the crisis of antibiotic resistant microorganisms. Nonetheless, very little about this biological synthesis is understood. This aimed at finding solution to the already mentioned challenges of antibiotic resistance and water treatment.

1.4 Rationale of the study

An environment-friendly and eco-efficient method with marginal safety to human and animal's health is required for synthesis of composite nanomaterial for the treatment of antibiotic resistant microorganism, dye degradation and water treatment. Different approaches have been used for the synthesis of core shell nanoparticles. There are cheaper, effective and expedient methods, which are used for the development of nanoparticles. However, they are detrimental to the environment and a threat to human and animal's life. The impact imposed by chemicals in the treatment of water do not only affect animals and human but has a negative impact on political and economic viability of the country. Therefore, there is a need for synthesis of new materials, which are effective and have the same mechanism of action as the chemical flocculants to ensure the safety of humans and the ecosystem. The use of the extracts of microorganisms or plants for the synthesis of nanomaterial is as a favourable tactic. However, high production cost, low efficiency or activity of this biological entities and poor understanding of the mechanism of action of this biological compounds limit their utilization particularly at industrial scale. Hence, the current study is aimed at finding better and effective ways of synthesising the core shell nanoparticles.

1.5 Aim

To biological synthesize iron and copper core-shell, iron and copper nanoparticles, characterise and determine their application in wastewater, dye removal and antimicrobial activity.

1.6 Objectives

- To extract and purify bioflocculant from *Alcaligenes faecalis.*
- To synthesis iron-core shell, iron and copper nanoparticles using bioflocculant.
- To characterize as-synthesised bioflocculant passivated/capped nanoparticles.
- To test the flocculating activity of biosynthesized nanoparticles using kaolin clay.
- To examine the antimicrobial effect of biosynthesized nanoparticles.
- To apply biosynthesized nanoparticles Fe@Cu Core-shell, Cu, Fe nanoparticles on wastewater treatment and dye removal.
- To test the biosafety of synthesized nanoparticles.
- To assess the biodegradability and stability of the synthesized nanoparticles.

1.7 Ethical consideration

My research does not fall into any category that requires special ethical obligations. However, general lab practice (GLP) were observed at all times to minimise risk and to protect other lab users. Chemicals and all the microbial media were treated with caution to minimize risk. Lastly, microbes, nutrients agars and nutrients broths were discarded into designated containers at all times.

1.8 Chapters overview

The chapters presented in this thesis are in a form of manuscripts which have been and will be submitted for consideration in science journals, except for the general introduction, literature review and the conclusion chapters. Chapter 1 provides an overview of what the thesis is about including the study aim and objectives, and Chapter 2 looks at the previous research findings on the topic. Chapter 3, 4, 5, 6, 7, 8, 9, 10 and 11 are presented in the form of research manuscripts. Each chapter clearly indicates the method of research, results, discussion and conclusion. The description of the chapters is as follow:

Chapter 3 - Biosynthesis and Characterization of Copper Nanoparticles Using a Bioflocculant Extracted from *Alcaligenes faecalis*: This chapter is compiled in accordance with the guidelines and is publication in the Journal *Advanced Science, Engineering and Medicine* Vol. 11, 1–7, 2019; doi:10.1166/asem.2019.2448.

Chapter 4 - Optimization and Application of Bioflocculant Passivated Copper Nanoparticles in the Wastewater Treatment. This chapter is compiled in accordance with the guidelines and is publication in the Journal *International Journal of Environmental Research and Public Health,* 16**,** 2185; doi:10.3390/ijerph16122185.

Chapter 5 - Biosynthesis of bioflocculant passivated copper nanoparticles, characterization and application. This chapter is compiled in accordance with the guidelines and is under review in the Journal *Physics and Chemistry of the Earth.*

Chapter 6 - Green synthesis of iron nanoparticles by a bioflocculant from marine *Alcaligenes faecalis* HCB2 and characterization. This chapter is compiled in accordance with the journal guidelines and is yet to be submitted for publication.

Chapter 7 - Biosynthesis, characterization, and application of iron nanoparticles: in dye removal and as antimicrobial agent. This chapter is compiled in accordance with the journal guidelines and is yet to be submitted for publication.

Chapter 8 - A comparative study between $Fe_{@}Cu$ Core-shell nanoparticles with iron and copper nanoparticles synthesized using a bioflocculant, their applications and biosafety. This chapter is compiled in accordance with the journal guidelines and is yet to be submitted for publication.

Chapter 9 - Application and biosafety of the Fe@Cu core-shell nanoparticles. This chapter is compiled in accordance with the journal guidelines and was presented in a conference proceeding.

Chapter 10 - Synthesis optimization of Fe@Cu Core-shell nanoparticles, characterization and application. This chapter is compiled in accordance with the journal guidelines and is yet to be submitted.

Chapter 11 - Green synthesis of Fe@Cu nanoparticles by a polysaccharide bioflocculant and characterization. This chapter is compiled in accordance with the journal guidelines and is yet to be submitted.

Chapter 12 - Wastewater treatment by a polymeric bioflocculant and iron nanoparticles synthesized from a bioflocculant.

Chapter 13 - Is the general conclusion and recommendations for future prospects on the topic.

1.8 References

ASHAJYOTHI, C., HARISH, K. H., DUBEY, N. & CHANDRAKANTH, R. K. 2016. Antibiofilm activity of biogenic copper and zinc oxide nanoparticles-antimicrobials collegiate against multiple drug resistant bacteria: a nanoscale approach. *Journal of Nanostructure in Chemistry,* 6**,** 329-341.

ASTEFANEI, A., NÚÑEZ, O. & GALCERAN, M. T. 2015. Characterisation and determination of fullerenes: a critical review. *Analytica chimica acta,* 882**,** 1-21.

BEIK, J., ABED, Z., GHOREISHI, F. S., HOSSEINI-NAMI, S., MEHRZADI, S., SHAKERI-ZADEH, A. & KAMRAVA, S. K. 2016. Nanotechnology in hyperthermia cancer therapy: From fundamental principles to advanced applications. *Journal of Controlled Release,* 235**,** 205-221.

DREADEN, E. C., ALKILANY, A. M., HUANG, X., MURPHY, C. J. & EL-SAYED, M. A. 2012. The golden age: gold nanoparticles for biomedicine. *Chemical Society Reviews,* 41**,** 2740-2779.

FAN, J., GUO, Y., WANG, J. & FAN, M. 2009. Rapid decolorization of azo dye methyl orange in aqueous solution by nanoscale zerovalent iron particles. *Journal of Hazardous Materials,* 166**,** 904-910.

FONOVICH, T. M. 2013. Sudan dyes: are they dangerous for human health? *Drug and chemical toxicology,* 36**,** 343-352.

HISATOMI, T., KUBOTA, J. & DOMEN, K. 2014. Recent advances in semiconductors for photocatalytic and photoelectrochemical water splitting. *Chemical Society Reviews,* 43**,** 7520-7535.

KARLSSON, H. L., CRONHOLM, P., HEDBERG, Y., TORNBERG, M., DE BATTICE, L., SVEDHEM, S. & WALLINDER, I. O. 2013. Cell membrane damage and protein interaction induced by copper containing nanoparticles—Importance of the metal release process. *Toxicology,* 313**,** 59-69.

KAUR, P., THAKUR, R., MALWAL, H., MANUJA, A. & CHAUDHURY, A. 2018. Biosynthesis of biocompatible and recyclable silver/iron and gold/iron core-shell nanoparticles for water purification technology. *Biocatalysis and Agricultural Biotechnology,* 14**,** 189-197.

KHAN, I., SAEED, K. & KHAN, I. 2017. Nanoparticles: Properties, applications and toxicities. *Arabian Journal of Chemistry*.

LEONG, K. H., CHU, H. Y., IBRAHIM, S. & SARAVANAN, P. 2015. Palladium nanoparticles anchored to anatase TiO2 for enhanced surface plasmon resonance-stimulated, visible-light-driven photocatalytic activity. *Beilstein journal of nanotechnology,* 6**,** 428.

MAJDALAWIEH, A., KANAN, M. C., EL-KADRI, O. & KANAN, S. M. 2014. Recent advances in gold and silver nanoparticles: synthesis and applications. *Journal of nanoscience and nanotechnology,* 14**,** 4757-4780.

MUKHERJEE, R., KUMAR, R., SINHA, A., LAMA, Y. & SAHA, A. K. 2016. A review on synthesis, characterization, and applications of nano zero valent iron (nZVI) for environmental remediation. *Critical Reviews in Environmental Science and Technology,* 46**,** 443-466.

NAICKER, K., CUKROWSKA, E. & MCCARTHY, T. 2003. Acid mine drainage arising from gold mining activity in Johannesburg, South Africa and environs. *Environmental pollution,* 122**,** 29-40.

REBAH, F. B. & SIDDEEG, S. 2017. Cactus an eco-friendly material for wastewater treatment: a review. *Journal of Materials and Environmental Sciences,* 8**,** 1770-1782.

RIETER, W. J., TAYLOR, K. M., AN, H., LIN, W. & LIN, W. 2006. Nanoscale metal− organic frameworks as potential multimodal contrast enhancing agents. *Journal of the American Chemical Society,* 128**,** 9024-9025.

SARAVANAN, R., GUPTA, V., PRAKASH, T., NARAYANAN, V. & STEPHEN, A. 2013. Synthesis, characterization and photocatalytic activity of novel Hg doped ZnO nanorods prepared by thermal decomposition method. *Journal of Molecular Liquids,* 178**,** 88-93.

SINGHAL, G., BHAVESH, R., KASARIYA, K., SHARMA, A. R. & SINGH, R. P. 2011. Biosynthesis of silver nanoparticles using Ocimum sanctum (Tulsi) leaf extract and screening its antimicrobial activity. *Journal of Nanoparticle Research,* 13**,** 2981-2988.

THOMAS, J. R., SILVERMAN, S. & NELSON, J. 2015. *Research methods in physical activity, 7E*, Human kinetics.

TIWARI, D. K., BEHARI, J. & SEN, P. 2008. Application of nanoparticles in wastewater treatment 1.

ZAIMY, M., JEBALI, A., BAZRAFSHAN, B., MEHRTASHFAR, S., SHABANI, S., TAVAKOLI, A., HEKMATIMOGHADDAM, S., SARLI, A., AZIZI, H. & IZADI, P. 2016. Coinhibition of overexpressed genes in acute myeloid leukemia subtype M2 by

gold nanoparticles functionalized with five antisense oligonucleotides and one anti-CD33 (+)/CD34 (+) aptamer. *Cancer gene therapy,* 23**,** 315.

ZIERVOGEL, G., NEW, M., ARCHER VAN GARDEREN, E., MIDGLEY, G., TAYLOR, A., HAMANN, R., STUART-HILL, S., MYERS, J. & WARBURTON, M. 2014. Climate change impacts and adaptation in South Africa. *Wiley Interdisciplinary Reviews: Climate Change,* 5**,** 605-620.

Chapter 2 Literature review

2.1 The flocculation process

The flocculation process is applicable to wastewater, municipal water, bioprocessing of coal and wastewater generated from other industrial process such as fermentation and downstream (Yokoi et al., 2002). Due to low cost and good flocculating efficiencies, traditional flocculants such as aluminium sulphate and polyaluminium chloride have played a major role in the flocculation process (Zaki et al., 2013). Nevertheless, these chemical flocculants have been found to be detrimental to the human health and environment. Bioflocculation is a process in which the microorganisms secreted macromolecules are used to flocculate, remove or settle particles in water (Xia et al., 2018).

2.2 Different types of flocculants

Chemicals that stimulate flocculation by aggregation of colloids and other suspended particles, forming a floc are called flocculants (Ugbenyen and Okoh, 2014). Both organic and inorganic flocculants have been employed in the purification of water in various industries. This include, organic synthetic polymers, inorganic aluminium or ferric salt (Guo et al., 2018). Natural flocculants have also been used in various downstream processes such as treatment of wastewater, purification of potable water and fermentation and food industries (Karthiga devi and Natarajan, 2015). Commonly, the flocculants categories are: organic synthetic flocculants which includes (polyacrylamide derivatives); inorganic flocculants which includes (polyaluminium chloride) and natural occurring flocculants which includes the secondary secretion (bioflocculants) from microorganisms (Sun et al., 2012).

Flocculants of chemical nature have been used widely in the process of flocculation due to the cost effectiveness and flocculating efficiency. Nonetheless, some environmental and health concerns have been raised through their usage. Hence, urgent attention is required in the application of these biodegradable, environmental friendly flocculants to replace chemically synthesized flocculants, through biotechnological process of water treatment (bioflocculation). Microorganisms such as, fungi, algae and bacteria are reported as the excellent source for extracellular polymers such as glycoprotein and polysaccharides. Normally environment for bioflocculant producing microorganisms isolation includes, soil, wastewater, activated sludge and marine sediment (Zhang et al., 2013).

2.3 Effect of effluent discharge from dyes on water pollution

Large volumes of water and chemicals are consumed by textile industries while the processing of textiles. The chemical composition of reagent for textiles used are diverse, ranging from organic compounds to inorganic products and polymers (Tan et al., 2015). More than 100,000 dyes are commercially available and over 10,000 tons of dyes are produced annually (Tan et al., 2015). The complexity and synthetic nature of most dyes makes it difficult to decolourise due to the various factors such as structural variations, acidic, basic, azo, diazo, disperse, metal complex and anthroquinone based dyes (Pinheiro et al., 2004). Treating textile dye effluent aerobically by municipal sewage systems does not decolourize the dyes (Robinson et al., 2001).

Water soluble, brightly coloured, reactive and acidic dyes are the most problematic to treat, due to the ability to pass through conventional treatment system. Moreover, the municipal aerobic system which is dependent on biological activity, are inefficient in removing these dyes (Khan and Goyal, 2007). Dyes, which do not ionise in aqueous solution are said to be non-ionic. Fear arises as most dyes are made from aromatic compounds and benzidine which is known to be carcinogenic (Baughman and Perenich, 1988).

2.4 Production of bioflocculant

Microbial produced flocculants by marine microorganisms have recently received considerable amount of attention as a results of their non-toxic, biodegradability and disregard secondary pollutants (Karthiga devi and Natarajan, 2015). So far, numerous bioflocculant producing microorganisms have been reported, including algae, bacteria, yeast, actinobacteria and bacteria (Manivasagan et al., 2015). Bioflocculant producing microorganisms are mainly producers of natural organic substances which have the ability to flocculate suspended cells and solids. Until now, microorganisms which produce bioflocculants have been reported, were bacteria, fungi, algae, yeast, and actinobacteria (Manivasagan et al., 2015). Polysaccharides, glycoproteins and proteins are the most constituents of the bioflocculants. Among these bio-macromolecules, polysaccharide-based bioflocculant received most attention.

2.4.1 *Alcaligenes faecalis*

The habitat of *A. faecalis* is water and soil. It possess peritrichous flagellar arrangement which allows for motility (Manz et al., 1995). The organism is Gram-negative, rod-shaped organism, can be viewed under light microscope with a diameter of 0.5-2.6 μm. It requires oxygen for grow i.e. an aerobic microbe, with optimal temperatures between 20-37 °C. It is most

commonly seen in the clinical laboratories and causes opportunistic infections. Most moist items such as nebulizers, respirators, and lavage fluids harbour this microorganism. Infection caused by *A. faecalis* is usually in the form of a urinary tract infection (Gunderson et al., 1981).

2.5 Bioflocculant production conditions

2.5.1 Inoculum size and nutrients availability

Inoculum size is an important parameter in the production of bioflocculant (Mabinya et al., 2012). Among various physiological properties, inoculum size plays an important role in cell growth and secondary metabolites production (Gong et al., 2008). An inoculum size prolongs the lag phase of bacteria growth and a large inoculum size forms niche and inhibits bioflocculant production (Zhang et al., 2013). Insufficient inoculum size prolongs the lag phase of microbial growth there by delaying bioflocculant production; hence, bioflocculants are produced during late phase of exponential growth. However, large inoculum sizes deplete nutrients faster as there will be competition amongst microorganisms. The bioflocculant production by *Oceanobacillus sp*. was reported to be optimum at inoculum size 2% (Cosa et al., 2011). While on another study the *Shinella albus* optimum inoculum size for bioflocculant production was 1% (Li et al., 2016).

All microorganisms require nutrients as their energy source for growth (Liu et al., 2016). Different carbon sources vary in the extent to which they affect bioflocculant production by different microorganisms (Gao et al., 2006). Literature reports that, nitrogen sources are important nutrient factor that enhance bioflocculant production whereby microorganisms utilise either organic or inorganic nitrogen sources, or both, to produce bioflocculant. Examples of organic nitrogen sources were listed as peptone, urea, yeast extract and casein. While the inorganic are ammonium chloride, ammonium sulphate and sodium nitrate (Abd El-Salam et al., 2017).

2.5.2 Initial pH, temperature and speed

Bioflocculant production is highly dependent on pH, and some organisms prefer acidic conditions while others prefer neutral to alkaline conditions (Tavassoli et al., 2012). Electric charge of the cells and redox reactions is affected by the initial pH of the culture medium which in turn affects assimilation of nutrients and enzymatic reaction (Okaiyeto et al., 2015a). *Virgibacillus sp.* was reported to produce bioflocculant at acidic pH (Cosa et al., 2011). Another study reported that the organism produced bioflocculant at optimum pH of 7 which is

neutral (Okaiyeto et al., 2016). Literature report shows the bioflocculant production by *Klebsiellus sp.* TG-1. at alkaline pH (Adebayo-Tayo and Adebami, 2017). Temperature of the cultivation medium is one of the most important factors for bioflocculant production (Li-Fan and Cheng, 2010). Optimum temperature is required for activation of enzymes which are responsible for bioflocculant production. Literature reports that the optimum temperature for bioflocculant production ranges between 25 and 37 °C (Abd El-Salam et al., 2017). *Citrobacter sp.* TKF04 was reported to produce bioflocculant at a cultivation temperature of 30 °C, where optimum enzymatic reactions are usually attained at the growth optimum conditions. Agitation of cultivation medium determines dissolved oxygen concentration which in turn influences nutrients absorption and enzymatic reaction (Gao et al., 2006). Shaker speed 140-160 rpm was reported to be the optimum speed for bioflocculant production (Sekelwa et al., 2013). However, differences in shaking speed could be due to different oxygen requirements for different microorganisms at different growth phases (Adebayo-Tayo and Adebami, 2017).

2.6 Extraction and purification of the bioflocculant

Bioflocculant extraction is achieved using solvent extraction technique. Absolute ethanol is used as an extracting solvent while chloroform and butanol are employed in purification processes. Literature reports on the very low yield for bioflocculant production, however, the yield could be improved by consortium, which is the combination of more than one microorganisms in a culture broth (Kurane and Matsuyama, 1994). A purified bioflocculant yield of 8.203 g/L was reported in a consortium medium (Zhang et al., 2013). Contrary, a much lower yield in the consortium of *Methylobacterium* sp. Obi and *Actinobacterium sp* was reported (Luvuyo et al., 2013).

2.7 Factors affecting flocculation process

2.7.1 Effect of viscosity and time on flocculation

The amount of time the flocculant is suspended in a solution has the effect on viscosity which in turn affect the flocculation process (Owen et al., 2002). After 1 hr of polyacrylamide dissolved in a solution the viscosity of the solution was similar to that of water. The amount of dissolved polymer at this moment does not alter the viscosity to a great degree. With the increase in time up to 3 hrs, the viscosity rapidly increased as well which was followed by sharp decrease at 5 hrs (Owen et al., 2002). After 7 hrs minimal changes to viscosity occurred and also the activity of the flocculant was minimal.

2.7.2 Effect of pH and metal ions on bioflocculant activity

Optimum flocculating activity was observed at pH 3.0 and it decreased gradually until pH 12 (Toeda and Kurane, 1991). At acidic pH the bioflocculant ionises completely which in turn enhance the flocculation process. Cations enhance the flocculation process by stabilizing the negatively charged suspension and that of the functional groups of the bioflocculant, to form bridge between the particles (Wu and Ye, 2007). Addition of bivalent or trivalent cations showed to have a synergistic effect on the flocculation process as opposed to monovalent cation. The synergistic effect was observed to decrease in the order of trivalent to bivalent to monovalent with the least effect on flocculation process (Toeda and Kurane, 1991).

2.7.3 Effect of agitation on flocculation

Aggregation was observed to be inversely proportional to agitation. At 100 rpm large volumes of aggregates were rapidly formed and fast settling rates were observed (Farrow and Swift, 1996). With the increased agitation 200 rpm, aggregation and settling was rapidly reduced. Further increase in agitation led to minor deterioration in performance of a flocculant (Owen et al., 2002).

2.7.4 Thermal stability of the purified bioflocculant

At lower temperatures both the bioflocculant and the kaolin particles are likely to absorb the hydrogen ions (H^+), subsequently weakening the kaolin and bioflocculant complex mediated by cations (Aljuboori et al., 2015). The increase in heat reduces the flocculating ability of the flocculant and the enzyme activity is affect as some enzymes denature at higher temperatures. Flocculating activity decreased by 15% in a bioflocculant when it was heated at 100 °C for 15 min,while 20% decrease was observed when the bioflocculant was heated for 20 min at 50 °C (Gong et al., 2008).

2.8 Nanoparticles

Particulate dispersions or solid particles with size range between 1-100 nm. Different nanoparticles can be obtained depending on the method of their preparation (Nanospheres or Nanocapsules). Properties such as, melting point, lower specific magnetization, and specific optical properties have attracted considerable amount of attention to most researchers (Amouri et al., 2012). Distinct optical properties of metal nanoparticles has attracted great interest in different applications such as bio-sensing, catalysis and drug delivery. Moreover, metal

nanoparticles are most studied by researchers due to optoelectronic, physiochemical properties and surface enhanced resonance (Kirubha and Palanisamy, 2014). Well organised nanomaterials consisting of two, three, or more types of individual nanocomponents are termed core shell (core@shell, core/shell or core-shell) (Gawande et al., 2015). Seed growth and chemical reduction technique are commonly used when synthesising bimetallic nanoparticles with core-shell structures. The synthesis procedure usually involves metal ion reduction by reducing agent and capped by another stabilizing agent. The environmental risk posed by such reactive chemicals resulted to a need for nontoxic, clean and environmental friendly approaches for nanoparticles synthesis (Allafchian et al., 2016).

2.9 Different classes of core-shell material

Core-shell nanomaterial can be categorised into different classes namely, organic/organic, inorganic/inorganic, inorganic/organic and organic/inorganic (Gudiksen et al., 2002). Core shell nanomaterial possess enhanced and/or multifunctional capabilities due to versatile and conducive compositions (Lauhon et al., 2002).

2.9.1 Hollow core-shell nanoparticles

Hollow core-shell nanoparticles, the core is sacrificed using diverse conditions specific to the core materials: calcination or dissolution method is used to remove organic nanomaterial, while strong acid or base is used to remove inorganic material (Wang et al., 2018). Core material removal offers some additional advantages depending on its application. The example of the most common hallow core shell nanoparticles include, inorganic oxide shell based. These types are prepared from the precursors separately or during calcination. Titanium, silica or ceria (sometimes combined) are often used because of their versatility in crafting (Chen et al., 2018).

2.9.2 Core-multishell nanoparticles

Core-multishell nanoparticles results from coating the core with similar or different material, and these types have been explored recently by researchers for different applications ranging from biology to catalytic functions (Erokhin et al., 2014). These types of nanoparticles (NPs) are generally designed to utilize different functionalities than just to protect the core material. Moreover, the core can be shielded by the inner layers from outer layers, which may at times not be compatible with each other. Recently the focus of many researchers is on the optical and electronic properties of the core-multishell nanomaterial (Erokhin et al., 2014).

2.10 Properties and factors affecting core shell nanoparticles formation

2.10.1 Water amount in the reaction

The high consideration of composite nano-sized structures is due to change in properties of individual elements and enhanced functionalities as compared to that of individual elements (Aguirre et al., 2011). Unique properties possessed by nanocomposite material include, biomedical, electrical and catalytic (Lin et al., 2006). Water content is an important factor on the crystallization and nucleation rate in the core-shell nanomaterial formation (Sanpui et al., 2008). Lower water content resulted in faster core-shell nanoparticles formation, which could be probably due to faster crystallization rate of the synthesis solution. At the same time the increase in the amount of water in the mother liquor decreased the formation of core shell material. This is due to low crystal growth, as a result the shell could not form completely (Huang et al., 2008).

2.10.2 Effect of synthesis time

When the synthesis time was increased to 2 hrs, core shell nanoparticles weight increased and it remained the same after the longer than 2 hrs. This is indicating the completion of crystallization at 2 hrs, which also indicates that synthesis time should not be too long, 2 hrs was enough to achieve excellent core shell formation performance (Zhou et al., 2017).

2.11 The use of bioflocculant for nanoparticles synthesis

Bioflocculant produced by marine microbial have received great attention in recent years. Owing to their non-toxic, biodegradability and negligible secondary pollution (Salehizadeh and Shojaosadati, 2001). The composition of bioflocculants is mainly biological macromolecules such as protein, nucleic acid, polysaccharides and glycoprotein (Shih et al., 2001). The use of bioflocculants is seen in various biotechnological processes such as food, wastewater treatment and downstream processes. Polymers of monosaccharides are called polysaccharides. There are different sources for polysaccharide production such as plant extract, and different microorganisms (Shih et al., 2001). Polysaccharides are usually used as stabilizing and reducing agents in nanoparticles synthesis, owing to their highly stable nature, non-toxic, safe, biodegradable and hydrophilic (Koenker and Hallock, 2001). Application of polysaccharide base bioflocculant in high-performance nanomaterial production is highly profitable, this is due to their ability to form liquid crystal in aqueous solution (Manivasagan et al., 2015).

2.12 Possible application of core-shell nanomaterial

2.12.1 Dye degradation

Many direct dyes have a disazo and trisazo structures, which are the largest class of dyes (60-70%) with the greatest variety of colours (Bae and Freeman, 2007). The intensive colour of dyes is a major challenge to the textile industry to discharge the effluent, as the presence of small amount of dye is noticeable. Wastewater generated from textile mills usually have intense colour, have high biological oxygen demand (BOD) and chemical oxygen demand (COD) (Işik and Sponza, 2003). They are also said to contain, sulphates, acidity, chlorides, phenolic compounds and numerous heavy metals (Jais et al., 2017). Some biotransformation products and azo dyes have been found to be toxic to aquatic ecosystem, and some of the compounds are mutagenic and carcinogenic (Verma, 2008). The water soluble azo dyes can cause receiving water bodies to become coloured even at lower concentration of 10-50 mg/L (Anliker, 1977). The main source of toxic discharge in aquatic environment is textile industries (Sponza, 2003). Manufacturing industries use dyes in different application fields such as printing, plastics, rubber, cosmetics, food processing and leather tanning (Yagub et al., 2014). About 1-15% of these dyes are lost in wastewater during processing. Due to the mutagenic, carcinogenic and teratogenic nature of the compounds contained in dyes, water contaminated does not only affect ground water and surface water but also impact human health and disrupts the ecological system (Morrow et al., 2000). High thermal and chemical stability of dyes makes them to resist degradation by light, heat, and oxidants in nature. Nano composite material are a promising alternative to dye degradability (Shu et al., 2015).

2.12.2 Antimicrobial and antifungal effect of core-shell material

With the emergence of antibiotic resistant microorganisms, it is imperative that researchers find the alternative methods to treat these microorganisms. The use of composite nanomaterial for testing the antimicrobial effect against selected strains of bacteria and fungi has been documented (Sanpui et al., 2008). The findings revealed that composite materials have the potential to inhibit the pathogenic organism, the findings were comparable to that of standard antibiotics (amoxicillin). These findings are of great significance in water purification as it provides both water purification and elimination of pathogens (Padmavathy and Vijayaraghavan, 2008).

2.13 Application of flocculants in textile industries

Pollution of water by both organic and inorganic pollutants has become an important concern of this era. Worldwide textile industry is viewed as one of the biggest contributors in water pollution as a result of different chemicals that are utilized during various textile processes (Ali, 2010). Discharged unused effluents from textile industries contain toxic chemicals with high level of toxicity, colour, turbidity, chemical oxygen demand (COD) and biological oxygen demand (BOD). These discharged effluents if released without proper treatment, affect the environment badly (Pinheiro et al., 2004). Therefore, it is of utmost important to treat and remove pollutants in our water bodies. A number of methods have been used for the treatment of industrial effluents such as constructed wetlands, electrocoagulation and membrane filtration. A major role has been played by all these technologies in industrial effluent management. However, the main shortcomings of these methods are either they produce huge amount of sludge or they are more expensive (Patil et al., 2011).

Composite material has been used to carry out the treatment of industrial discharge which significantly provide heavy metal ions recoveries up to 97-98% yield (Sajayan et al., 2017). Nevertheless, metal ions adsorbed on exhausted composite material cannot be removed by applying any method. A procedure to desorption of metal ions from the surface of hybrid metals is time consuming and expensive. Hence, hybrid metals, inorganic flocculants are used extensively due to the effectiveness for the organic pollutant removal from water bodies (Guo and Chen, 2017). Furthermore, polymeric residues which are produced by organic flocculants are known to be carcinogenic and neurotoxic. Also, the non-biodegradability of flocculants causes problem for the treatment of sludge (Shahadat et al., 2017).

2.14 Nanoparticles toxicity

Nanoparticles have various industrial and medical applications, however, there are some toxicities which are associated with nanomaterials and is necessary to have basic knowledge about nanoparticles toxicities to be able to properly encounter them (Bahadar et al., 2016). During numerous human activities nanoparticles (NPs) enter the environment surreptitiously through soil, air and water. Nevertheless, great concerns have been raised as the results of deliberately application of NPs for the treatment of the environment through injection or dumps to aquatic system or soil (Khan et al., 2017). Properties of NPs such as high reactivity, small size and great capacity, could become lethal to the cell by inducing harmful and toxic effects.

Through literature, NPs can enter organisms through inhalation or ingestion, due to the small size nature, NPs can translocate within the body to different tissues and organs where toxicology effect may occur (Khan et al., 2017). Application of NPs such as silver nanoparticles (AgNPs) in various consumer products results in their release to the aquatic environment and in turn result in dissolved Ag and have a toxic effect on aquatic life (Navarro et al., 2008). The portal entry for NPs is respiratory system and it represent potential target for toxicity as it receives the entire cardiac output (Montalescot et al., 2013). Application of NPs in nanobiotechnology has received progress and early acceptance, however, prolonged exposure at different concentrations cause a potential adverse health effects (Montalescot et al., 2013). The ability of NPs to organise around protein is one of the toxic abilities of NPs, but, this depends on the shape, size, curvature and surface characteristics such as charge, functional groups and free energy (Khan et al., 2017).

2.15 References

ABD EL-SALAM, A. E., ABD-EL-HALEEM, D., YOUSSEF, A. S., ZAKI, S., ABU-ELREESH, G. & EL-ASSAR, S. A. 2017. Isolation, characterization, optimization, immobilization and batch fermentation of bioflocculant produced by Bacillus aryabhattai strain PSK1. *Journal of Genetic Engineering and Biotechnology,* 15**,** 335-344.

ADEBAYO-TAYO, B. C. & ADEBAMI, G. E. 2017. Production, Characterization and Effect of Cultural Condition on Bioflocculant Produced by Alcaligenes aquatilis AP4. *Journal of Applied Life Sciences International,* 14**,** 1-12.

AGUIRRE, M. E., RODRÍGUEZ, H. B., SAN ROMÁN, E., FELDHOFF, A. & GRELA, M. A. 2011. Ag@ ZnO core–shell nanoparticles formed by the timely reduction of Ag+ ions and zinc acetate hydrolysis in N, N-dimethylformamide: mechanism of growth and photocatalytic properties. *The Journal of Physical Chemistry C,* 115**,** 24967-24974.

ALI, H. 2010. Biodegradation of Synthetic Dyes—A Review. *Water, Air, & Soil Pollution,* 213**,** 251-273.

ALJUBOORI, A. H. R., IDRIS, A., AL-JOUBORY, H. H. R., UEMURA, Y. & ABUBAKAR, B. I. 2015. Flocculation behavior and mechanism of bioflocculant produced by Aspergillus flavus. *Journal of environmental management,* 150**,** 466-471.

ALLAFCHIAN, A., JALALI, S. A. H., BAHRAMIAN, H. & AHMADVAND, H. 2016. Preparation, characterization, and antibacterial activity of NiFe2O4/PAMA/Ag–TiO2 nanocomposite. *Journal of Magnetism and Magnetic Materials,* 404**,** 14-20.

AMOURI, H., DESMARETS, C. & MOUSSA, J. 2012. Confined nanospaces in metallocages: guest molecules, weakly encapsulated anions, and catalyst sequestration. *Chemical reviews,* 112**,** 2015-2041.

ANLIKER, R. 1977. Color chemistry and the environment. *Ecotoxicology and environmental safety,* 1**,** 211-237.

BAE, J.-S. & FREEMAN, H. S. 2007. Aquatic toxicity evaluation of new direct dyes to the Daphnia magna. *Dyes and Pigments,* 73**,** 81-85.

BAHADAR, H., MAQBOOL, F., NIAZ, K. & ABDOLLAHI, M. 2016. Toxicity of nanoparticles and an overview of current experimental models. *Iranian biomedical journal,* 20**,** 1.

BAUGHMAN, G. L. & PERENICH, T. A. 1988. Fate of dyes in aquatic systems: I. Solubility and partitioning of some hydrophobic dyes and related compounds. *Environmental Toxicology and Chemistry: An International Journal,* 7**,** 183-199.

CHEN, M., HE, Y., WANG, X. & HU, Y. 2018. Complementary enhanced solar thermal conversion performance of core-shell nanoparticles. *Applied Energy,* 211**,** 735-742.

COSA, S., MABINYA, L. V., OLANIRAN, A. O., OKOH, O. O., BERNARD, K., DEYZEL, S. & OKOH, A. I. 2011. Bioflocculant production by Virgibacillus sp. Rob isolated from the bottom sediment of Algoa Bay in the Eastern Cape, South Africa. *Molecules,* 16**,** 2431-2442.

EROKHIN, A., LOKTEVA, E., YERMAKOV, A. Y., BOUKHVALOV, D., MASLAKOV, K., GOLUBINA, E. & UIMIN, M. 2014. Phenylacetylene hydrogenation on Fe@ C and Ni@ C core–shell nanoparticles: about intrinsic activity of graphene-like carbon layer in H2 activation. *Carbon,* 74**,** 291-301.

FARROW, J. & SWIFT, J. 1996. A new procedure for assessing the performance of flocculants. *International Journal of Mineral Processing,* 46**,** 263-275.

GAO, J., BAO, H.-Y., XIN, M.-X., LIU, Y.-X., LI, Q. & ZHANG, Y.-F. 2006. Characterization of a bioflocculant from a newly isolated Vagococcus sp. W31. *Journal of Zhejiang University Science B,* 7**,** 186-192.

GAWANDE, M. B., GOSWAMI, A., ASEFA, T., GUO, H., BIRADAR, A. V., PENG, D.-L., ZBORIL, R. & VARMA, R. S. 2015. Core–shell nanoparticles: synthesis and applications in catalysis and electrocatalysis. *Chemical Society Reviews,* 44**,** 7540-7590.

GONG, W.-X., WANG, S.-G., SUN, X.-F., LIU, X.-W., YUE, Q.-Y. & GAO, B.-Y. 2008. Bioflocculant production by culture of Serratia ficaria and its application in wastewater treatment. *Bioresource technology,* 99**,** 4668-4674.

GUDIKSEN, M. S., LAUHON, L. J., WANG, J., SMITH, D. C. & LIEBER, C. M. 2002. Growth of nanowire superlattice structures for nanoscale photonics and electronics. *Nature,* 415**,** 617.

GUNDERSON, J. G., KOLB, J. E. & AUSTIN, V. 1981. The diagnostic interview for borderline patients. *The American Journal of Psychiatry*.

GUO, H., HONG, C., ZHANG, C., ZHENG, B., JIANG, D. & QIN, W. 2018. Bioflocculants' production from a cellulase-free xylanase-producing Pseudomonas boreopolis G22 by degrading biomass and its application in cost-effective harvest of microalgae. *Bioresource Technology,* 255**,** 171-179.

GUO, J. & CHEN, C. 2017. Sludge conditioning using the composite of a bioflocculant and PAC for enhancement in dewaterability. *Chemosphere,* 185**,** 277-283.

HUANG, J., LIU, Y., HOU, H. & YOU, T. 2008. Simultaneous electrochemical determination of dopamine, uric acid and ascorbic acid using palladium nanoparticle-loaded carbon nanofibers modified electrode. *Biosensors and Bioelectronics,* 24**,** 632-637.

IŞIK, M. & SPONZA, D. T. 2003. Effect of oxygen on decolorization of azo dyes by Escherichia coli and Pseudomonas sp. and fate of aromatic amines. *Process Biochemistry,* 38**,** 1183-1192.

JAIS, N. M., MOHAMED, R., AL-GHEETHI, A. & HASHIM, M. A. 2017. The dual roles of phycoremediation of wet market wastewater for nutrients and heavy metals removal and microalgae biomass production. *Clean Technologies and Environmental Policy,* 19**,** 37-52.

KARTHIGA DEVI, K. & NATARAJAN, K. A. 2015. Production and characterization of bioflocculants for mineral processing applications. *International Journal of Mineral Processing,* 137**,** 15-25.

KHAN, B. & GOYAL, D. G. 2007. *Microbial decolorization of triphenylmethane dyes.*

KHAN, I., SAEED, K. & KHAN, I. 2017. Nanoparticles: Properties, applications and toxicities. *Arabian Journal of Chemistry*.

KIRUBHA, E. & PALANISAMY, P. 2014. Green synthesis, characterization of Au–Ag core–shell nanoparticles using gripe water and their applications in nonlinear optics and surface enhanced Raman studies. *Advances in Natural Sciences: Nanoscience and Nanotechnology,* 5**,** 045006.

KOENKER, R. & HALLOCK, K. F. 2001. Quantile regression. *Journal of economic perspectives,* 15**,** 143-156.

KURANE, R. & MATSUYAMA, H. 1994. Production of a bioflocculant by mixed culture. *Bioscience, biotechnology, and biochemistry,* 58**,** 1589-1594.

LAUHON, L. J., GUDIKSEN, M. S., WANG, D. & LIEBER, C. M. 2002. Epitaxial core–shell and core–multishell nanowire heterostructures. *Nature,* 420**,** 57.

LI-FAN, L. & CHENG, W. 2010. Characteristics and culture conditions of a bioflocculant produced by Penicillium sp. *Biomedical and environmental sciences,* 23**,** 213-218.

LI, Y., XU, Y., LIU, L., JIANG, X., ZHANG, K., ZHENG, T. & WANG, H. 2016. First evidence of bioflocculant from Shinella albus with flocculation activity on harvesting of Chlorella vulgaris biomass. *Bioresource Technology,* 218**,** 807-815.

LIN, J. M., LIN, H. Y., CHENG, C. L. & CHEN, Y. F. 2006. Giant enhancement of bandgap emission of ZnO nanorods by platinum nanoparticles. *Nanotechnology,* 17**,** 4391.

LIU, H., WANG, H. & QIN, H. 2016. Characteristics of hydrogen and bioflocculant production by a transposon-mutagenized strain of Pantoea agglomerans BH18. *International Journal of Hydrogen Energy,* 41**,** 22786-22792.

LUVUYO, N., NWODO, U. U., MABINYA, L. V. & OKOH, A. I. 2013. Studies on bioflocculant production by a mixed culture of Methylobacterium sp. Obi and Actinobacterium sp. Mayor. *BMC biotechnology,* 13**,** 62.

MABINYA, L. V., COSA, S., NWODO, U. & OKOH, A. I. 2012. Studies on bioflocculant production by Arthrobacter sp. Raats, a freshwater bacteria isolated from Tyume River, South Africa. *International journal of molecular sciences,* 13**,** 1054-1065.

MANIVASAGAN, P., KANG, K.-H., KIM, D. G. & KIM, S.-K. 2015. Production of polysaccharide-based bioflocculant for the synthesis of silver nanoparticles by Streptomyces sp. *International Journal of Biological Macromolecules,* 77**,** 159-167.

MANZ, W., AMANN, R., SZEWZYK, R., SZEWZYK, U., STENSTRÖM, T.-A., HUTZLER, P. & SCHLEIFER, K.-H. 1995. In situ identification of Legionellaceae using 16S rRNA-targeted oligonucleotide probes and confocal laser scanning microscopy. *Microbiology,* 141**,** 29-39.

MONTALESCOT, G., SECHTEM, U., ACHENBACH, S., ANDREOTTI, F., ARDEN, C., BUDAJ, A., BUGIARDINI, R., CREA, F., CUISSET, T. & DI MARIO, C. 2013. 2013 ESC guidelines on the management of stable coronary artery disease: the Task Force on the management of stable coronary artery disease of the European Society of Cardiology. *Eur Heart J,* 34**,** 2949-3003.

MORROW, C., MOORE, D. E. & LOCKNER, D. 2000. The effect of mineral bond strength and adsorbed water on fault gouge frictional strength. *Geophysical research letters,* 27**,** 815-818.

NAVARRO, E., BAUN, A., BEHRA, R., HARTMANN, N. B., FILSER, J., MIAO, A.-J., QUIGG, A., SANTSCHI, P. H. & SIGG, L. 2008. Environmental behavior and ecotoxicity of engineered nanoparticles to algae, plants, and fungi. *Ecotoxicology,* 17**,** 372-386.

OKAIYETO, K., NWODO, U. U., MABINYA, L. V. & OKOH, A. I. 2015. Bacillus toyonensis Strain AEMREG6, a Bacterium Isolated from South African Marine Environment Sediment Samples Produces a Glycoprotein Bioflocculant. *Molecules,* 20**,** 5239.

OKAIYETO, K., NWODO, U. U., OKOLI, S. A., MABINYA, L. V. & OKOH, A. I. 2016. Implications for public health demands alternatives to inorganic and synthetic flocculants: bioflocculants as important candidates. *MicrobiologyOpen,* 5**,** 177-211.

OWEN, A., FAWELL, P., SWIFT, J. & FARROW, J. 2002. The impact of polyacrylamide flocculant solution age on flocculation performance. *International journal of mineral processing,* 67**,** 123-144.

PADMAVATHY, N. & VIJAYARAGHAVAN, R. 2008. Enhanced bioactivity of ZnO nanoparticles—an antimicrobial study. *Science and technology of advanced materials,* 9**,** 035004.

PATIL, S. V., PATIL, C. D., SALUNKE, B. K., SALUNKHE, R. B., BATHE, G. & PATIL, D. M. 2011. Studies on characterization of bioflocculant exopolysaccharide of Azotobacter indicus and its potential for wastewater treatment. *Applied biochemistry and biotechnology,* 163**,** 463-472.

PINHEIRO, H. M., TOURAUD, E. & THOMAS, O. 2004. Aromatic amines from azo dye reduction: status review with emphasis on direct UV spectrophotometric detection in textile industry wastewaters. *Dyes and pigments,* 61**,** 121-139.

ROBINSON, T., MCMULLAN, G., MARCHANT, R. & NIGAM, P. 2001. Remediation of dyes in textile effluent: a critical review on current treatment technologies with a proposed alternative. *Bioresource technology,* 77**,** 247-255.

SAJAYAN, A., SEGHAL KIRAN, G., PRIYADHARSHINI, S., POULOSE, N. & SELVIN, J. 2017. Revealing the ability of a novel polysaccharide bioflocculant in bioremediation of heavy metals sensed in a Vibrio bioluminescence reporter assay. *Environmental Pollution,* 228**,** 118-127.

SALEHIZADEH, H. & SHOJAOSADATI, S. 2001. Extracellular biopolymeric flocculants: recent trends and biotechnological importance. *Biotechnology advances,* 19**,** 371-385.

SANPUI, P., MURUGADOSS, A., PRASAD, P. D., GHOSH, S. S. & CHATTOPADHYAY, A. 2008. The antibacterial properties of a novel chitosan–Ag-nanoparticle composite. *International journal of food microbiology,* 124**,** 142-146.

SEKELWA, C., ANTHONY, U. M., VUYANI, M. L. & ANTHONY, O. I. 2013. Characterization of a thermostable polysaccharide bioflocculant produced by Virgibacillus species isolated from Algoa bay. *African Journal of Microbiology Research,* 7**,** 2925-2938.

SHAHADAT, M., TENG, T. T., RAFATULLAH, M., SHAIKH, Z. A., SREEKRISHNAN, T. R. & ALI, S. W. 2017. Bacterial bioflocculants: A review of recent advances and perspectives. *Chemical Engineering Journal,* 328**,** 1139-1152.

SHIH, I., VAN, Y., YEH, L., LIN, H. & CHANG, Y. 2001. Production of a biopolymer flocculant from Bacillus licheniformis and its flocculation properties. *Bioresource technology,* 78**,** 267-272.

SHU, Z., CHEN, Y., ZHOU, J., LI, T., YU, D. & WANG, Y. 2015. Nanoporous-walled silica and alumina nanotubes derived from halloysite: controllable preparation and their dye adsorption applications. *Applied Clay Science,* 112**,** 17-24.

SPONZA, D. T. 2003. Investigation of extracellular polymer substances (EPS) and physicochemical properties of different activated sludge flocs under steady-state conditions. *Enzyme and Microbial Technology,* 32**,** 375-385.

SUN, J., ZHANG, X., MIAO, X. & ZHOU, J. 2012. Preparation and characteristics of bioflocculants from excess biological sludge. *Bioresource Technology,* 126**,** 362-366.

TAN, K. B., VAKILI, M., HORRI, B. A., POH, P. E., ABDULLAH, A. Z. & SALAMATINIA, B. 2015. Adsorption of dyes by nanomaterials: recent developments and adsorption mechanisms. *Separation and Purification Technology,* 150**,** 229-242.

TAVASSOLI, T., MOUSAVI, S., SHOJAOSADATI, S. & SALEHIZADEH, H. 2012. Asphaltene biodegradation using microorganisms isolated from oil samples. *Fuel,* 93**,** 142-148.

TOEDA, K. & KURANE, R. 1991. Microbial flocculant from Alcaligenes cupidus KT201. *Agricultural and Biological Chemistry,* 55**,** 2793-2799.

UGBENYEN, A. & OKOH, A. 2014. Characteristics of a bioflocculant produced by a consortium of Cobetia and Bacillus species and its application in the treatment of wastewaters. *Water SA,* 40**,** 140-144.

VERMA, Y. 2008. Acute toxicity assessment of textile dyes and textile and dye industrial effluents using Daphnia magna bioassay. *Toxicology and industrial health,* 24**,** 491-500.

WANG, Z., QUAN, X., ZHANG, Z. & CHENG, P. 2018. Optical absorption of carbon-gold core-shell nanoparticles. *Journal of Quantitative Spectroscopy and Radiative Transfer,* 205**,** 291-298.

WU, J.-Y. & YE, H.-F. 2007. Characterization and flocculating properties of an extracellular biopolymer produced from a Bacillus subtilis DYU1 isolate. *Process Biochemistry,* 42**,** 1114-1123.

XIA, X., LAN, S., LI, X., XIE, Y., LIANG, Y., YAN, P., CHEN, Z. & XING, Y. 2018. Characterization and coagulation-flocculation performance of a composite flocculant in high-turbidity drinking water treatment. *Chemosphere,* 206**,** 701-708.

YAGUB, M. T., SEN, T. K., AFROZE, S. & ANG, H. M. 2014. Dye and its removal from aqueous solution by adsorption: a review. *Advances in colloid and interface science,* 209**,** 172-184.

YOKOI, H., OBITA, T., HIROSE, J., HAYASHI, S. & TAKASAKI, Y. 2002. Flocculation properties of pectin in various suspensions. *Bioresource Technology,* 84**,** 287-290.

ZAKI, S. A., ELKADY, M. F., FARAG, S. & ABD-EL-HALEEM, D. 2013. Characterization and flocculation properties of a carbohydrate bioflocculant from a newly isolated Bacillus velezensis 40B. *Journal of environmental biology,* 34**,** 51.

ZHANG, X., SUN, J., LIU, X. & ZHOU, J. 2013. Production and flocculating performance of sludge bioflocculant from biological sludge. *Bioresource Technology,* 146**,** 51-56.

ZHOU, Z., SONG, J., TIAN, R., YANG, Z., YU, G., LIN, L., ZHANG, G., FAN, W., ZHANG, F. & NIU, G. 2017. Activatable singlet oxygen generation from lipid hydroperoxide nanoparticles for cancer therapy. *Angewandte Chemie International Edition,* 56**,** 6492-6496.

Chapter 3 : ARTICLE 1: Biosynthesis and Characterization of Copper Nanoparticles Using a Bioflocculant Extracted from *Alcaligenes faecalis* HCB2

Nkosinathi G. Dlamini[1*], Albertus K. Basson[1], and V. S. R. Rajasekhar Pullabhotla[2*]

[1]Bioflocculation Research Group, Department of Biochemistry and Microbiology

[2]Department of Chemistry, University of Zululand, Private Bag X1001, Kwa-Dlangezwa, 3886, South Africa.

Received: 3 January 2019; Accepted: 13 June 2019; Published: (November 2019)

Abstract: Bioflocculant from *Alcalegenis faecalis* HCB2 was used in the eco-friendly synthesis of the copper nanoparticles. Nanoparticles were characterized using a scanning electron microscope (SEM), transmission electron microscopy (TEM), UV-visible spectroscopy, thermo gravimetric analysis (TGA) and Fourier Transform Infrared Spectroscopy (FT-IR). The transmission electron microscopy images showed close to spherical shapes with an average particle size of ~53 nm. Energy dispersive X-ray spectroscopy analysis confirmed the presence of the Cu nanoparticles and also the other elements such as O, C, P, Ca, Cl, Na, K, Mg, and S originated from the bioflocculant. FT-IR results showed the presence of the –OH and $–NH_2$ groups, aliphatic bonds, amide and Cu–O bonds. Powder X-ray diffraction peaks confirmed the presence of (111) and (220) planes of fcc structure at 2° of 33° and 47° respectively with no other impurity peaks.

Keywords: Bioflocculant, Copper Nanoparticles, Electron Microscopy, Biosynthesis.

3.1 Introduction

Nanoparticles are the part of an emerging field of science Nanotechnology, which refers to the synthesis and development of numerous nanomaterials with size range from 1–100 nm [1]. A series of different techniques have been developed to synthesized nanoparticles of different sizes, composition and shapes [2]. These techniques include both physical and chemical methods; the physical method includes laser ablation and high-energy irradiation technique [3]. While chemical method includes chemical reduction techniques by reducing agents. Most common method used for nanoparticles formation such, as physical (condensation evaporation) and chemical (oxidation and reduction) methods are very efficient traditional methods. However, both methods have been found to have some shortcomings. One may require a large amount of energy and the other may involve the use of toxic and expensive chemicals, which may results in the binding of the nanoparticles on the surface of these chemicals. Copper nanoparticles (CuNPs) have attracted a considerable amount of interest to researchers due to the properties they possess such as, low production cost and mainly their antibacterial effectiveness. In comparison with precious metals for instance gold, silver or palladium, copper nanoparticles have shown the advantages such as high surface area to volume ratio, catalytic activity, optical and magnetic properties [4]. However, their immediate oxidation when exposed in air becomes the main challenge in their preparation and preservation. Inert atmospheric conditions such as under nitrogen, argon have been used to overcome this problem of oxidation, also reducing agents are used for protecting or capping copper salt used [5]. Reducing and capping agents that are used in the synthesis found to have toxic effects and are very expensive. Naturally occurring secretion by microorganisms (bioflocculants) have attracted considerable interest due to their harmlessness, biodegradability, and negligible secondary pollution. To overcome the toxicity-associated difficulties of reducing agents and to synthesise CuNPs in environment friendly route, we have exploited the use of bioflocculant in our chemical reduction process. Here bioflocculant work both as reducing and as protecting agent, which make the process nontoxic, economical and environment friendly. There is an increased demand for several metallic and non-metallic nanoparticles over the past decades. In this present study, we have adopted a biosynthesis method for the synthesis of copper nanoparticles using bioflocculant from *Alcaligenes feacalis* and copper sulphate salt as precursors. Nanoparticles were characterized using various analytical techniques such a as scanning electron microscope (SEM), UV-visible spectroscopy, thermo gravimetric analysis (TGA), Fourier Transform Infrared Spectroscopy (FT-IR) and transmission electron

microscopy (TEM). This new synthesis method shows excellent stability being eco-friendly. Scanning electron microscopy-energy dispersive spectroscopy (SEM-EDX) technique revealed that the significant presence of copper nanoparticles encapsulated with bioflocculant.

3.2 Materials and Methods

3.2.1 Source of Bioflocculant and Production Medium

The bioflocculant was extracted from *Alcalegenis faecalis*, which was previously isolated from marine environment and was identified as *Alcalegenis faecalis* through Inqaba laboratories. The bioflocculant production medium was prepared in accordance to a description by Zhang et al. [6] and it was composed of glucose (20 g), $MgSO_4 \cdot 7H_2O$, (0.2 g), $(NH4)_2SO_4$ (0.2 g), K_2HPO_4 (5 g), urea (0.5 g), yeast extract (0.5 g) and KH_2PO_4 (2 g). In a litre of filtered seawater at pH 8 and sterilized by autoclaving at 121–124 °C for 15 min. After autoclave, the medium was then allowed to cool and was inoculated with fresh culture, which was resuscitated a previous day, and it was then incubated in a shaking incubator for 72 hrs at 30 °C at a speed of 165 rpm.

3.2.2. Extraction and Purification of Bioflocculant

The culture broth taken out after 72 hrs of fermentation and centrifuged at 4,000 rpm at 4 °C for 30 min. This was done in order to remove cells and insoluble substances, the supernatant was then transferred into a clean container and cell were discarded. One litre of distilled water was then added into a supernatant and was centrifuged again at 4,000 rpm for 15 min at 4 °C. Two volumes of ethanol were added to the supernatant, agitated and the solution was stored at 4 °C for 12 hrs. A precipitate was formed and vacuum-dried, to which 100 mL of distilled water was added and the mixture of chloroform and *n*-butyl alcohol (5:2 v/v) was added. After stirring, the mixture was allowed to stand for 12 hrs at room temperature. The supernatant was then vacuum-dried in order to obtain a purified bioflocculant.

3.2.3. Synthesis of Copper Nanoparticles

The synthesis of copper nanoparticles was achieved using a method described by Chen et al. [7] with some minor modifications; 0.5 g of purified bioflocculant was added into a 200 mL solution of 3 mM $CuSO_4$. The mixture was agitated until a homogenous solution was achieved; foil was then used to cover the mouth of the conical flask containing the solution to prevent the interference of foreign material. The solution was left unstirred at room temperature for 24 hrs. Bioflocculant solution was used as a control for this experiment and formation of nanoparticles

was confirmed through physical observation and characterization. After 24 hrs, formation of a blue precipitate was observed and the synthesized nanoparticles were collected using centrifuge at 4 °C, 4000 rpm for 30 min. The as-synthesised nanoparticles were vacuum-dried overnight and stored for further characterization.

3.2.4. Characterization of As-Synthesized Copper Nanoparticles

Thermogravimetric analysis measurements were performed using a Perkin-Elmer Thermal Analysis Pyris 6 TGA in a closed perforated aluminium pan, under nitrogen gas with a flow rate of 40 cc/min and with a heating rate starting from 22 to 900 °C at 10.00 °C /min under constant flow of nitrogen gas. The as-synthesized bioflocculant passivated copper nanoparticles decomposition studies were in accordance with Piyo et al. [8]. Varian Cary 50 Conc UV-Vis spectrophotometer was used to carry out optical measurements of the synthesized copper nanoparticles, whereby 0.1 mL of the sample was taken and diluted with 2 mL of deionized water. Samples were placed in quartz cuvettes (1 cm path length). The absorption measurements were conducted in the wavelength region 300–700 nm wavelength range operated at a resolution of 1 nm and at room temperature conditions. Fourier Transform-Infrared (FT-IR) spectroscopy was used as part of structural elucidation to identify and confirm the functional groups present in the bioflocculant and the as-synthesized copper nanoparticles. For FT-IR measurements, pure solid samples were dried and ground to a fine powder and the spectra were recorded using a Tensor 27, Bruker FT-IR spectrophotometer with a resolution of 4 cm^{-1} in the range of 4000–200 cm^{-1}. Infrared spectra of both the bioflocculant and the as-synthesized copper nanoparticles were obtained. Morphology and compositional information of the synthesized copper nanoparticles was determined using scanning electron microscope and energy dispersive spectroscopy technique using a JEOL JSM-6100 microscope equipped with an energy-dispersive X-ray analyser (EDX). The images were taken with an emission current of 100 μA by a Tungsten (W) filament and an accelerator voltage of 10 kV. A small quantity of dry samples was placed on copper stubs using double-sided carbon tape and carbon coated using the JEOL vacuum evaporator. The working distance was varied between 5 and 10 mm. For EDX measurements on the samples were then performed using the JEOL JSM 6100 SEM with Bruker Quantax Esprit software. The elemental composition of as-synthesised copper nanoparticles was recorded. TEM images for the copper nanoparticles were obtained using a JEOL 1010 transmission electron microscope. The specimens were prepared by using a micropipette to place a diluted drop of suspension in toluene on a copper grid (150 mesh). The samples were allowed to dry completely at room temperature. Samples were viewed at

100 kV as the accelerating voltage. The images were captured digitally using a Megaview III camera, stored and measured using Soft Imaging System iTEM software. The crystallinity of the dried copper nanoparticles and bioflocculant was studied using the powder X-ray diffraction technique and the patterns were recorded using a Bruker D8 Advance diffractometer equipped with Cu-Kα radiation (λ= 1.5406 Å) at 40 kV, 40 mA at room temperature. The dried samples were placed on a flat sample holder and were scanned between 5 to 90° with steps of 0.05 in a 0.03°/s scan rate and step size of 0.00657.

3.3 Results and Discussion

3.3.1 Thermogravimetric Results of the Purified Bioflocculant and As-Synthesized Copper Nanoparticles

Thermogravimetric analysis was performed on purified bioflocculant and as-synthesised copper nanoparticles to reveal their behaviour when exposed to very high temperature. According to Kumari et al. [9], bioflocculant thermal degradation generally occurs in two phases. Phase one involves the loss of moisture which is due to increase in temperature up to about 150, which in turn results to weight loss. The second phase is brought about depolymerisation of the structure of the bioflocculant at temperatures above 400 °C. Figure 1 indicates the weight loss of about 20% at about 100 to 200 °C and about 29% weight loss at 500 °C. The further increase in temperature resulted in more weight loss. The first weight loss could be attributed to the moisture content loss in the bioflocculant [10]. These findings are similar to the one documented in the study by Okaiyeto et al. [11]. However, the findings are contrary to those documented in another study conducted by Yim et al. [12], where bioflocculant p-KG03 produced by marine dinoflagellate *Gyrodinium impudicum* KG03, weight loss was initially observed at 40–230 °C and remaining weight loss was noticed at around 310 °C. The complete decomposition of the bioflocculant is observed at temperatures above 800 °C. Three phases that can be noticed in the thermogravimetric analysis of cooper nanoparticles (Fig. 3.1). The first phase is seen approximately from temperature 40 to 120 °C, which could be the result of loss in moisture content or drying of residual solvent, which was used during purification. The second phase is observed at temperatures around 150 °C and below 200 °C, this could be related to decomposition of polymer, which in turn resulted in weight loss. Moreover, further increase in temperature resulted in more weight loss in the synthesized nanoparticles. These findings suggest that as-synthesized nanoparticles are thermostable as they are able to maintain weight above 60% even at temperatures above 500 °C. Contrary to the findings in a study conducted by Lee et al. [13], where weight gain of about

20% was observed at 180 °C and stopped at 600 °C. This could be related to thermal oxidation of copper nanoparticles to form copper oxide.

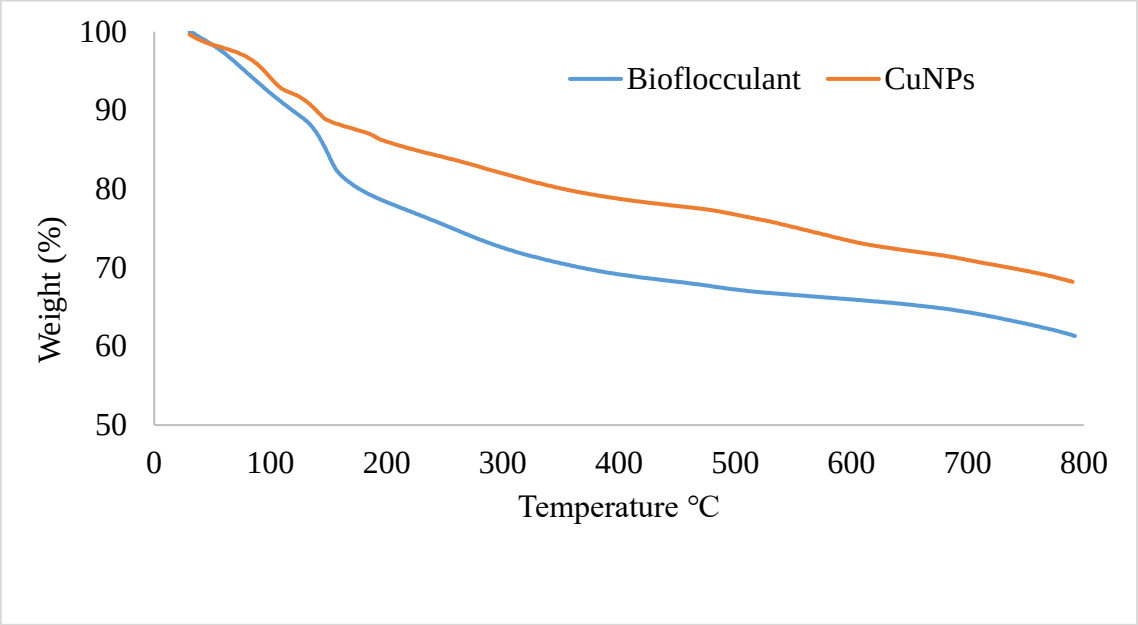

Figure 3.1 : Thermogravimetric analysis of both bioflocculant and copper nanoparticles.

3.3.2 UV-Visible Spectroscopy Results of the Purified Bioflocculant and As-Synthesized Copper Nanoparticles

Figure 3.2 represents UV-visible spectra of the bioflocculant and as-synthesised copper nanoparticles. The recorded spectra from both the bioflocculant and copper nanoparticles solution showed the plasmon resonance (SPR) spectra with absorbance 200–700 nm and the peak maxima for both the bioflocculant and as-synthesized particles was observed at around 290–300 nm, which could be ascribed to the formation of Cu nanoparticles. The change in colour of the bioflocculant from white to blue indicated the formation of copper nanoparticles. CuNPs exhibited green colour in a solution due to surface plasmon vibration in CuNPs.

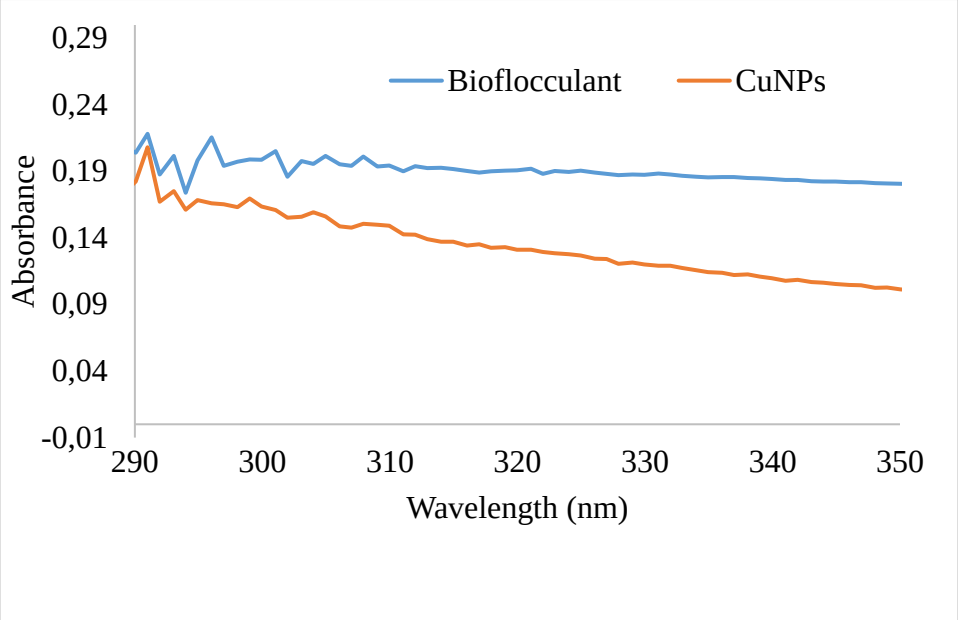

Figure 3.2: UV-Visible absorption spectra of the bioflocculant and synthesized copper nanoparticles.

3.3.3 FT-IR Results of the Purified Bioflocculant and As-Synthesized Copper Nanoparticles

Shojaodasati and Salehizadeh [14] states that microorganism produce bioflocculant with different composition chemical composition. Purified bioflocculants flocculating activity solely depends on the chemical structure, which is correlated to the functional groups present in the molecule. Xiong et al. [15] documented that the functional groups present in the molecule also serve as a binding site for different colloids in suspension. Different functional groups present in the molecule were revealed by the Fourier transform infrared (FT-IR) spectroscopy analysis. Figure 3.3 shows FT-IR spectra of the bioflocculant and copper nanoparticles showing various functional groups. The band at 3276 cm^{-1} (bioflocculant) and 3408 cm^{-1} (copper nanoparticles) showed the presence of hydroxyl (−OH) group and amine ($-NH_2$) group in the samples. The weak band at 2182 cm^{-1} in both the samples can be designated to the presence of aliphatic bonds. The peak located at 1670 cm^{-1} indicates the presence of an amide group. The vibrational peaks at 1077 cm^{-1} (bioflocculant) and 1022 cm^{-1} (copper nanoparticles) are analogous to the C–O stretching in alcohols, which confirms the −OH group presence. The vibrational bands observed at 596 cm^{-1} is typical of Cu–O bonds in the as-synthesised copper nanoparticles. The peaks between 1,000–^{1},100 cm^{-1} suggests the presence of saccharide derivatives. The FT-IR spectrum of the bioflocculant passivated copper nanoparticles showing all the functional groups that are characteristic of the bioflocculant.

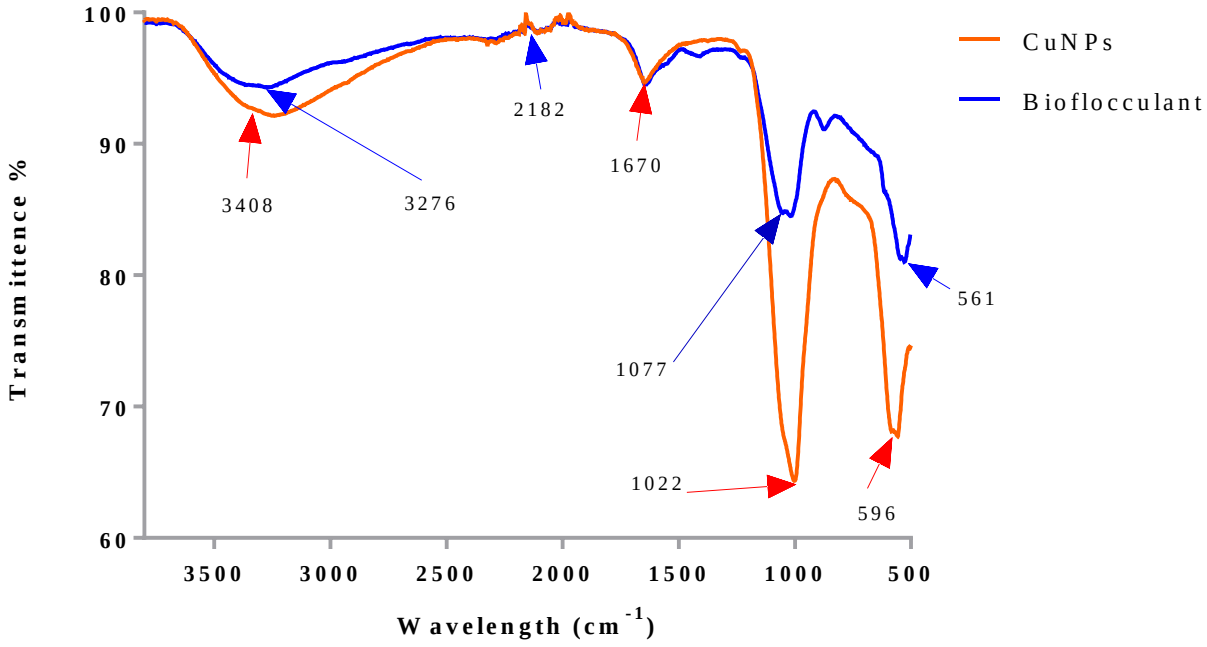

Figure 3.3: FT-IR spectra of the bioflocculant and copper nanoparticles.

3.3.4 Electron Microscopy Results of the Purified Bioflocculant and As-Synthesized Copper Nanoparticles

3.3.4.1 SEM-EDX Results of the Purified Bioflocculant and As-Synthesized Copper Nanoparticles

The SEM-EDX results show various elements present in the purified bioflocculant and as-synthesized bioflocculant passivated copper nanoparticles are illustrated in the Figure 3.4 Elements such as O, C, P, Ca, Cl, Na, K, Mg, and S were found to be present in the purified bioflocculant at the concentration of weight by percentage (wt%). Oxygen was the highest with 29 % while sulphur was the least with just 0.6% (Fig. 4(a)). The presence of the elements in bioflocculant play an important role in the structure and flocculating activity [8]. Furthermore, the presence of various elements brings about flexibility and stability to the bioflocculant and CuNPs. The presence of elements such as oxygen, carbon suggest that the bioflocculant is predominately carbohydrates in nature, also the absence of nitrogen confirms that it cannot be a glycoprotein [16]. In a study by Okaiyeto et al. [11] similar results were obtained in a bioflocculant MBF-UFH, where elements such as: C, O, Na, Mg, P, S, Cl, K and Ca were found. In the synthesized copper nanoparticles, the elements present were O, Cu, P, Mg, Ca, Cl and S. These findings reveal that oxygen with 37 wt.% followed by copper with 35.8 wt.% (Fig. 4(b)) which is an indication that the synthesis of copper nanoparticles was a success. It can be therefore deduced that the presence of copper in the highest percentage is as the results

of copper binding onto the surface of the bioflocculant. The results of the bioflocculant alone did not have any copper present.

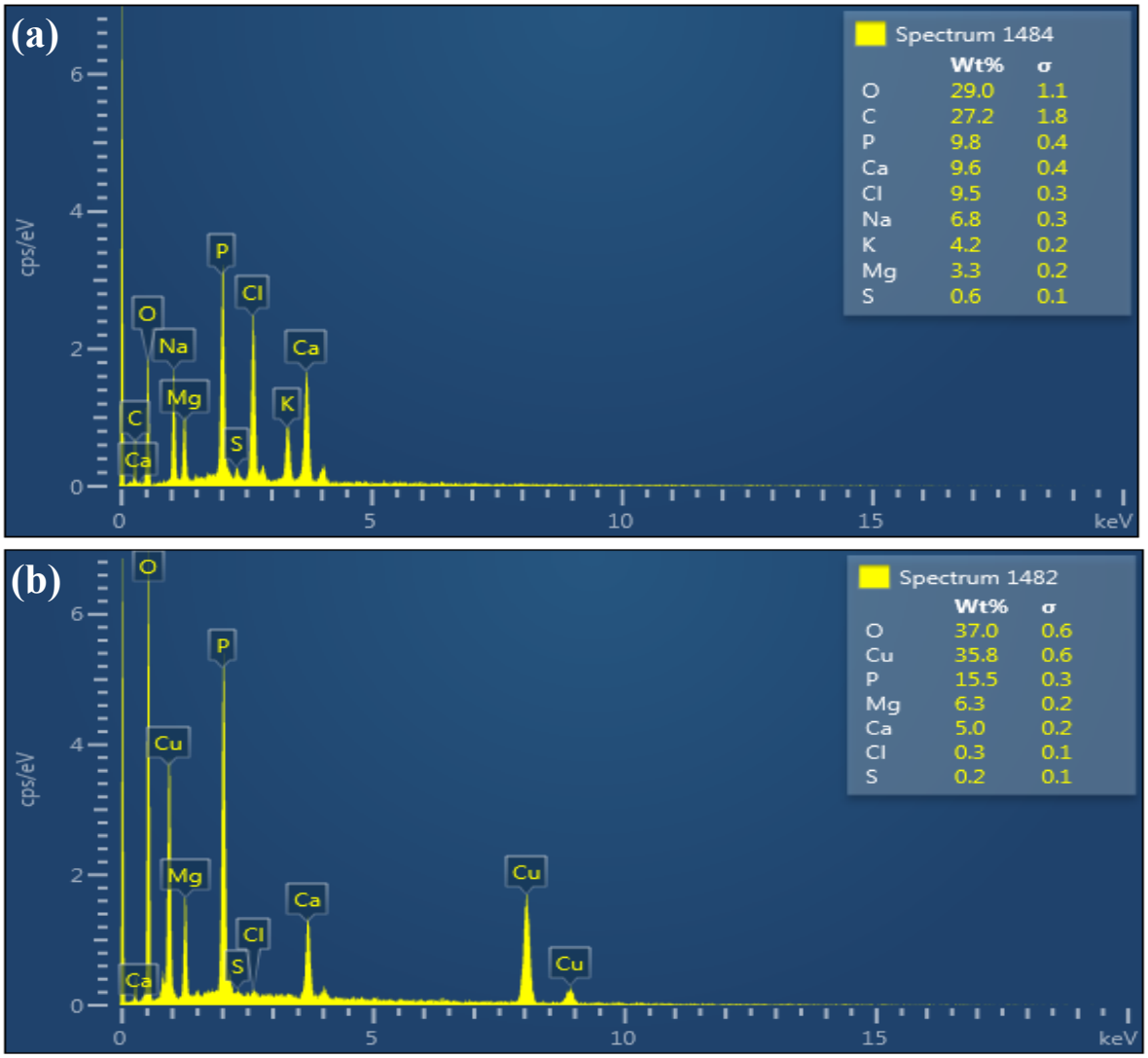

Figure 3.4: Energy dispersive X-ray spectrum of (a) bioflocculant and (b) copper nanoparticles passivated with bioflocculant.

3.3.4.2 SEM Results of the Purified Bioflocculant and As-Synthesized Copper Nanoparticles

Figure 3.5 shows the scanning electron micrograph of the purified bioflocculant and copper nanoparticles. The morphology of the synthesized copper nanoparticles and bioflocculant indicate an amorphous nature of the material. The morphological surface of the bioflocculant is similar to that of synthesized nanoparticles but with much bigger particle size. The synthesized nanoparticles seem to be spherical in shape and are agglomerated.

3.3.4.3 TEM Results of the Purified Bioflocculant and As-Synthesized Copper Nanoparticles

The morphology of the synthesized CuNPs was studied using TEM. Sample preparation for TEM was achieved by keeping a drop of colloidal solution on a copper grid. The sample was dried at room temperature before placing it on the specimen holder. A thin sample was irradiated with a sharp high-energy electron beam focused by magnetic lenses. The electron intensity distribution of the beam after interaction with the sample was imaged onto a fluorescent screen by the objective lens and the post objective lens system. Images were recorded by a digital CCD camera reproduced or displayed on a computer monitor. The results showed that the average particle size was 54 nm from TEM images, and seems spherical in shape as shown in Figure 3.6. To confirm the particle size, the intense peak from the X-ray diffract gram was used. From the Scherrer equation: $D = K\lambda/\beta \cos\theta$ the particles size was found to be ~53.56 nm, which is in good agreement with the average particle size calculated from the TEM analysis

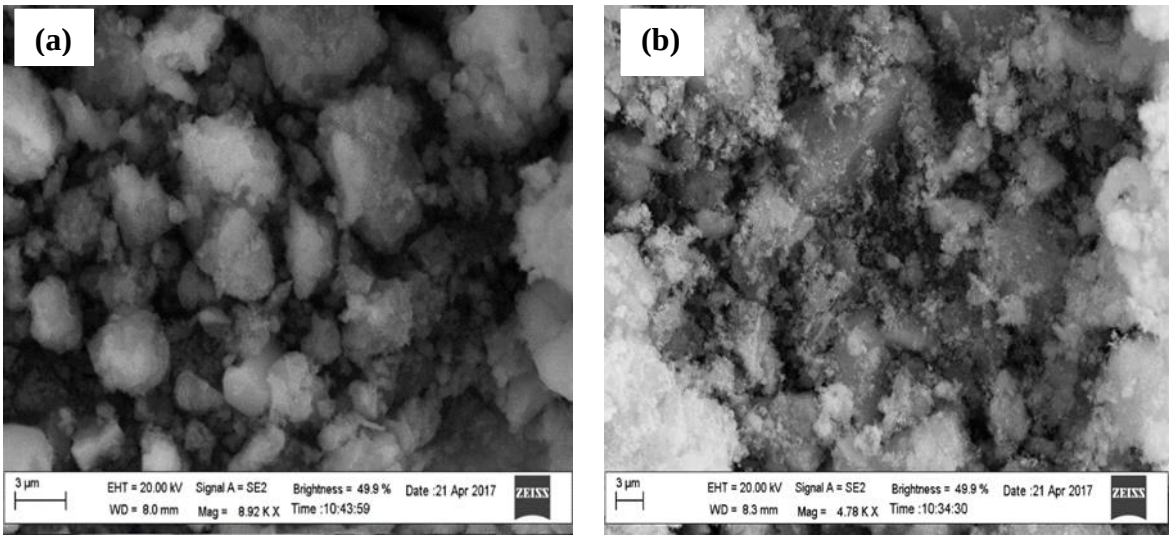

Figure 3.5: SEM images of (a) purified bioflocculant and (b) synthesised copper nanoparticles.

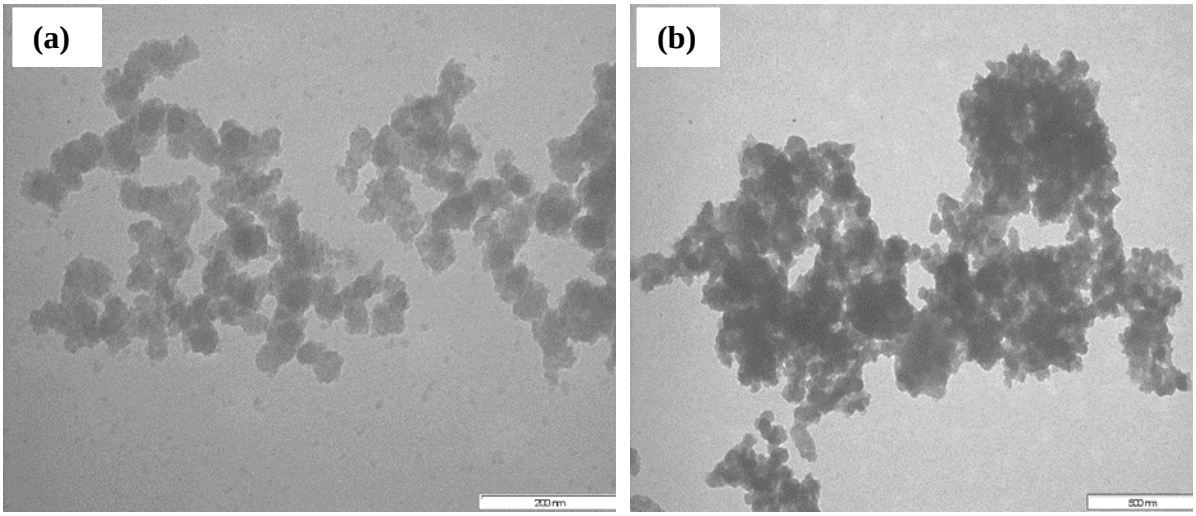

Figure 3.6: TEM images (a and b) of copper nanoparticles at 200 and 500 nm scale.

3.3.5 Bioflocculant and As-Synthesized Copper Nanoparticles

Figure 3.7 illustrates the X-ray diffraction patterns of the purified bioflocculant and as-synthesised copper nanoparticles. The XRD patterns of the bioflocculant is shown in the Figure 7(a), several peaks were observed between the 20° and 30° 2 θ angle. The peaks broadening in the XRD patterns of the solids is generally attributed to particle size effects. Smaller particle size is signified by broader peaks; it can be deduced that the bioflocculant possess much smaller particles of the nano size. Figure 7(b) shows XRD patterns of as-synthesised copper nanoparticles produced from a bioflocculant. In comparison to a copper standard (JCPDS 04-0836), the characteristic diffraction peaks of copper were observed at around 33° and 47° 2 θ. They correspond to the (111) and (220) planes of the fcc structure. No other peaks due to impurity were detected in the sample. Based on the findings it can be deduced that it is possible to produce pure copper nanoparticles using this method. Sharp diffraction peaks result from moderate temperature. This is an indication of growth of quality CuNPs at moderate conditions. The synthesized copper nanoparticles were revealed crystalline in nature. Intense Bragg reflections suggested that strong X-ray scattering centres in the crystalline phase could be due to the bioflocculant from which the nanoparticles were synthesized. Therefore, XRD result suggests that the crystallization of the bio-organic phase occurred on the surface of the copper nanoparticles or vice versa. The peaks broadening in the XRD patterns of the solids is generally attributed to particle size effects. Smaller particle size is signified by broader peaks. Moreover, broader peaks may also signify the effects due to experimental conditions on the nucleation and growth of the crystal nuclei. By using Debye-Scherrer's equation the particles size was calculated. The size of crystallite was ~53 nm, which indicates a higher surface area and surface to volume ratio of the nanoparticle

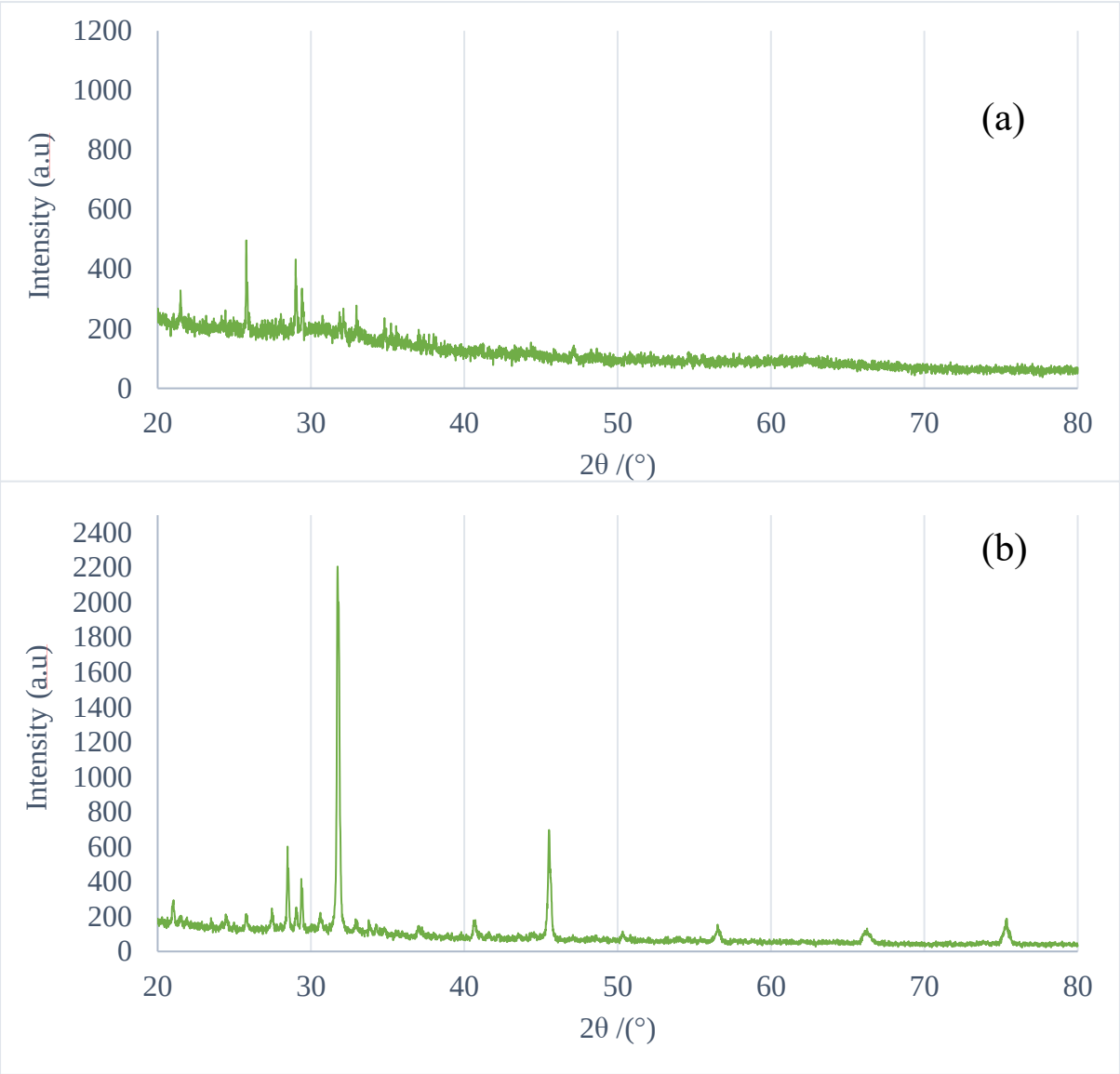

Figure 3.7: X-ray diffraction patterns of the (a) bioflocculant and (b) as-synthesized copper nanoparticles.

3.4 Conclusion

Copper nanoparticles were successful synthesized using a purified bioflocculant from *Alcaligenes faecalis* HCB2 and the synthesis method proved to be efficient, effective and eco-friendly since it uses biodegradable bioflocculant. The elements present in the synthesized copper nanoparticles were: O, Cu, P, Mg, Ca, Cl, and S; with 37 wt.% of oxygen and 35.5 wt.% of copper. FT-IR results showed the presence of the –OH and $–NH_2$, aliphatic, amide groups in both the purified bioflocculant and as-synthesised copper nanoparticles. The vibrational band at 596 cm−1 is typical of Cu–O bonds, ascertains the presence of the cupper nanoparticles in the as-synthesised material. TEM images revealed close to spherical shaped particles with an average particle size of ~53 nm, which is in good agreement with that of the calculated

using the Scherrer equation from XRD results. Powder X-ray diffraction peaks revealed the crystalline nature of the synthesised material with no impurities and are in correlation with the copper standard (JCPDS 04-0836). The characteristic diffraction peaks of copper were observed at around 33° and 47° 2θ, corresponding to the (111) and (220) planes of the fcc structure.

Acknowledgments: The authors would like to acknowledge the Electron Microscopy Unit at the University of KwaZulu-Natal, Westville campus, for providing support by letting us use the TEM and SEM-EDX facilities for the characterization of nanomaterials. Rajasekhar Pullabhotla would like to acknowledge the Research and Innovation Office, University of Zululand for the financial support in the form of Project S 451/12 and National Research Foundation (NRF, South Arica) for the financial support in the form of the Incentive Fund Grant (Grant No: 103691).

3.5 References

1. Dubchak, S., Ogar, A., Mietelski, J. and Turnau, K., 2010. Influence of silver and titanium nanoparticles on arbuscular mycorrhiza colonization and accumulation of radiocaesium in Helianthus annuus. *Spanish Journal of Agricultural Research*, pp.103–108.

2. Fawcett, A.A., Iyer, G.C., Clarke, L.E., Edmonds, J.A., Hultman, N.E., Mcjeon, H.C., Rogelj, J., Schuler, R., Alsalam, J. and Asrar, G.R., 2015. Can Paris pledges avert severe climate change? *Science, 350*, pp.1168–1169.

3. Sun, S. and Zeng, H., 2002. Size-controlled synthesis of magnetite nanoparticles. *Journal of the American Chemical Society, 124*, pp.8204–8205.

4. Umer, A., Naveed, S., Ramzan, N. and Rafique, M.S., 2012. Selection of a suitable method for the synthesis of copper nanoparticles. *Nano, 7*, p.1230005.

5. Lu, A.H., Salabas, E.E.L. and Schüth, F., 2007. Magnetic nanoparticles: Synthesis, protection, functionalization, and application. *Angewandte Chemie International Edition, 46*, pp.1222–1244.

6. Okaiyeto, K., Nwodo, U.U., Mabinya, L.V. and Okoh, A.I., 2015. Bacillus toyonensis strain AEMREG6, a bacterium isolated from South African marine environment sediment samples produces a glycoprotein bioflocculant. *Molecules, 20*, pp.5239.

7. Sathiyanarayanan, G., Kiran, G.S. and Selvin, J., 2013. Synthesis of silver nanoparticles by polysaccharide bioflocculant produced from marine *Bacillus subtilis* MSBN17. *Colloids and Surfaces B: Biointerfaces, 102*, pp.13–20.

8. Luo, Z., Chen, L., Chen, C., Zhang, W., Liu, M., Han, Y. and Zhou, J., 2014. Production and characteristics of a bioflocculant by *Klebsiella pneumoniae* YZ-6 isolated from human saliva. *Applied Biochemistry and Biotechnology, 172*, pp.1282–1292.

9. Venkatesh, P., Balraj, M., Ayyanna, R., Ankaiah, D. and Arul, V., 2016. Physicochemical and biosorption properties of novel exopolysaccharide produced by Enterococcus faecalis. *LWT-Food Science and Technology, 68*, pp.606–614.

10. Zhang, L., He, R. and Gu, H.-C., 2006. Oleic acid coating on the monodisperse magnetite nanoparticles. *Applied Surface Science, 253*, pp.2611–2617. 11. Okaiyeto, K., Nwodo, U.U.,

11. Okoli, S.A., Mabinya, L.V. and Okoh, A.I., 2016. Implications for public health demands alternatives to inorganic and synthetic flocculants: Bioflocculants as important candidates. *Microbiology Open, 5*, pp.177–211.

12. Yim, J.H., Kim, S.J., Ahn, S.H. and Lee, H.K., 2007. Characterization of a novel bioflocculant, p-KG03, from a marine dinoflagellate, Gyrodinium impudicum KG03. *Bioresource Technology, 98,* pp.361–367.

13. Lee, D.-J. and Chang, Y.-R., 2018. Bioflocculants from isolated stains: A research update. *Journal of the Taiwan Institute of Chemical Engineers, 87,* pp.211–215.

14. Salehizadeh, H. and Shojaosadati, S., 2001. Extracellular biopolymeric flocculants: Recent trends and biotechnological importance. *Biotechnology Advances, 19,* pp.371–385.

15. Xiong, Y., Wang, Y., Yu, Y., Li, Q., Wang, H., Chen, R. and He, N., 2010. Production and characterization of a novel bioflocculant from Bacillus licheniformis. *Appl. Environ. Microbiol., 76,* pp.2778–2782.

16. Karthiga Devi, K. and Natarajan, K.A., 2015. Production and characterization of bioflocculants for mineral processing applications. *International Journal of Mineral Processing, 137,* pp.15–25.

Chapter 4 : ARTICLE 2: Optimization and Application of Bioflocculant Passivated Copper Nanoparticles in the Wastewater Treatment

Nkosinathi Goodman Dlamini [1]*, Albertus Kotze Basson [1] and Viswanadha Srirama Rajasekhar Pullabhotla [2]*

1 Department of Biochemistry and Microbiology, University of Zululand, Private Bag X1001, KwaDlangezwa 3886, South Africa; BassonA@unizulu.ac.za

[2]Department of Chemistry, University of Zululand, Private Bag X1001, KwaDlangezwa 3886, South Africa

***** Correspondence: nathidlamini03@gmail.com (N.G.D.); PullabhotlaV@unizulu.ac.za (V.S.R.P.); Tel.: +27-35-902-6155 (V.S.R.P.)

Received: 23 May 2019; Accepted: 13 June 2019; Published: 20 June 2019

Abstract: Nanotechnology offers a great opportunity for efficient removal of pollutants and pathogenic microorganisms in water. Copper nanoparticles were synthesized using a polysaccharide bioflocculant and its flocculation, removal efficiency, and antimicrobial properties were evaluated. The synthesized nanoparticles were characterized using thermogravimetric, UV-Visible spectroscopy, Fourier-transform infrared spectroscopy (FT-IR), powder X-ray diffraction, scanning electron microscope (SEM), and transmission electron microscope (TEM). The highest flocculation activity (FA) was achieved with the lowest concentration of copper nanoparticles (0.2 mg/mL) with 96% (FA) and the least flocculation activity was 80% at 1 mg/mL. The copper nanoparticles (CuNPs) work well without the addition of the cation as the flocculation activity was 96% and worked best at weak acidic, neutral, and alkaline pH with the optimal FA of 96% at pH 7. Furthermore, the nanoparticles were found to be thermostable with 91% FA at 100 °C. The synthesized copper nanoparticles are also high in removal efficiency of staining dyes, such as safranin (92%), carbol fuchsine (94%), malachite green (97%), and methylene blue (85%). The high removal efficiency of nutrients such as phosphate and total nitrogen in both domestic wastewater and Mzingazi river water was observed. In comparison to ciprofloxacin, CuNPs revealed some remarkable properties, as they are able to kill both the Gram-positive and Gram-negative microorganisms.

Keywords: copper nanoparticles; flocculation activity; removal efficiency; wastewater treatment

4.1 Introduction

Surface water has different constituents, which need to be removed for the supply of potable water systems. These constituents that need to be removed can be subdivided into colloidal solids, settleable suspended solids, and dissolved solids [1,2]. The treatment of drinking water mostly consists of flocculation, filtration, and disinfection processes. The dosing of a coagulant in water results in the destabilization of negatively charged particles, which results in bigger flocs through a flocculation process, which is known as coagulation [3]. Efficient flocculation is described as the gentle water movement, which results in the gathering of small flocs to form larger masses better suitable for removal by clarification and finally by filtration. Flocculation is an extensively used technology in wastewater treatment, due to its convenience, cheapness, energy-efficiency, easy running, and environmental friendliness [4]. In urban areas, atmospheric deposition, vegetation, and fertilizers are a primary source of nutrients. Nutrients load can also be significantly added through maintenance, construction, and soil management through the addition of fertilizer in the process of reviving injured vegetation [5]. Moreover, nitrogen can result in nitrate and nitrite ions that are part of the nitrogen cycle and occur naturally. Nitrite in excess concentrations can cause diseases. In fish, nitrites can produce a condition known as “brown blood disease” and in warm-blooded animals, it directly reacts with haemoglobin to produce methemoglobin [6].

Industrialization is good for the economic growth of any country. However, industrial growth in many instances produces a huge amount of waste, which ends up reaching the water bodies if untreated. The global growth of waste-producing industries is increasingly becoming a problem to the environment and it is a major contributing factor in water pollution [7]. Synthetic flocculants seem to be the only option. Some of these synthetic flocculants have been found to cause adverse effect to human health and the environment [8]. The process of using flocculants to aggregate and floc colloidal and freely suspended particles is called flocculation (IUPAC, 1997) [9]. Flocculants have various biotechnological applications in wastewater, drinking water treatment, the removal of dye solutions, inorganic solid suspensions, and industrial downstream processing [10]. There are inorganic flocculants, organic flocculants, and naturally occurring flocculants, such as polyaluminum chloride and polyacrylamide derivatives, respectively [2]. Naturally occurring flocculants are usually in a form of extracellular polymers (EPS) of proteins, glycoproteins, lipids, glycolipids, polysaccharides (such as cellulose), and nucleic acids [11]. Nanoparticles are part of an emerging field of

science that refer to the synthesis and development of numerous nanomaterials with size ranges of 1–100 nm [12]. Specifically, copper nanoparticles (CuNPs) have attracted a considerable amount of interest from researchers due to the properties they possess such as low production cost and antibacterial effectiveness. In comparison with precious metals, for instance, gold, silver, or palladium, copper nanoparticles have a high surface-area-to-volume ratio, catalytic activity, optical, and magnetic properties [13]. However, their immediate oxidation when exposed to air becomes the main challenge in their preparation and preservation. The synthesis of these materials in an inert atmosphere such as nitrogen or argon have been used by several researchers to overcome this problem. Reducing agents and capping agents that are used in the synthesis have been found to have toxic effects and are very expensive.

To overcome the toxicity resulting from the use of reducing agents, we synthesized CuNPs using a green and environmentally friendly route, in this synthesis; we have employed bioflocculant in the chemical reduction process. A bioflocculant can function both as a reducing and protecting agent for the copper nanoparticles. This makes the process nontoxic, economical, and friendly to the environment [14]. The current paper is aimed at the optimization and application of bioflocculant passivated copper nanoparticles in wastewater treatment. The impact imposed by chemicals in the treatment of water do not only affect animals and humans, but also has a negative impact on environment. The current study contributes towards an environmentally friendly and eco-efficient method with marginal safety to human and animal's health. The as-synthesized composite nanomaterial has shown its applications in the treatment of antibiotic resistant microorganism, dye degradation, and water treatment.

4.2 Materials and Methods

4.2.1 Synthesis of Copper Nanoparticles

In total, 3 mM copper sulphate solution was prepared in distilled water. After which, 0.5 g of pure bioflocculant was added and the mixture was shaken for 5–10 min in a shaking incubator at room temperature. The mixture was left standing for 24 hrs at room temperature and the resulting precipitate was collected by centrifugation at 8000 rpm for 15 min at 4 °C. The synthesis of copper nanoparticles was monitored through physical observation and characterization. Control was a copper sulphate solution without bioflocculant [15].

4.2.2 Characterization of As-Synthesized Copper Nanoparticles

Thermogravimetric analysis measurements were performed on the as-synthesized copper nanoparticles using a Perkin-Elmer Thermal Analysis Pyris 6 TGA (PerkinElmer, Inc., Waltham, Massachusetts 02451, USA). The nitrogen gas flow rate was maintained at 40 cc/min with ramping of the temperature from 22 to 900 °C at 10 °C /min. The optical measurements of the as-synthesized copper nanoparticles were carried out using Varian Cary 50 Conc UV–Vis spectrophotometer (Agilent Technologies, California 95051, USA). The UV-Vis analysis on the dilute samples of the nanoparticles were conducted using the wavelength region 300–700 nm operated using the 1 nm resolution and at room temperature conditions. Fourier transform-infrared (FT-IR) analysis was performed on the bioflocculant and as-synthesized nanoparticles using the Tensor 27, Bruker FT-IR spectrophotometer with a resolution of 4 cm^{-1} in the range of 4000–200 cm^{-1}. The pure dry samples were ground to fine powder and were used in the analysis to identify the functional groups present [15]. JEOL JSM-6100 microscope equipped with an energy-dispersive X-ray analyzer (EDX) (JEOL USA, Inc., Peabody, Massachusetts 01960, USA) was used for morphological study of the as-synthesized copper nanoparticles. The SEM images were taken using the Tungston (W) filament operated at an emission current of 100 µA and an accelerating voltage of 10 kV. The dry samples of small quantities were placed on copper stubs using double-sided carbon tape and coated with the carbon with the help of a JEOL vacuum evaporator. The working distance was maintained at 5–10 nm. JEOL JSM 6100 SEM with Bruker Quantax Esprit software (JEOL USA, Inc., Peabody, Massachusetts 01960, USA) was used for the EDX measurements. JEOL 1010 transmission electron microscope (JEOL USA, Inc., Peabody, Massachusetts 01960, USA) was used to obtain the TEM images. The specimens were prepared by placing a drop of diluted sample on the copper grid (150 mesh size). The samples were viewed at 100 kV accelerating

voltage and digital images were captured using Megaview III camera. Bruker D8 Advance diffractometer equipped with Cu-Kα radiation (λ= 1.5406 Å) was used to study the crystallinity of the as-synthesized copper nanoparticles. The dry powder samples were placed on the sample holder and diffraction patterns were recorded at room temperature using 40 kV and 40 mA [14].

4.2.3 Test for Flocculation Activity of Copper Nanoparticles

A solution of kaolin clay consisting of 4 g in 1 L distilled water was prepared. Then, 100 mL of the prepared solution was transferred into 3 separate 150 mL conical flask; thereafter, 2 mL (0.2 mg/mL) solution of the nanoparticles was added, 3 mL $CaCl_2$ (1%) solution was also added, and the mixture was shaken for 1 min and transferred to 100 mL graduated measuring cylinders. The mixture was left to stand for 5 min before supernatant was taken for analysis [16]. Flocculation activity was calculated according the following equation:

$$\text{Flocculation activity, } FA = \frac{[A-B]}{A} X\ 100 \quad (1)$$

A is optical density of control at 550 nm and B is optical density of sample at 550 nm.

4.2.4 Optimization of Copper Nanoparticles in Flocculation Activity

Different parameters such as dosage, cations, pH, temperature, and speed were evaluated for their effect on flocculation activity. For dosage effect, 0.2–1.0 mg/mL range was used, after obtaining the dosage that resulted in the maximum flocculation activity. Different cations were tested including monovalent, divalent, and trivalent cations. Furthermore, different pH was evaluated in the range of 3–12 and thereafter, the thermostability of the nanoparticles was evaluated in the temperature range of 50–100 °C. Finally, the effect of speed was conducted by varying speed from 0–220 rpm. These were all done to ascertain which conditions favor the optimal flocculation activity [17].

All data were collected in triplicates with mean and standard deviation values determined where differences were considered significant at 0.05 at confidence level ($p > 0.05$) by the use of Graph Pad Prism. Version 6 and data were analyzed using One-way of variances (ANOVA).

4.2.5 Removal Efficiency of Dyes by Copper Nanoparticles

Decolorization experiments were performed, where 1 mL of copper nanoparticles was added into a 50 mL dye solution (4 g/L), after which the mixture was shaken for a minute and was left to stand for 10 min at room temperature. Test dyes (g/L) included (safranin, methylene

blue, carbol fuchsine, malachite green). The supernatant was taken for analysis using UV-VIS Spectrophotometer after the mixture had been stirred for a minute and allowed to settle for 10 min. The absorbance of each sample was measured at the maximum wavelength of each dye. Decolorization efficiency was calculated using the formula below:

$$RE\ (\%) = \frac{[C0-C]}{C0}\ X\ 100 \qquad (2)$$

Where C0 is the initial value and C is the value after the flocculation treatment. Based on the initial and final dye concentrations, it is important to measure residual concentration of the dye in the samples after treatment [18].

4.2.6 Application of Nanoparticles in the Treatment of Wastewater

Wastewater samples were collected from the Vulindlela water treatment plant, Tendele coal mine, and Mzingazi River to ascertain removal efficiency (RE) of pollutants by nanoparticles in the water sample. NaOH or HCl was used for adjusting pH value when necessary. The wastewater sample was then poured into a 100 mL beaker and 2 mL of 0.2 mg/mL nanoparticles were added, and the mixture was stirred at the designed agitation speed for 10 min, and then allowed to stand for 30 min. The supernatant was taken for analysis using spectrophotometer at 680 nm and the residual Chemical oxygen demand (COD), Biochemical oxygen demand (BOD), total nitrogen, and phosphate were measured. To measure the total nitrogen, sulphate, COD, and BOD, test kits were used following manufacturer's protocol. The removal efficiency (RE) of the pollutants was calculated using a same equation as indicated above.

4.2.7 Antimicrobial Activity Test for Synthesized Nanoparticles

Test bacteria of choice were first resuscitated by inoculation into the sterile nutrient broth and incubated at 37 °C overnight. After which, 1 mL from each culture was inoculated into separate test tubes containing 9mLof sterile nutrient, the test tubes were labelled with *Escherichia coli*, *Bacillus pumilus*, *Citrobacter freundii,* and *Klebsiella pneumoniae*. The culture was then incubated overnight at 37 °C. The absorbance of each organism was then determined at 600 nm using a UV-visible spectrophotometer to ascertain the turbidity of each organism. The turbidity of all the organisms was then adjusted using fresh sterile nutrient broth to attain an absorbance of 0.1–0.5, which is within McFarland accepted standard.

4.2.7.1 Minimum Inhibitory Concentration (MIC)

A method described by Maliehe et al. [19] was adopted. The minimal inhibitory concentration (MIC) of the synthesized copper nanoparticles was determined. MIC is described as the lowest concentration of the CuNPs required to inhibit microorganisms. Quantitative determination of the synthesized nanoparticles was achieved through the use of 96-well plates. All the wells of the 96-well plates were inoculated with 50 µL of sterile nutrient broth. Then, 0.2 g of CuNPs was dissolved into 2 mL of distilled water. The solution of CuNPs (50 µL) was then poured into the first row of 96-well plates containing nutrient broth, and mixed. A 3-fold dilution was then performed whereby (50 µL) from row A was taken to row B of the 96-micro-well plates and it was mixed again, and another (50 µL) was taken from row B to other subsequent rows until all the wells had the CuNPs in different concentrations. The (50 µL) in the last column was discarded so that the total volumes of all the 96 wells is (50 µL). Selected bacteria strains were then added (50 µL) into corresponding wells. The antibiotic Ciprofloxacin (40%) was used as a positive control, while distilled water was used as a negative control. The plates were then incubated at 37 °C overnight. *P-iodonitrotetrazolium* violet (INT) solution was used as an indicator after the incubation period. Then, 40 µL of 0.2 mg/mL INT solution was added to each well and further incubated at 37 °C for 30 min. The presence of a reddish color indicated the reduction of INT to formazan by a metabolic active microorganism. The absence of the reddish colour (clear) was an indication of inactivity of microorganisms since INT was not broken down to form formazan. All the tests were conducted in triplicates and mean values were taken.

4.2.7.2. Minimum Bactericidal Concentration (MBC)

MBC was determined by using the agar dilution method. A loop full of the culture of each strain from the wells that indicated no colour change was streaked on a Muller Hilton nutrient agar. The plates were incubated at 37 °C for 12 hrs. The lowest concentration of CuNPs that exhibited the complete killing of the test organisms was considered as the MBC [20].

4.3 Results and Discussion

4.3.1 Characterization Results of Purified Bioflocculant and As-Synthesized Copper Nanoparticles

Three phases were noticed in the thermogravimetric analysis of as-synthesized copper nanoparticles. The first phase is observed from 40–120 °C due to the loss of moisture, the second phase appeared around 150–200 °C and could be attributed to the decomposition of polymer, and the third phase was observed at higher temperatures due to more weight loss from the samples [15]. The UV-Visible spectra of the bioflocculant and as-synthesized copper nanoparticles showed peak maxima at around 290–300 nm that could be ascribed to Cu nanoparticles formation [15]. Different functional groups viz., hydroxyl (-OH) group and amine (-NH2) group were present in the molecule representing the bands at 3276 cm^{-1} (bioflocculant) and 3408 cm^{-1} (copper nanoparticles). The weak band at 2182 cm^{-1} and the peak located at 1670 cm−1 in both samples indicates the aliphatic bonds and amide group. The presence vibrational band for Cu-O bonds can be observed at 596 cm^{-1}. The presence of saccharide derivatives can be observed as peaks between 1000–1100 cm^{-1} [15].

SEM-EDX results illustrated the presence of O, C, P, Ca, Cl, Na, K, Mg, and S elements in the purified bioflocculant. The presence of O, Cu, P, Mg, Ca, Cl, and S elements in the as-synthesized nanoparticles represent the passivation of the copper nanoparticles with the bioflocculant [15]. The SEM images shows the amorphous nature of the purified bioflocculant and copper nanoparticles. The larger particle sizes can be observed for the bioflocculant passivated copper nanoparticles. The copper nanoparticles appear to be close to spherical in shape and are aggregated [15]. The TEM image revealed the average particle size of 54 nm and close to spherical shape. The particle size was found to be ~53.56 nm using the Scherrer equation: $D = (K \lambda)/ (\beta \cos \theta)$ [15]. Powder X-ray diffraction patterns for as-synthesized copper nanoparticles showed the characteristic peaks at around 33° and 47° 2θ corresponding to (111) and (220) planes of the fcc structure, which are in good agreement with the copper standard (JCPDS 04-0836) [15]. Figures 4.1 and 4.2 show the TEM and SEM-EDX images of synthesized copper nanoparticles. From the TEM image, it is evident that as-synthesized copper nanoparticles were agglomerated and has close to spherical shape. The EDX results confirms the presence of copper in a sample, which is an indication that the bioflocculant could be used as a capping agent in nanoparticles synthesis. The detailed characterization results of the as-synthesized nanoparticles can be found elsewhere [15].

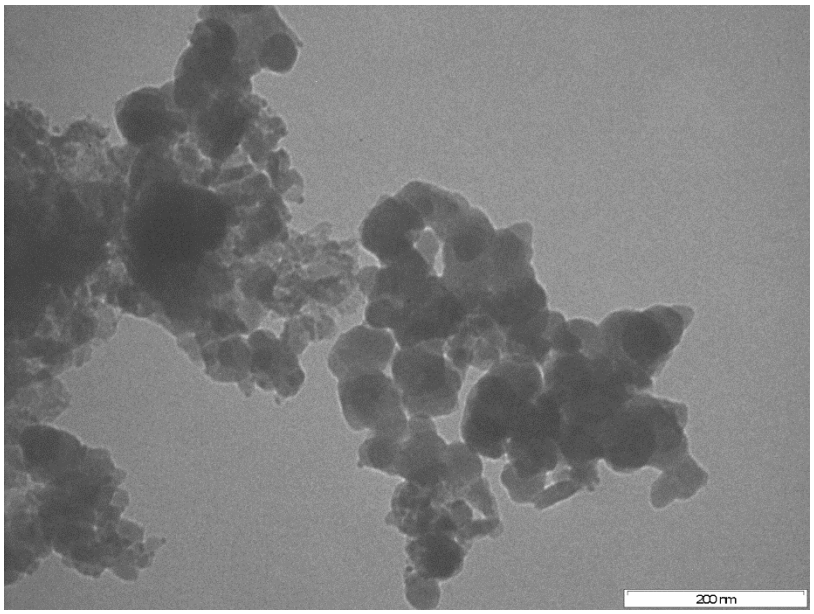

Figure 4.1: TEM (transmission electron microscope) image of as-synthesized copper nanoparticles at 200 nm scale.

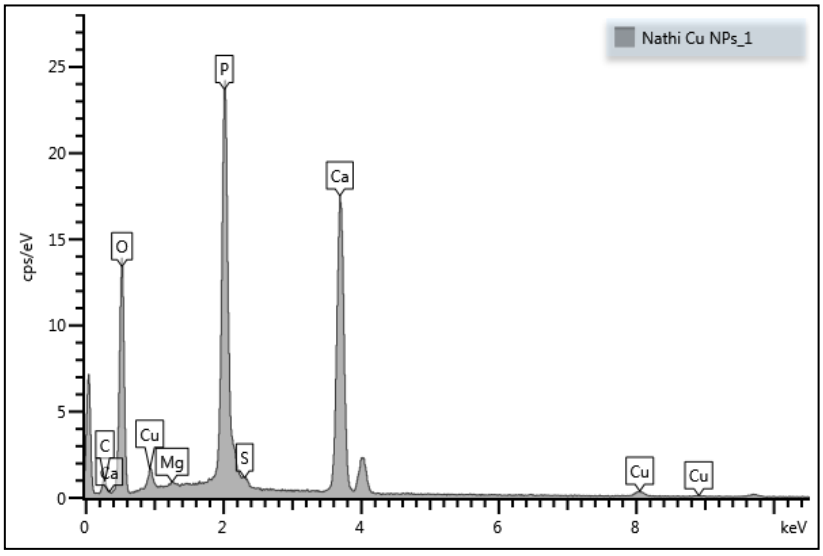

Figure 4.2: SEM-EDX (scanning electron microscope-energy-dispersive X-ray analyzer) image of as-synthesized copper nanoparticle.

4.3.2 Effect of Dosage on Flocculation Activity of Nanoparticles

Figure 4.3 represents the results obtained during the determination of the effect the copper nanoparticles concentration on flocculation activity. The flocculation activity of copper nanoparticles decreased proportionally with the increase in dosage concentration. The amount of nanoparticles powder required for optimal flocculation is called dosage size. The different concentration of copper nanoparticles (CuNPs) solution was prepared and its flocculation activity was evaluated. Various concentrations were prepared by dissolving different amounts

of CuNPs powder in the concentration of 0.2, 0.4, 0.6, 0.8, and 1 mg/mL in distilled water. Each of them dittos was dissolved in 50 mL distilled water. After which 1 L of kaolin clay solution was prepared whereby 4 g of kaolin clay powder was dissolved in a liter of distilled water. Three milliliters of 1% (w/v) CaCl2 and 2 mL of CuNPs solution was added into a 500 mL conical flask containing 100 mL of kaolin clay and then agitated for 1 min. The mixture was transferred to a graduated 100 mL measuring cylinder and left to stand for 5 min. The supernatant was taken for analysis in a spectrophotometer with a wavelength of 500 nm. As depicted in Figure 4.1, the nanoparticles flocculate best at a low dosage as the highest flocculation activity was achieved at 0.2 mg/mL with the flocculation activity of 96%. The increase in dosage concentration resulted in a decrease in flocculation activity. The highest flocculation activity was achieved at the lowest dosage of 0.2 mg/mL. According to Peng et al. [21], excessive addition of the flocculants results in destabilized kaolin particles suspension, which in turn results in repulsion of negatively charged kaolin particles. The increase in dosage concentration results into decrease in flocculation activity. This could be due to the blocking of the binding site of kaolin particles by the excess flocculating agent [20]. Most literature reports on the low dosage with the concentrations between 10–50 mg/L are more effective in flocculation activity [21]. Contrary to these findings, the bridging phenomena could not be effectively formed when the dosage of the bioflocculant was too low [22].

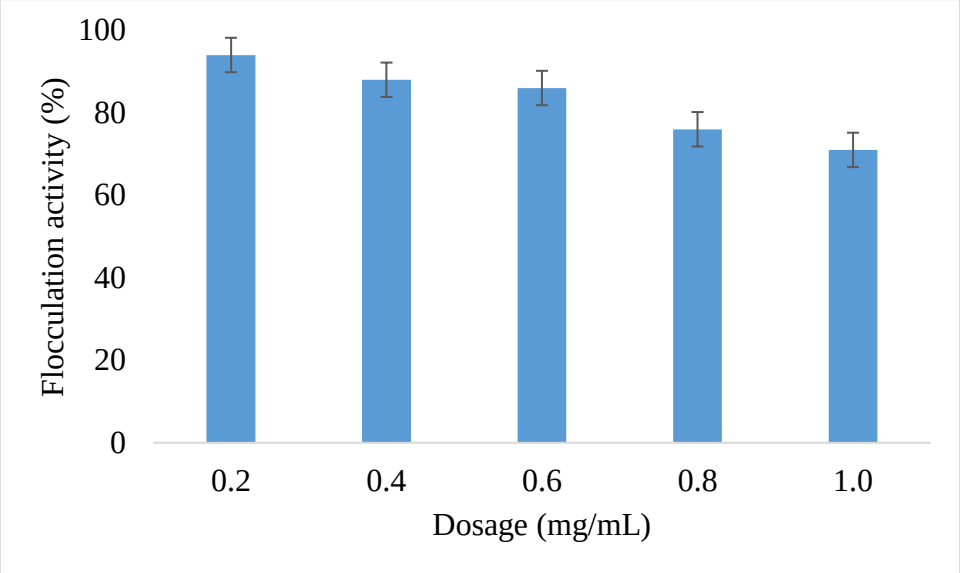

Figure 4.3: Effect of copper nanoparticles dosage on flocculation activity. (Refer to index data Table 4.3).

4.3.3 The Effect of pH on Flocculation Activity of Copper Nanoparticles

Figure 4.4 shows the effect of pH on flocculation activity of copper nanoparticles. CuNPs work best in weak acidic, neutral, and alkaline pH. Key factors that influence the flocculation process include the pH of the reaction mixture [23]. The flocculant charge status and surface characteristics of the colloidal particles may be altered by pH, which in turn may affect flocculating efficiency [24]. Different flocculants have been reported to produce flocculating efficiency with optimal activity at varying pH values. NaOH and HCl were used to adjust kaolin solution's pH whenever it was necessary. Figure 4.4 shows a strong flocculation activity that can be observed over a wide range of pH 3–12. The maximum flocculation activity of 96% was achieved at neutral pH 7 implying that the adjustment of pH would not be necessary for achieving high flocculation with these nanoparticles. However, at acidic pH, low flocculation activity was observed (55% at pH 3). This might be due to the bioflocculant, which showed different electric states at different pH, thus affecting the bridging efficiency of the bioflocculant for clay powder [25]. At alkaline pH, the flocculation activity remained constant from pH 10–12 with flocculation activity above 75%. A method described by Yu-sen et al. [26] was adopted to ascertain the presence of copper ions in the flocculated water sample; whereby, 50 mL of flocculated sample was centrifuged at 4000 rpm for 30 min. Subsequently, 50 mL of the supernatant containing soluble copper was removed 0.05 M of ammonium was added and there was no presence of blue precipitate observed, which indicated the absence of copper ions.

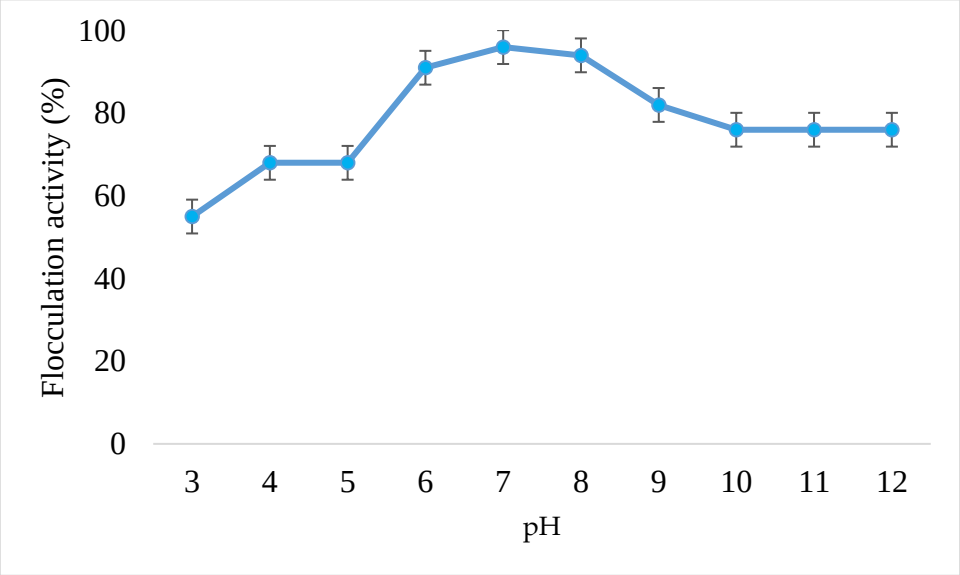

Figure 4.4: Effect of pH on the flocculation activity of synthesized copper nanoparticles. (Refer to index data Table 4.4).

4.3.4 The effect of cations on flocculation activity of copper nanoparticles

Table 4.1 represents the results obtained during the determination of the effect of cations on flocculation activity of CuNPs. Synthesized CuNPs are cations independent as the flocculation activity was above 95% without addition of cations.

Table 4.1: Effect of cations on flocculation activity of CuNPs.

Cations	Flocculation activity (%) ± SD
Control	96±2.08
Fe^{3+}	86±3.74
Mn^{2+}	97±1.52
Ba^{2+}	95±3.46
K^{+}	96±2.88
Li^{+}	97±1.15
Na^{+}	86±1.15

Values represent mean ± deviation of replicate readings. (Refer to index data Table 4.5).

The effect of cations on flocculation activity of CuNPs was investigated and all cations enhanced the flocculation activity. The synthesized copper nanoparticles without the addition of cations control was the second highest with a flocculation activity of 96%. According to a study conducted by Li et al. [27] trivalent, divalent, and monovalent cations have stimulated the adsorption of bioflocculant on the suspended kaolin particles by decreasing the negative charge of both the polymer and particles. This stimulation process of flocculation activity was observed in a bioflocculant produced by Bacillus licheniforms and Bacillus circulans when Al^{3+} and Ca^{2+} were used [28]. Cations neutralize and stabilize the negative charge of the functional groups of colloidal kaolin particles in solution and the bioflocculant [27]. Synthesized copper nanoparticles are more effective without the addition of cation with 96% flocculation activity. This makes the synthesized nanoparticles commercially valuable.

4.3.5 The Temperature Effect on Flocculation Activity of Copper Nanoparticles

Figure 4.5 shows the effect of temperature on flocculation activity of copper nanoparticles. CuNPs were found to be heat stable with a flocculation activity above 90%.

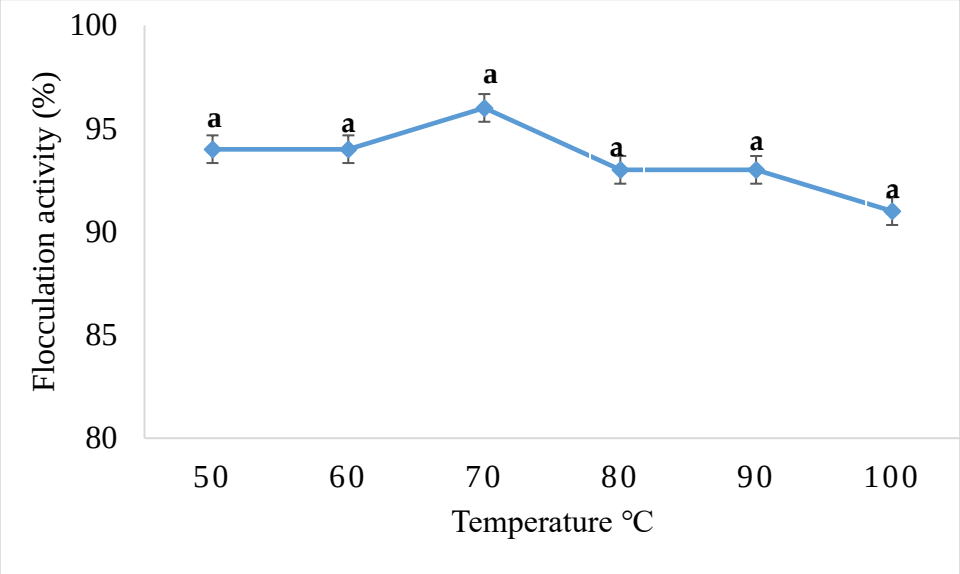

Figure 4.5: Effect of temperature on flocculation activity of CuNPs. Percentage flocculating activities with letter (a) are significantly ($p < 0.05$). (Refer to index data Table 4.6).

The relationship between temperature and flocculating efficiency of the synthesized nanoparticles was examined at a temperature range from 50–100 °C [29]. The synthesized nanoparticles were subjected to different temperatures using a water bath for 30 min; this was done to ascertain its stability when subjected to higher temperatures. The synthesized nanoparticles retained over 90% flocculation activity, suggesting that the nanoparticles were very stable. The highest flocculation activity was achieved below 70 °C, increase in temperature resulted in slightly decreased flocculating efficiency, but the difference was not significant in terms of statistical analysis. Therefore, it was deduced that the nanoparticles were thermo-stable, and its flocculation activity was not affected when the temperature was elevated. The presence of protein or peptide in the structure of a bioflocculant was generally linked to its sensitivity to heat, while sugars containing bioflocculants were more heat resistant. It can be concluded that the bioflocculant from which the nanoparticles were synthesized contains more sugar than protein [30]. The thermal stability of the synthesized nanoparticles may be due to the hydroxyl group found in the bioflocculant that is responsible in the formation of hydrogen bonds in its structure [9].

4.3.6 The Effect of Shaking Speed on Flocculation Activity of Copper Nanoparticles

Figure 4.6 shows the effect of shaking speed on flocculation activity of copper nanoparticles. Speed is one of the parameters, which influences flocculation activity. Synthesized CuNPs work well in all ranges of speed evaluated. The agitation effect on flocculation activity was assed using a shaking incubator. The solution of 100 mL kaolin clay was mixed with 2 mL copper nanoparticles, the mixture was placed inside the shaking incubator for 1 min at different speeds, and flocculation activity was measured. The highest flocculation activity was observed at 220 rpm. However, the nanoparticles worked effectively without agitation with 88% flocculation activity, which indicates that the synthesized nanoparticles can work well without agitation.

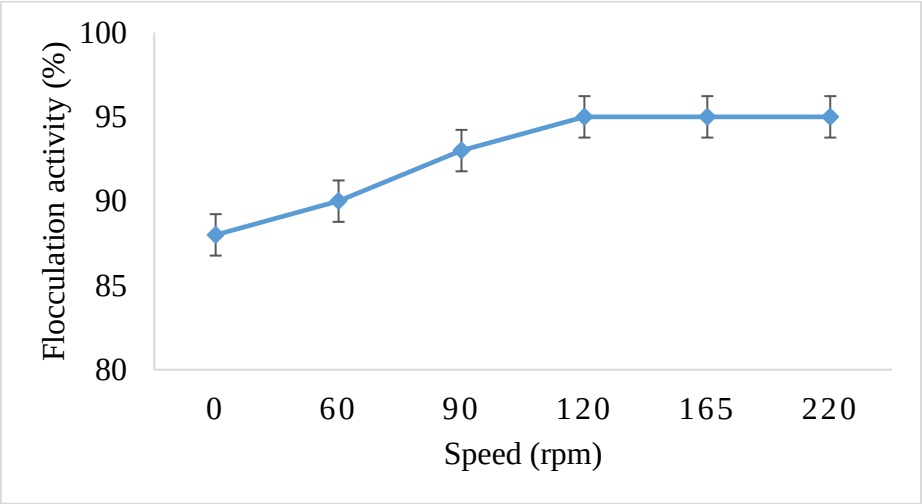

Figure 4.6: Effect of agitation speed on flocculation activity of CuNPs. (Refer to index data Table 4.7).

4.3.7 The Effect of Copper Nanoparticles on Staining Dye Removal

Figure 7 illustrates effect of copper nanoparticles on staining dye removal. The synthesized nanoparticles have a high affinity for all examined dyes with removal efficiency above 85%. These copper nanoparticles are effective to remove dyes in wastewater from different industries like the clothing industries.

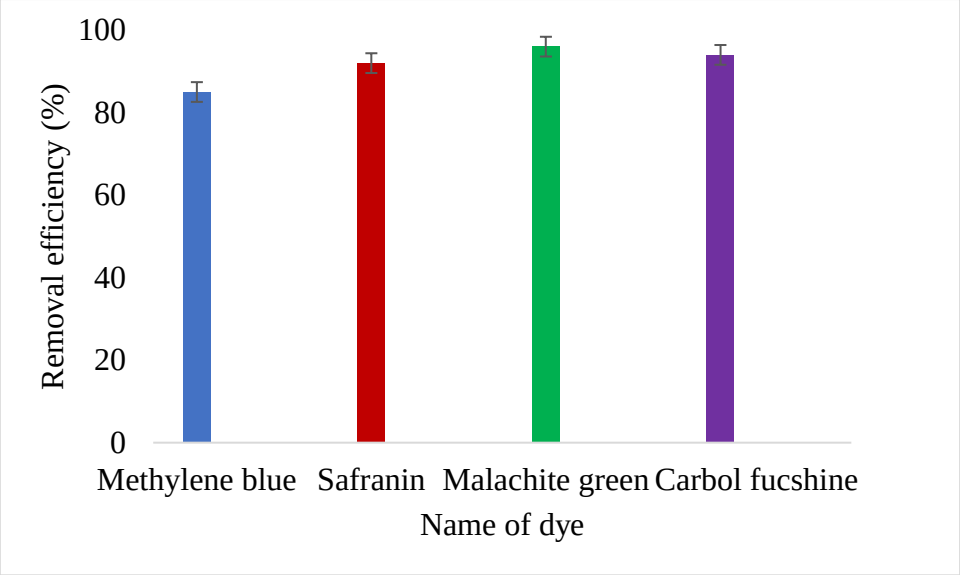

Figure 4.7: Effect of copper nanoparticles on staining dye removal. (Refer to index data Table 4.8).

The dye removal potential of copper nanoparticles synthesized from a bioflocculant was investigated. Synthesized nanoparticles were able to remove all different dyes. This could be attributed to the aggregation of particles due to bridging and charge neutralization as reported previously [31]. When the particles extend from the surface into a solution for a distance greater than the distance over which the antiparticle repulsion acts, bridging occurs. The synthesized nanoparticles possess huge potential for removing stain in all dyes that were tested. Concentration of nanoparticles remained constant (0.2 mg/mL) and this demonstrated the nanoparticles were effective because removal efficiency was above 80% in all removal efficiency was above 80% in all dyes without the addition of cations. This was contrary to the findings reported by Deng et al. [32] where the removal efficiency of dyes directly depended on high concentrations of the bioflocculant. The functional groups present in the polymer must be able to interact with sites on the surface of the colloidal particle in order to be effective [29].

Table 4.2: Removal of pollutants in different water samples by copper nanoparticles

Table 4.2 shows the removal of nutrients (nitrate, phosphate, and total nitrogen), metals (aluminium and sulphate), and BOD and COD in coal mine wastewater, domestic wastewater, and Mzingazi river water. The nanoparticles showed some remarkable properties for pollutants removal.

Flocculant	Types of wastewater	Types of pollutants in water	Water quality before treatment (mg/L)	Water quality after treatment (mg/L)	Removal efficiency (%)
CuNPs	Coal mine water	Phosphate	2.00	0.3	85
		Sulphate	0.55	0.13	76
		COD	154	11.2	93
		BOD	123.2	5.0	96
	Domestic wastewater	Phosphate	7.6	1.5	80
		Total nitrogen	155	17.0	89
		Nitrate	20.6	7.7	63
		Aluminium	0.86	0.33	62
		Sulphate	1.7	0.61	64
		COD	2.313	0.654	72
		BOD	123.2	4.123	96
	Mzingazi River water	Phosphate	85.7	7.521	92
		Total nitrogen	0.223	0.108	52
		COD	3.300	0.278	92
		BOD	133	15.0	89

4.3.8 Removal Efficiency of Pollutants in Wastewater

In Table 4.2 above, copper nanoparticles showed the ability to remove P and S in coalmine water. A water sample from a local coalmine was used to ascertain the removal efficiency of synthesized copper nanoparticles. Elements such as P and S were tested. The synthesized copper nanoparticles showed some remarkable ability to remove these elements. The results suggest that copper nanoparticles can be a suitable alternative to replace chemical flocculants. The bioflocculant-passivated nanoparticles provide properties such as degradability and friendliness to the environment that the chemical flocculants lack. High levels of COD and BOD in water do not support aquatic life [33]. The presence of N, P, and S in high concentrations in water prompt eutrophication. The application of copper nanoparticles for removal of these pollutants from domestic wastewater, coalmine water, and industrial wastewater was determined. The synthesized nanoparticles had the best removal efficiency for COD and BOD with 93% and 96% removal efficiency, respectively, contrary to the polyamine flocculants, which could remove up to 89% of COD in dye wastewater [2]. The removal efficiency of the copper nanoparticles could be attributed to the surface structure, chemical components, and functional groups. The findings suggest that the synthesized copper nanoparticles possess high potential for industrial application. Furthermore, the effectiveness of CuNPs recommends that they also have the potential to reduce the adverse effects of chemical flocculants being used. The ability of CuNPs to reduce the tested water quality parameters signifies their multi-functionality. Over the years, there has been a significant increase in nutrients in lakes in response due to the increased discharge of domestic wastewater, pollution from agricultural practices and urban development [33]. Nutrients enrichment, especially nitrate and nitrogen has been considered as the main threat to marine water. This may result in eutrophication, which, in turn, affects the cost of producing potable water. The synthesized copper nanoparticles had effectively removed aluminium, nitrate, and total nitrogen in domestic wastewater. The bioflocculant could not effectively remove these pollutants in wastewater, therefore it can be concluded that copper nanoparticles are more effective. As depicted in Table 4.2, the synthesized nanoparticles were found to be most effective in BOD removal in domestic wastewater with 96% removal efficiency. Varying amounts of phosphate can be considered as a result of washing, from farm soil to waterbodies. The presence of phosphate in water stimulates the growth of aquatic plants and plankton, which provide food for fish and this increased growth may increase the population growth of fish and improve overall water quality. Even so, excess of phosphate may cause wild growth of aquatic

plants and algal; this may, in turn, result in eutrophication or over-fertilization of receiving waters. As a result, eutrophication or over-fertilization may cause the decay of vegetation and quality of life due to decreased dissolved oxygen levels. Toxicity of phosphate to people and animals could occur from an extremely high levels of phosphate [33]. Table 4.2 shows the ability of nanoparticles to remove phosphate in the Mzingazi River. The copper nanoparticles had a removal efficiency below 40% when it was tested as per the test kit manufacturer's protocol. However, when it was left standing for a week, there was a drastic increase in phosphate removal up to 90% as depicted in Table 4.2. These results suggest that contact time is an important factor in the efficiency of nanoparticles. Eutrophication continues to be the primary concern for water quality and phosphorus and nitrogen are the primary nutrients implicated in eutrophication [34]. As can be seen from the results, the copper nanoparticles could remove up to 52% of total nitrogen.

4.3.9 Minimal Inhibitory Concentration, Minimal Bactericidal Concentration in mg/mL for Copper Nanoparticles

Table 4.3 shows the MIC and MBC of the synthesized copper nanoparticles in comparison with the ciprofloxacin. The synthesized nanoparticles showed some remarkable properties against both Gram-positive and Gram-negative organisms; the least MIC and MBC was observed against *B. pumilus and E. coli.*

Table 4.3: Minimal inhibitory concentration, minimal bactericidal concentration in mg/ml for copper nanoparticles.

	Ciprofloxacin		CuNPs	
Strains of bacteria	MIC	MBC	MIC	MBC
B. pumilus	-	-	3.13	6.25
E. coli	3.125	6.25	6.25	12.5
A. freundii	1.56	3.13	12.5	12.5
K. pneumoniae	1.56	3.13	12.5	25.0

Copper nanoparticles were evaluated for their antimicrobial effect in comparison with ciprofloxacin, which was used as a control for the experiment. Further, 20 µL ciprofloxacin was used and all the Gram-negative organisms show the inhibitory effect of ciprofloxacin. However, *B. pumilus,* which is Gram-positive, could still grow in the presence of both low and high concentration of ciprofloxacin. On the other hand, copper nanoparticles showed some remarkable properties for inhibiting and killing both the Gram-positive and Gram-negative

organisms. In addition, 96-well microplate technique was used, against four strains of both Gram-positive and Gram-negative pathogenic organisms. The antimicrobial effect of copper nanoparticles was found to be more prominent on Gram-negative organisms and remarkable properties against Gram-positive were observed, where *B. pimillus* had low MIC of 3.13 mg/mL concentration. Gram-positive bacteria lack the outer membrane and the constituents of the CuNPs are directly in contact with the phospholipid bilayer of the cell [18].

4.4 Conclusions

The synthesized copper nanoparticles showed an excellent flocculation property at a low concentration of 0.2 mg/mL. They flocculate independent of cation, are thermostable, and work at weak acidic, neutral, and alkaline pH. Agitation (shaking speed) is not required for the effectiveness of the synthesized nanoparticles in flocculation. They possess great properties for pollutants removal in coal mine water, domestic wastewater, and river water. Over 89% of COD and BOD removal efficiency was observed for both the coal mine and river water. Furthermore, they are able to remove staining dyes at a low concentration of 0.2 mg/mL and 10 min contact time. The remarkable properties for the removal of staining dyes suggest that the synthesized nanoparticles can be used in removing dye effluents from wastewater. When evaluated for antimicrobial activity against both Gram-negative and Gram-positive bacteria, they were able to inhibit and kill all the tested strains at the lowest concentration of 3.13 mg/mL.

Author Contributions: Conceptualization, A.K.B. and V.S.R.P.; formal analysis, N.G.D. and V.S.R.P.; investigation, N.G.D.; supervision, A.K.B. and V.S.R.P.; writing—original draft, N.G.D.; writing—review and editing, V.S.R.P.

Funding: National Research Foundation (NRF, South Arica) for the financial support in the form of the Incentive Fund Grant (Grant No: 103691).

Acknowledgments: Nkosinathi Dlamini would like to acknowledge the Council for Scientific and Industrial Research (CSIR, South Africa) for the financial assistance in the form of the Ph.D. bursary. The authors would like to acknowledge the Electron Microscopy Unit at the University of KwaZulu-Natal, Westville campus, for providing support by letting us use the TEM and SEM-EDX facilities for the characterization of nanomaterials. Rajasekhar Pullabhotla would like to acknowledge the National Research Foundation (NRF, South Arica) for the financial support in the form of the Incentive Fund Grant (Grant No: 103691).

Conflicts of Interest: The authors declare that there is no conflict of interest.

4.5 References

1. Naidoo, S.; Olaniran, A. Treated wastewater e_uent as a source of microbial pollution of surface water resources. Int. J. Environ. Res. Public Health **2014**, 11, 249–270. [CrossRef] [PubMed]

2. Yue, Q.Y.; Gao, B.Y.;Wang, Y.; Zhang, H.; Sun, X.;Wang, S.G.; Gu, R.R. Synthesis of polyamine flocculants and their potential use in treating dye wastewater. J. Hazard. Mater. **2008**, 152, 221–227. [CrossRef] [PubMed]

3. Renault, F.; Sancey, B.; Badot, P.; Crini, C. Chitosan for coagulation/flocculation processes—An eco-friendly approach. Eur. Polym. J. **2009**, 45, 1337–1348. [CrossRef]

4. Ma, J.; Shi, J.; Ding, L.; Zhang, H.; Zhou, S.; Wang, Q.; Fu, X.; Jiang, L.; Fu, K. Removal of emulsified oil from water using hydrophobic modified cationic polyacrylamide flocculants synthesized from low-pressure UV initiation. Sep. Purif. Technol. **2018**, 197, 407–417. [CrossRef]

5. Kumar, M.; Puri, A. A review of permissible limits of drinking water. Indian J. Occup. Environ. Med. **2012**, 16, 40.

6. Davis, A.P.; Shokouhian, M.; Sharma, H.; Minami, C. Water quality improvement through bioretention media: Nitrogen and phosphorus removal. Water Environ. Res. **2006**, 78, 284 293. [CrossRef]

7. Agrawal, A.; Sahu, K.; Pandey, B. Solid waste management in non-ferrous industries in India. Resour. Conserv. Recycl. **2004**, 42, 99–120. [CrossRef]

8. Okaiyeto, K.; Nwodo, U.U.; Okoli, S.A.; Mabinya, L.V.; Okoh, A.I. Implications for public health demands alternatives to inorganic and synthetic flocculants: Bioflocculants as important candidates. Microbiol. Open **2016**, 5, 177–211. [CrossRef]

9. Ugbenyen, A.; Okoh, A. Characteristics of a bioflocculant produced by a consortium of Cobetia and Bacillus species and its application in the treatment of wastewaters. Water SA **2014**, 40, 140–144. [CrossRef]

10. Thakur, V.; Singha, A.; Thakur, M. Surface modification of natural polymers to impart low water absorbency. Int. J. Polym. Anal. Charact. **2012**, 17, 133–143. [CrossRef]

11. Zhang, C.-L.; Cui, Y.-N.;Wang, Y. Bioflocculant produced from bacteria for decolorization, Cr removal and swine wastewater application. Sustain. Environ. Res. **2012**, 22, 129–134.

12. Gharge, V.G.; Gore, M.M. and Yadav, A. Di_erent techniques for preparation of nanoemulsion with characterisation and various application of it—A review. World J. Pharm. Res. **2017**, 15, 112–128. [CrossRef]
13. Kanhed, P.; Birla, S.; Gaikwad, S.; Gade, A.; Seabra, A.B.; Rubilar, O.; Duran, N.; Rai, M. In vitro antifungal efficacy of copper nanoparticles against selected crop pathogenic fungi. Mater. Lett. **2014**, 115, 13–17. [CrossRef]
14. Sathiyanarayanan, G.; Kiran, G.S.; Selvin, J. Synthesis of silver nanoparticles by polysaccharide bioflocculant produced from marine Bacillus subtilis MSBN17. Colloids Surf. B Biointerfaces **2013**, 102, 13–20. [CrossRef]
15. Dlamini, N.G.; Basson, A.K.; Pullabhotla, V.S.R.R. Biosynthesis and characterization of copper nanoparticles using a bioflocculant extracted from Alcaligenes faecalis HCB2. Adv. Sci. Eng. Med. **2019**, 11, 1–7. [CrossRef]
16. Xia, X.; Lan, S.; Li, X.; Xie, Y.; Liang, Y.; Yan, P.; Chen, Z.; Xing, Y. Characterization and coagulation-flocculation performance of a composite flocculant in high-turbidity drinking watertreatment. Chemosphere **2018**, 206, 701–708. [CrossRef]
17. Agunbiade, M.; Pohl, C.; Ashafa, O. Bioflocculant production from Streptomyces platensis and its potential for river and waste water treatment. Br. J. Microbiol. **2018**. [CrossRef]
18. Buthelezi, S.P.; Olaniran, A.O.; Pillay, B. Textile dye removal from wastewater e_uents using bioflocculants produced by indigenous bacterial isolates. Molecules **2012**, 17, 14260–14274. [CrossRef]
19. Maliehe, S.; Shandu, S.J.; Basson, K.A. The antibacterial and antidiarreal activities of the crude methanolic Syzygium cordatum [S. Ncik, 48 (UZ)] fruit pulp and seed extracts. J. Med. Plants Res. **2015**, 9, 884–891. [CrossRef]
20. Elo, J.N. A sensitive and quick microplate method to determine the minimal inhibitory concentration of plant extracts for bacteria. Planta Med. **1998**, 64, 711–713. [CrossRef]
21. Peng, L.; Yang, C.; Zeng, G.; Wang, L.; Dai, C.; Long, Z.; Liu, H.; Zhong, Y. Characterization and application of bioflocculant prepared by Rhodococcus erythropolis using sludge and livestock wastewater as cheap culture media. Appl. Microbiol. Biotechnol. **2014**, 98, 6847–6858. [CrossRef]
22. Gao, J.; Bao, H.Y.; Xin, M.X.; Liu, Y.X.; Li, Q.; Zhang, Y.F. Characterization of a bioflocculant from a newly isolated Vagococcus sp. W31. J. Zhejiang Univ. Sci. B **2006**, 7, 186–192. [CrossRef]

23. Gong, W.-X.; Wang, S.-G.; Sun, X.-F.; Liu, X.-W.; Yue, Q.-Y.; Gao, B.-Y. Bioflocculant production by culture of Serratia ficaria and its application in wastewater treatment. Bioresour. Technol. **2008**, 99, 4668–4674. [CrossRef]
24. Zaki, S.A.; Elkady, M.F.; Farag, S.; Abd-El-Haleem, D. Characterization and flocculation properties of a carbohydrate bioflocculant from a newly isolated Bacillus velezensis 40B. J. Environ. Biol. **2013**, 34, 51.
25. Wang, L.; Ma, F.; Qu, Y.; Sun, D.; Li, A.; Guo, J.; Yu, B. Characterization of a compound bioflocculant produced by mixed culture of Rhizobium radiobacter F2 and Bacillus sphaeicus F6. World J. Microbiol. Biotechnol. **2011**, 27, 2559–2565. [CrossRef]
26. Yu-sen, E.L.; Vidic, R.D.; Stout, J.E.; Victory, L.Y. Negative e_ect of high pH on biocidal e_cacy of copper and silver ions in controlling Legionella pneumophila. Appl. Environ. Microbiol. **2002**, 68, 2711–2715.
27. Li, Y.; Xu, Y.; Liu, L.; Jiang, X.; Zhang, K.; Zheng, T.; Wang, H. First evidence of bioflocculant from Shinella albus with flocculation activity on harvesting of Chlorella vulgaris biomass. Bioresour. Technol. **2016**, 218, 807–815. [CrossRef]
28. Liu,W.;Wang, K.; Li, B.; Yuan, H.; Yang, J. Production and characterization of an intracellular bioflocculant by Chryseobacterium daeguense W6 cultured in low nutrition medium. Bioresour. Technol. **2010**, 101, 1044–1048. [CrossRef]
29. Aljuboori, A.H.R.; Idris, A.; Al-joubory, H.H.R.; Uemura, Y.; Abubakar, B.I. Flocculation behavior and mechanism of bioflocculant produced by Aspergillus flavus. J. Environ. Manag. **2015**, 150, 466–471. [CrossRef]
30. Sun, J.; Zhang, X.; Miao, X.; Zhou, J. Preparation and characteristics of bioflocculants from excess biological sludge. Bioresour. Technol. **2012**, 126, 362–366. [CrossRef]
31. Salehizadeh, H.; Shojaosadati, S. Extracellular biopolymeric flocculants: Recent trends and biotechnological importance. Biotechnol. Adv. **2001**, 19, 371–385. [CrossRef]
32. Deng, S.; Yu, G.; Ting, Y.P. Production of a bioflocculant by Aspergillus parasiticus and its application in dye removal. Colloids Surf. B Biointerfaces **2005**, 44, 179–186. [CrossRef]
33. Tiwary, R. Environmental impact of coal mining on water regime and its management. Water Air Soil Pollut. **2001**, 132, 185–199. [CrossRef]
34. Gao, C.; Zhu, J.; Zhu, J.; Gao, X.; Dou, Y.; Hosen, Y. Nitrogen export from an agriculture watershed in the Taihu Lake area, China. Environ. Geochem. Health **2004**, 26, 199–207. [CrossRef]

Chapter 5 : ARTICLE 3: Biosynthesis of bioflocculant passivated copper nanoparticles, characterization and application

Nkosinathi Goodman Dlamini[a] *, Albertus Kotze Basson [a], Viswanadha Srirama Rajasekhar Pullabhotla [b], Jean Simonis[c]

[a] Department of Biochemistry and Microbiology, University of Zululand, Private Bag X1001, KwaDlangezwa, 3886, South Africa

[b] Department of Chemistry, University of Zululand

[c] Department of Hydrology, University of Zululand

*Correspondence: E-Mail nathidlamini03@gmail.com (N.G.D.);
PullabhotlaV@unizulu.ac.za (V.S.R.P.)
Tel. +27 35 902 6155 (V.S.R.P.)

Abstract: Bioflocculant capped copper nanoparticles (CuNPs) were successfully synthesized through the reduction of copper sulphate solution by the bioflocculant. The synthesize nanoparticles were verified by Scanning electron microscope equipped with elementary detector (SEM), X-ray diffractometer (XRD), Fourier Transform Infrared Spectrophotometer (FT-IR), Transmission electron microscopy (TEM), Thermogravimetric analysis (TGA) and UV spectroscope. CuNPs were applied in the treatment of both the domestic and industrial wastewater, removal of dyes and were confirmed for the antimicrobial effect against both Gram negative and Gram-positive microorganisms. The synthesized nanoparticles showed great potential for industrial application when compared to the chemical flocculant. The highest flocculating activity and removal efficiency was observed at the lowest dosage of 0.2 mg/mL. Moreover, both the Minimal inhibitory concentration (MIC) and Minimal bactericidal concentration (MBC) were observed at the concertation of 12.5 µL.

Keywords: Bioflocculant, Synthesis, Characterization, Antimicrobial activity, Removal efficiency

5.1 Introduction

Metallic nanoparticles utilization in numerous medical applications and biotechnological applications represent the most studied area of the nanomaterial science (Kaur et al., 2015). A major problem in the world is environmental pollution (Prasertsan et al., 2006). The environment, human and aquatic animals are in serious threat due to discharges of wastes from households and industries into the various water bodies without proper treatment (Zaki et al., 2014). In various industrial processes, flocculants are therefore, frequently used for the aggregation of cellular materials and colloidal substances (Salehizadeh and Shojaosadati, 2001).

Water cause about 80% of infections in developing countries and approximately a billion people have no access to clean to water facilities. Industrial effluents results into a loss of many lives as a result of waterborne diseases and cancer (Tiwari et al., 2008). Flocculation is the process which is applied in wastewater treatment, coal bioprocessing and downstream processing in fermentation (Fujita et al., 2000). Leading role in flocculation processes have been played by traditional flocculants, such as polyaluminium chloride, aluminium sulphate and polyacrylamide flocculants due to their good flocculating activity and low cost (He et al., 2010, Cosa et al., 2011, Mabinya et al., 2012). Nonetheless, the detrimental health problems such as cancer, neurodegradation (Alzheimer's disease) and neurotoxicity have been linked to this flocculants has led to search for alternatives (Rudén, 2004, Nontembiso et al., 2011). Moreover, ban has been place by some developed countries over the use of hazardous flocculants (Xiong et al., 2010).

With the emerging of antibiotic resistant microorganisms, and with the ever increasing health cost, researchers are searching for new, low cost and effective antimicrobial agents (Ashajyothi et al., 2016). The emerging area of research is use of nanoparticle-based antimicrobial agents due to its broad spectrum activity compare to drugs (Durán et al., 2010). Synthetic dyes from text tile industries cause pollution to water bodies and have negative impact to human life because of the carcinogenic nature they possess (Li et al., 2008). For this reason, it is imperative to remove dyes from water to protect the aquatic environment and human. Application of nanoparticles with high removal efficiency is considered one of the promising methods for dye removal (Khan et al., 2017).

5.2 Material and Methods

5.2.1 Materials

The bioflocculant was extracted from an isolate, which was previously isolated from the marine environment and was identified as *Alcaligenes faecalis* through Inqaba Biotec, South Africa. The bioflocculant production medium was prepared in accordance to a description by Maliehe et al. (2016) and it was composed of glucose (20 g), $MgSO4{\cdot}7H_2O$ (0.2 g), (NH4)2SO4 (0.2 g), K_2HPO4 (5 g), urea (0.5 g), yeast extract (0.5 g) and KH_2PO4 (2 g) in a litre of filtered seawater at pH 8 and sterilized by autoclaving at 121 °C for 15 min. After autoclave, the medium was then allowed to cool and was inoculated with fresh culture, which was resuscitated the previous day. The broth was then incubated in a shaking incubator for 72 hrs at 30 °C at a speed of 165 rpm (Maliehe et al., 2016).

5.2.2 Extraction and purification of the bioflocculant

Extraction and purification of the bioflocculant was done following a description by Okaiyeto et al. (2013) where the culture broth was taken out after 72 hrs of growth and centrifuged at 4,000 rpm at 4 °C for 30 min. This was done in order to remove cells and insoluble substances. The supernatant was then transferred into a clean container and the cells were discarded. 1 litre of distilled water was then added into the supernatant and was centrifuged again at 4 °C for 15 min. Two volumes of ethanol were added to the supernatant, agitated and the solution was stored at 4 °C for 12 hrs. After 12 hrs the precipitate was vacuum-dried and 100 mL of distilled water was added. A mixture of chloroform and *n*-butyl (5:2 v/v*)* was also added. After stirring, the mixture was left to stand for 12 hrs at room temperature. The supernatant was then vacuum-dried in order to obtain a purified bioflocculant (Okaiyeto et al., 2013).

5.2.3 Synthesis of copper nanoparticles

The synthesis of copper nanoparticles was achieved using a method described by Dlamini et al. (2019) with some minor modifications; 0.5 g of purified bioflocculant was added into a 200 mL solution of 3 mM $CuSO_4$. The mixture was agitated until a homogenous solution was achieved. Foil was then used to cover the mouth of the conical flask containing the solution, prevent the interference of foreign material. The solution was left unstirred at room temperature for 24 hrs. The bioflocculant solution was used as a control for this experiment and synthesis of nanoparticles was confirmed through physical observation and characterization, after 24 hrs. A blue precipitate was observed and the synthesized nanoparticles were collected using

centrifuge at 4 °C, 4000 rpm for 30 min. and vacuum-dried overnight and sample stored for characterization (Dlamini et al., 2019b).

5.2.4 Characterization of copper nanoparticles

SEM was used for better image at 1000 keV i.e. wavelengths of resolution. Morphology and elementary analysis of the synthesized nanoparticles was determined using scanning electron microscope equipped with elementary detector (SEM-Sipma-VP-03-67). BRUKER D8 Advance X-Ray Diffractometer operated at 40 kV, 40 mA, with copper monochromatized CuKα1 radiation of wavelength λ=1.5406 Å was used to investigate the phase composition and crystallinity of the bioflocculant. XRD was recorded in the 2θ range from 20° to 80° at scanning steps of 0.03°. Perkin-Elmer spectrophotometer was used to investigate UV-vis spectrum of the synthesized copper nanoparticles. 0.1 mL of the sample was taken and diluted with 2 mL of deionized water. As a function of time of reaction the investigation was conducted in the wavelength region 300 to 700 nm operated at a resolution of 1 nm. Fourier Transform-Infrared (FTIR) spectroscopy was used to identify and confirm the functional groups present in the bioflocculant (Tensor 27, Bruker FT-IR spectrophotometer). TEM images for the copper nanoparticles were obtained using a JEOL 1010 transmission electron microscope. The specimens were prepared by using a micropipette to place a diluted drop of suspension in toluene on a copper grid (150 mesh). The samples were allowed to dry completely at room temperature. Samples were viewed at 100 kV as the voltage accelerates. The images were captured digitally using a Megaview III camera, stored and measured using Soft Imaging System iTEM software. The as-synthesized bioflocculant passivated copper nanoparticles decomposition was studied using a thermo-gravimetric instrument in accordance to (Cosa et al., 2013). High temperatures with range 22 to 900 °C was used to heat the bioflocculant passivated copper nanoparticles, at a constant rate of 10 °C min^{-1} under constant flow of nitrogen gas.

5.2.5 Flocculation activity

A description by Nwodo et al. (2012) was used for measuring flocculation activity. 0.3 mL of 1% $CaCl_2$ and 0.2 mL of 0.002 g/L copper nanoparticles were added into 100 mL of Kaolin suspension (4.0 g/L) in a 200 mL conical flask. The mixture was shaken for 1 min at 165 rpm and it was then transferred into 100 mL measuring cylinder and allowed to stand for 5 min. 2 mL of the upper layer was withdrawn carefully and optical density was read using a spectrophotometer at 550 nm wavelength (Nwodo et al., 2012). For a control, same procedure

was repeated excluding the CuNPs solution. All the results were taken in triplicates and flocculation activity was calculated using the following equation:

$$\text{Flocculating Activity (\%)} = \frac{A-B}{A} X\ 100 \quad (1)$$

Where A is the optical density of control at 550 nm and B is the optical density of a sample at 550 nm.

5.2.6 Water treatment

Samples of water from different industries were examined in accordance to a method described by Okaiyeto et al. (2016). One sample was collected from a domestic water treatment plant (Vulindlela water treatment plant). The next sample was collected from Tendele coal mine. The last sample was collected from local industries Empangeni. To test flocculating activity of copper nanoparticles against different wastewater sample the following followed. 100 mL of wastewater was poured in a flask and 3 mL of 1 % $CaCl_2$ solution was added into the flask containing the wastewater samples after which 2 mL of copper nanoparticles were added into a flask. Mixture was then shaken vigorously for 1 min. using shaking incubator after which the mixture was transferred into graduated 100 mL measuring cylinder. It was allowed to stand for 5 min. before the upper phase was taken for analysis using UV-visible spectrophotometer at 550 nm optical density. The flocculating activity and removal efficiency of dissolved heavy metals of the synthesized nanoparticles was compared to that of bioflocculant and chemical flocculent (iron chloride) (Okaiyeto et al., 2016).

The biological oxygen demand (BOD), chemical oxygen demand (COD), nitrogen (N), phosphorus (P), sulphur (S), aluminium (Al) and calcium (Ca) in wastewater were measured with spectro-quant (Pharo 300, Merck KGaA, Germany), before and after application of the copper nanoparticles. The removal efficiency (RE) of the pollutants was calculated by the following equation:

$$RE(\%) = \frac{Ci - Cf}{Ci}\ X100 \quad (2)$$

Where: C_i is the initial value and C_f is the final value after the flocculation treatment of the sample.

5.2.7 Staining dye removal

Decolourization experiments was performed in accordance to description by Buthelezi et al. (2012). Staining dyes, carbolfuchsine, safranin, malachite green and methylene blue were studied. The dye solution with 5 g/L concentration was prepared. 100 mL of the dye solution

was transferred into 250 mL conical flasks after which 2 mL of 0.2 mg/mL of copper nanoparticles was added. The mixture was vigorously shaken for 1 min. at 165 rpm and transferred to a graduated measuring cylinder. The mixture was allowed to stand for 10 min. and the upper phase was taken for analysis using UV-visible spectrophotometer at 550 nm. The residual concentration of the dye in the samples was then calculated, and the decolourization efficiency was calculated based on the initial dye and final dye concentrations after treatment (Buthelezi et al., 2012).

5.2.8 Antimicrobial activity

5.2.8.1 Minimal inhibitory concentration

A method described by Eloff (1998), was adapted. The minimal inhibitory concentration (MIC) of the synthesized copper nanoparticles was determined. MIC is described as the lowest concentration of the CuNPs required to inhibit microorganisms. Quantitative determination of the synthesized nanoparticles was achieved through the use of 96-well plates. All the wells of 96-well plates were inoculated with 50 µL of sterile nutrient broth. O.2 g of CuNPs was dissolve into 2 mL of distilled water. The solution of CuNPs (50 µL) was the poured into the first row of 96-well containing nutrient broth and mixed. A 3-fold dilution was then performed whereby (50 µL) from row A was taken to row B of the 96 micro-well plates and it was mixed again and another (50 µL) was taken from row B to other subsequent rows until all the well had the CuNPs in different concentrations. The (50 µL) in the last column was discarded so that the total volumes of all the 96-wells is (50 µL). Selected bacteria strains were then added (50 µL) into corresponding wells. The antibiotic Ciprofloxacin (40 %) was used as a positive control, while distilled water was used as a negative control. The plates were then incubated at 37 °C overnight. *P-iodonitrotetrazodium* violet (INT) solution was used as an indicator after incubation period. 40 µL 0f 0.2 mg/mL INT solution was added to each well and further incubated at 37 °C for 30 min. the presence of a reddish colour indicated the reduction of INT to formazan by metabolic active microorganism. The absence of reddish colour (clear) was an indication of inactivity of microorganisms since INT was not broken down to form formazan. All the tests were conducted in triplicates and mean values were taken (Eloff, 1998).

5.2.8.1 Minimal bactericidal concentration

MBC was determined through using the agar dilution method. A loop full of culture of each strain from the well, which indicated no colour change, was streak on a Muller Hilton nutrient agar. The plates were incubated at 37 °C for 12 hrs. The lowest concentration of CuNPs that

exhibited the complete killing of the test organisms were considered as the MBC (Maliehe et al., 2015).

5.2.9 Data analysis

All data were collected in triplicates with mean and standard deviation values determined where differences were considered significant at 0.05 at confidence level ($p > 0.05$) by the use of Graph Pad Prism Version 6 and data were analysed using One-way of variances (ANOVA).

5.3 Results and discussion

5.3.1 Elementary analysis of bioflocculant and copper nanoparticles

The results from the SEM-EDX show the different elements present in the purified bioflocculant in Figure 5.1a and copper nanoparticles Figure 5.1b. The bioflocculant is composed of elements such as: O, C, P, Ca, Cl, Na, K, Mg, and S. Copper was the second highest present element, signifying binding of copper onto the bioflocculant see Figure 5.1b.

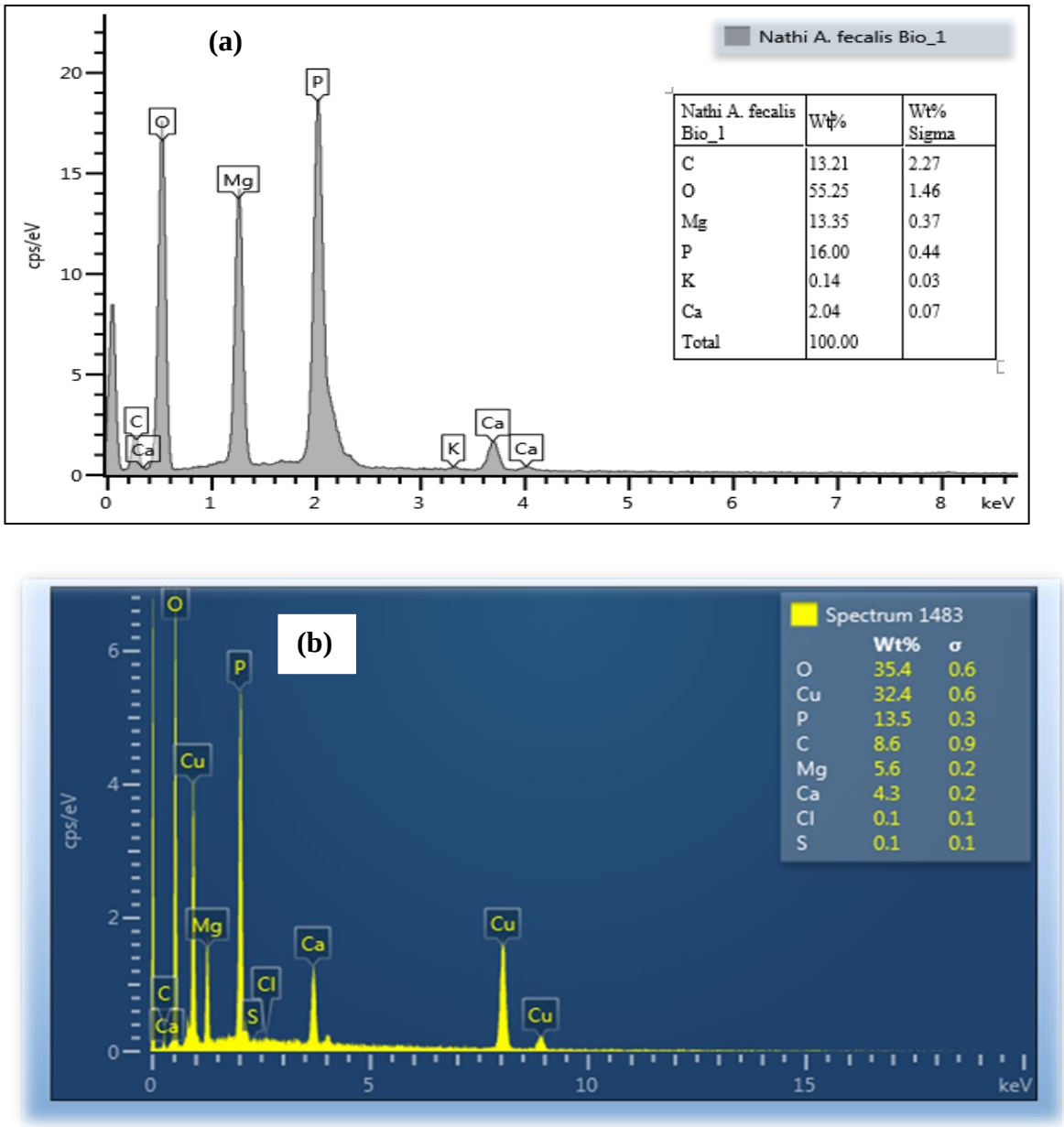

Figure 5.1: SEM-EDX of bioflocculant (A) and CuNPs (B).

Elements such as O, C, P, Ca, Cl, Na, K, Mg, and S were found to be present in the purified bioflocculant at the concentration of weight by percentage (Wt %). Oxygen was the highest

with 29% while sulphur was the least with 0.6. The presence of the elements in bioflocculant play an important role in the structure and flocculating activity (Cosa et al., 2013). Furthermore, the presence of various elements brings about flexibility and stability to the bioflocculant and CuNPs. Elements such as oxygen and carbon suggest that the bioflocculant is predominately carbohydrates in nature and the absence of nitrogen confirms that it cannot be a glycoprotein (Pathak et al., 2015). Similar results were obtained in the bioflocculant MBF-UFH where elements such as: C, O, Na, Mg, P, S, Cl, K and Ca were found (Okaiyeto et al., 2013). In the synthesized copper nanoparticles, the elements present were: O, Cu, P, Mg, Ca, Cl, and S. These findings reveal that oxygen with 37 Wt. % followed by copper with 35.5 Wt. % which is an indication that the synthesis of copper nanoparticles was a success. It can be therefore concluded that the presence of the highest percentage copper bind onto the surface of the bioflocculant. The original bioflocculant alone did not have any copper present Figure 1 A and B respectively.

5.3.2 Surface morphology of both bioflocculant and synthesized copper nanoparticles

Figures 5.2 (a and b) illustrates the surface morphology of both the bioflocculant and nanoparticles. These analyses was done using the SEM. The morphological surface of the bioflocculant is similar to the synthesized nanoparticles but a bigger particle size.

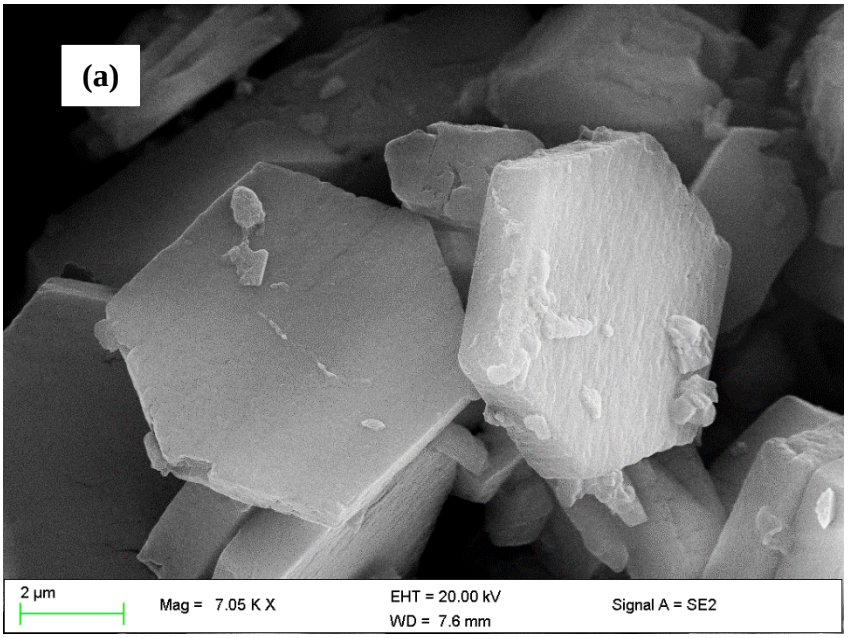

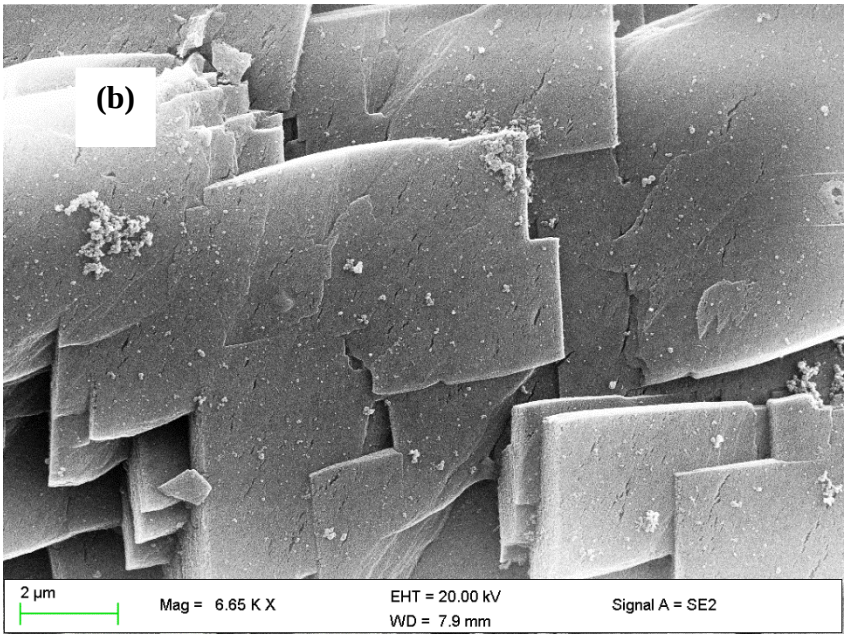

Figure 5.2: SEM image of synthesised copper nanoparticles (a) and bioflocculant (b).

Figure 5.2 (a) and (b) shows the scanning electron micrograph of the copper nanoparticles and the purified bioflocculant. The morphology of the synthesized copper nanoparticles and bioflocculant indicate an amorphous structure. The surface morphology of the flocculants plays a significant role during the formation of flocs (ZHANG et al., 2007). Poor or effective formation of flocs may be accounted for by the structure of the flocculant. The structures of bioflocculants can be amorphous, porous or crystal-like. The synthesized copper nanoparticles are agglomerated which could be due to electric static force between the particles.

5.3.3 UV-visible spectra for both the bioflocculant and copper nanoparticles

Figure 5.3 represents the UV-visible spectra of the bioflocculant and copper nanoparticles at a wavelength of 350 nm. The findings revealed no straight peaks, which could be due to some impurities in the samples.

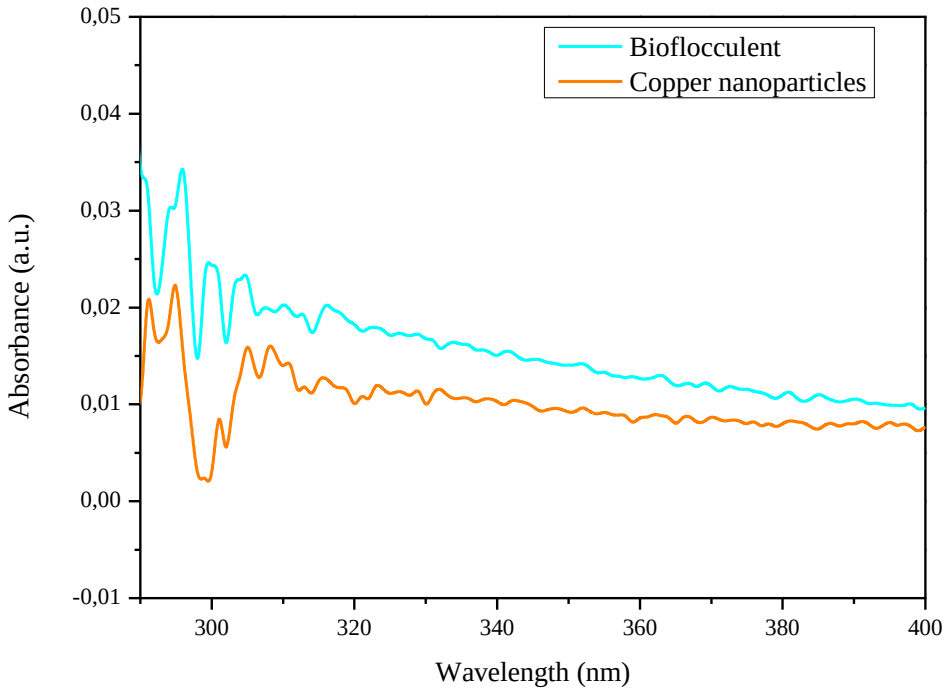

Figure 5.3: UV-visible spectra of the bioflocculant and synthesized nanoparticle.

Figure 5.3 shows UV-Vis spectroscopy recorded from both the bioflocculant and copper nanoparticles solution. This showed the plasmon resonance (SPR) spectra with absorbance 200-350 nm and the pic maxima for both the bioflocculant and the synthesized particles was observed at around 280 nm. This could be ascribed to the formation of Cu nanoparticles. The change in colour of the bioflocculant from white to blue indicated the formation of copper nanoparticles. CuNPs exhibited a green colour in solution due to surface plasmon vibration in CuNPs. Shift in exact position of the SPR band depend on the properties of the individual particle, these properties include shape, size and capping agents.

5.3.4 Functional groups found in both the bioflocculant and copper nanoparticles

Figure 5.4 shows the band at 3256 cm^{-1} (bioflocculant) and 3282 cm^{-1} (copper nanoparticles). This showed the presence of hydroxyl (OH) group and amine (NH_2) group in the samples.

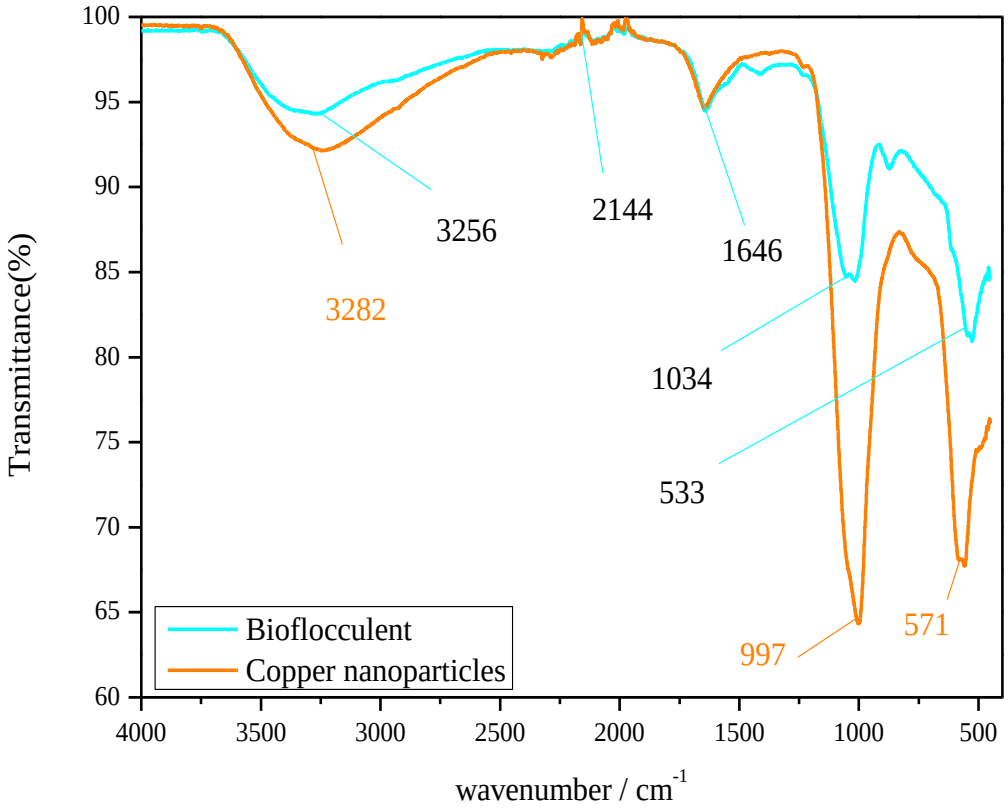

Figure 5.4: FT-IR spectra of bioflocculant and copper nanoparticles.

Salehizadeh and Shojaosadati (2001) states that microorganisms produce bioflocculants with different chemical composition. Purified bioflocculants flocculating activity solely depends on the chemical structure, which is correlated to the functional groups present in the molecule. Xiong et al. (2010) contended that the functional groups present in the molecule also serve as a binding site for different colloids in suspension. Different functional groups present in the molecule were revealed by the Fourier-transform infrared (FTIR) spectroscope analysis (Salehizadeh and Shojaosadati, 2001).

5.3.5 TEM image of copper nanoparticles

Figures 5.5 shows the approximation of size, range of nanoparticles. The synthesized copper nanoparticles seems to be spherical in shape and agglomerated.

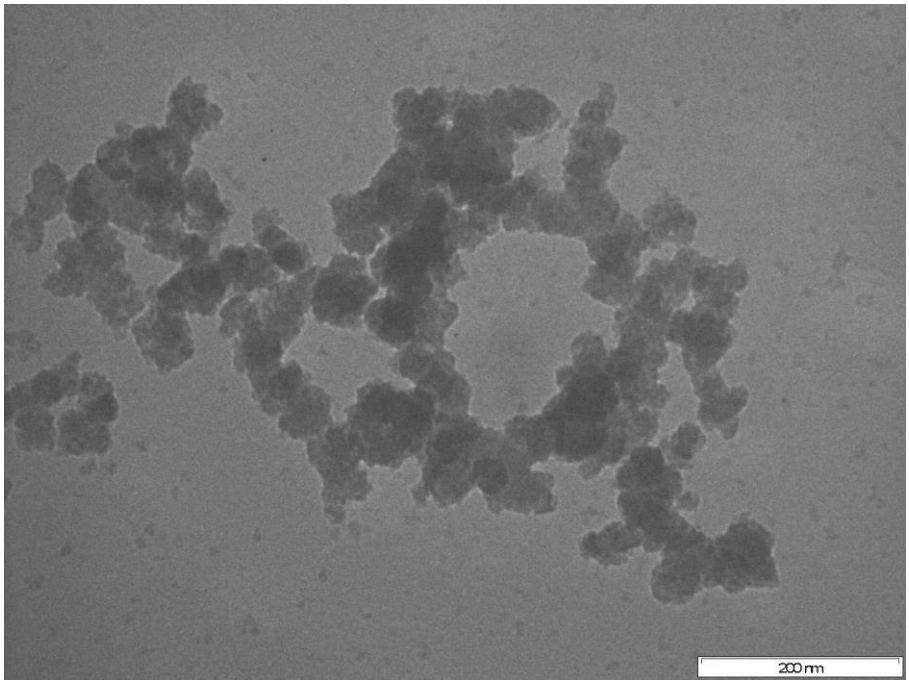

Figure 5.5: TEM image of copper nanoparticles at 200nm scale.

The morphology of the synthesized CuNPs was characterized using TEM. Sample preparation for TEM was achieved by keeping a drop of colloidal solution on a copper grid. The sample was dried at room temperature before placing it in the specimen holder. A thin sample was irradiated with a sharp high-energy electron beam focused by magnetic lenses. The electron intensity distribution of the beam after interaction with the sample was imaged onto a fluorescent screen by the objective lens and the post objective lens system. Images were recorded by a digital CCD camera reproduced or displayed on a computer monitor. The results showed that the average particle size was 100 nm, and seems spherical in morphology as shown

5.3.6 X-ray diffraction pattern of the bioflocculant and the copper nanoparticles

Figure 6 illustrates an X-ray pattern of the CuNPs at angle (2thetha) and deep pics were seen between 30 and 50 angle. The pattern looks similar to that of standard copper nanoparticles.

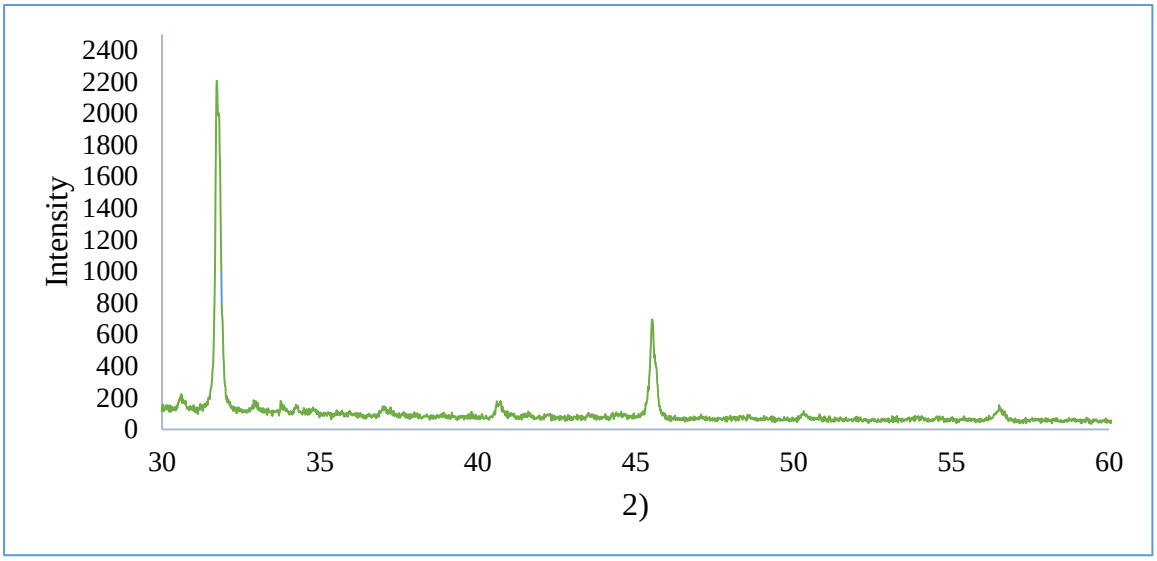

Figure 5.6: X-ray diffraction pattern of copper nanoparticles.

Figure 5.6 shows XRD patterns of copper nanoparticles, synthesized from a bioflocculant. In comparison to a copper standard (JCPDS 04-0836), the characteristic diffraction peaks of copper were observed at around 33˚ and 47˚ 2θ angle. They correspond to the (111) and (220) planes of the fcc structure. No other impurity peaks were detected in the sample. Based on the findings, it could be therefore concluded that it is possible to produced pure nanoparticles using a bioflocculant with copper salt. Sharpening of the diffraction peaks results from moderate temperature. This is an indication of growth of CuNPs and their improved quality. The synthesized copper nanoparticles were revealed crystalline in nature. Intense Bragg reflections suggested that strong X-ray scattering centres in the crystalline phase could be due to the bioflocculant from which the nanoparticles were synthesized. Therefore, XRD result suggested that the crystallization of the bioorganic phase occurred on the surface of the copper nanoparticles. The peaks broadening in the XRD patterns of the solids is generally attributed to particle size effects. Broader peaks signified smaller particle sizes. Moreover, broader peaks may also signify the effects due to experimental conditions on the nucleation and growth of the crystal nuclei. The Debye-Scherrer's equation was used to calculate the particles size. The size of crystallite was in the range of 6-10 nm, which indicated a high surface area and surface area to volume ratio of the nanoparticles.

5.3.7 Effect of copper nanoparticle dosage on flocculating activity

Figure 5.7 represents the results obtained during the determination of the effect the copper nanoparticles concentration on flocculating activity. The flocculating activity of copper nanoparticles decreased proportionally with the increase in dosage concentration.

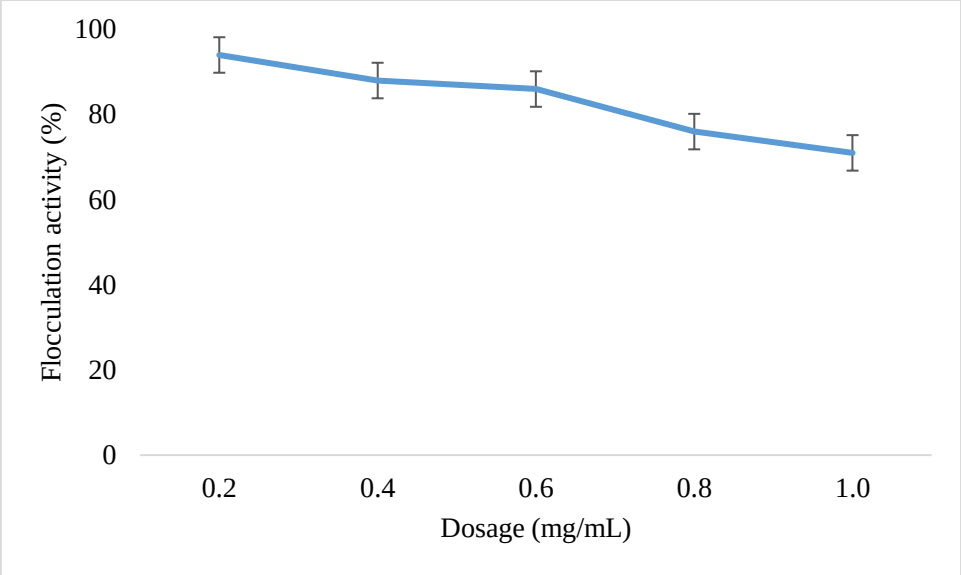

Figure 5.7: Dosage effect on flocculation activity. (Refer to index data Table 5.7).

The amount of nanoparticles powder required for optimal flocculation is called *dosage size.* The different concentration of CuNPs solution was prepared and its flocculating activity was evaluated. Various concentrations were prepared by dissolving different amounts of CuNPs powder in concentration of 0.2, 0.4, 0.6, 0.8 and 0.1 mg/mL in distilled water. Each of the ditto were dissolved in 50 mL distilled water. After which a litre of kaolin clay solution was prepared where by 4 g of kaolin clay powder was dissolved in a litre of distilled water. Three millilitres of 1 % (w/v) $CaCl_2$ and 2 mL of CuNPs solution was added into a 250 mL conical flask containing 100 mL of kaolin clay and then agitated for 1 min. The mixture was transferred to a graduated 100 mL measuring cylinder and left to stand for 5 min. The supernatant was taken for analysis in a spectrophotometer with a wavelength of 500 nm. As depicted in the Figure 7 the nanoparticles flocculate best at low dosage as the highest flocculating activity was achieved at 0.2 mg/mL with flocculating activity of 96%. The increase in dosage concentration resulted in decrease in flocculating activity.

5.3.8 Flocculating efficiency of CuNPs, iron chloride and bioflocculant

Figure 8 shows the flocculating efficiency of CuNPs in comparison to that of $FeCl_3$ and bioflocculant. Different wastewater samples were examined including kaolin, coal mine wastewater, industrial wastewater and domestic wastewater.

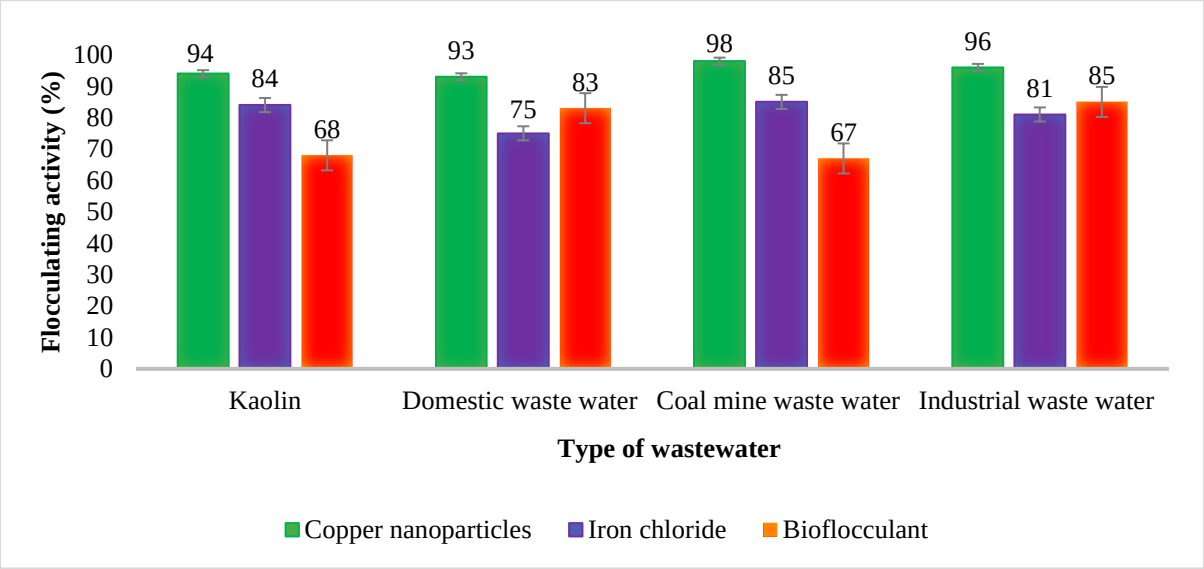

Figure 5.8: Flocculation activity of CuNPs, iron chloride and bioflocculant. (Refer to index data Table 5.8).

Commercial flocculants are considered cost effective due to their high flocculating efficiency; however, their secondary pollutants have a negative effect on the environment. Contrary, bioflocculants are environmental friendly but they are not as effective compare to chemical flocculants. In this particular study, the aim was to compare the effectiveness of CuNPs, which were synthesized from the bioflocculant against the commercial flocculant (iron chloride) and pure bioflocculant. The results were outstanding in all the tested wastewater samples as the flocculation activity was above 80 %. These findings suggested the multifunctionality of the synthesized nanoparticles. However, to obtain maximum efficiency more optimization needs to be done on the synthesized CuNPs.

5.3.9 Pollutants removal in coal mine wastewater

Table 5.1 shows the removal efficiency of pollutants in coal mine wastewater by copper nanoparticles. CuNPs has a high removal efficiency for phosphorus and sulphur.

Table 5.1: Removal of pollutants metals in coalmine wastewater.

Type of flocculant	Water quality before treatment			Water quality after treatment			Removal efficiency (%)		
	P (mg/L)	S (mg/L)	Ca (mg/L)	P (mg/L)	S (mg/L)	Ca (mg/L)	P	S	Ca
CuNPs	2.0±0.0	0.55±0.1	56±0.0	0.3±0	0.13±0.1	17±0.0	85	76	71
Bioflocculant	2.0±0.0	0.55±0.1	56±0.0	1.3±0	0.10±0	15±0.0	37	72	73
$FeCl_3$	2.0±0.0	0.55±0.1	56±0.0	0.5±0	0.24±0	18±0.0	75	56	68

Industrialization is good for the economic growth of any country. However, industrial growth in many instances produce a huge amount of waste, which end up reaching the water, bodies if untreated. Water samples from a local coal mine was use to ascertain the removal efficiency of synthesized copper nanoparticles. Elements such as P, S, and Ca were tested. The synthesized copper nanoparticles showed some remarkable ability to remove these elements. Removal was better than for the bioflocculant and the synthetic flocculant. The results suggest that the copper nanoparticle can be a suitable alternative to replace chemical flocculants. The nanoparticles provided properties such as degradability and friendliness to the environment, which the chemical flocculants lack.

5.3.10 Effect of copper nanoparticles on staining dye removal

Figure 9 illustrates effect of copper nanoparticles on staining dye removal. The synthesized nanoparticles have a high affinity for all examined dyes with removal efficiency above 85%. These copper nanoparticles are effective to remove dyes in wastewater from different industries like the clothing industries.

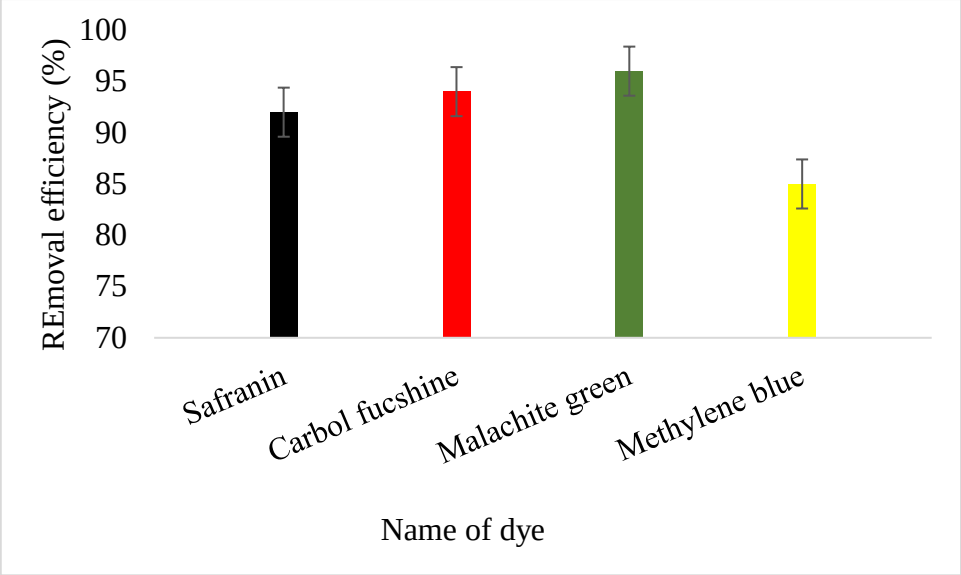

Figure 5.9: Effect of copper nanoparticles on dye removal. (Refer to index data Table 5.9).

The dye removal potential of copper nanoparticles synthesized from a bioflocculant was investigated. Synthesized nanoparticles were able to remove all different dyes. This could be by causing aggregation of particles due to bridging and charge neutralization as reported previously (Salehizadeh and Shojaosadati, 2001). When the particles extend from the surface into a solution for a distance greater than the distance over which the antiparticle repulsion acts bridging occurs. This results into a biopolymer adsorb into other particles resulting into floc formation (Guibai and Gregory, 1991). The synthesized nanoparticles possess huge potential for removing all dyes, which were tested. Concentration of nanoparticles remained constant (0.2 mg/mL) and this demonstrated that the nanoparticles were effective because removal efficiency was above 80% in all dyes without the addition of cations. Contrary, the removal efficiency of dyes directly depended on high concentration of the bioflocculant. The functional groups present in the polymer must be able to interact with sites on the surface of the colloidal particle in order to be effective (Deng et al., 2005).

Table 5.2: The removal efficiency of BOD and COD in coalmine wastewater by CuNPs.

Flocculants type	Water quality before treatment		Water quality after treatment		Removal Efficiency (%)	
	BOD mg/mL	COD mg/mL	BOD mg/mL	COD mg/mL	BOD mg/mL	COD mg/mL
CuNPs	123.2±0.0	154±0.0	5±0.0	17±0.0	96	89
Bioflocculant	123.2±0.0	154±0.0	27±0.0	37±0.0	75	78
$FeCl_3$	123.2±0.0	154±0.0	31±0.0	29±0.0	72	81

High levels of COD and BOD in water do not support aquatic life (Poff and Zimmerman, 2010). The presence of N, P and S in high concentrations in water prompt eutrophication. The application of bioflocculant and copper nanoparticles for removal of these pollutants from domestic wastewater, coalmine water and industrial wastewater, were determined in comparison with iron chloride. The synthesized nanoparticles had the best removal efficiency compared to bioflocculant and iron chloride for COD, BOD (Poff and Zimmerman, 2010). The removal efficiency of the copper nanoparticles could be attributed to the surface structure, chemical components and to the functional groups. The results were contrary to other findings reported in literature Zhang et al. (2012); Ugbenyen et al. (2012) whereby the purified bioflocculant had the highest removal efficiencies of pollutants in wastewater. The findings suggested that the synthesized copper nanoparticles possess high potential for industrial application. Furthermore, the effectiveness of CuNPs recommend that they also have potential to reduce adverse effects of chemical flocculants being used (Zhang et al., 2012, Ugbenyen et al., 2012). The ability for CuNPs to reduce the tested water quality parameters signifies their multi functionality.

5.3.11 Minimal inhibitory concentration, minimal bactericidal concentration for CuNPs in mg/mL

Table 5.3 shows the MIC and MBC of the synthesized copper nanoparticles compare to ciprofloxacin. The synthesized nanoparticles showed some remarkable properties against both Gram-positive and Gram-negative organisms, the least MIC and MBC was observed against *K. pneumoniae* and *A. freundii.*

Table 5.3: Minimal inhibitory concentration and minimal bactericidal concentration in mg/mL for CuNPs.

	CuNPs		Ciprofloxacin	
Bacterial strains	MIC	MIC	MIC	MIC
E. coli	6.25	6.25	3.125	6.25
B. pumilus	3.125	3.125	-	-
A. freundii	12.5	12.5	1.56	1.56
K. pneumoniae	12.5	12.5	1.56	1.56

Ciprofloxacin is an antibiotic used to treat a number of bacterial infections both Gram positive and Gram negative. Ciprofloxacin (20 µL) was used as a positive control in this study. The inhibitory effect of ciprofloxacin was observed in all the Gram-negative tested microorganisms. However, the Gram-positive (*B. pumilus*) could still grow in the presence of both high and low concentration of ciprofloxacin. Contrary, the synthesized nanoparticles had a remarkable effect in both Gram positive and Gram-negative organisms. Even though the antimicrobial activity of the synthesized CuNPs was more prominent on Gram-negative organisms, it also showed some remarkable abilities against Gram-positive *B. pumilus.* Gram-positive bacteria lack the outer membrane; the constituents of the CuNPs are directly in contact with the phospholipid bilayer of the cell (Maliehe et al., 2015). Gram-negative microorganisms have outer membrane, which is approximately 7 to 8 nm in addition to a thin peptidoglycan layer. The presence of this layer in Gram-negative bacterial provides protection against antimicrobial compounds and chemotherapy. This is due to the protective liposaccharides layer that exhibit antigenicity and resistance against antimicrobial agents (Levy and Marshall, 2004). The ability of the CuNPs to inhibit the growth of all the Gram-negative bacteria suggest that the synthesized CuNPs may have the potential to overcome resistance of Gram-negative bacteria.

5.4 Conclusion

Copper nanoparticles were successful synthesized using a purified bioflocculant. Synthesized nanoparticles were characterized and applied in wastewater treatment, stain removal and its antimicrobial effect was evaluated. The removal efficiencies were determined using different water samples, one from coalmine water the other from domestic and industrial wastewater respectively. In the treatment of wastewater, the synthesized nanoparticles worked better compared to both the iron chloride and bioflocculant. The CuNPs possess some good properties in terms of staining dye affinity as it had above 80 % removal efficiency in the staining dye tests. The elemental composition of CuNPs compare to that bioflocculant revealed that, there was huge significant increase in copper with 37.8 Wt. % while there was no copper present in the bioflocculant. Thermogravimetric analysis of both the bioflocculant and CuNPs showed that the synthesized nanoparticles are more thermally stable compared to bioflocculant. The synthesized particles possessed some antimicrobial properties, to all selected test strain positive results were obtained. The bioflocculant alone did not give any positive results, suggesting that the antimicrobial property was due to copper presence.

Author Contributions: Conceptualization, A.K.B. and V.S.R.P.; formal analysis, N.G.D. and V.S.R.P.; investigation, N.G.D.; supervision, A.K.B. and V.S.R.P.; writing—original draft, N.G.D.; writing—review and editing, V.S.R.P.

Acknowledgments: Nkosinathi Dlamini would like to acknowledge the Council for Scientific and Industrial Research (CSIR, South Africa) for the financial assistance in the form of the Ph.D. bursary. The authors would like to acknowledge the Electron Microscopy Unit at the University of KwaZulu-Natal, Westville campus, for providing support by letting us use the TEM and SEM-EDX facilities for the characterization of nanomaterials. Rajasekhar Pullabhotla would like to acknowledge the National Research Foundation (NRF, South Arica) for the financial support in the form of the Incentive Fund Grant (Grant No: 103691) and Research Developmental Grants for Rated Researchers (Grant No: 116363).

Declaration of interest

The authors declare that there is no conflict of interest.

5.5 References

ASHAJYOTHI, C., HARISH, K. H., DUBEY, N. & CHANDRAKANTH, R. K. 2016. Antibiofilm activity of biogenic copper and zinc oxide nanoparticles-antimicrobials collegiate against multiple drug resistant bacteria: a nanoscale approach. *Journal of Nanostructure in Chemistry,* 6**,** 329-341.

BUTHELEZI, S. P., OLANIRAN, A. O. & PILLAY, B. 2012. Textile dye removal from wastewater effluents using bioflocculants produced by indigenous bacterial isolates. *Molecules,* 17**,** 14260-14274.

COSA, S., MABINYA, L. V., OLANIRAN, A. O., OKOH, O. O., BERNARD, K., DEYZEL, S. & OKOH, A. I. 2011. Bioflocculant production by Virgibacillus sp. Rob isolated from the bottom sediment of Algoa Bay in the Eastern Cape, South Africa. *Molecules,* 16**,** 2431-2442.

COSA, S., UGBENYEN, A. M., MABINYA, L. V., RUMBOLD, K. & OKOH, A. I. 2013. Characterization and flocculation efficiency of a bioflocculant produced by a marine Halobacillus. *Environmental technology,* 34**,** 2671-2679.

DENG, S., YU, G. & TING, Y. P. 2005. Production of a bioflocculant by Aspergillus parasiticus and its application in dye removal. *Colloids and surfaces B: Biointerfaces,* 44**,** 179-186.

DLAMINI, N. G., BASSON, A. K. & PULLABHOTLA, V. S. R. 2019. Optimization and Application of Bioflocculant Passivated Copper Nanoparticles in the Wastewater Treatment. *International Journal of Environmental Research and Public Health,* 16**,** 2185.

DURÁN, N., MARCATO, P. D., CONTI, R. D., ALVES, O. L., COSTA, F. & BROCCHI, M. 2010. Potential use of silver nanoparticles on pathogenic bacteria, their toxicity and possible mechanisms of action. *Journal of the Brazilian Chemical Society,* 21**,** 949-959.

ELOFF, J. N. 1998. A sensitive and quick microplate method to determine the minimal inhibitory concentration of plant extracts for bacteria. *Planta medica,* 64**,** 711-713.

FUJITA, M., IKE, M., TACHIBANA, S., KITADA, G., KIM, S. M. & INOUE, Z. 2000. Characterization of a bioflocculant produced by Citrobacter sp. TKF04 from acetic and propionic acids. *Journal of Bioscience and Bioengineering,* 89**,** 40-46.

GUIBAI, L. & GREGORY, J. 1991. Flocculation and sedimentation of high-turbidity waters. *Water Research,* 25**,** 1137-1143.

HE, J., ZOU, J., SHAO, Z., ZHANG, J., LIU, Z. & YU, Z. 2010. Characteristics and flocculating mechanism of a novel bioflocculant HBF-3 produced by deep-sea bacterium mutant Halomonas sp. V3a'. *World Journal of Microbiology and Biotechnology,* 26**,** 1135-1141.

KAUR, P., THAKUR, R., BARNELA, M., CHOPRA, M., MANUJA, A. & CHAUDHURY, A. 2015. Synthesis, characterization and in vitro evaluation of cytotoxicity and antimicrobial activity of chitosan–metal nanocomposites. *Journal of Chemical Technology & Biotechnology,* 90**,** 867-873.

KHAN, I., SAEED, K. & KHAN, I. 2017. Nanoparticles: Properties, applications and toxicities. *Arabian Journal of Chemistry*.

LEVY, S. B. & MARSHALL, B. 2004. Antibacterial resistance worldwide: causes, challenges and responses. *Nature medicine,* 10**,** S122.

LI, Q., MAHENDRA, S., LYON, D. Y., BRUNET, L., LIGA, M. V., LI, D. & ALVAREZ, P. J. 2008. Antimicrobial nanomaterials for water disinfection and microbial control: potential applications and implications. *Water research,* 42**,** 4591-4602.

MABINYA, L. V., COSA, S., NWODO, U. & OKOH, A. I. 2012. Studies on bioflocculant production by Arthrobacter sp. Raats, a freshwater bacteria isolated from Tyume River, South Africa. *International journal of molecular sciences,* 13**,** 1054-1065.

MALIEHE, S., SHANDU, S. J. & BASSON, K. A. 2015. The antibacterial and antidiarreal activities of the crude methanolic Syzygium cordatum [S. Ncik, 48 (UZ)] fruit pulp and seed extracts. *Journal of Medicinal Plants Research,* 9**,** 884-891.

MALIEHE, T., SIMONIS, J., BASSON, A., REVE, M., NGEMA, S. & XABA, P. 2016. Production, characterisation and flocculation mechanism of bioflocculant TMT-1 from marine Bacillus pumilus JX860616. *African Journal of Biotechnology,* 15**,** 2352-2367.

NONTEMBISO, P., SEKELWA, C., LEONARD, M. V. & ANTHONY, O. I. 2011. Assessment of bioflocculant production by Bacillus sp. Gilbert, a marine bacterium isolated from the bottom sediment of Algoa Bay. *Marine drugs,* 9**,** 1232-1242.

NWODO, U. U., AGUNBIADE, M. O., GREEN, E., MABINYA, L. V. & OKOH, A. I. 2012. A freshwater Streptomyces, isolated from Tyume river, produces a predominantly extracellular glycoprotein bioflocculant. *International journal of molecular sciences,* 13**,** 8679-8695.

OKAIYETO, K., NWODO, U., MABINYA, L. & OKOH, A. 2013. Characterization of a bioflocculant produced by a consortium of Halomonas sp. Okoh and Micrococcus sp. Leo. *International journal of environmental research and public health,* 10**,** 5097-5110.

OKAIYETO, K., NWODO, U. U., OKOLI, S. A., MABINYA, L. V. & OKOH, A. I. 2016. Implications for public health demands alternatives to inorganic and synthetic flocculants: bioflocculants as important candidates. *MicrobiologyOpen,* 5**,** 177-211.

PATHAK, M., DEVI, A., BHATTACHARYYA, K., SARMA, H., SUBUDHI, S. & LAL, B. 2015. Production of a non-cytotoxic bioflocculant by a bacterium utilizing a petroleum hydrocarbon source and its application in heavy metal removal. *Rsc Advances,* 5**,** 66037-66046.

POFF, N. L. & ZIMMERMAN, J. K. 2010. Ecological responses to altered flow regimes: a literature review to inform the science and management of environmental flows. *Freshwater Biology,* 55**,** 194-205.

PRASERTSAN, P., DERMLIM, W., DOELLE, H. & KENNEDY, J. 2006. Screening, characterization and flocculating property of carbohydrate polymer from newly isolated Enterobacter cloacae WD7. *Carbohydrate polymers,* 66**,** 289-297.

RUDÉN, C. 2004. Acrylamide and cancer risk—expert risk assessments and the public debate. *Food and Chemical Toxicology,* 42**,** 335-349.

SALEHIZADEH, H. & SHOJAOSADATI, S. 2001. Extracellular biopolymeric flocculants: recent trends and biotechnological importance. *Biotechnology advances,* 19**,** 371-385.

TIWARI, D. K., BEHARI, J. & SEN, P. 2008. Application of nanoparticles in wastewater treatment 1.

UGBENYEN, A., COSA, S., MABINYA, L., BABALOLA, O. O., AGHDASI, F. & OKOH, A. 2012. Thermostable bacterial bioflocculant produced by Cobetia spp. isolated from Algoa Bay (South Africa). *International journal of environmental research and public health,* 9**,** 2108-2120.

XIONG, Y., WANG, Y., YU, Y., LI, Q., WANG, H., CHEN, R. & HE, N. 2010. Production and characterization of a novel bioflocculant from Bacillus licheniformis. *Appl. Environ. Microbiol.,* 76**,** 2778-2782.

ZAKI, S., ELTARAHONY, M., ELKADY, M. & ABD-EL-HALEEM, D. 2014. The use of bioflocculant and bioflocculant-producing Bacillus mojavensis strain 32A to synthesize silver nanoparticles. J Nanomater 2014: 1–7.

ZHANG, C.-L., CUI, Y.-N. & WANG, Y. 2012. Bioflocculant produced from bacteria for decolorization, Cr removal and swine wastewater application. *Sustainable Environment Research,* 22**,** 129-134.

ZHANG, Z.-Q., BO, L., XIA, S.-Q., WANG, X.-J. & YANG, A.-M. 2007. Production and application of a novel bioflocculant by multiple-microorganism consortia using brewery wastewater as carbon source. *Journal of Environmental Sciences,* 19**,** 667-673.

Chapter 6 ARTICLE 4: Green synthesis of iron nanoparticles by a bioflocculant from marine *Alcaligenes faecalis* HCB2 and characterization

Dlamini NG [a]*, Basson A.K[a], Rajasekhar Pullabhotla VSR [b]*,

[a] Department of Biochemistry and Microbiology, University of Zululand, Private Bag X1001, KwaDlangezwa, 3886, South Africa

[b] Department of Chemistry, University of Zululand

***** Author to whom correspondence should be addressed; E-Mail: nathidlamini03@gmail.com; PullabhotlaV@unizulu.ac.za

Tel. +27-73 0985921/ +27-359026155

Abstract: Iron, the most ubiquitous of the transition metals and the fourth most plentiful metal in the Earth's crust is the structural backbone of our modern infrastructure. It is therefore ironic that as a nanoparticle, iron has been somewhat neglected in favor of its own oxides as well as other metals such as cobalt, nickel, gold, and platinum. This study reports the green synthesis of iron nanoparticles using a bioflocculant and characterization. The materials were characterized using Scanning Electron Microscopy (SEM), Transmission Electron Microscopy (TEM), X-ray diffractometer, Fourier Transform Infrared Spectroscopy (FT-IR), Thermogravimetric analysis (TGA) and UV-Vis absorption spectroscopy. Spherical morphology was observed in iron nanoparticles (FeNPs) and elements such as Oxygen and iron 65.25 % with oxygen having 47.94 followed by iron with 17.31%. Broad peaks are seen between 20° and 30° for the as-synthesized iron nanoparticles. FTIR shows the band at 3154 cm^{-1} (bioflocculant) and 3244 cm^{-1} (iron nanoparticles). This showed the presence of hydroxyl (OH) group and amine (NH2) group in the samples.

Keywords: Bioflocculant, Iron nanoparticles, Synthesis, Characterization

6.1 Introduction

Polysaccharide from microbial origin such as bioflocculants are emerging stabilizing and reducing agents for synthesis of nanoparticles (Sathiyanarayanan et al., 2013). Commonly, bioflocculant pause less threat to the environment due to their biodegradability, nontoxicity nature as compare to organic and synthetic flocculants (Singh et al., 2000a). However, the production media which is used for bioflocculant production is very expensive which render them not to be commercial viable for application in industries (Sathiyanarayanan et al., 2013). Polysaccharide bioflocculants form a variety of liquid crystals easily in aqueous solution, they can be used for high-performance nanomaterial production. Moreover, they have hemiacetal reducing end, hydroxyl groups and other functionalities which aid as reducing and stabilizing agent during formation of metallic nanoparticles (Mata et al., 2009).

The great interest in iron nanoparticles is due to its magnetic properties. Among the most used magnetic materials is iron (Huber, 2005). Iron nanoparticles have been reported to be able to transform wide range of common environment contaminants such as chlorinated organic solvent (Zhang et al., 2003). Iron nanoparticles ability to rapidly reduce ground water redox potential is vital to chemical reduction of contaminants and is also essential for stimulating biodegradability of chlorinated solvents (Mata et al., 2009).

Trace amount of iron nanoparticles addition reduces the standard potential quickly, hydrogen gas is generated and divalent iron is produced. These are favourable growth conditions for anaerobic microorganisms (Sun et al., 2006). The application of iron nanoparticles in the removal of viruses in water is reported to be successful, viruses are very small and cannot be removed by technologies such as membrane filtration. Viruses such as MS-2 and ΦX174 were successfully removed by commercial available iron granules, it was concluded that both physical adsorption and inactivation occurred (You et al., 2005). In present study the bioflocculant from marine species was used for the synthesis of nanoparticles.

6.2 Material and Methods

6.2.1 Culture medium

A culture medium consisting of glucose (20 g), KH_2PO_4 (2.0 g), $(NH_4)_2SO_4$ (0.20 g), $MgSO_4 \cdot 7H_2O$ (0.20 g), yeast extract (0.50 g), urea (0.50 g) and K_2HPO_4 (5.0 g) was used to culture a bioflocculant producing bacteria. A bioflocculant producer was previously isolated and identified as *Alcalegenis faecalis* by sRNA sequencing through Inqaba Biotech, South Africa. 1 litre of filter sea water at pH (8) and the optimum pH was adjusted using NaOH and HCl. The medium was sterilized by autoclave at 121 ºC for 15 min. After which, the medium was left to cool at room temperature before it was inoculated with 1 % freshly resuscitated inoculum and incubated for 72 hrs at 30 ºC shaking at 165 rpm (Gong et al., 2008).

6.2.2 Extraction and purification of the bioflocculant

To extract the bioflocculant after 72 hrs of incubation the broth was centrifuged at 4,000 rpm at 4 ºC for 30 min to separate cells from the supernatant. A litre of distilled water was added onto the supernatant and was further centrifuged for 15 min under same conditions previously described. Two litres of absolute ethanol were added and the mixture was left for 12 hrs at 4 ºC to allow for precipitate formation. The crude bioflocculant was purify using 100 mL distilled water and the mixture of chloroform and *n*-butyl (5:2 v/v*)*. Mixture was stirred and was left to stand at room temperature for further 12 hrs before it was vacuum dried to obtain pure bioflocculant (Okaiyeto et al., 2015b).

6.2.3 Synthesis of iron nanoparticles

0.5 g of polysaccharide bioflocculant was added into a solution containing $FeCl_3$ (10 mL, 0.2 M) in a flask. After which NaOH (10 mL, 5.0 M) was added to prevent agglomeration of synthesized nanoparticles, the mixture was left to stand at room temperature until colour changed was observed which indicated nanoparticles formation. Resulted precipitate was centrifuged at 4,000 rpm, 4 ºC for 15 min. The control used was bioflocculant solution without the addition of iron chloride. Synthesized nanoparticles were washed by absolute ethanol and characterized (Swierczewska et al., 2016).

6.2.4 Characterization of copper nanoparticles

SEM was used for better image at 1000 keV i.e. wavelengths of resolution. Morphology and elementary analysis of the synthesized nanoparticles was determined using scanning electron microscope equipped with elementary detector (SEM-Sipma-VP-03-67). BRUKER D8 Advance X-Ray Diffractometer operated at 40 kV, 40 mA, with copper monochromatized CuKα1 radiation of wavelength λ=1.5406 Å was used to investigate the phase composition and crystallinity of the bioflocculant. XRD was recorded in the 2θ range from 20° to 80° at scanning steps of 0.03°.

Perkin-Elmer spectrophotometer was used to investigate UV-vis spectrum of the synthesized iron nanoparticles. 0.1 ml of the sample was taken and diluted with 2 ml of deionized water. As a function of time of reaction the investigation was conducted in the wavelength region 300 to 700 nm operated at a resolution of 1 nm. Fourier Transform-Infrared (FT-IR) spectroscopy was used to identify and confirm the functional groups present in the bioflocculant (Tensor 27, Bruker FT-IR spectrophotometer).

TEM images for the iron nanoparticles were obtained using a JEOL 1010 transmission electron microscope. The specimens were prepared by using a micropipette to place a diluted drop of suspension in toluene on a copper grid (150 mesh). The samples were allowed to dry completely at room temperature. Samples were viewed at 100 kV as the voltage accelerates. The images were captured digitally using a Megaview III camera, stored and measured using Soft Imaging System iTEM software.

The as-synthesized bioflocculant passivated iron nanoparticles decomposition was studied using a thermo-gravimetric instrument. High temperatures with range 22 to 900 ºC was used to heat the bioflocculant passivated copper nanoparticles, at a constant rate of 10 ºC min^{-1} under constant flow of nitrogen gas.

6.3 Results and discussion

6.3.1 The functional groups present in the bioflocculant and iron nanoparticles

Figure 6.1 shows the band at 3154 cm^{-1} (bioflocculant) and 3244 cm^{-1} (iron nanoparticles). This showed the presence of hydroxyl (OH) group and amine (NH2) group in the samples. The weak band at 1782 cm^{-1} in both the samples can be designated to the presence of aliphatic bonds. The peak located at 1252 cm^{-1} indicates the presence of an amide group. The vibrational peaks at 1252 cm^{-1} (bioflocculant) and 1256 cm^{-1} (iron nanoparticles) are analogous to the C-O stretching in alcohols, which confirms the OH group presence.

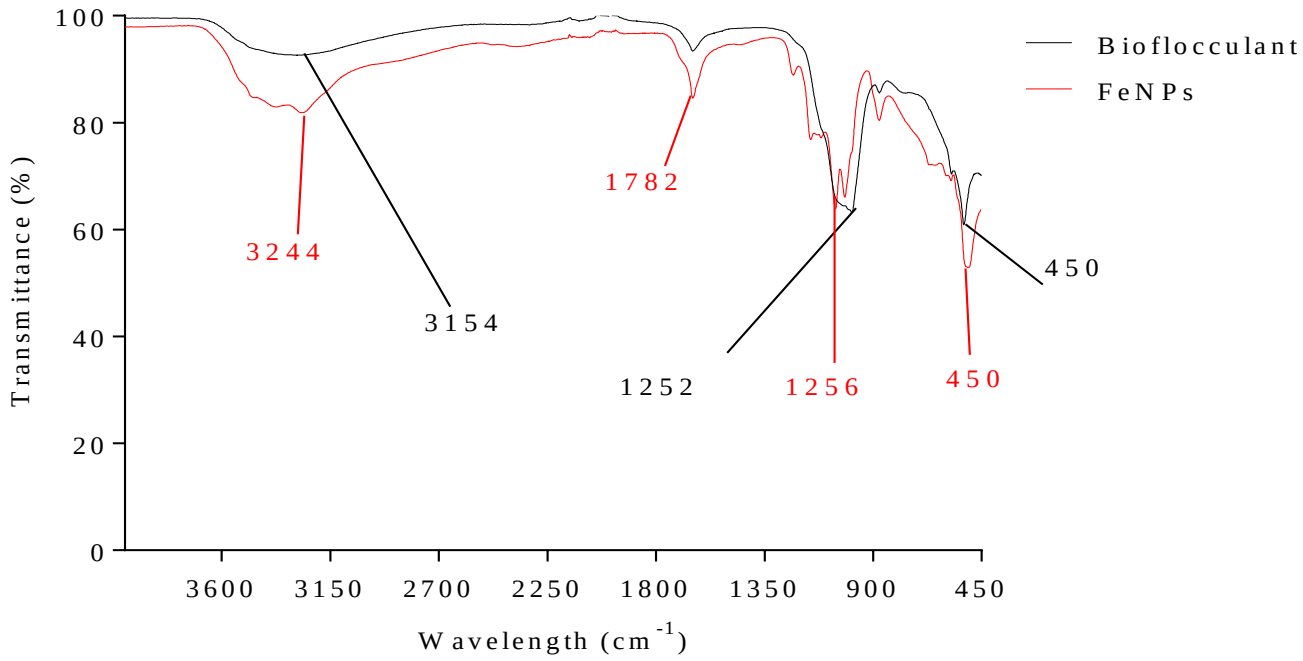

Figure 6.1: FT-IR of the bioflocculant and iron nanoparticles.

Figure 6.1 shows the band at 3154 cm^{-1} (bioflocculant) and 3244 cm^{-1} (iron nanoparticles). The two bands at 3154 and 3244 cm^{-1} showed the presence of hydroxyl group (OH) and amine group (NH_2) in the sample. The hydroxyl group plays a significant role of reducing and stabilizing nanoparticles during synthesis (Mata et al., 2009). The vibration band at 450 cm^{-1} Is typical of Fe-O bond in the synthesized iron nanoparticles 1000-900 cm^{-1} suggest the presence of polysaccharides derivatives. This was further confirmed by the thermostability of the synthesized nanoparticles when they were subjected at different temperatures during flocculation evaluation (Guo et al., 2013). Different functional groups present in the molecule were revealed by the Fourier-transform infrared (FTIR) spectroscope analysis.

6.3.2 Elementary analysis of the bioflocculant

Figure 6.2 the results from the SEM-EDX, show the different elements present in the purified bioflocculant. The bioflocculant is composed of elements such as: O, P, Mg, C, K and Ca. The element with the highest Wt% was carbon with 13.21Wt% while Ca was the least with just 2.04 Wt%. No iron was present in the bioflocculant.

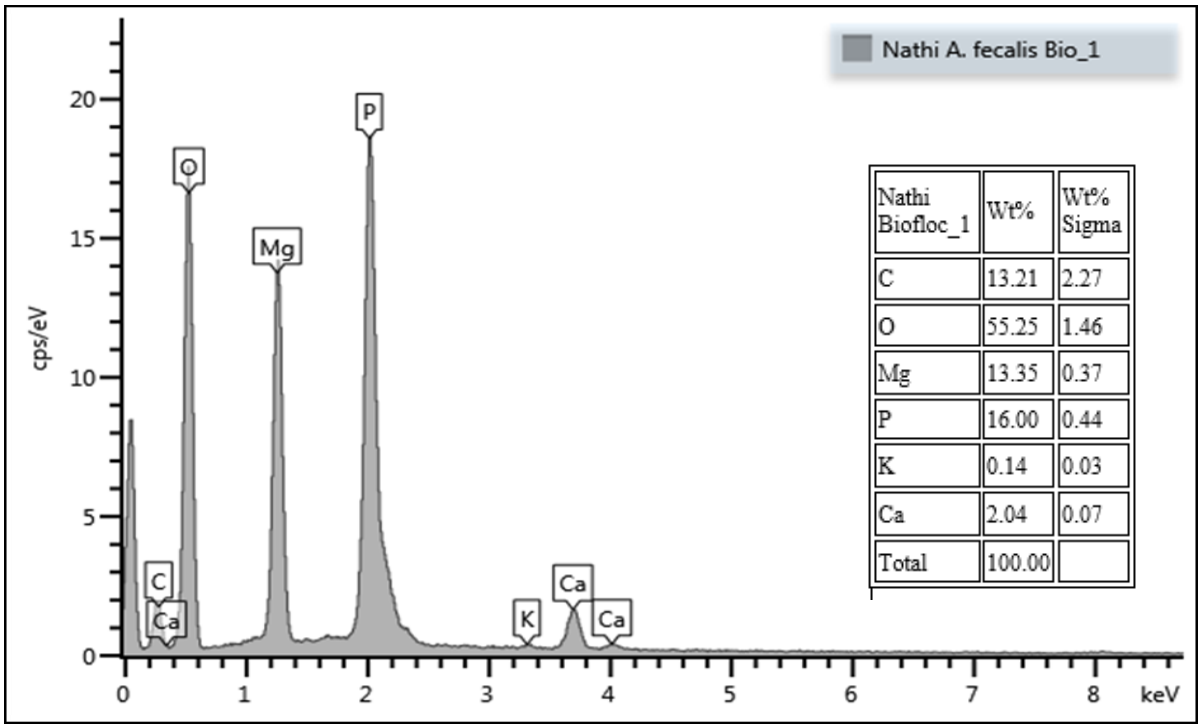

Nathi Biofloc_1	Wt%	Wt% Sigma
C	13.21	2.27
O	55.25	1.46
Mg	13.35	0.37
P	16.00	0.44
K	0.14	0.03
Ca	2.04	0.07
Total	100.00	

Figure 6.2: Different elements present in the bioflocculant: SEM-EDX.

As indicated in Figure 6.2 oxygen is the most abundant element in the sample with 55.25 Wt% while K was found to be the least with 0.14 Wt%. The presence of elements plays an important role in the structure of the bioflocculant. Moreover, the presence of elements brings about flexibility and stability in the bioflocculant. Subudhi et al. (2016) states that presences of elements such as oxygen and carbon in a bioflocculant is an indication that the bioflocculant consist mostly of carbohydrates and absence of nitrogen further confirms that it cannot be a glycoprotein. Bioflocculants which are predominantly of carbohydrates are thermostable as compared to glycoprotein bioflocculants (Subudhi et al., 2016).

6.3.3 Elementary analysis of iron nanoparticles

The results from the SEM-EDX, show the different elements present in iron nanoparticles. Figure 6.3 shows that elements such as O, Fe, P, C, Ca, Cu and K were present in the sample. Iron was the second highest present element in the sample signifying the binding of iron onto the bioflocculant.

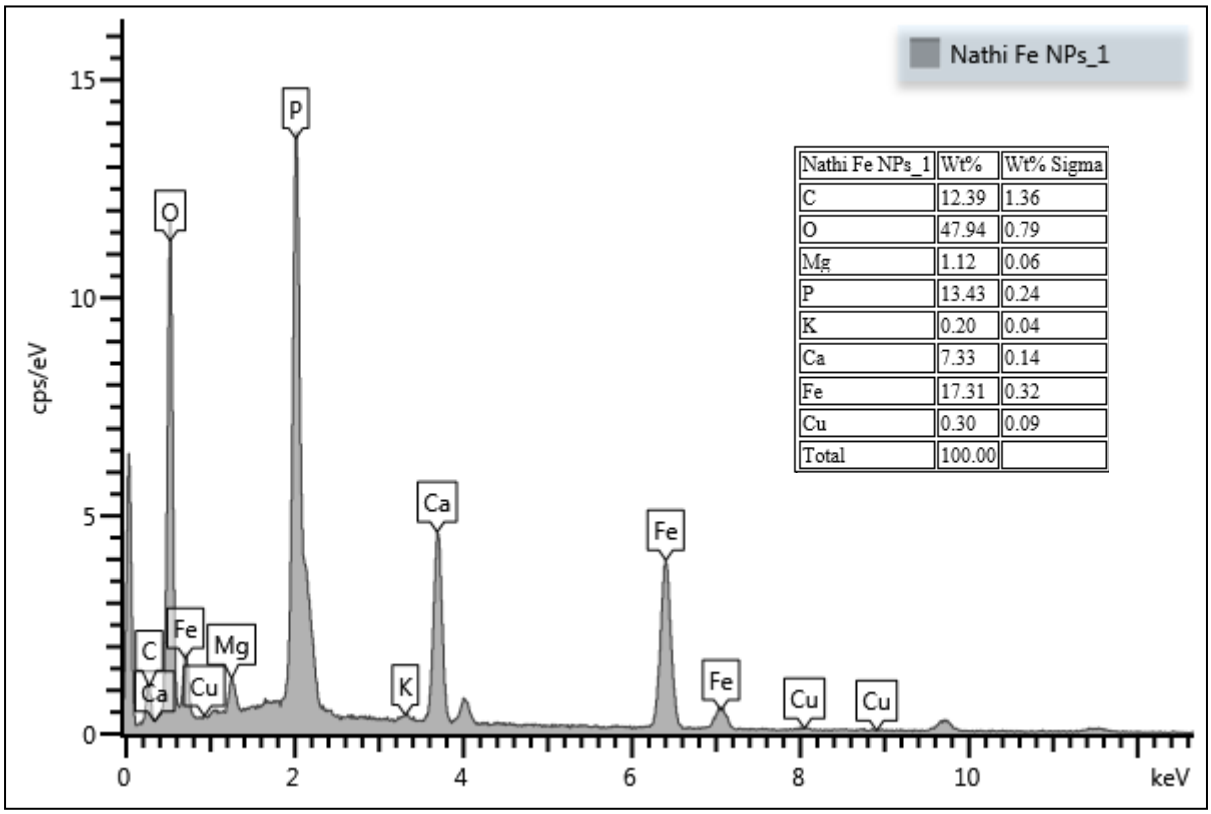

Nathi Fe NPs_1	Wt%	Wt% Sigma
C	12.39	1.36
O	47.94	0.79
Mg	1.12	0.06
P	13.43	0.24
K	0.20	0.04
Ca	7.33	0.14
Fe	17.31	0.32
Cu	0.30	0.09
Total	100.00	

Figure 6.3: Different elements present in the iron nanoparticles: SEM-EDX.

In comparison to the pure bioflocculant, nanoparticles in Figure 6.3 indicate that oxygen in the highest element present followed by iron with 17 Wt%. Indicating that the iron metal was able to bind onto the surface of the bioflocculant thereby producing nanoparticles. Elements such as Mg, P, K, Ca maybe as the results of the growth medium that was used for the extraction of the bioflocculant. As depicted in the above figure there was no iron present in the bioflocculant, which is the further confirmation of the nanoparticles synthesis.

6.3.4 SEM morphology of bioflocculant and iron nanoparticles

Figures 6.4 (A and B) illustrates the surface morphology of both the bioflocculant and nanoparticles. These analyses was done using the SEM. The morphology of the pure bioflocculant is hexagonal in shape (A) and surface morphology of iron nanoparticles is amorphous (B).

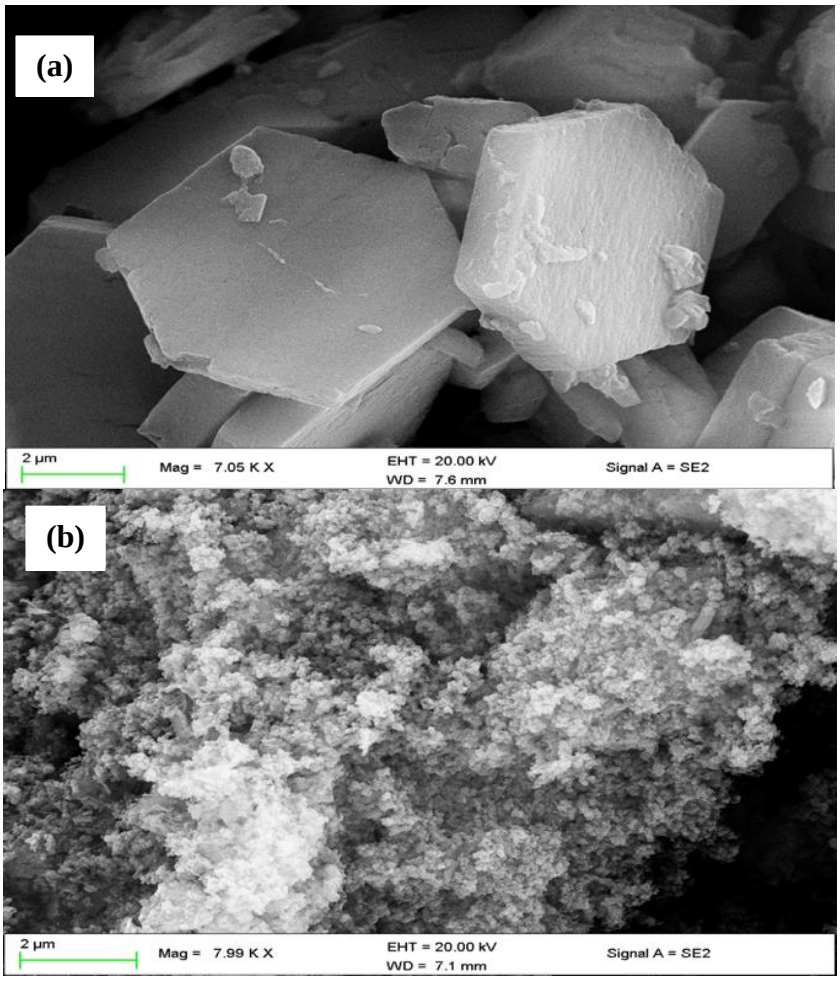

Figure 6.4: SEM image of the bioflocculant (a) and nanoparticles (b).

Figure 6.4 (a) and (b) shows scanning electron micrograph of bioflocculant and iron nanoparticles. Morphological changes are observed, the bioflocculant shape changed from hexagonal to amorphous when the iron was incorporated. Nanoparticles surface area maybe reactive due to the very small size they possess which constitutes to large surface area to volume (Handy et al., 2008). Forces such as van der Waals forces, electrostatic attraction or hydrophobic interaction can now act on the particles as the results of shorter distances between particles which ultimately aggregate particles during agglomeration (Handy et al., 2008).

Large surface area aid during flocculation suspended particles bind to the surface of the particle thereby forming larger flocks, which can faster easily.

6.3.5 TEM images of bioflocculant and iron nanoparticles

Images in Figures 6.5 and 6.6 of the bioflocculant and iron nanoparticles, show the approximation of size, range of nanoparticles. The synthesized iron nanoparticles seems to be spherical in shape and agglomerated.

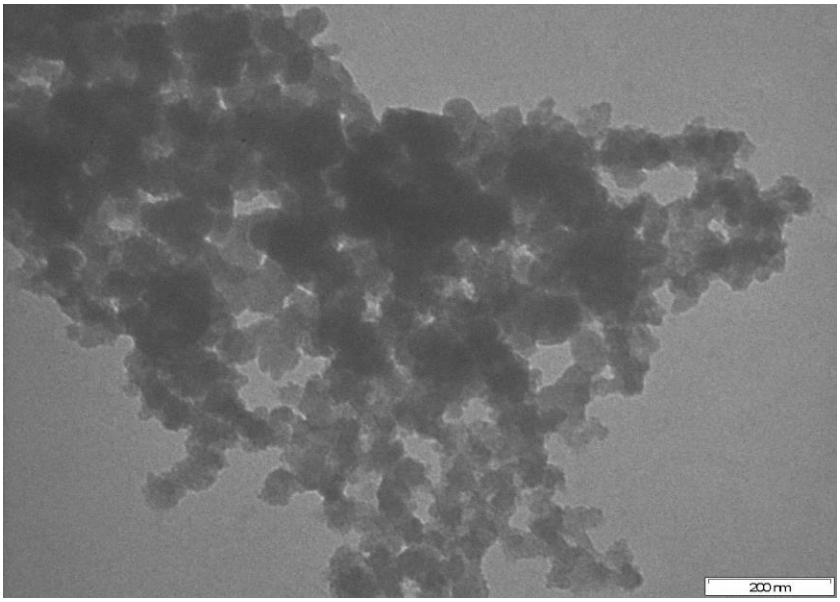

Figure 6.5: TEM image of the bioflocculant at 200nm scale.

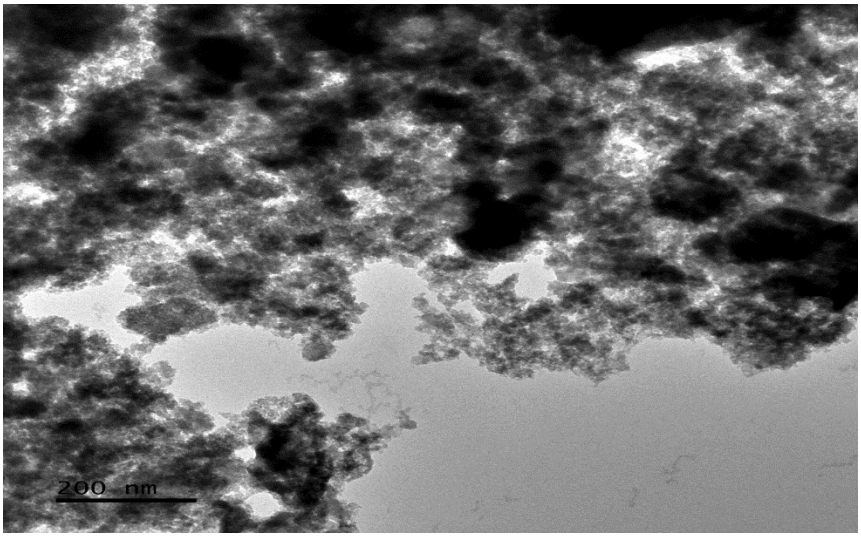

Figure 6.6: TEM image of iron nanoparticles at 200nm scale.

The TEM picture was somewhat blurred, perhaps by the surfactant matrix. Selected area electron diffraction on the iron nanoparticles failed to show any discernible electron diffraction indicating that the iron nanoparticles are amorphous. From Figure 6.5, it can be seen that the bioflocculant is clustered and single particles could be observed. The TEM image of this sample reveals that the majority of the sample is highly agglomerated.

6.3.6 X-ray diffraction results of bioflocculant and as-synthesized iron nanoparticles

Figure 6.7 illustrates the X-ray diffraction patterns of the purified bioflocculant and as-synthesised iron nanoparticles.

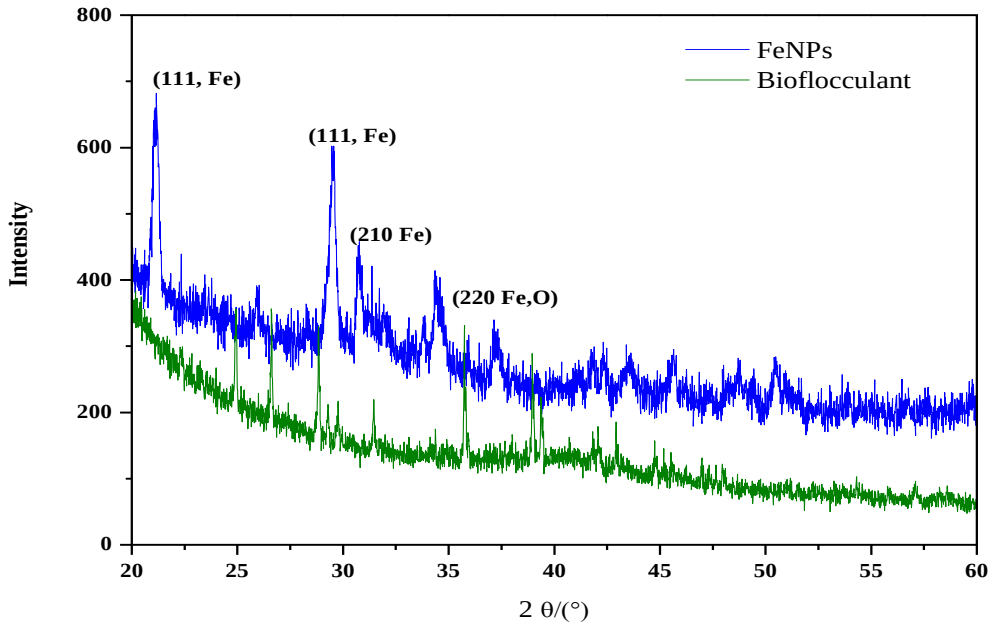

Figure 6.7: XRD of bioflocculant and FeNPs nanoparticles.

In figure 7, the broad peaks are seen between 2θ ~ 24°, 29°, 30° and 35° for the as-synthesized iron nanoparticles. For bioflocculant, the peak is observed at 2θ ~ 27°, 30° and 35° as depicted in figure 7. Consequently, crystallization of the bioorganic phase occurred on the surface of the iron nanoparticles or vice versa as suggested by the XRD results. The broadening of peaks in the XRD patterns of solids is mainly attributed the effect of particles size. Smaller particle size is signified by broad peaks. Furthermore, broader peaks may also signify the effects due to experimental conditions on the nucleation and growth of the crystal nuclei. Debye-Scherrer's

equation was used for calculating the particles size. The size of crystallite was ~53 nm which indicates a higher surface area and surface to volume ratio of the nanoparticles.

6.3.7 TGA analysis of bioflocculant and iron nanoparticles

Thermogravimetric analysis was performed to reveal the behavior under the heat on the bioflocculant and the iron nanoparticles. This analysis gives information of pyrolytic property of the material when exposed to high temperatures. Figure 6.8 indicates a cumulative weight loss of about 20% at about 150 °C and 36% cumulative weight loss at 700 °C. About 35% weight loss was observed at 200 °C in Figure 6.9.

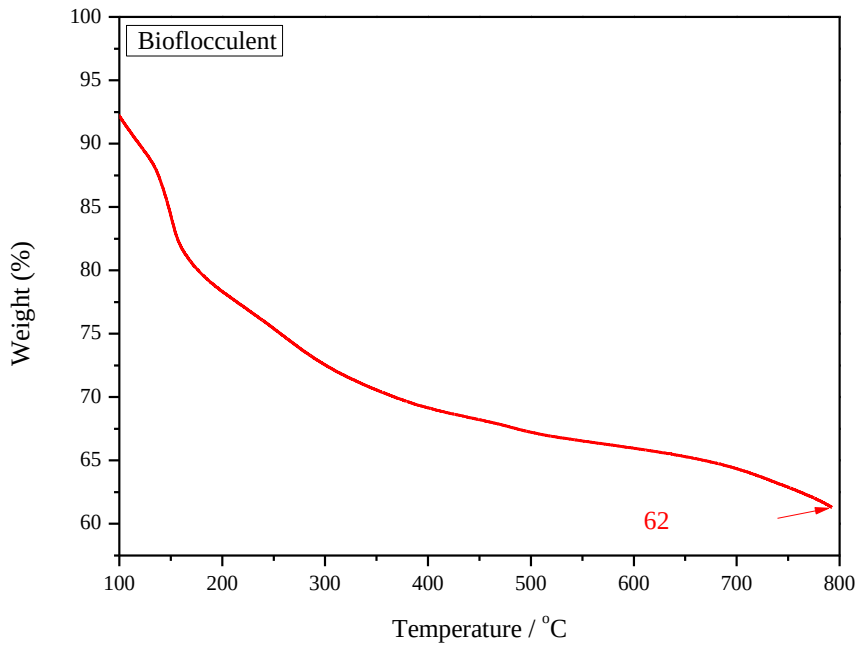

Figure 6.8: TAG analysis such of the bioflocculant.

Two phases of thermal degradation generally occur in a bioflocculant thermal. The first degradation phase is brought by loss of moisture which is due to increase in temperature up to about 150 °C which in turn results to weight loss. The second phase is brought about structure of the bioflocculant depolymerisation at temperatures above 400 °C. Behaviour of bioflocculant properties was investigated using thermogravimetric analysis (TGA) in the temperatures 30-800 °C. This technique enables us to comprehend the pyrolysis of the bioflocculant when exposed to very high temperature (Cosa et al., 2013). About 20% weight lost between 100 to 200 °C and at 500 °C, about 29% weight loss was observed from figure 8. The first weight loss could be as the result of moisture loss (Kumar and Anand, 1998).

Similarly, Okaiyeto (2015) documented similar findings. Contrary, different results were obtained for the bioflocculant p-KG03 produced by marine dinoflagellate *Gyrodinium impudicum* KG0, weight loss was initially observed at 40-230 °C (Yim et al., 2007).

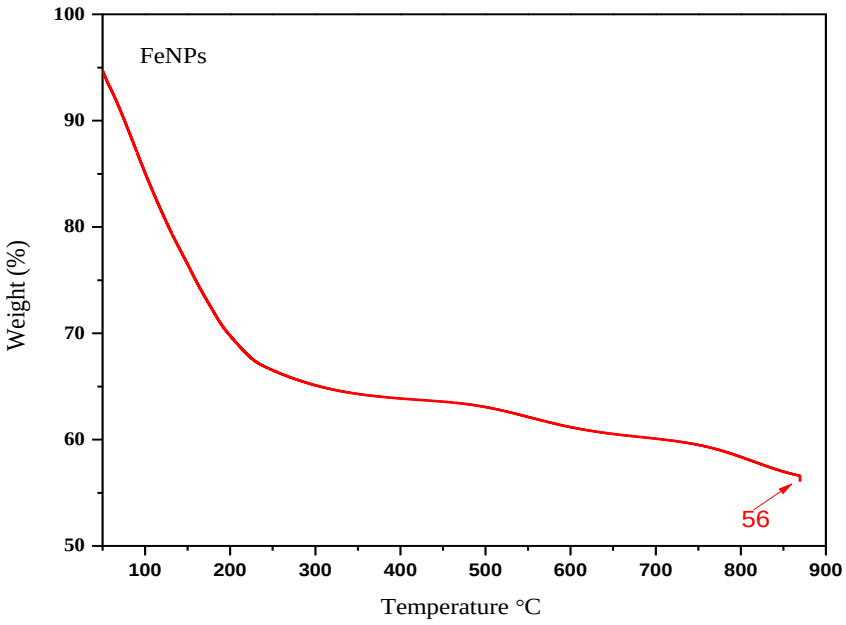

Figure 6.9: Thermogravimetric analysis of FeNPs.

Figure 6.9 elicits three phases in a TGA of iron nanoparticles. The first phase could be the result of loss in moisture content or drying of residual solvent that was used during purification is seen approximately from temperature 40 to 200 °C. The second phase is observed at temperatures around 400 °C, this could be related to decomposition of polymer that in turn resulted in weight loss. Moreover, further increase in temperature resulted in more weight loss in the synthesized nanoparticles. These findings suggest that synthesized nanoparticles are thermostable as they are able to maintain weight above 60% even at temperatures above 700 °C. This was related to thermal oxidation of iron nanoparticles to form iron oxide.

6.3.8 UV–vis spectrum of iron nanoparticles

Figure 6.10 represents the UV-visible spectrum of the iron nanoparticles at a wavelength of 300 nm. The findings revealed no straight peaks. This could be due to some impurities in the sample.

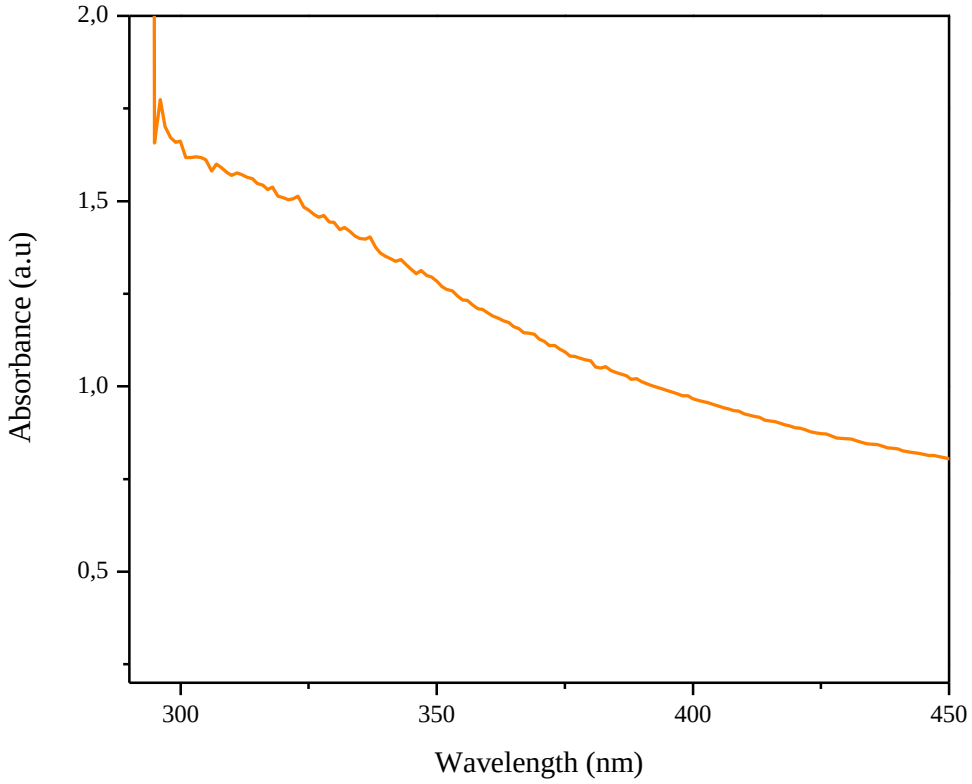

Figure 6.10: UV–vis spectrum of the as-synthesize FeNPs.

From Figure 6.10 UV-vis spectroscopy recorded from iron nanoparticles solution. This showed the plasmon resonance (SPR) spectra with absorbance 300-350 nm and the pic maxima for the synthesized particles was observed at around 300 nm. However, the no intensity of peaks could we observed and this may be due to impurities in the sample. This further explained that the reaction mixture's color changed rapidly from yellow to dark after the reaction between bioflocculant and $FeCl_3$. This could be ascribed to the formation of Fe nanoparticles. The change in colour of the bioflocculant from white to pale yellow colour indicated the formation of iron nanoparticles. FeNPs exhibited a pale yellow colour in solution due to surface plasmon vibration in FeNPs. Shift in exact position of the SPR band depend on the properties of the individual particle, these properties include shape, size and capping agents.

6.4 Conclusion

The synthesis iron nanoparticles revealed the presence of hydroxyl group (OH) and amine group (NH_2) in the sample. In comparison to a bioflocculant, there was no iron present in the pure bioflocculant and 17.31 Wt% iron was observed in the iron nanoparticles. Suggesting that iron was incorporated onto the bioflocculant. Furthermore, elements such as O, P, C, Ca, Cu and K were present in the sample. This can be attributed to the medium which was used for bioflocculant production. The size of crystallite was ~53 nm which indicates a higher surface area and surface to volume ratio of the nanoparticles. The synthesized nanoparticles are thermostable as they are able to maintain weight above 60% even at temperatures above 700 ℃. UV-vis spectrum illustrated the plasmon resonance (SPR) spectra with absorbance 300-350 nm and the pic maxima for the synthesized particles was observed at around 300 nm.

Declaration of interest

The authors declare that there is no conflict of interest.

Acknowledgements

Nkosinathi Dlamini would like to acknowledge the Council for Scientific and Industrial Research (CSIR, South Africa) for the financial assistance in the form of the Ph.D. bursary. Rajasekhar Pullabhotla would like to acknowledge the National Research Foundation (NRF, South Arica) for the financial support in the form of the Incentive Fund Grant and Research Developmental Grants for Rated Researchers (Grant No: 103691 and 116363).

Author Contributions: Conceptualization, A.K.B. and V.S.R.P.; formal analysis, N.G.D. and V.S.R.P.; investigation, N.G.D.; supervision, A.K.B. and V.S.R.P.; writing—original draft, N.G.D.; writing—review and editing, V.S.R.P.

Funding: National Research Foundation (NRF, South Arica) for the financial support in the form of the Incentive Fund Grant (Grant No: 103691) and Research Developmental Grants for Rated Researchers (Grant No: 103691 and 116363).

6.5 References

GONG, W.-X., WANG, S.-G., SUN, X.-F., LIU, X.-W., YUE, Q.-Y. & GAO, B.-Y. 2008. Bioflocculant production by culture of Serratia ficaria and its application in wastewater treatment. *Bioresource technology,* 99**,** 4668-4674.

GUO, S.-L., ZHAO, X.-Q., WAN, C., HUANG, Z.-Y., YANG, Y.-L., ALAM, M. A., HO, S.-H., BAI, F.-W. & CHANG, J.-S. 2013. Characterization of flocculating agent from the self-flocculating microalga Scenedesmus obliquus AS-6-1 for efficient biomass harvest. *Bioresource technology,* 145**,** 285-289.

HANDY, R. D., VON DER KAMMER, F., LEAD, J. R., HASSELLÖV, M., OWEN, R. & CRANE, M. 2008. The ecotoxicology and chemistry of manufactured nanoparticles. *Ecotoxicology,* 17**,** 287-314.

HUBER, D. L. 2005. Synthesis, properties, and applications of iron nanoparticles. *Small,* 1**,** 482-501.

MATA, Y., TORRES, E., BLAZQUEZ, M., BALLESTER, A., GONZÁLEZ, F. & MUNOZ, J. 2009. Gold (III) biosorption and bioreduction with the brown alga Fucus vesiculosus. *Journal of hazardous materials,* 166**,** 612-618.

OKAIYETO, K., NWODO, U. U., MABINYA, L. V., OKOLI, A. S. & OKOH, A. I. 2015. Characterization of a Bioflocculant (MBF-UFH) Produced by Bacillus sp. AEMREG7. *International journal of molecular sciences,* 16**,** 12986-13003.

SATHIYANARAYANAN, G., KIRAN, G. S. & SELVIN, J. 2013. Synthesis of silver nanoparticles by polysaccharide bioflocculant produced from marine Bacillus subtilis MSBN17. *Colloids and Surfaces B: Biointerfaces,* 102**,** 13-20.

SINGH, R., TRIPATHY, T., KARMAKAR, G., RATH, S., KARMAKAR, N., PANDEY, S., KANNAN, K., JAIN, S. & LAN, N. 2000. Novel biodegradable flocculants based on polysaccharides. *CURRENT SCIENCE-BANGALORE-,* 78**,** 798-803.

SUBUDHI, S., BISHT, V., BATTA, N., PATHAK, M., DEVI, A. & LAL, B. 2016. Purification and characterization of exopolysaccharide bioflocculant produced by heavy metal resistant Achromobacter xylosoxidans. *Carbohydrate polymers,* 137**,** 441-451.

SUN, Y.-P., LI, X.-Q., CAO, J., ZHANG, W.-X. & WANG, H. P. 2006. Characterization of zero-valent iron nanoparticles. *Advances in colloid and interface science,* 120**,** 47-56.

SWIERCZEWSKA, M., HAN, H., KIM, K., PARK, J. & LEE, S. 2016. Polysaccharide-based nanoparticles for theranostic nanomedicine. *Advanced drug delivery reviews,* 99**,** 70-84.

YOU, Y., HAN, J., CHIU, P. C. & JIN, Y. 2005. Removal and inactivation of waterborne viruses using zerovalent iron. *Environmental science & technology,* 39**,** 9263-9269.

ZHANG, W., HE, H., FENG, Y. & DA, S. 2003. Separation and purification of phosphatidylcholine and phosphatidylethanolamine from soybean degummed oil residues by using solvent extraction and column chromatography. *Journal of Chromatography B,* 798**,** 323-331.

Chapter 7 ARTICLE 5: Biosynthesis, characterization, and application of iron nanoparticles: in dye removal and as antimicrobial agent

Dlamini G Nkosinathi [a]*, Basson K Albertus [a], Shandu Jabulani[a], Mavuso Sboniso[a], Rajasekhar VSR Pullabhotla [b]*

[a] Department of Biochemistry and Microbiology, University of Zululand, Private Bag X1001, KwaDlangezwa, 3886, South Africa

[b] Department of Chemistry, University of Zululand

***** Correspondence; E-Mail: nathidlamini03@gmail.com; PullabhotlaV@unizulu.ac.za

Tel. +27- 35 9026155 / +27-79 6828 444

Abstract: Green protocols for synthesizing nanoparticles have demonstrated numerous benefits and advantages, which include environmental friendliness, good efficacy and possess less threat to human. The aim of this study was to biosynthesize, characterize and evaluate the effectiveness of biosynthesized iron nanoparticles. The bioflocculant was extracted using a solvent extraction method and purified by 100 mL distilled water and a mixture of chloroform and butanol (5:2 v/v). Iron nanoparticles (FeNPs) were successfully synthesized through the chemical reduction method, where 0.5 g of bioflocculant was mixed with 3 mM iron sulphate ($FeSO_4$) solution and left to stand at room temperature for 24 hrs. Characterization of the as-synthesised nanoparticles was achieved through the use of a Scanning Electron Microscope (SEM), Energy Dispersive X-ray Spectroscopy (EDX), and Fourier-Transform Infrared spectroscopy (FT-IR). The various parameters that effect on flocculation activity were evaluated, with optimum flocculation activity at a dosage size of 0.4 mg/mL (88%). The FeNPs were found to be cation-dependent Mg^{2+} (82%) and flocculate both in acidic pH 3 and in alkaline pH 11 with (93%) flocculation activity. The synthesized FeNPs are thermostable as they maintain flocculation activity above 80% at 100 ºC temperatures.

Key words: dye removal, flocculation activity, iron nanoparticles, optimization.

7.1 Introduction

Freshwater is a major source of water for human and animals. Industrialization, population growth and changes in climate have resulted in water scarcity in most countries, especially developing countries (Vörösmarty et al., 2004). There are general methods that are applied in water purification, which include, boiling, filtration, sedimentation and salting-in method (Buthelezi et al., 2012). Chemicals used are of viewed as the better water treatment tools as they are highly efficient and cheaper. However, the inadequacy is that they have been found to be environmentally unfriendly and detrimental to human health (Exley et al., 2006).

Conversely, bioflocculants have recently gained a huge interest to most researchers because of remarkable properties they possess. Bioflocculants are defined as secondary metabolites which are produced by microorganisms during growth (Lee and Chang, 2018). These unique properties which bioflocculants possess, include biodegradability eco-friendliness and the fact that they cause less secondary pollution. Their method of production is very expensive irrespective of how good they are, give lower yield and are not as effective as chemical flocculants. This makes them not to be industrially viable (Ugbenyen and Okoh, 2014).

Nanoparticles are defined as particles with size ranged from 1-100 nm and have modified chemical, physical properties (Shinde and More, 2009). Various methods have been reported on the synthesis of nanoparticles. This includes both physical and chemical methods. However, both methods have limitations. For an example, one being the consumption of a lot of energy and the other may involve the use of toxic chemicals. To overcome these shortcomings, metallic nanoparticles have been synthesised using the biosynthesis procedure and used in the water treatment (Devatha et al., 2016).

In this present study, we report on the synthesis of iron nanoparticles (FeNPs) using a bioflocculant from *A. faecalis* HCB2, an isolate from marine water. Recently the use of biological entities such as bioflocculant and plant extracts are used as both the capping and reducing agents in the synthesis of nanoparticles. This is due to the functional groups they possess. This can act as reducing agents (Muthulakshmi et al., 2017). The production of nanoparticles using bioflocculants is simple, rapid and dependable amongst the other methods and this can be achieved under the mild and controlled conditions (Sathiyanarayanan et al., 2013). The synthesized FeNPs were optimized for flocculation, dye degradation and antimicrobial activity.

7.2 Methodology

7.2.1 Extraction and purification of the bioflocculant produced by *A. faecalis* HCB2

The *Alcaligenes faecalis* was previously isolated from marine environment Sodwana Bay, KwaZulu-Natal province of South Africa, verified using nucleotide sequencing of the 16S rRNA. Preservation methods for bacterial strains were taken into consideration and stored at -80 ºC. The bioflocculant production medium was prepared according to the method given by He et al. (2007). Filtered natural marine water was used to prepare a production medium and was sterilized by autoclaving for 15 min. at 120 ºC. Bioflocculant was extracted and purified, where culture medium was inoculated with the *A. faecalis* HCB2 and incubated for 3 days at 30 ºC with a shaking speed of 160 rpm. The mixture was centrifuged at (5000 × rpm, 4 ºC, for 30 min.), the supernatant was collected and subjected into 2000 mL ethanol for extraction and allowed to precipitate at 4 ºC for 12 hrs. The precipitate was vacuum dried, the crude bioflocculant that was obtained dissolved in100 mL of distilled water, and a mixture of 79 mL chloroform, 21 mL butanol was added and left for 12 hrs at 25 ºC to allow sedimentation of cell-free supernatant finally collected and vacuum dried (He et al., 2009).

7.2.2 Biological synthesis of iron nanoparticles and characterization

Iron sulphate ($FeSO_4$) was used as the metal precursor for the synthesis of iron nanoparticles. FeNPs were synthesised according to method described by Dlamini et al. (2019) where 0.5 g of pure bioflocculant was dissolved in 0.2 M ($FeSO_4$) and 10 mL of 5.0 M sodium hydroxide (NaOH) solution was added to prevent agglomeration of nanoparticles. The mixture was left overnight at room temperature and colour change was observed, which was an indication for the formation of nanoparticles. To harvest the synthesised nanoparticles the mixture was centrifuged at 5000 rpm at 4 ºC for 15 min. resulting precipitate was vacuum dried at 25 ºC for 24 hrs. Physical observation of the mixture and characterization was done to confirm the formation of FeNPs. The negative control was prepared by excluding bioflocculant in the iron solution (Dlamini et al., 2019b). TEM and SEM techniques were used to identify the surface morphology and elemental composition of the biosynthesised FeNPs. FT-IR spectroscopy technique was used to verify functional groups present in the as-synthesised iron nanoparticles.

7.2.3 Evaluation of Flocculation activity of the biosynthesised FeNPs

Different solutions of the iron nanoparticles having concentrations (0.2, 0.4, 0.6 and 0.8 mg/mL) were prepared by diluting FeNPs with distilled water to obtain respective concentration. Kaolin clay was used as the test material. 4 g/L of kaolin solution was prepared with distilled water, where the 100 mL of kaolin solution, 2 mL of FeNPs and 3 mL of 1% $CaCl_2$ was transferred into a 300 mL conical flask (Cosa et al., 2011). The mixture was vigorously mixed for the 1 min then transferred into a measuring cylinder (100 mL), and then allowed to settle and form sediments for 5 min. at 25 ºC. This procedure was also followed for the control, where 2 mL nanoparticles were replaced by 2 mL distilled water. The clear top layer of the supernatant was pipetted into a cuvette to determine the flocculation activity (Karthiga devi and Natarajan, 2015). The UV-visible spectrophotometer was used to measure the optical density (OD_{550nm}) of the liquid (1 cm beneath the fluid level); the result was used to calculate the flocculating rate of the FeNPs and control. The formula that was used to calculate the flocculation activity is as given below:

$$FA(\%) = \frac{A - B}{A} X\ 100 \qquad (1)$$

Where A and B are for optical density at 550 nm of the blank control and the suspension treated by FeNPs respectively.

7.2.3.1 Effect of cations on flocculating activity

A wide variety of cations containing solution were used to replace 1% $CaCl_2$ salt solution ranging from monovalent (LiCl & NaCl), divalent ($MgCl_2$ & $CaCl_2$) and trivalent ($FeCl_3$) at the same concentration then the control without cations was also prepared. To measure the flocculating activity, same procedure that was used in the effect of dosage size.

7.2.3.2 Effect of pH and temperature on flocculating activity

The (100 mL) kaolin clay suspension's pH was adjusted with either NaOH or HCl in a pH range (3 to 11), the addition of 2 mL of FeNPs and 3 mL of the cations that showed highest flocculating activity. The flocculation activity was assessed using previously described methods. The FeNPs were subjected to high temperatures (50-100 ºC) in a water bath for 30 min. after which a flocculation activity was calculated using a method described above (Cosa et al., 2011).

7.2.4 Antimicrobial assay

7.2.4.1 Bacterial strains reviving step

Bacterial strains (Gram positive and Gram negative) were transferred into separate sterile nutrient broth, then the broth was incubated at 37 ºC for 12 hrs. 1 mL of *Bacillus subtilis* CSM5 and *Escherichia coli* ATCC 25922 were transferred into different 9 mL sterile nutrient broth contained in the test tubes. The mixture was incubated at 37 ºC for 12 hrs. UV-Visible spectrophotometer (600 nm) was used to determine the bacterial turbidity/absorbance; the turbidity was adjusted to be in line with the McFarlan standards (0.5).

7.2.4.2 Minimum inhibitory concentration (MIC)

Nutrient broth (23 g) was prepared using 1000 mL of distilled water and sterilized by autoclaving for 15 min. at 120 ºC. Streptomycin (50 µL) was used as a positive control. A series of dilutions factor was prepared using 96 micro wells plates. Sterile nutrient broth (50 µL) was poured in all wells followed by addition of 50 µL of bacterial strain into the corresponding wells from highest concentration to the lowest concentration. FeNPs (50 µL) was added into the corresponding wells then streptomycin (50 µL) was added into corresponding well where distilled water participated as a negative control. The colour changes were observed after the addition of 40 µL from a solution 0.2 mg/mL of p-iodonitrotetrazolium (INT) indicator in the solutions after overnight incubation at 37 ºC (Maliehe et al., 2015).

7.2.5 Dye removal efficiency by nanoparticles

Removal efficiency (RE) experiment was conducted, where 2 mL of iron nanoparticles with concentration (0.2 mg/mL) and 3 mL of 1% Mg^{2+} was added into 100 mL solution of each dye with a concentration of 4 g/L. Safranin, methylene blue, methylene orange, and malachite green are the dyes which were used. The mixture was left at room temperature for 5 min before the supernatant was taken for analysis at a maximum wavelength for each dye. The removal efficiency was calculated using the formula below:

$$RE\ (\%)\frac{C0 - C1}{C1} X\ 100 \qquad (2)$$

Where: C_0 is the initial value and C_1 is the value after the flocculation treatment.

7.2.6 Statistical analysis

The experimental data was collected in triplicates and error bars on the Figures represent the standard deviation of the data. All data were subjected to one-way variance analysis using graph pad prism version 6.1, where a significant level of $p<0.05$ was used.

7.3 Results and discussion

7.3.1 Morphology of iron nanoparticles observed under SEM

Figure 7.1 shows the approximation of size range of nanoparticles. The synthesized iron nanoparticles seem to be granular like and agglomerated.

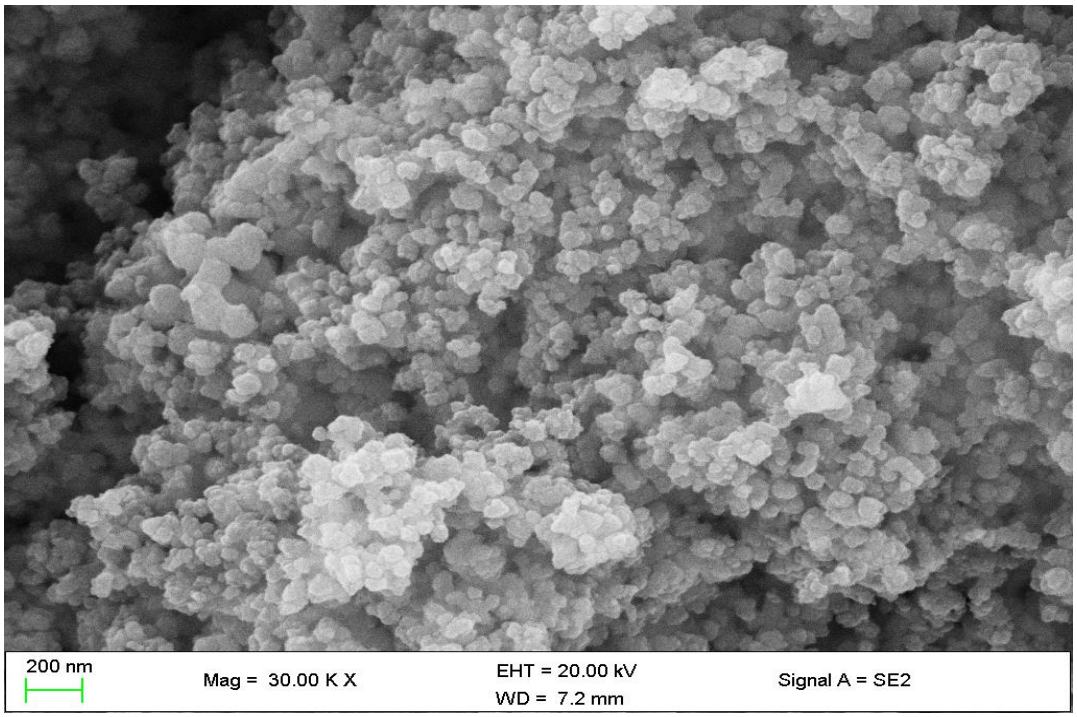

Figure 7.1: SEM image of iron nanoparticles at 200 nm scale.

The morphology characterization of iron nanoparticles was achieved using Scanning Electron Microscope (SEM). As depicted in a Figure 1 above, the synthesized nanoparticle resembles a granular like morphology and seems to be agglomerated together. Morphology plays an important role during flocculation. Materials with increased surface area turn to have an affinity to bind suspended solids which in turn results in improved removal efficiency and improved flocculation activity (Xia et al., 2018). The agglomeration could be due to the result of forces between the particles.

7.3.2 Elemental analysis of iron nanoparticles

Figure 7.2 shows the results of SEM-EDX analysis, where one can notice the various elements present in the synthesised nanoparticles. The composition includes O, Fe, P, Ca, Mg, Cu and K. The element with the highest Wt.% was O with 47.94 Wt.%, while K was the least with just 0.20 Wt.%.

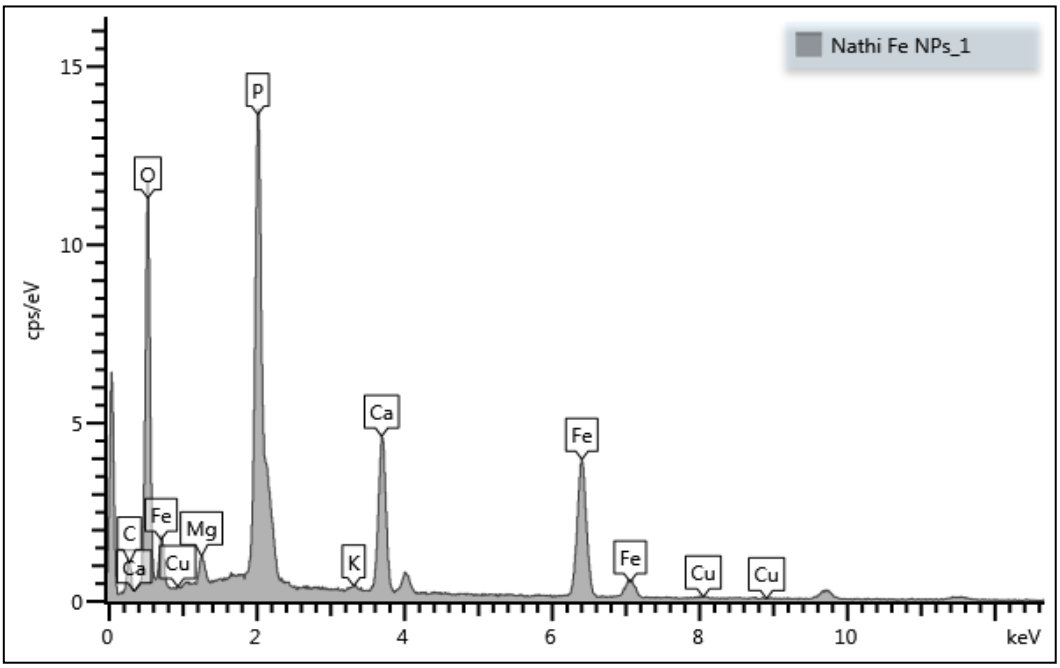

Figure 7.2: SEM-EDX results of iron nanoparticles.

The bioflocculant, which was used for the synthesis of iron nanoparticles, consisted mainly of sugars, which constitute the high carbon and glucose content in the sample. The high amount of iron present in the sample is an indication of iron incorporation, which confirms the formation of the bioflocculant passivated iron nanoparticles. Furthermore, iron is the next highest element present in the sample after oxygen with 17.31Wtpercentage. The presence of oxygen and carbon in the sample is an indication that the bioflocculant, which was used for synthesis, is polysaccharide in nature.

7.3.3 The functional groups present in the bioflocculant and iron nanoparticles

Figure 7.3 shows FT-IR spectrum of the bioflocculant and the synthesised iron nanoparticles. The band at 3244 cm^{-1} (iron nanoparticles) represents the presence of hydroxyl (-OH) group and amine ($-NH_2$) group in the samples. The weak band at 1646 cm^{-1} could be designated to the presence of aliphatic bonds. The peak located at 978 cm^{-1} indicates the presence of an

amide group. The vibrational peaks at 523 cm^{-1} is analogous to the C-O stretching in alcohols, which confirms the -OH group presence.

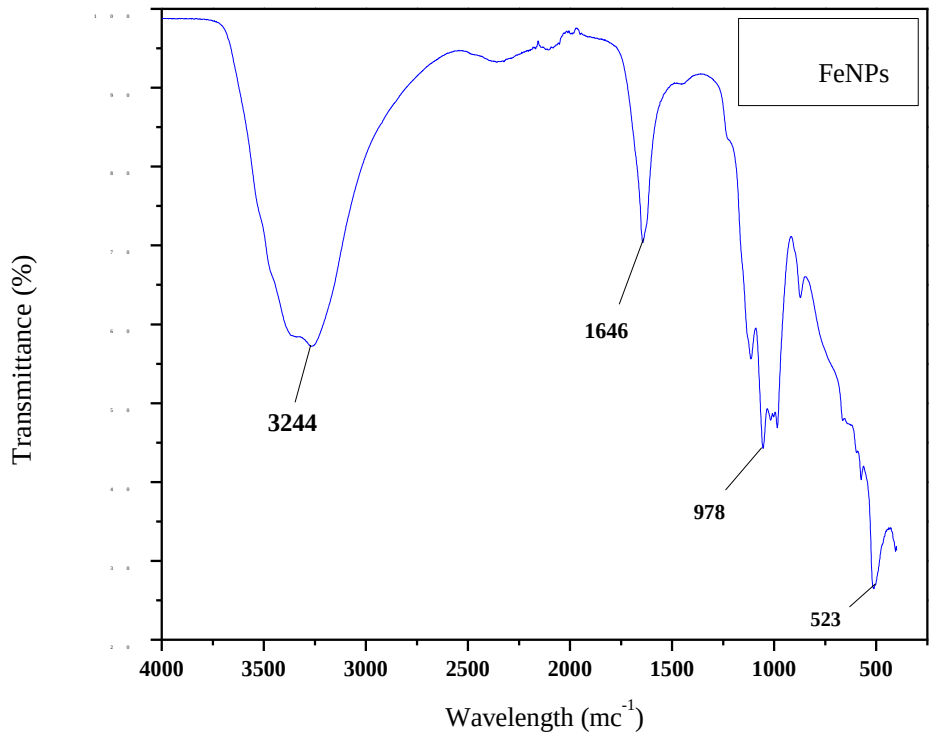

Figure 7.3: FT-IR spectrum of the iron nanoparticles.

The different functional groups showed by Fourier-Transform Infrared Spectroscopy (FT-IR) play an important role during the formation of nanoparticles. Biological entities such as plant extract and bioflocculant are said to possess functional groups which reduce metals salts to form nanoparticles (Muthulakshmi et al., 2017). Moreover, functional groups act as binding sites for suspended particles to flocs which results into flocculation (Gao et al., 2006). The two bands at 3244 cm^{-1} shows the presence of hydroxyl group which is highly negatively charged and this group provided the site for adsorption of positively charged metal ions in the solution, hence the formation of FeNPs. The band at 1646 cm^{-1} revealed the presence of an amine group, which significantly permits the FeNPs chain to be spread evenly because of the electrostatic forces. The presence of -OH and C-O groups signifies that the bioflocculant mainly consists of polysaccharides.

7.3.4 Effect of dosage size on flocculation activity

Figure 7.4 below shows the dosage flocculation activity on iron nanoparticles, 0.4 mg/mL gave the highest flocculation activity of 82%.

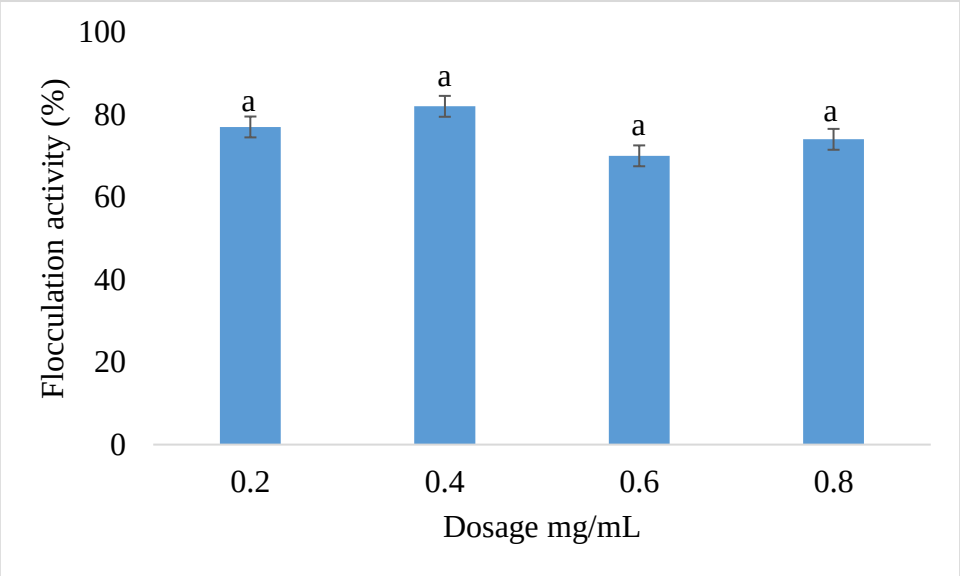

Figure 7.4: Dosage effect on flocculation activity. Percentage flocculating activities with letter (a) are significantly ($p<0.05$) different. (Refer to index data Table 7.4).

To determine the optimum dosage concentration, different dosage sizes of FeNPs were analysed for their flocculation activity ranging from 0.2-0.8 mg/mL. Okaiyeto et al. (2015) explained the mechanism of high viscosity generation caused by high dosage concentration which also hinders the rate at which solid particles in solution settles (Okaiyeto et al., 2015a). In this current study, the similar observation was made. Figure 7.4 Shows the optimum flocculation activity of 88 % at a concentration of 0.4 mg/mL, where the increase in the concentration caused a slight decrease in the flocculation activity. However, Analysis of Variance One-way (ANOVA) revealed that the difference between optimum (0.4 mg/mL) concentration and the lowest (0.2 mg/mL) concentration was not significant statistically, which allowed the use of 0.2 mg/mL for subsequent experiments. These results are similar to those obtained by Cosa et al. (2013), where the bioflocculant produced by *Halobacillus sp*. had an optimal dosage of 0.4 mg/mL. The slight decrease in flocculation activity of FeNPs may be due to high viscosity formed by high concentration present in the solution. This tends to block the adsorption site for molecule and hindered the movement motion of FeNPs to flocculate the suspended particles in the solution (Cosa et al., 2013).

7.3.5 Effect of cations on Flocculation activity of iron nanoparticles

Table 7.1 below represents the results of cations effect on flocculation activity. The synthesized nanoparticles were found to be cation dependent with 46% flocculation activity in the absence of cation.

Table 7.1: Cations effect on flocculation activity

Cations	Flocculation activity (%) ± SD
Control	46 ± 2.03^{b}
Fe^{3+}	85 ± 2.72^{a}
Mg^{2+}	82 ± 1.53^{a}
Ca^{2+}	82 ± 3.64^{a}
Li^{+}	72 ± 1.15^{a}
Na^{+}	72 ± 1.15^{a}

Values represent mean ± deviation of replicate readings. Flocculation activities percentage with different letters (a & b) are significantly ($p<0.05$) different. (Refer to index data Table 7.5).

Ungbenyen and Okoh (2014) stated the role of the metallic ions that contain divalent and trivalent charges. This is to elevate the initial adsorption/binding of the polymer on the particles by lowering the negative charge on both polymer and particles in the solution. In the present study, divalent metals showed high flocculation activity this was due to electrostatic force between the FeNPs and the kaolin clay, since the clay contain a negative charge the interaction was elevated by Mg^{2+} which showed 82% flocculation activity as depicted in Table 7.1 Although identical results were observed for Ca^{2+}, the statistical analyser showed that there were no statistical differences since these cations are also micronutrient and are essential to the living system. Any one of these cations two can be used, but in this study, magnesium was preferred because of its physical and chemical properties as well as availability. The control proved that the FeNPs are cation dependant as it showed the lowest flocculation activity (Ugbenyen and Okoh, 2014).

7.3.6 Effect of pH on Flocculation activity of iron nanoparticles

Figure 7.5 indicates the effect of pH on the flocculation activity of iron nanoparticles; the nanoparticles flocculate well at all pH ranges (acidic, neutral, and alkaline). However, the optimum flocculation was achieved at an alkaline pH of 11 with 93% flocculation activity.

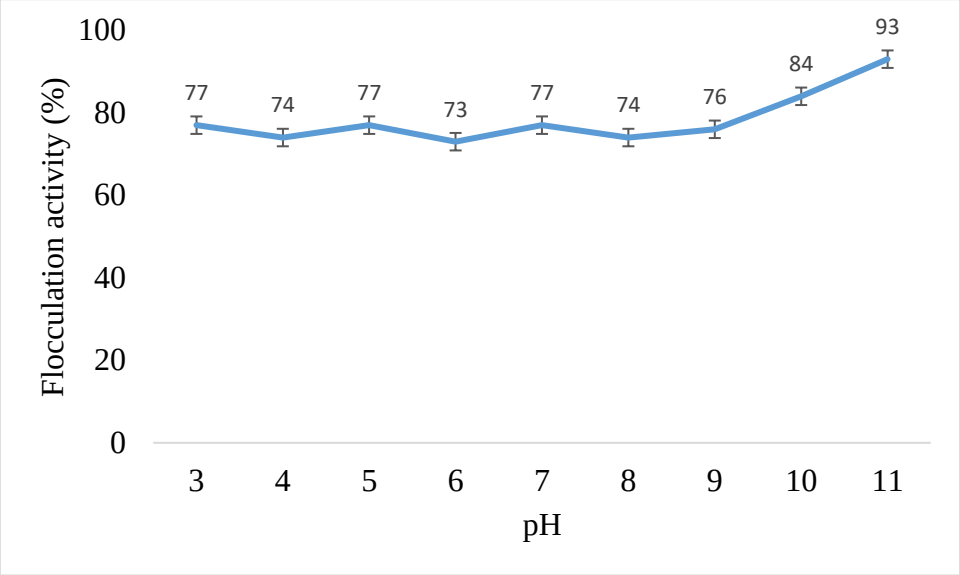

Figure 7.5: Effect of pH on flocculation activity. (Refer to index data Table 7.6).

The pH plays a vital role during the flocculation (Yang et al., 2009). The flocculation activity of the biosynthesised FeNPs was evaluated at a concentration of 0.4 mg/mL within the pH range of 3-11. The flocculation activity was highly effective at a wide range of pH with a flocculation activity above 70% with an optimum of 93% at pH 11. This may be due to the environment in which the microorganism was isolated, i.e. marine environment, which is more alkaline. The functional groups that were revealed by FT-IR spectroscopy facilitated the flocculation where they ionised more at the basic condition and attracted more particles forming the flocs in the solution. Since the FeNPs were mostly composed of polysaccharides that are more stable in harsh conditions. This could justify the consistency in flocculation activity of above 70% and even at the extremely acidic environment. The pH stability of the FeNPs signifies the potential for industrial application to treat water without adjustments of the pH during the purification, which can in turn reduce cost as it reported that bioflocculant limitation in the industrial application includes low efficiency and cost (Bo et al., 2012).

7.3.7 Effect of temperature on Flocculation activity of iron nanoparticles

Figure 7.6 below reveals the thermostability of iron nanoparticles. The results indicate that the synthesized nanoparticles are heat stable as they retained up to 88% flocculation at 100 °C.

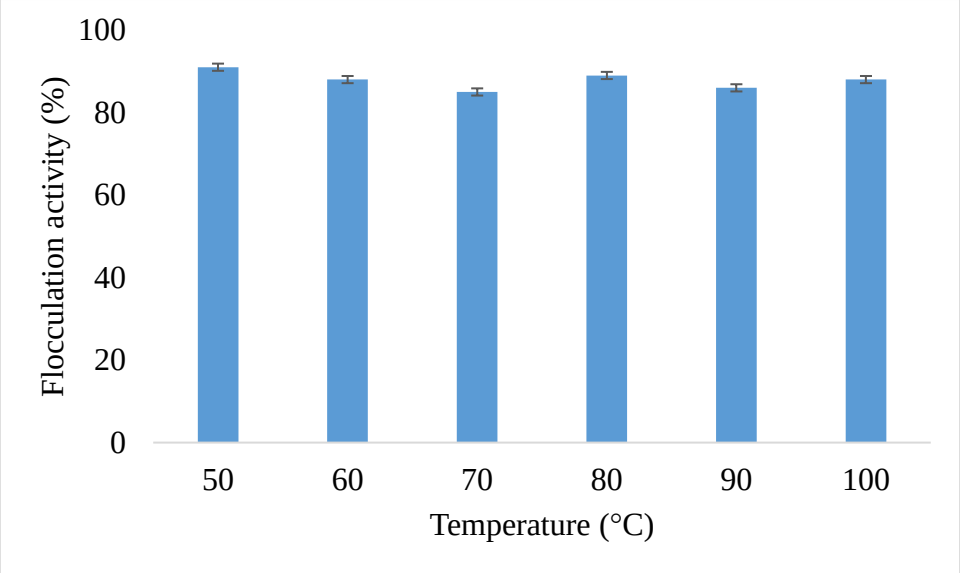

Figure 7.6: Effect of temperature on flocculating activity. (Refer to index data Table 7.7).

The iron nanoparticles synthesised through chemical reduction between the bioflocculant and iron sulphate were subjected to different temperatures to evaluate their flocculation activity and thermal stability. Since there were no statistical differences and the flocculation activity was above 80%, this could be attributed to the properties of iron to withstand high temperature. Moreover, the bioflocculant which was used consisted mainly of polysaccharides. These constitute the backbone of FeNPs (Sun et al., 2012). This also facilitated to obtain such results which are similar to those obtained when the bioflocculant produced by *Bacillus sp*. were thermally stable when exposed to various temperatures because of the carbohydrate composition (Zaki et al., 2013). The results obtained in this study show the potential of the FeNPs to be applied even in high temperature processes at an industrial scale.

7.3.8 Antimicrobial effect of iron nanoparticles

Table 7.2 represents the antimicrobial activity of iron nanoparticles in comparison with *Streptomycin*. There was no antimicrobial activity on the synthesized nanoparticles.

Table 7.2: Antimicrobial test

	FeNPs	*Streptomycin*
Bacterial Strain	MIC (mg/mL)	MIC (mg/mL)
E. coli	None	6.25
B. subtulis	None	3.125

The antimicrobial activity assay was done to evaluate the effect of the biosynthesized FeNPs on to gram positive and Gram-negative bacterial strain. The test strains were *E.coli* which is a gram negative and gram positive *B. subtilis.* The results were negative for both strains, this is due to the transport system of the organism, and for example, *E. coli* produces sidophores, which facilitates the absorption of iron by the cell and *B. subtilis.* Most bacterial species use iron as a core factor in different proteins (Olsen et al., 2005). This may be the reason for non-inhibitory effect on both test strains and it may be as the result of low concentration of FeNPs (0.2 mg/mL) which was used. Contrary to this, the study where zero valent iron nanoparticles revealed some remarkable antimicrobial properties when *S. aureus* and *E.coli* were used (Mahdy et al., 2012).

7.3.9 Staining dye removal

Table 7.3 below shows the effect of iron nanoparticles on staining dyes removal. The nanoparticles were very poorly performed in the removal of dyes.

Table 7.3: Removal efficiency (RE) of dyes by nanoparticles.

	Dye type	RE (%)		Dye type	RE (%)
FeNPs	Methylene blue	20	FeNPs + Mg^{2+}	Methylene blue	31
	Malachite green	39		Malachite green	48
	Safranin	5		Safranin	12
	Methylene orange	45		Methylene Orange	58

The effect of iron nanoparticle on removal was evaluated and removal efficiency (RE) was calculated. A 2 mL of 0.2 mg/mL iron nanoparticles were mixed with 100 mL of 4 g/L of dye solution, the mixture was left standing for 5 min, and the supernatant was withdrawn and analysed using UV-VIS Spectrophotometer Pharo 300 Spectroquant® at 620 nm. The removal efficiency was very poor for all the dyes tested. However, there was a slight increase in removal efficiency when the cation was added. The synthesized nanoparticles were able to achieve up to 58% (RE) on methylene blue. To improve the effectiveness of nanoparticles a dosage and time contact may be increased.

7.4 Conclusion

Iron nanoparticles were synthesized using a polysaccharide bioflocculant and characterized using SEM, TEM, and FT-IR techniques. The nanoparticles revealed a granular like morphology and the elementary analysis revealed the significant increase of iron (Fe) in the sample. The functional groups included hydroxyl and amine which signify that the bioflocculant consisted mainly of polysaccharide. The optimum dosage was found to be 0.4 mg/mL however, statistics revealed that 0.2 mg/mL can also flocculate effectively. Cation effect was evaluated and divalent cations were found to be the most effective with flocculation above 80% and were found to be pH dependent and thermostable. The FeNPs showed potential to remove basic dyes in the presence of magnesium ions and were found not to have any inhibitory effect on microorganisms.

Declaration of interest

The authors declare that there is no conflict of interest.

Acknowledgements

Nkosinathi Dlamini would like to acknowledge the Council for Scientific and Industrial Research (CSIR, South Africa) for the financial assistance in the form of the Ph.D. bursary. The authors would like to acknowledge the Electron Microscopy Unit at the University of KwaZulu-Natal, Westville campus, for providing support by letting us use the TEM and SEM-EDX facilities for the characterization of nanomaterials. Rajasekhar Pullabhotla would like to acknowledge the National Research Foundation (NRF, South Arica) for the financial support in the form of the Incentive Fund Grant (Grant No: 103691) and Research Developmental Grants for Rated Researchers (Grant No: 116363).

7.5 References

Bo, X., Gao, B., Peng, N., Wang, Y., Yue, Q., & Zhao, Y. (2012). Effect of dosing sequence and solution pH on floc properties of the compound bioflocculant–aluminum sulfate dual-coagulant in kaolin–humic acid solution treatment. *Bioresource technology, 113*, 89-96.

Buthelezi, S. P., Olaniran, A. O., & Pillay, B. (2012). Textile dye removal from wastewater effluents using bioflocculants produced by indigenous bacterial isolates. *Molecules, 17*(12), 14260-14274.

Cosa, S., Mabinya, L. V., Olaniran, A. O., Okoh, O. O., Bernard, K., Deyzel, S., & Okoh, A. I. (2011). Bioflocculant production by Virgibacillus sp. Rob isolated from the bottom sediment of Algoa Bay in the Eastern Cape, South Africa. *Molecules, 16*(3), 2431-2442.

Cosa, S., Ugbenyen, A. M., Mabinya, L. V., Rumbold, K., & Okoh, A. I. (2013). Characterization and flocculation efficiency of a bioflocculant produced by a marine Halobacillus. *Environmental technology, 34*(18), 2671-2679.

Devatha, C. P., Thalla, A. K., & Katte, S. Y. (2016). Green synthesis of iron nanoparticles using different leaf extracts for treatment of domestic waste water. *Journal of Cleaner Production, 139*, 1425-1435. doi:https://doi.org/10.1016/j.jclepro.2016.09.019

Dlamini, N. G., Basson, A. K., & Pullabhotla, V. S. R. (2019). Optimization and Application of Bioflocculant Passivated Copper Nanoparticles in the Wastewater Treatment. *International journal of environmental research and public health, 16*(12), 2185.

Exley, C., Korchazhkina, O., Job, D., Strekopytov, S., Polwart, A., & Crome, P. (2006). Non-invasive therapy to reduce the body burden of aluminium in Alzheimer's disease. *Journal of Alzheimer's Disease, 10*(1), 17-24.

Gao, J., Bao, H.-y., Xin, M.-x., Liu, Y.-x., Li, Q., & Zhang, Y.-f. (2006). Characterization of a bioflocculant from a newly isolated Vagococcus sp. W31. *Journal of Zhejiang University Science B, 7*(3), 186-192.

He, J., Zhen, Q., Qiu, N., Liu, Z., Wang, B., Shao, Z., & Yu, Z. (2009). Medium optimization for the production of a novel bioflocculant from Halomonas sp. V3a′ using response surface methodology. *Bioresource technology, 100*(23), 5922-5927.

Karthiga devi, K., & Natarajan, K. A. (2015). Production and characterization of bioflocculants for mineral processing applications. *International journal of mineral processing, 137*, 15-25. doi:https://doi.org/10.1016/j.minpro.2015.02.007

Lee, D.-J., & Chang, Y.-R. (2018). Bioflocculants from isolated stains: A research update. *Journal of the Taiwan Institute of Chemical Engineers, 87*, 211-215. doi:https://doi.org/10.1016/j.jtice.2018.03.037

Mahdy, S. A., Raheed, Q. J., & Kalaichelvan, P. (2012). Antimicrobial activity of zero-valent iron nanoparticles. *International Journal of Modern Engineering Research, 2*(1), 578-581.

Maliehe, S., Shandu, S. J., & Basson, K. A. (2015). The antibacterial and antidiarreal activities of the crude methanolic Syzygium cordatum [S. Ncik, 48 (UZ)] fruit pulp and seed extracts. *Journal of Medicinal Plants Research, 9*(33), 884-891.

Muthulakshmi, L., Rajini, N., Varada Rajalu, A., Siengchin, S., & Kathiresan, T. (2017). Synthesis and characterization of cellulose/silver nanocomposites from bioflocculant reducing agent. *International Journal of Biological Macromolecules, 103*, 1113-1120. doi:https://doi.org/10.1016/j.ijbiomac.2017.05.068

Okaiyeto, K., Nwodo, U. U., Mabinya, L. V., & Okoh, A. I. (2015). Bacillus toyonensis Strain AEMREG6, a Bacterium Isolated from South African Marine Environment Sediment Samples Produces a Glycoprotein Bioflocculant. *Molecules, 20*(3), 5239.

Olsen, K. N., Larsen, M. H., Gahan, C. G., Kallipolitis, B., Wolf, X. A., Rea, R., . . . Ingmer, H. (2005). The Dps-like protein Fri of Listeria monocytogenes promotes stress tolerance and intracellular multiplication in macrophage-like cells. *Microbiology, 151*(3), 925-933.

Sathiyanarayanan, G., Kiran, G. S., & Selvin, J. (2013). Synthesis of silver nanoparticles by polysaccharide bioflocculant produced from marine Bacillus subtilis MSBN17. *Colloids and Surfaces B: Biointerfaces, 102*, 13-20.

Shinde, A. J., & More, H. N. (2009). Nanoparticles: As Carriers for Drug Delivery System. *Research Journal of Pharmaceutical Dosage Forms and Technology, 1*(2), 80-86.

Sun, J., Zhang, X., Miao, X., & Zhou, J. (2012). Preparation and characteristics of bioflocculants from excess biological sludge. *Bioresource technology, 126*, 362-366. doi:https://doi.org/10.1016/j.biortech.2012.08.042

Ugbenyen, A., & Okoh, A. (2014). Characteristics of a bioflocculant produced by a consortium of Cobetia and Bacillus species and its application in the treatment of wastewaters. *Water SA, 40*(1), 140-144.

Vörösmarty, C., Lettenmaier, D., Leveque, C., Meybeck, M., Pahl-Wostl, C., Alcamo, J., . . . Kabat, P. (2004). Humans transforming the global water system. *Eos, Transactions American Geophysical Union, 85*(48), 509-514.

Xia, X., Lan, S., Li, X., Xie, Y., Liang, Y., Yan, P., . . . Xing, Y. (2018). Characterization and coagulation-flocculation performance of a composite flocculant in high-turbidity drinking water treatment. *Chemosphere, 206*, 701-708. doi:https://doi.org/10.1016/j.chemosphere.2018.04.159

Yang, Z.-H., Huang, J., Zeng, G.-M., Ruan, M., Zhou, C.-S., Li, L., & Rong, Z.-G. (2009). Optimization of flocculation conditions for kaolin suspension using the composite flocculant of MBFGA1 and PAC by response surface methodology. *Bioresource technology, 100*(18), 4233-4239.

Zaki, S. A., Elkady, M. F., Farag, S., & Abd-El-Haleem, D. (2013). Characterization and flocculation properties of a carbohydrate bioflocculant from a newly isolated Bacillus velezensis 40B. *Journal of environmental biology, 34*(1), 51.

Chapter 8 : ARTICLE 6: A comparative study between Fe@Cu core-shell nanoparticles with iron and copper nanoparticles synthesized using a bioflocculant, their applications and biosafety

Dlamini Nkosinathi Goodman [a]*, Basson Albertus Kotze [a], Rajasekhar Pullabhotla VSR [b]*,

[a] Department of Biochemistry and Microbiology, University of Zululand, Private Bag X1001, KwaDlangezwa, 3886, South Africa

[b] Department of Chemistry, University of Zululand

***** Correspondence; E-Mail: nathidlamini03@gmail.com; PullabhotlaV@unizulu.ac.za

---

Abstract: Nanotechnology addresses numerous environmental problems such as wastewater treatment. Ground water, surface water and wastewater that is contaminated by toxic organic, inorganic solutes and pathogenic microorganisms can now be treated through the application of nanotechnology. This paper focuses mainly on the synthesis of single metallic and core-shell metallic nanoparticles using a greener approach and application of these materials in the wastewater treatment. Characterization of the as-synthesised material was achieved through the use of Fourier transform - infrared spectroscopy (FTIR), Thermogravimetric analysis (TGA), Scanning Electron Microscope (SEM), Transmission Electron Microscopy (TEM), and X-Ray diffraction (XRD). In their application, the effect of various parameters on the flocculation activity were evaluated. Both the CuNPs and Fe@Cu core-shell nanoparticles have shown the best flocculation activity at a concentration of 0.2 mg/mL with over 90% activity, while the dosage size with a concentration of 0.4 mg/mL was optimal for FeNPs. The FeNPs were found to be cation dependent, while CuNPs and Fe@Cu core-shell nanoparticles flocculate in the absence of a cation and flocculate both in acidic and alkaline pH. All the synthesized nanoparticles are thermostable and maintain flocculation activity above 80% at 100 ºC. Both the Fe@Cu core-shell and CuNPs were found to be effective in removing dyes with the removal efficiency above 89% and were found to be effective in removal of COD & BOD in Mzingazi river water and mine wastewater with over 80% removal efficiency. Moreover, the synthesized nanoparticles showed some remarkable antimicrobial properties when evaluated against Gram-positive and Gram-negative microorganisms.

Keywords: Bioflocculant, Copper nanoparticles, Characterization, Fe@Cu core-shell nanoparticles, Removal efficiency.

8.1 Introduction

Water contamination by a series of compounds, more specifically heavy metals, dying pigments from textile industries, and other suspended toxic particles, remains a threat to environment and public health. Consequently, measures should be taken to control the discharge of these toxic products to the environment and water bodies (Li et al., 2013). Numerous methods have been employed to remove contaminants from wastewater both physically and chemically which includes, ion-exchange, flocculation, reverse osmosis, electrodialysis and neutralization (Abdel-Halim and Al-Deyab, 2011, Crini, 2005).

Flocculation is the most popular of the above mentioned techniques due to its economic viability and effectiveness. The flocculation technique uses flocculants namely: organic synthetic flocculants, inorganic flocculants and naturally occurring bioflocculants (Shih et al., 2001). Numerous textile industries use dyes in their product processing; as a result, water contaminated with dyes released as a by-product (Moussavi and Mahmoudi, 2009). Environmental and health concerns have been raised over the use of organic and inorganic flocculants, while bioflocculants are environmental friendly, biodegradable and possess no health hazards (Shih et al., 2001).

Inorganic particles with nano size, of either simple or composite, possess exceptional physico-chemical properties which render them effective for various nanotechnological applications such as biomedical, biological and pharmaceutical (Sondi and Salopek-Sondi, 2004). The opportunity to develop water supply systems for the future generation is provided by nanotechnology. The current water system is relying on conveyance and centralized system are no longer sustainable. Nanotechnology is envisaged to provide high performance, highly efficient, flexible and multifunctional processes which will result to affordable water treatment solutions (Qu et al., 2013). With the emergence of antibiotic resistant microorganisms to multiple antibiotics, contamination of water poses a major threat to public health (Kolář et al., 2001).

Here, we provide the use of bioflocculant passivated nanoparticles from *Alcaligenes faecalis* HCB2 of marine origin for the treatment of wastewater, river water and dye removal. Furthermore, this provides the cytotoxicity test of nanoparticles on HEK293 human embryonic cells and MCF7 breast cancer cells. Lastly, the study seeks to ascertain the biodegradation of nanoparticles by microorganisms from soil samples collected from dried sludge from domestic wastewater.

8.2 Material and methods

8.2.1 Synthesis of FeNPs, CuNPs and Fe@Cu core-shell nanoparticles

3.0 mM solution of iron sulphate and copper sulphate solution in distilled water was prepared separately. After which 0.5 g of pure bioflocculant was added in both solutions, both mixtures were shaken for 5-10 min in a shaking incubator at room temperature. The mixture was left standing for 24 hrs at room temperature. The resulting precipitate was collected by centrifugation at 8000 rpm 15 min. The synthesis of both the copper and iron nanoparticles was monitored through physical observation and characterization. The control was maintained without addition of iron sulphate and copper sulphate with the experimental flask containing purified bioflocculant (Dlamini et al., 2019a).

A modified method was describes by Yu et al. (2017) was adopted for the synthesis of Fe@Cu core-shell nanoparticles. Different volumes of FeNPs, 10, 20 and 30 mL was mixed successively with a solution of $CuSO_4$ (0.003 M) in glucose (6.0 mL). This reaction was allowed to continue for 20 min and resulting precipitates were collected through centrifugation at 15000 rpm @ 4 °C for 30 min (Yu et al., 2017).

8.2.2 Test for flocculation activity of CuNPs, FeNPs and Fe@Cu core-shell nanoparticles

A solution of kaolin clay consisting of 4.0 g in 1000 mL distilled water was prepared. 50 mL of the prepared solution was then transferred into 3 separate 150 mL conical flask, thereafter 2.0 mL (0.2 mg/mL) solution of the nanoparticles was added and 3.0 mL $CaCl_2$ (1.0 g/L) solution was also added. The mixtures were shaken for a minute and transferred to 100 mL graduated measuring cylinders. The mixture was left to stand for 5 min before the supernatant was taken for analysis (Xia et al., 2018). Flocculation activity was calculated according the following equation:

Flocculation activity $\text{FA } \% = \frac{[A-B]}{A} \text{ X } 100$ (1)

A = Optical density of Control at 550 nm & B= Optical density of Sample at 550 nm

8.2.3 Application of CuNPs, FeNPs and Fe@Cu core-shell nanoparticles on treatment of wastewater

Wastewater sample were collected from Vulindlela water treatment plant, KwaDlangezwa, KwaZulu Natal, RSA to ascertain removal efficiency (RE) of pollutants by nanoparticles in the water samples. NaOH (0.1 M) and/or HCl (0.1 M) solutions were used for adjusting pH value when necessary. The wastewater sample was then poured in 1000 mL beakers and the nanoparticles were added. The mixture was stirred at 360 rpm agitation speed for 10 min, and then allowed to stand for 30 min. The supernatants were taken for analysis using UV-Vis spectrophotometer Pharo 300 Spectroquant® at 680 nm and the residual COD, BOD, total nitrogen, phosphate contents. The removal efficiency (RE) of the pollutants was calculated by the following equation:

$$RE\ (\%) = \frac{C0-C1}{C0}\ X\ 100 \qquad (2)$$

Where: C_0 is the initial value and C_1 is the value after the flocculation treatment. The flocculating efficiency of the synthesised nanoparticles and the conventionally used chemical flocculants was compared. The chemical flocculant used was ferric chloride (Agunbiade et al., 2018).

8.2.4 Application of nanoparticles on dye removal

Decolourization experiments were conducted where 1.0 mL of copper nanoparticles was added into a 50 mL dye solution, after which 1.0 mL of $CaCl_2$ (1 wt %) was added (Gong et al., 2008). Experiment dyes (4 g/L) included (safranin, methylene blue, methylene orange, malachite green), then NaOH solutions (10 wt %) was used to adjust the pH of the suspension to 8. The supernatants were taken for analysis after the mixture had been stirred for a minute and allowed to settle for 10 min, using a spectrophotometer. The absorbance of each sample was measured at the maximum wavelength of each dye. Decolourization efficiency was calculated using the (RE) equation as indicated above (Dlamini et al., 2019b).

8.2.5 Biosafety of CuNPs, FeNPs and Fe@Cu core-shell nanoparticles

A method described by Daniels and Singh (2019) was used to ascertain cytotoxicity of the nanoparticles using a human embryonic kidney (HEK 293) and breast cancer cells (MCF-7). 96-well-plate were used for plating the cells with cell suspensions of 1×10^5 cells/mL concentrations. After 48 hrs incubation the cells were seeded with different concentrations of

nanoparticles (25-100 µg/µL) using a tenfold serial dilution method, media containing 1 % of foetal bovine serum (FBS) were used for the administration of nanoparticles and the plates were returned to the incubator for 48 hrs. Tetrazolium salt (Sigma) was added as an indicator after 48 hrs of incubation to ascertain cell viability. 15 µL of MTT (5 mg/mL) in phosphate buffered saline (PBS) was added to each well and incubated at 37 °C for 4 hrs. After sucking off from the wells the medium with MTT and the formed formazan crystals were dissolved in 100 µL of dimethyl sulfoxide (DMSO). The optical density of the solutions was measured at 570 nm using a micro plate reader. The % cell inhibition was determined using following formula:

$$\text{Cell viability}(\%) = \frac{F1}{F0}\ X\ 100 \qquad (3)$$

Where F_1 and F_0 are the final values obtained after and before treatment with the nanoparticles, respectively (Daniels and Singh, 2019).

8.2.6 Antimicrobial effect of CuNPs, FeNPs and Fe@Cu core-shell nanoparticles

8.2.6.1 Bacterial strains resuscitation

To determine the antimicrobial activity of nanoparticles (CuNPs, FeNPs & Fe@Cu core-shell) were tested against Gram-positive and Gram-negative microorganisms. *Bacillus subtilis* CSM5 and *Escherichia coli* ATCC 25922 (1.0 mL) were inoculated into different 9.0 mL sterile nutrient broth contained in the test tubes. The inoculum was incubated at 37 ºC for 24 hrs. Spectrophotometer (600_{nm}) was used to determine the bacterial turbidity/absorbance. The turbidity was adjusted to be in line with the McFarlan standards (0.5).

8.2.6.2 Minimum Inhibitory Concentration (MIC) and Minimum Bactericidal Concentration (MBC)

The antimicrobial activity study was achieved through 96 microplate well method with 40 % ciprofloxacin as a positive control in this experiment. A series of (50 µL) dilutions were prepared using 96 micro wells plates. Sterile nutrient broth (50 µL) was poured in all wells followed by addition of 50 µL of bacterial strain into the corresponding wells from highest concentration until the lowest concentration. To achieve the required concentration 50 µL nanoparticles (CuNPs, FeNPs & Fe@Cu core-shell) was added into to the first row of 96 microplate's wells which was followed by a series of dilutions from the highest concentration

to the lowest. Distilled water was used as a negative control for this experiment while *p*-iodonitrotetrazolium (INT) was used as an indicator (Maliehe et al., 2015).

The minimal inhibitory concentration (MIC) of the synthesized nanoparticles was determined as described by Eloff (1998). The MBC was determined through using the agar dilution method. A loop full of culture of each strain from the well indicated no colour change, were streak on a Muller Hilton nutrient agar. The plates were incubated at 37 °C for 12 hrs. The lowest concentration of nanoparticles that exhibited the complete killing of the test organisms were considered as the MBC (Eloff, 1998).

8.2.7 Biodegradability of the synthesized nanoparticles

To ascertain biodegradability of the synthesized nanoparticles (CuNPs, FeNPs & Fe@Cu core-shell) a method described by Mittal et al. (2013) was adopted with some minor modifications. Soil samples were collected from Vulindlela wastewater treatment plant using sterile Petri dishes (Mittal et al., 2013). Domestic wastewater is regularly discharged in the plant, which makes the wastewater treatment plant a great environment for growth of diverse microorganisms, which are capable of degrading a variety of compounds. The plant is located close to the University of Zululand, RSA. After which 4.0 g of soil sample was mixed with 0.2 g of nanoparticles. To ensure that microbes in the soil sample are kept alive, the effluent from the treatment plant was consistently sprinkled in the soil sample. A soil sample of 4.0 g and 0.2 g of the nanoparticles was left uncovered to mimic the environment from which the microbes were sampled. At the end of every week the soil sample was firstly dried using a microwave oven at 37 °C before it was weighed (Kale et al., 2007). This was performed in order to monitor the biodegradation process and was done for 7 weeks. The following formula was used to calculate the remaining weight of the flocculant after degradation: $Wr = Wm - Ws$

Where Wr is the remaining weight after degradation, Wm weight of the mixture of soil sample & nanoparticles and Ws is the weight of the soil. All the experiments were conducted in triplicates and the mean values were collected.

8.2.8 Experimental, software and statistical analysis

All data was collected in triplicates and the error bars in the Figures show the standard deviations of the data. Data was subjected to One-way analysis of variances (ANOVA) using Graph Pad Prism™ 6.1. A significant level of $p<0.05$ was used.

8.3 Results and discussion

8.3.1 Effect of nanoparticles concentration on flocculation activity

Figure 8.1 is the representative of the results obtained during the evaluation of nanoparticles (FeNPs, CuNPs and Fe@Cu core-shell) effect of dosage concentration on the effect of flocculation activity. Fe@Cu core-shell nanoparticles had the highest flocculation activity compared to both FeNPs and CuNPs.

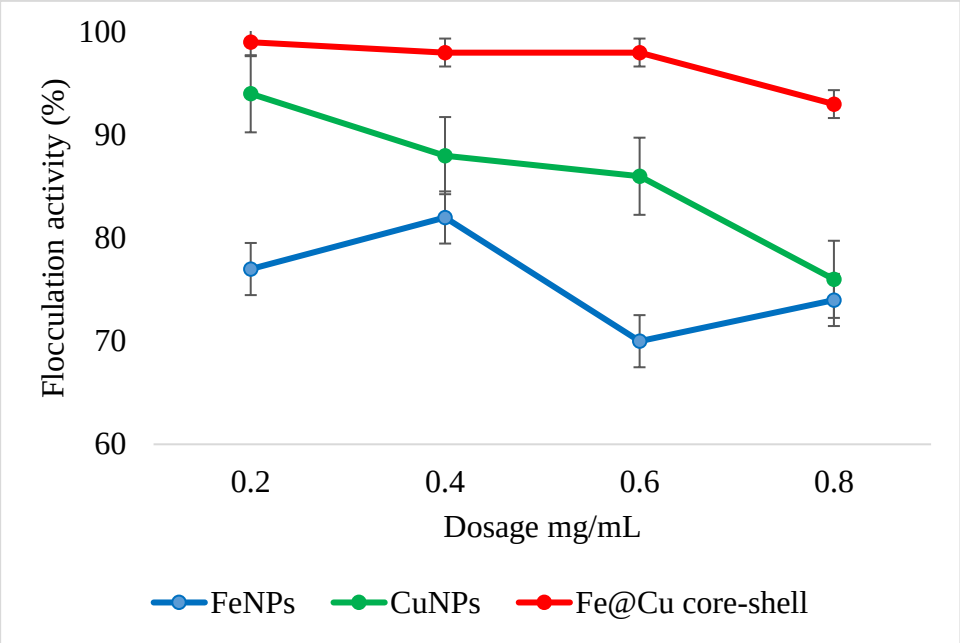

Figure 8.1: Effect of nanoparticles dosage concentration on the flocculation activity. (Refer to index data Table 8.1).

Dosage size is defined as the amount of required flocculant powder for optimal flocculation activity. Different nanoparticles concentrations were prepared by dissolving different milligrams (0.2 - 0.8 mg/mL) of nanoparticles (FeNPs, CuNPs & Fe@Cu core-shell) in distilled water. Each of the ditto were dissolved in 50 mL distilled water. After which 4.0 g of kaolin clay was dissolved in 1.0 L of distilled water. 2.0 mL of nanoparticles (FeNPs, CuNPs and Fe@Cu core-shell) solutions and 3.0 mL of 1 % (w/v) $CaCl_2$ and was added into a 500 mL conical flask containing 100 mL of kaolin clay and agitated for 1 min. The mixture was transferred to a 100 mL graduated measuring cylinder and left to stand for 5 min. The supernatant was analysed in a UV-Vis spectrophotometer Pharo 300 Spectroquant® at 550 nm. As shown in Figure 1, CuNPs and Fe@Cu core-shell nanoparticles had the highest flocculation activity of 99 and 96% respectively at a low concentration of 0.2 mg/mL while the optimum

flocculation activity for FeNPs was achieved at 0.4 mg/mL with 82% flocculation activity. With the increased dosage concentration of the nanoparticles, flocculation activity for both CuNPs and Fe@Cu core-shell started to decrease. Contrary to this, the flocculation activity of FeNPs kept on fluctuating with the increase in dosage of nanoparticles concentration. Core-shell nanoparticles worked efficiently at low concentration with 99% flocculation activity at 0.2 mg/mL. Excessive addition of the flocculants results in destabilized kaolin particles suspension, which in turn results into repulsion of negatively charged kaolin particles. The increase in dosage concentration results into decrease in flocculation activity (Xia et al., 2018). This could be due to blocking of the binding site of kaolin particles by excess flocculating agent. Contrary to these findings the bridging phenomena could not be effectively formed when the dosage of the bioflocculant was too low (Gong et al., 2008).

8.3.2 Effect of cations on flocculation activity

Table 8.1 below represents the results obtained during the determination of the effect of cations on flocculation activity of nanoparticles (FeNPs, CuNPs & Fe@Cu core-shell). Both CuNPs and Fe@Cu core-shell nanoparticles are cation independent as the flocculation activity was above 95% without addition of cations. While the FeNPs were highly dependent on a cation because the flocculation activity was below 50% in the absence of cation.

Table 8.1: Effect of cations presence on the flocculation activity.

Flocculant type	Cations FA(%)±SD			
	Control	Na^{+}	Ca^{2+}	Fe^{3+}
CuNPs	96 ± 0.0^{a}	86 ± 0.1^{b}	$94\pm0.0^{a,b}$	97 ± 0.2^{a}
FeNPs	42 ± 0.1^{d}	73 ± 0.0^{c}	$82\pm0.1^{b,c}$	85 ± 0.3^{b}
Fe@Cu core-shell	95 ± 0.3^{a}	97 ± 0.2^{a}	99 ± 0.2^{a}	97 ± 0.0^{a}

Values represent mean ± deviation of replicate readings. Percentage flocculating activities with different letters (a, b, c & d) are significantly ($p<0.05$) different. (Refer to index data Table 8.2).

Cations have stimulating effect on the adsorption of bioflocculant on the suspended kaolin particles by decreasing the negative charge of both the polymer and particles. Cations neutralise and stabilise the negative charge of the functional groups of colloidal kaolin particles in solution and the bioflocculant (Abd El-Salam et al., 2017). Iron nanoparticles are cation dependent with 85% flocculation activity when Fe^{3+} was used as opposed to 46% flocculation

activity when there was no cation present. Contrary to this, the synthesized copper nanoparticles are more effective without the addition of cation with 96% flocculation activity. In comparison to both iron and copper nanoparticles, Fe@Cu core-shell nanoparticles proved to have best flocculation ability. All the cations (monovalent, divalent and trivalent) enhanced the flocculation of Fe@Cu core-shell nanoparticles. However, it was observed that the flocculation activity was above 95% in the absence of cation.

8.3.3 The effect of pH on nanoparticles flocculation activity

Figure 8.2 shows the effect of pH on flocculation activity of nanoparticles. Fe@Cu core-shell nanoparticles work best in all pH ranges, while CuNPs was observed to flocculate less at acidic pH with the maxim flocculation observed at neutral pH. On the other hand, FeNPs flocculate best at alkaline pH.

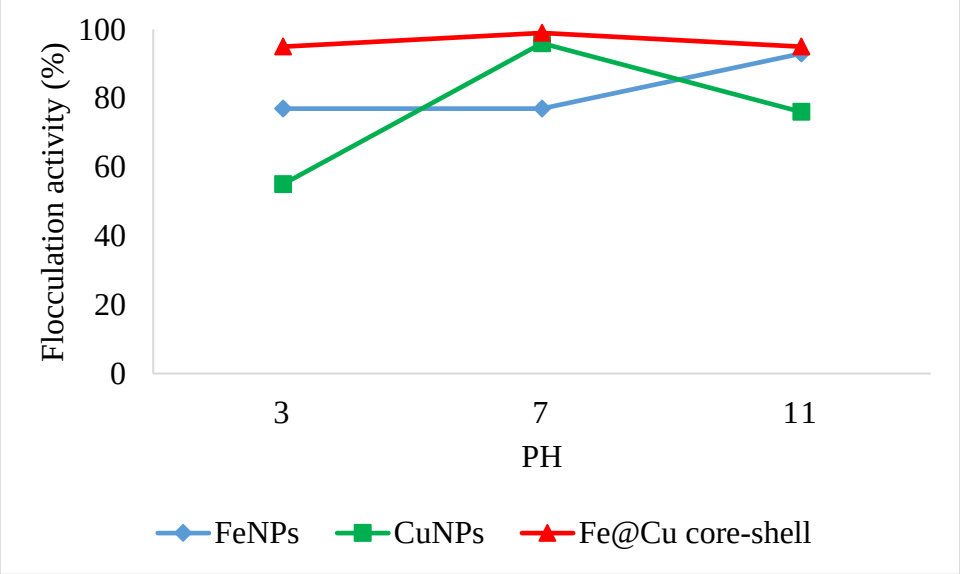

Figure 8.2: The effect of pH on nanoparticles flocculation activity. (Refer to index data Table 8.3).

One of the key factors which influence the flocculation process is pH of the reaction mixture (Zaki et al., 2013). The flocculant charge status and surface characteristics of the colloidal particles may be altered by pH which in turn may affect flocculating efficiency (Xia et al., 2018). Different flocculants have been reported to produce flocculating efficiency with optimal activity at varying pH values (Karthiga devi and Natarajan, 2015). NaOH (0.1 M) and HCl

(0.1 M) solutions were used to adjust the pH of the kaolin solutions whenever it was necessary. It can be observed from Figure 8.2 that a strong flocculation activity at all pH ranges for Fe@Cu core-shell nanoparticles, from strong acidic to strong alkaline pH the flocculation activity was

above 95%. These findings are in good agreement with the literature which states that Fe@Cu core-shell nanoparticles can with stand harsh conditions such as extreme pH and temperatures and have improved properties as opposed to single metal nanoparticles (Zhu et al., 2012). The FeNPs flocculation activity remained constant at 77% both at acidic and neutral pH and there was significantly sharp increased from 77-95% at an alkaline pH suggesting that FeNPs were more efficient in an alkaline pH.

Maximum flocculation activity of 96% was achieved at neutral pH 7 for CuNPs nanoparticles implying that the adjustment of pH would not be necessary for achieving high flocculation. However, at acidic pH, low flocculation activity was observed (55 % at pH 3). This could be due to the bioflocculant from which nanoparticles were synthesized have shown different electric charges at different pH, affecting the bridging efficiency of the nanoparticles (Zhu et al., 2012). Consequently, it could be deduced that the spatial arrangement of charge at pH 3 were not encompassing. *Bacillus velezenis* 404 bioflocculant was found to be stable at pH range of 3-9 and the optimum flocculation ability was reached at pH 7 (Xia et al., 2008). Like many other flocculants reported in literature, the synthesized copper nanoparticles flocculate in a wide range of pH suggesting that it is a stable at different pH's with an optimum flocculation activity at pH 7.

8.3.4 Thermostability of nanoparticles

Figure 8.3 shows the effect of temperature on flocculation activity of nanoparticles (FeNPs, CuNPs & Fe@Cu core-shell). All synthesized nanoparticles were found to be thermally stable with a flocculation activity above 88% at 100 °C.

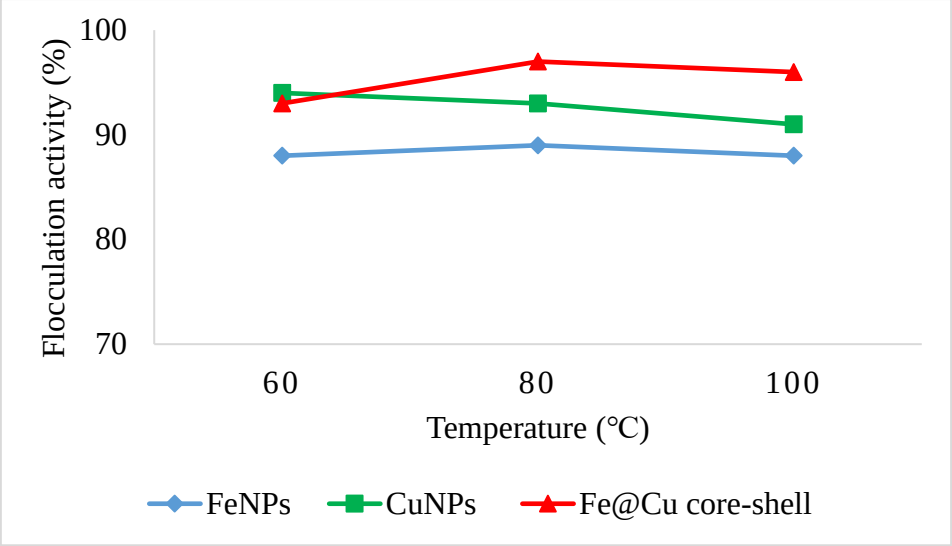

Figure 8.3: Effect of temperature on the flocculation activity. (Refer to index data Table 8.4).

The relationship between temperature and flocculating efficiency of the synthesized nanoparticles was examined at temperatures 60, 80 and 100 °C (Sun et al., 2012). The synthesized nanoparticles were subjected to different temperatures using a water bath for 30 min. This was to ascertain its stability when subjected to higher temperatures. Both the CuNPs and Fe@Cu core-shell nanoparticles retained over 90% flocculation activity. FeNPs retained over 88% flocculation suggesting that the nanoparticles were very stable. The flocculation activity for all synthesized nanoparticles remained at 88% throughout the temperatures with the Fe@Cu core-shell having the highest flocculation. Therefore, it was deduced that the nanoparticles were thermo-stable and its flocculation activity was not affected when the temperature was elevated. Heat sensitivity of the bioflocculant is linked to the presence of peptide or protein in the bioflocculant structure, while bioflocculant with sugar containing structure is heat resistant (Salehizadeh and Shojaosadati, 2001). The bioflocculant, which was used for nanoparticles synthesis, is polysaccharide and contains hydroxyl groups. The presence of the hydroxyl group could be responsible for the thermal stability of nanoparticles. Moreover, the Fe@Cu core-shell nanoparticles are resistant to harsh conditions and this is due to the synergistic effect between a core and a shell (Lin et al., 2017).

8.3.5 The effect of nanoparticles on dye removal

Figure 8.4 illustrates the effect of nanoparticles (FeNPs CuNPs and Fe@Cu core-shell) on dye removal. Both the CuNPs and Fe@Cu core-shell nanoparticles have a high affinity for all examined dyes with removal efficiency above 85%. FeNPs were found to be very poor in

removing staining dyes with highest removal efficiency of 58%. The Fe@Cu core-shell nanoparticles were effective with over 90% removal efficiency for all tested dyes.

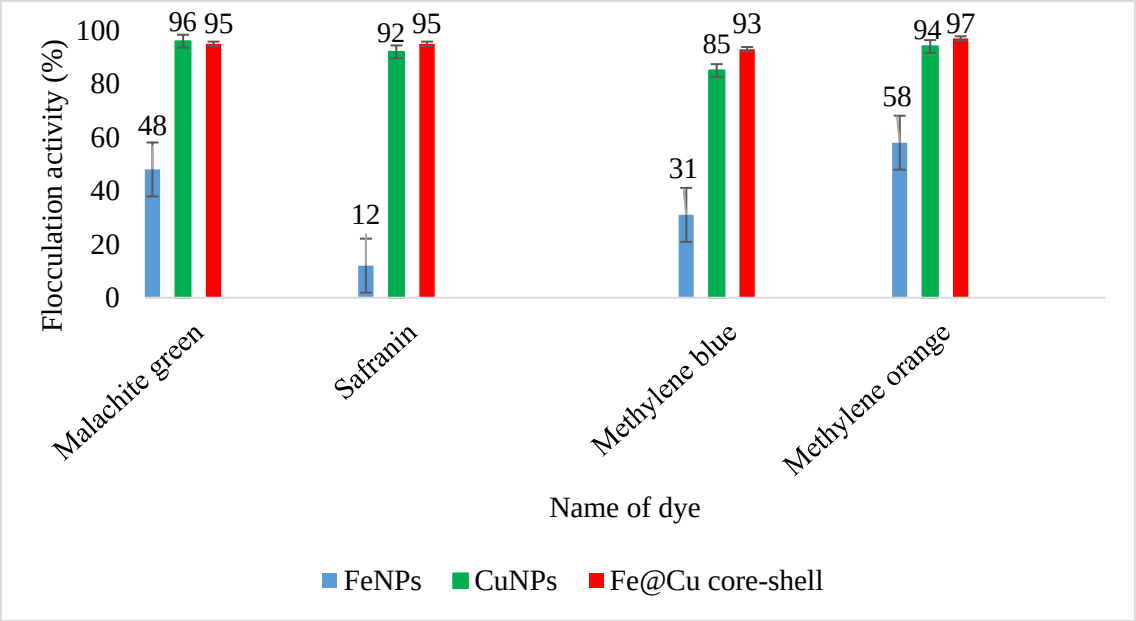

Figure 8.4: Effect of nanoparticles on the removal of staining dyes. (Refer to index data Table 8.5).

The potential of nanoparticles (FeNPs, CuNPs and Fe@Cu core-shell) to remove staining dye was investigated. Copper and Fe@Cu core-shell nanoparticles were able to remove all different dyes. While iron nanoparticles had an avarage of below 50% removal efficiency. All the experiment were carried out at room temperature. The optimum dosage concentration for each nanoparticles was found to be as 0.2 mg/mL for CuNPs and 0.4 mg/mL for FeNPs. It is clear from Figure 4 that both the CuNPs and Fe@Cu core-shell nanoparticles were able to remove all the dyes and Fe@Cu core-shell had the highest removal efficiency of above 90% for all the tested dyes. Iron nanoparticles had the poorest results with the romoval efficiency delow 50% for most of the dyes. Poor perfomance of the FeNPs could be attributted parameters such as low dosage of the nanoparticles, pH of the dye solution and insufficient contact time between dye solution and FeNPs nanoparticles. Contrary to this, a study by Shahwan et al. (2011) iron nanoparicles removed both the methylene blue and methylene orange completely. Howerer,

the concentration 50 mg/L could only manage to remove both methylene blue and methyl orage after 6 hrs (Shahwan et al., 2011).

8.3.6 The removal of nutrients in Vulindlela wastewater

Table 8.2 below shows the removal of phosphate and total nitrogen from Vulindlela wastewater by different nanoparticles. All the nanoparticles have an affinity for total nitrogen but Fe@Cu core-shell nanoparticles were more effective to both phosphate and total nitrogen removal compare to iron and copper nanoparticles.

Table 8.2: Phosphate and total nitrogen removal from Vulindlela wastewater by nanoparticles.

Type of flocculants	Water quality before treatment (control)		Water quality after treatment (flocculants)		Removal efficiency (%)	
	Phosphate (mg/L)	Total nitrogen (mg/L)	Phosphate (mg/L)	Total nitrogen (mg/L)	Phosphate (mg/L)	Total nitrogen (mg/L)
CuNPs	3.38±0.0	0.127±0.0	1.62±0.1	0.022±0.0	52	83
FeNPs	3.38±0.0	0.127±0.0	1.64±0.0	0.019±0.0	51	85
Fe@Cu core-shell	3.38±0.0	0.127±0.0	0.09±0.0	0.020±0.0	97	84

Phosphorus is an essential element for the growth of plants and animals. However, it is very toxic in its elemental form as it can result in the formation of PO_4^{3-} and is subjected to accumulation (Kumar and Puri, 2012). There are three forms of phosphate which exist: Met-pho sulphate, orthophosphate and organically bound phosphate. A different chemical formula is contained in each compound, ortho forms are produced naturally and are found in sewage. Ortho forms are important in nature and results from poly phosphate forms, which are used for treating boiler water and in detergents. Breakdown of organic pesticides, which contain phosphate, results into the occurrence of ortho forms. Table 8.2 shows that Fe@Cu core-shell nanoparticles were able to remove up to 97% phosphate in wastewater in comparison to copper and iron nanoparticles.

8.3.7 The removal of nutrients in Mzingazi river water

Table 8.3 below shows the removal of phosphate and total nitrogen from Mzingazi river water by different nanoparticles. Both the iron and copper nanoparticles showed to have poor removal efficiency for total nitrogen but Fe@Cu core-shell nanoparticles were more effective with 94% removal efficiency.

Table 8.3: Phosphate and total nitrogen removal from Mzingazi river water by nanoparticles.

Type of flocculants	Water quality before treatment (control)		Water quality after treatment (flocculants)		Removal efficiency (%)	
	Phosphate (mg/L)	Total nitrogen (mg/L)	Phosphate (mg/L)	Total nitrogen (mg/L)	Phosphate (mg/L)	Total nitrogen (mg/L)
CuNPs	85.7±0.0	0.223±0.0	7.521±0.1	0.108±0.0	92	52
FeNPs	85.7±0.0	0.223±0.0	9.102±0.0	0.127±0.0	90	45
Fe@Cu core-shell	85.7±0.0	0.223±0.0	0.109±0.0	0.014±0.0	99	94

Varying amounts of phosphate can be washed from farm soil to waterbodies. The presence of phosphate in water stimulates the growth of aquatic plants and plankton which provide food for fish and increases the population growth of fish and also improve the overall water quality. Even the excess of phosphate may cause wild growth of aquatic plants and algal, resulting into eutrophication or over-fertilization of receiving waters. As a result, eutrophication may decay vegetation and quality life due to decreased dissolved oxygen levels. Toxicity of phosphate to people and animals could occur from extremely high levels of phosphate (Kumar and Puri, 2012). The ability of nanoparticles to remove phosphate in Mzingazi river is shown in Table 3. All the nanoparticles had removal efficiency below 40 %. However, when wastewater treated with nanoparticles was left standing for a week, there was a drastic increase in phosphate removal up to 90 % as depicted in Table 8.3.

This results suggest that contact time is an important factor in the efficiency of nanoparticles. Eutrophication continues to be the primary concern to water quality and phosphorus and nitrogen are the primary nutrients implicated on eutrophication (Davis et al., 2006). In urban areas, atmospheric deposition, vegetation and fertilizers are primary sources of nutrients. Nutrients load can also be significantly added through maintenance, construction and soil

management through the addition of fertilizers in the process of reviving injured vegetation (Davis et al., 2006). Moreover, nitrogen can result in nitrate and nitrite ions which are part of nitrogen cycle and occur naturally. In fish, nitrites can produce a condition known as “brown blood disease” and in warm-blooded animals it directly reacts with haemoglobin to produce methaemoglobin. The ability of red blood cells to transport haemoglobin is destroyed by methaemoglobin (Kumar and Puri, 2012). As shown in Table 8.3, Fe@Cu core-shell nanoparticles could remove up to 94 % of total nitrogen in comparison to both iron and copper nanoparticles with 45 and 52 % respectively. Therefore, it can be deduced that Fe@Cu core-shell nanoparticles are more effective to remove phosphate and total nitrogen from river water.

8.3.8 COD and BOD removal from domestic wastewater and Mzingazi river water

Table 8.4 below shows the removal efficiency for COD and BOD by nanoparticles (FeNPs, CuNPs & Fe@Cu core-shell) from Vulindlela wastewater and Mzingazi river water. The copper nanoparticles had the highest removal efficiency for both COD and BOD for all the water samples.

Table 8.4: Removal efficiency of COD and BOD from coal mine water and Mzingazi river water.

Flocculant	Types of waste water	Types of pollutants in water	Water quality before treatment (mg/L)	Water quality after treatment (mg/L)	Removal efficiency (%)
CuNPs	Coal mine water	COD	842	103	88
		BOD	123.2	4.123	96
	Mzingazi river water	COD	3.300	0.278	92
		BOD	136	14	89
FeNPs	Coal mine water	COD	842	204	76
		BOD	123.2	23	81
	Mzingazi river water	COD	3.300	1.700	48
		BOD	136	24	82
Fe@Cu core-shell	Coal mine water	COD	842	71	92
		BOD	123.2	3.413	97
	Mzingazi river water	COD	3.300	0.793	76
		BOD	136	70	94

Both the high amount of COD and BOD in water will result in decrease of dissolved oxygen (DO). Reduced oxygen dissolved lead to anaerobic conditions, which is detrimental to higher aquatic life forms. Higher amount of BOD in water indicates a high amount of nutrients in water. This condition is not healthy for the environment, as it also may result into alga boom.

Tendele coalmine wastewater, KwaZulu Natal, South Africa and Mzingazi river water were selected for the application of nanoparticles (FeNPs, CuNPs, and Fe@Cu core-shell) for the removal of COD and BOD. The COD and BOD for both water samples was measured before and after the application of nanoparticles. The COD for all the water samples was evaluated using COD Cell Test, photometric method 25 - 1500 mg/L Spectroquant®. Where 10 mL of the both untreated and treated wastewater samples were added in different COD cells and the cells were taken into a digester for 120 min at 150 °C after which the samples were taken for absorption analysis using UV-Vis spectrophotometer at 620 nm wavelength.

The concentration which was used for all the nanoparticles was 0.2 mg/mL and both the CuNPs and Fe@Cu core-shell nanoparticles exhibited good properties in all water samples for both the COD and BOD, with the Fe@Cu core-shell having the highest removal efficacy. Contrary to that FeNPs were very poor for all the water samples COD removal (<50%). However, for BOD, all three samples of nanoparticle (FeNPs, CuNPs, and Fe@Cu core-shell) were able to remove above 80 %. Contrary to this, the study on the effectiveness of bioflocculant on COD removal in industrial wastewater, it was revealed that bioflocculant could only remove up to 60 % of COD (Patil et al., 2011).

8.3.9 Flocculation of coalmine and Mzingazi river water

Figure 8.5 shows the flocculating efficiency of CuNPs, FeNPs, Fe@Cu core-shell nanoparticles and Ferric chloride. Different wastewater samples were examined including kaolin, coal mine wastewater and River water.

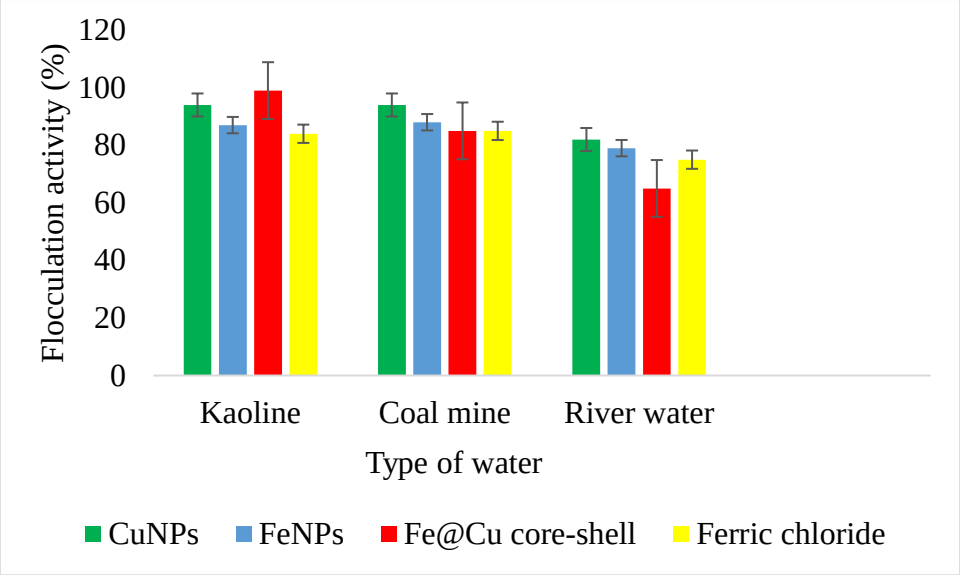

Figure 8.5: Flocculating efficiency of CuNPs, FeNPs and Fe@Cu core-shell nanoparticles and ferric chloride using kaolin clay, coal mine water and river water. (Refer to index data Table 8.6).

Several technologies have been reported in wastewater treatment methods such as physical, chemical and biological, etc. There are numerous sources of water contamination and this include industries, household. Industrial wastewater remains the largest contributor of the contamination (Lu et al., 2017). The current study aimed at comparing the flocculating efficiency of the synthesized nanoparticles CuNPs, FeNPs and Fe@Cu Core-shell with a commercial flocculant (ferric chloride). All the synthesized nanoparticles showed some remarkable ability to flocculate suspended particles in all the established water samples; however, CuNPs remained outstanding with a flocculation activity above 82% in all the samples. These findings suggest that nanoparticles, particularly, copper nanoparticles can be used to flocculate coal mine and river water. This could be an alternative to chemical flocculants that are harmful and non-degradable (Exley et al., 2006). All data was collected in triplicates and the error bars in the Figures show the standard deviations of the data.

8.3.10 Antimicrobial effect of nanoparticles

Table 8.5 shows the antimicrobial activity of nanoparticles (FeNPs, CuNPs & Fe@Cu core-shell) in comparison with Ciprofloxacin. Minimum Inhibitory Concentration (MIC) and Minimum Bactericidal Concentration (MBC) was observed for (CuNPs & Fe@Cu core-shell), while FeNPs nanoparticles did not have any antimicrobial effect on the verified strains.

Table 8.5: Antimicrobial activity of nanoparticles in comparison with ciprofloxacin

Bacterial strain	Antimicrobial agent	MIC (mg/mL)	MBC (mg/mL)
E. coli	FeNPs	-	-
	CuNPs	3.125	3.125
	Fe@Cu core-shell	1.563	1.563
	Ciprofloxacin	12.5	12.5
		MIC (mg/mL)	MBC (mg/mL)
B. subtilis	FeNPs	-	-
	CuNPs	3.125	3.125
	Fe@Cu core-shell	1.563	1.563
	Ciprofloxacin	6.25	6.25

Test bacterial strains for antimicrobial activity include a Gram-negative bacterium *E. coli* ATCC 25922 and a Gram-positive bacterium *Bacillus subtilis* CSM5. The antimicrobial activity study was achieved through 96 well microplate method while 40 % *ciprofloxacin* was used as a positive control in this experiment. Both the (CuNPs and Fe@Cu core-shell) nanoparticles showed some remarkable properties for MIC and MBC against all the strains. Iron nanoparticles did not show any antimicrobial effect. The MIC and MBC for the Fe@Cu Core-shell nanoparticles was achieved at the lowest concentration of 1.563 mg/mL for both strains. Similarly, the copper nanoparticles revealed some notable properties against the examined organisms. *B. subtilis* cell surface has carboxyl and amines group in abundant and copper is known to have greater affinity towards these groups which could be attributed to the sensitivity of *B. subtilis* against copper nanoparticles (Ruparelia et al., 2008). To evaluate the MBC, *p*-iodonitrotetrazolium (INT) indicator was used and all the wells which did not turn to red i.e. the wells, which had indicated a sensitivity towards the test strains, were further inoculated into a Muller Hilton agar and no growth was observed which indicated that both the copper and Fe@Cu core-shell nanoparticles have a bactericidal effect.

8.3.11 In-vitro cytotoxicity of nanoparticles

Figures 8.6, 8.7 and 8.8 illustrate the in-vitro cytotoxicity of nanoparticles (FeNPs, CuNPs and Fe@Cu core-shell) on HEK293 human embryonic cells and MCF7 breast cancer cells respectively.

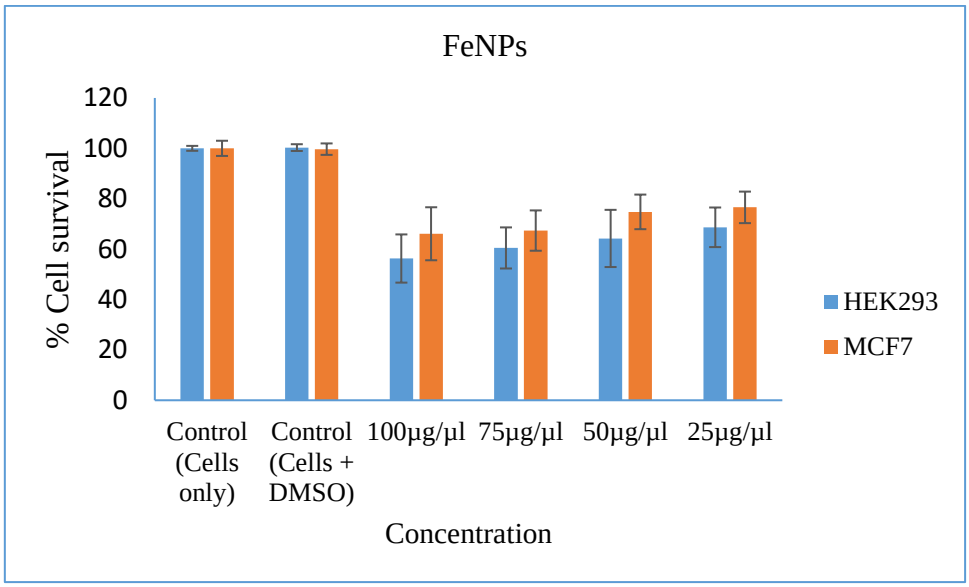

Figure 8.6: *In-vitro* cytotoxicity effect of FeNPs nanoparticles on HEK293 & MCF7 cells.

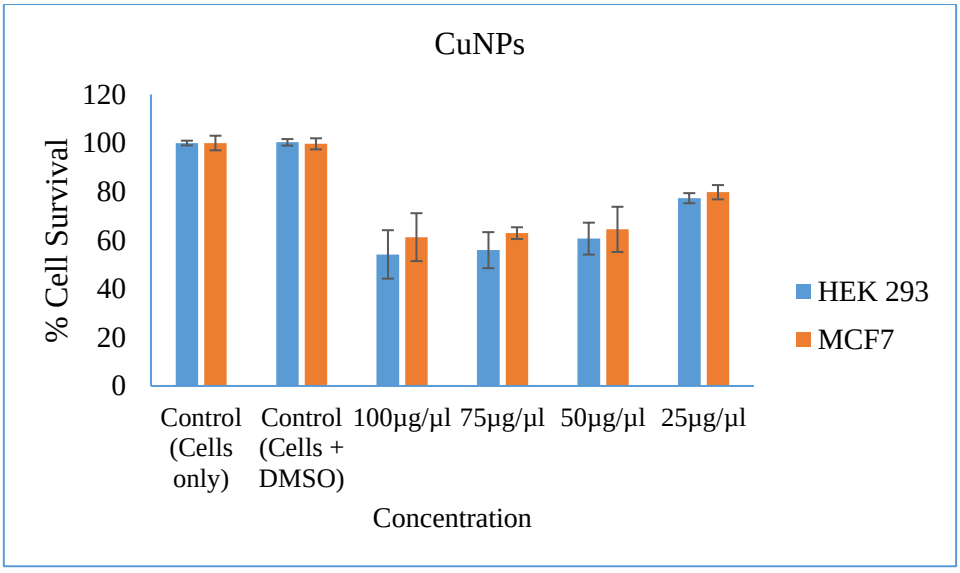

Figure 8.7: *In-vitro* cytotoxicity effect of CuNPs nanoparticles on HEK293 & MCF7 cells.

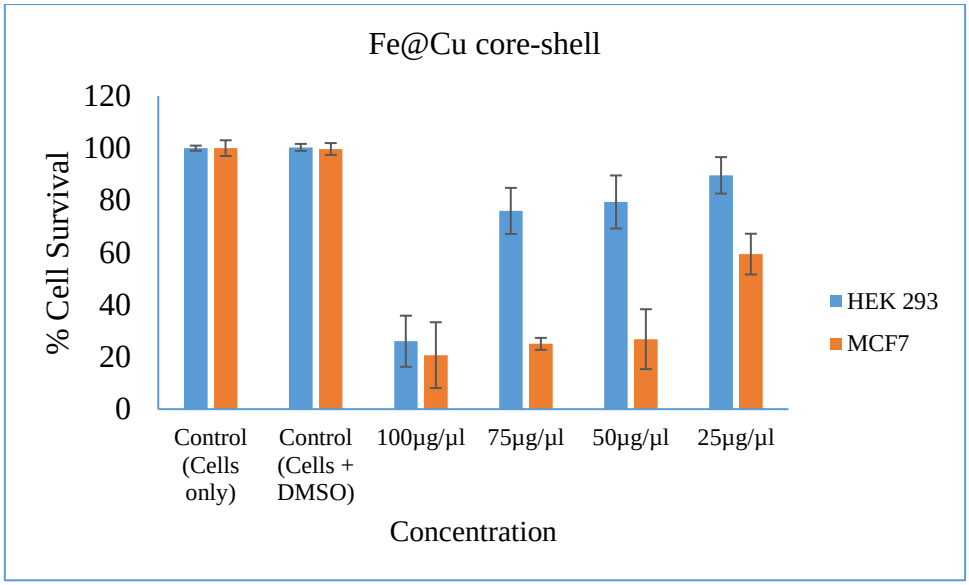

Figure 8.8: In-vitro cytotoxicity effect of Fe@Cu core-shell nanoparticles on HEK293 & MCF7 cells**.**

A flocculant that is safe and efficient is required for wastewater treatment. In this study, *in-vitro* cytotoxicity of nanoparticles (FeNPs, CuNPs, and Fe@Cu core-shell) was investigated using MTT reduction assay on HEK 293 and MCF7 cell lines. A compound used for the detection of viable cells and is based on the active metabolism of cells that are capable of converting MTT into a purple formazan is known as tetrazolium. From Figure 6, 7 and 8, all the nanoparticles at 25 µg/µL had cell viability over 70 % for HEK 293 and Fe@Cu core-shell had the highest cell viability of 89 %. With increased concentration up to 75 µg/µL the Fe@Cu core-shell maintained 75 % cell viability for normal cells that indicates that Fe@Cu core-shell nanoparticles may not be toxic to normal cells. The FeNPs revealed that 66 % cell of MCF-7 were still viable at the highest concentration of 100 µg/µL and 56% of HEK 293 cells were viable at the highest concentration of 100 µg/µL, which could therefore be deduced that the FeNPs are considered safe. Contrary to that CuNPs at 100 µg/µL showed 61 % cell activity for MCF7 and 54 % cell viability at the same highest concentration of 100 µg/µL This indicates that the CuNPs are safe to use at lower concentration.

8.3.12 Biodegradation of nanoparticles

Table 8.6 represents biodegradation results for nanoparticles CuNPs, FeNPs and Fe@Cu core-shell. The Fe@Cu core-shell nanoparticles in week one were less degraded in comparison to both CuNPs and FeNPs.

Table 8.6: Biodegradation study on nanoparticles (CuNPs, FeNPs and Fe@Cu core-shell).

Samples	Initial weight (g)	Weight of samples remaining per week (g) ± SD				
		1	2	3	4	5
CuNPs	0.17±0.00	0.17±0.00	0.17±0.00	0.10±0.00	0.03±0.00	0.00±0.00
FeNPs	0.21±0.00	0.21±0.00	0.19±0.00	0.12±0.00	0.01±0.00	0.00±0.00
Fe@Cu core-shell	0.23±0.00	0.23±0.00	0.16±0.00	0.08±0.00	0.02±0.01	0.00±0.00
Control (soil only)	4.00±0.00	4.00±0.00	4.00±0.00	4.00±0.00	4.00±0.00	4.00±0.00

Biodegradation studies results for the nanoparticles (FeNPs, CuNPs, and Fe@Cu core-shell) are presented in Table 8.6. All the bioflocculant-passivated nanoparticles were able to biodegrade completely after 5 weeks; however, the Fe@Cu core-shell nanoparticles drastically decreased in mass after two weeks. The initial mass of Fe@Cu core-shell nanoparticles decreased from 0.23 g to 0.16 g, which is over 60 % degradation. In the first two weeks, CuNPs could not degrade, the mass remained at the initial mass of 1.7 g. Similarly, the FeNPs mass decreased from 0.23 g to 0.19 g, which is just 4% degradation. This could be due to the structure modification of both FeNPs and CuNPs, thus making it difficult for enzymes to degrade in short space of time (Singh et al., 2000b).

8.4. Conclusion

Both CuNPs and Fe@Cu core-shell nanoparticles had the highest flocculation activity of 96 and 99 % respectively at a low concentration of 0.2 mg/mL, while the optimum flocculation activity for FeNPs was achieved at 0.4 mg/mL with 82 % flocculation activity. Iron nanoparticles are cation dependent with 85 % flocculation activity when Fe^{3+} was used as opposed to 46 % flocculation activity when there was no cation present. Contrary to this, CuNPs and Fe@Cu core-shell nanoparticles flocculate well without the addition of cations and are pH stable. Both CuNPs and Fe@Cu core-shell nanoparticles have remarkable ability to remove dyes, while FeNPs needs the addition of cation to yield RE above 50 %. The synthesized nanoparticles work well in removing both the COD and BOD in river water and coal mine wastewater. When evaluated for antimicrobial activity, both CuNPs were able to inhibit and kill the Gram-positive and Gram-negative microorganisms, while FeNPs did not show any antimicrobial activity. In the cytotoxicity study, all the nanoparticles showed to be safer to use at a low concentration 25 µg/µL, as the cell viability was above 70 % again HEK 293 and MCF7. After 7 weeks, all the nanoparticles were biodegraded by microorganisms.

Declaration of interest

The authors declare that there is no conflict of interest.

Acknowledgements

Nkosinathi Dlamini would like to acknowledge the Council for Scientific and Industrial Research (CSIR, South Africa) for the financial assistance in the form of the Ph.D. bursary. Rajasekhar Pullabhotla would like to acknowledge the National Research Foundation (NRF, South Arica) for the financial support in the form of the Incentive Fund Grant and Research Developmental Grants for Rated Researchers (Grant No: 103691 and 116363).

8.5. References

ABD EL-SALAM, A. E., ABD-EL-HALEEM, D., YOUSSEF, A. S., ZAKI, S., ABU-ELREESH, G. & EL-ASSAR, S. A. 2017. Isolation, characterization, optimization, immobilization and batch fermentation of bioflocculant produced by Bacillus aryabhattai strain PSK1. *Journal of Genetic Engineering and Biotechnology*, 15**,** 335-344.

ABDEL-HALIM, E. & AL-DEYAB, S. S. 2011. Removal of heavy metals from their aqueous solutions through adsorption onto natural polymers. *Carbohydrate Polymers*, 84**,** 454-458.

AGUNBIADE, M., POHL, C. & ASHAFA, O. 2018. Bioflocculant production from Streptomyces platensis and its potential for river and waste water treatment. *Brazilian Journal of Microbiology*.

CRINI, G. 2005. Recent developments in polysaccharide-based materials used as adsorbents in wastewater treatment. *Progress in polymer science,* 30**,** 38-70.

DANIELS, A. N. & SINGH, M. 2019. Sterically stabilized siRNA: gold nanocomplexes enhance c-MYC silencing in a breast cancer cell model. *Nanomedicine*.

DAVIS, A. P., SHOKOUHIAN, M., SHARMA, H. & MINAMI, C. 2006. Water quality improvement through bioretention media: Nitrogen and phosphorus removal. *Water Environment Research,* 78**,** 284-293.

DLAMINI, N. G., BASSON, A. K. & PULLABHOTLA, V. S. R. 2019a. Biosynthesis and Characterization of Copper Nanoparticles Using a Bioflocculant Extracted from *Alcaligenis faecalis* HCB2. *Advanced Science Engineering and Medicine,* 11**,** 1-7.

DLAMINI, N. G., BASSON, A. K. & PULLABHOTLA, V. S. R. 2019b. Optimization and Application of Bioflocculant Passivated Copper Nanoparticles in the Wastewater Treatment. *International Journal of Environmental Research and Public Health,* 16**,** 2185.

ELOFF, J. N. 1998. A sensitive and quick microplate method to determine the minimal inhibitory concentration of plant extracts for bacteria. *Planta medica,* 64**,** 711-713.

EXLEY, C., KORCHAZHKINA, O., JOB, D., STREKOPYTOV, S., POLWART, A. & CROME, P. 2006. Non-invasive therapy to reduce the body burden of aluminium in Alzheimer's disease. *Journal of Alzheimer's Disease,* 10**,** 17-24.

GONG, W.-X., WANG, S.-G., SUN, X.-F., LIU, X.-W., YUE, Q.-Y. & GAO, B.-Y. 2008. Bioflocculant production by culture of Serratia ficaria and its application in wastewater treatment. *Bioresource technology,* 99**,** 4668-4674.

KALE, G., AURAS, R., SINGH, S. P. & NARAYAN, R. 2007. Biodegradability of polylactide bottles in real and simulated composting conditions. *Polymer Testing,* 26**,** 1049-1061.

KARTHIGA DEVI, K. & NATARAJAN, K. A. 2015. Production and characterization of bioflocculants for mineral processing applications. *International Journal of Mineral Processing,* 137**,** 15-25.

KOLÁŘ, M., URBÁNEK, K. & LÁTAL, T. 2001. Antibiotic selective pressure and development of bacterial resistance. *International journal of antimicrobial agents,* 17**,** 357-363.

KUMAR, M. & PURI, A. 2012. A review of permissible limits of drinking water. *Indian journal of occupational and environmental medicine,* 16**,** 40.

LI, O., LU, C., LIU, A., ZHU, L., WANG, P.-M., QIAN, C.-D., JIANG, X.-H. & WU, X.-C. 2013. Optimization and characterization of polysaccharide-based bioflocculant produced by Paenibacillus elgii B69 and its application in wastewater treatment. *Bioresource technology,* 134**,** 87-93.

LIN, Z.-Z., HUANG, C.-L., HUANG, Z. & ZHEN, W.-K. 2017. Surface/interface influence on specific heat capacity of solid, shell and Core-shell nanoparticles. *Applied Thermal Engineering,* 127**,** 884-888.

LU, H., WANG, J., WANG, T., WANG, N., BAO, Y. & HAO, H. 2017. Crystallization techniques in wastewater treatment: An overview of applications. *Chemosphere,* 173**,** 474-484.

MALIEHE, S., SHANDU, S. J. & BASSON, K. A. 2015. The antibacterial and antidiarreal activities of the crude methanolic Syzygium cordatum [S. Ncik, 48 (UZ)] fruit pulp and seed extracts. *Journal of Medicinal Plants Research,* 9**,** 884-891.

MITTAL, H., MISHRA, S. B., MISHRA, A., KAITH, B., JINDAL, R. & KALIA, S. 2013. Preparation of poly (acrylamide-co-acrylic acid)-grafted gum and its flocculation and biodegradation studies. *Carbohydrate polymers,* 98**,** 397-404.

MOUSSAVI, G. & MAHMOUDI, M. 2009. Removal of azo and anthraquinone reactive dyes from industrial wastewaters using MgO nanoparticles. *Journal of hazardous materials,* 168**,** 806-812.

PATIL, S. V., PATIL, C. D., SALUNKE, B. K., SALUNKHE, R. B., BATHE, G. & PATIL, D. M. 2011. Studies on characterization of bioflocculant exopolysaccharide of

Azotobacter indicus and its potential for wastewater treatment. *Applied biochemistry and biotechnology,* 163**,** 463-472.

QU, X., ALVAREZ, P. J. & LI, Q. 2013. Applications of nanotechnology in water and wastewater treatment. *Water research,* 47**,** 3931-3946.

RUPARELIA, J. P., CHATTERJEE, A. K., DUTTAGUPTA, S. P. & MUKHERJI, S. 2008. Strain specificity in antimicrobial activity of silver and copper nanoparticles. *Acta biomaterialia,* 4**,** 707-716.

SALEHIZADEH, H. & SHOJAOSADATI, S. 2001. Extracellular biopolymeric flocculants: recent trends and biotechnological importance. *Biotechnology advances,* 19**,** 371-385.

SHAHWAN, T., SIRRIAH, S. A., NAIRAT, M., BOYACı, E., EROĞLU, A. E., SCOTT, T. B. & HALLAM, K. R. 2011. Green synthesis of iron nanoparticles and their application as a Fenton-like catalyst for the degradation of aqueous cationic and anionic dyes. *Chemical Engineering Journal,* 172**,** 258-266.

SHIH, I., VAN, Y., YEH, L., LIN, H. & CHANG, Y. 2001. Production of a biopolymer flocculant from Bacillus licheniformis and its flocculation properties. *Bioresource technology,* 78**,** 267-272.

SINGH, R. P., KARMAKAR, G., RATH, S., KARMAKAR, N., PANDEY, S., TRIPATHY, T., PANDA, J., KANAN, K., JAIN, S. & LAN, N. 2000. Biodegradable drag reducing agents and flocculants based on polysaccharides: materials and applications. *Polymer Engineering & Science,* 40**,** 46-60.

SONDI, I. & SALOPEK-SONDI, B. 2004. Silver nanoparticles as antimicrobial agent: a case study on E. coli as a model for Gram-negative bacteria. *Journal of colloid and interface science,* 275**,** 177-182.

SUN, J., ZHANG, X., MIAO, X. & ZHOU, J. 2012. Preparation and characteristics of bioflocculants from excess biological sludge. *Bioresource Technology,* 126**,** 362-366.

XIA, S., ZHANG, Z., WANG, X., YANG, A., CHEN, L., ZHAO, J., LEONARD, D. & JAFFREZIC-RENAULT, N. 2008. Production and characterization of a bioflocculant by Proteus mirabilis TJ-1. *Bioresource technology,* 99**,** 6520-6527.

XIA, X., LAN, S., LI, X., XIE, Y., LIANG, Y., YAN, P., CHEN, Z. & XING, Y. 2018. Characterization and coagulation-flocculation performance of a composite flocculant in high-turbidity drinking water treatment. *Chemosphere,* 206**,** 701-708.

YU, X., LI, J., SHI, T., CHENG, C., LIAO, G., FAN, J., LI, T. & TANG, Z. 2017. A green approach of synthesizing of Cu-Ag Core-shell nanoparticles and their sintering behavior for printed electronics. *Journal of Alloys and Compounds,* 724**,** 365-372.

ZAKI, S. A., ELKADY, M. F., FARAG, S. & ABD-EL-HALEEM, D. 2013. Characterization and flocculation properties of a carbohydrate bioflocculant from a newly isolated Bacillus velezensis 40B. *Journal of environmental biology,* 34**,** 51.

ZHU, C., CHEN, C., ZHAO, L., ZHANG, Y., YANG, J., SONG, L. & YANG, S. 2012. Bioflocculant produced by Chlamydomonas reinhardtii. *Journal of applied phycology,* 24**,** 1245-1251.

Chapter 9 : ARTICLE 7: Application and biosafety of the Fe@Cu core-shell nanoparticles

Dlamini Nkosinathi Goodman [a]*, Basson Albertus Kotze [a], Rajasekhar VSR Pullabhotla [b]*, Moganavelli Singh[c]

[a] Department of Biochemistry and Microbiology, University of Zululand, Private Bag X1001, KwaDlangezwa, 3886, South Africa

[b] Department of Chemistry, University of Zululand

School of life Sciences, University of KwaZulu-Natal, Private Bag X54001, South Africa

***** Corresponding Author; E-Mail: nathidlamini03@gmail.com; PullabhotlaV@unizulu.ac.za

Abstract: A broad range of applications and interesting properties of core-shell nanoparticles (CSNs) such as catalysis, sensors, material chemistry, biology, and water purification have gained the huge interest to most researchers in recent years. A dosage of 0.2 mg/mL was found to be the most effective as the flocculation activity (FA) was 99% and has an advantage to flocculate at a wider pH range of 3-11 (acidic, neutral and alkaline). Thermostability of the core-shell nanoparticles was evaluated between 60-100 ºC temperature, however, 96% flocculation activity was retained, indicating the thermal stability of the CSNs. The addition of cation, Ca^{2+}, improved the flocculation activity to the highest 99%. The high removal efficiency (RE) of COD, BOD, total nitrogen and phosphate was observed in all wastewater samples examined. The removal efficiency of the dyes was found to be above 93% for all dye samples. The Fe@Cu core-shell nanoparticles possess antimicrobial activity against both Gram-positive and Gram-negative microorganisms. The Minimal Inhibitory Concentration (MIC) and Bactericidal Minimal Concentration (MBC) was observed at a lower concentration of 1.563 mg/mL. Cell viability against HEK 293 and MCF7 was high at the lower concentration with the increase in concentration the decrease in cell viability was observed.

Key words: Application, Fe@Cu core-shell, nanoparticles, removal efficiency, synthesis

9.1 Introduction

A crucial aspect of our life is water, the essential feature of our planet. Ocean holds about 97% of our water and the only 1% of the fresh water is accessible for use (Corcoran, 2010). The world is facing crisis of both quality and quantity water since the beginning of the 21st century, this is due the industrialization, ever increasing population, food production practices, etc. Both liquid and solid waste is produced in every community and these wastes reach our water bodies. Wastewater contain nutrients which stimulates aquatic life growth and may also contain compounds which are toxic, i.e. mutagenic or carcinogenic compounds (Tchobanoglous et al., 1991).

The major water pollutants are colloids and are mostly kinetically unstable. This makes them hard to be removed, as they do not settle down under gravity (Santschi, 2018). Colloids possess a great challenge to be removed due to electrokinetic properties on their surface (Bampole and Bafubiandi, 2018). A physicochemical technique, which is often used to enhance flocs to form larger flocs that can be removed through sedimentation, floatation or filtration, is called flocculation (Abdullah et al., 2017). In the last decade, synthetic and chemical flocculants have been used in wastewater treatment due to high efficacy (Okaiyeto et al., 2016). Although, synthetic and chemical flocculants such as polyacrylamide derivatives and aluminum sulfate have high efficiency and are reported to be detrimental to both environment and human (Guo and Yu, 2014).

Material at nanoscale size with the cores (inner material) and shells (outer material) are traditionally defined as core-shell nanoparticles (CSNs) (Wang et al., 2013). Due to remarkable properties and application in diverse areas including catalysis, nanomaterial have attracted vast attention in the recent past. Furthermore, researchers over the past few decades have viewed conventional heterogeneous catalysts from a new perspective as the result of rapid nanotechnology development (Gawande et al., 2015). As a result, nanoparticles have been found to possess excellent properties in the wastewater application (Dlamini et al., 2019b, Tiwari et al., 2008)

The present paper aims to investigate the efficacy of Fe@Cu core-shell nanoparticles in the wastewater and river water treatment. For this purpose, removal efficacy of pollutants such as Chemical oxygen demand (COD), Biochemical oxygen demand (BOD), phosphate and total nitrogen was examined. Furthermore, this study seeks to establish the biosafety of core-shell nanoparticles synthesized using bioflocculant.

9.2 Material and Methods

9.2.1 Synthesis of Fe@Cu core-shell nanoparticles

To synthesize both iron and copper nanoparticles a series of steps were followed as described by Dlamini et al. (2019b); Dlamini et al. (2019a). A solution of both copper sulphate ($CuSO_4$) and iron sulphate ($FeSO_4$) were used. 3.0 mM of each solution was prepared separately and was added to 0.5 g of pure bioflocculant in a conical flask. The mixtures were allowed to stand at room temperate overnight and the control was the bioflocculant solution excluding the copper sulphate and iron sulphate. The synthesized nanoparticles were collected by centrifuge at 4000 rpm for 15 min at 4 °C (Dlamini et al., 2019b, Dlamini et al., 2019a).

To synthesize Fe@Cu core-shell nanoparticles a similar method with minor modifications as described by Yu et al. (2017) was followed. 3.0 mM solutions of $CuSO_4$ with different volumes of 10, 20, 30 mL was sequentially added to iron nanoparticles (FeNPs). The reaction was allowed to continue for 20 min after which the precipitate was harvested by centrifuge at 15000 rpm at 4 °C for 30 min (Yu et al., 2017).

9.2.2 Characterization of Fe@Cu core-shell nanoparticles

BRUKER D8 Advance Diffractometer operated at 40 kV, 40 mA, with graphite monochromatized CuKα1 radiation of wavelength λ=1.5406 Å was used to investigate the phase composition and crystallinity of the iron and copper nanoparticles. Diffraction pattern of the nanoparticles were recorded in the 2θ range from 20° to 80° at scanning steps of 0.03°. A sample of 0.1 mL was taken and diluted with 2 mL of deionized water to investigate UV–vis spectrum of copper nanoparticles, as a function of reaction time using a Perkin-Elmer spectrophotometer in the 300 to 700 nm wavelength region operated at a resolution of 1 nm. Field emission scanning electron microscopy (FESEM) (JSM-6700, JEOL, Japan) was used to examine synthesized nanoparticles. The synthesised nanoparticles were mounted on specimen stubs with double-sided adhesive tape coated with gold in a sputter coater. A drop of aqueous solution containing the nanoparticles was placed on carbon coated copper grids and dried under an infrared lamp (JEM 2010, JEOL, Japan) (accelerating voltage − 200.0 kV). Energy dispersive X-ray analysis (EDXA) combined with FESEM was used to ascertain the composition of the nanoparticles synthesized.

9.2.3 Evaluation of flocculation activity of Fe@Cu core-shell nanoparticles

F Kaolin clay (4 g/L) was used as the suspend solutes for experimentation. 100 mL of kaolin solution was mixed with 1% of 3 mL $CaCl_2$ and 2 mL of 0.2 mg/mL of Fe@Cu core-shell nanoparticles. The mixture was then transferred to a 250 mL conical flask and was shaken in the shaking incubator for 1 min at 165 rpm. After which the mixture was transferred to a graduated measuring cylinder and was allowed to stand for 5 min and the supernatant liquid was analyzed using a spectrophotometer at 550 nm. Flocculation activity (FA) was calculated using the equation below:

$$\text{Flocculation activity FA (\%)} = \frac{[A-B]}{A} \text{ X } 100 \quad (1)$$

Where: A and B are the optical density of both the sample and the control at 550 nm.

9.2.4 Application of Fe@Cu core-shell nanoparticles in dye removal and wastewater treatment

Mzingazi River water, domestic wastewater and coalmine wastewater were used to test the removal efficiency (RE) of Fe@Cu core-shell nanoparticles. To evaluate the RE of pollutants in all the water samples as described by Dlamini et al. (2019) was adopted. To examine the RE of COD, BOD, phosphate and total nitrogen test kits were used in accordance to manufacturer protocol and all the residuals were analyzed in a UV-Vis spectrophotometer Pharo 300 Spectroquant® at 680 nm. The RE of the pollutants was calculated by the following equation:

$$\text{RE (\%)} = \frac{C0-C1}{C0} \text{ X } 100 \quad (2)$$

Where: C_0 is the initial value and C_1 is the value after the flocculation treatment with Fe@Cu core-shell nanoparticles.

9.2.5 Antimicrobial activity of Fe@Cu core-shell nanoparticles

Bacillus subtilis CSM5 and *Escherichia coli* ATCC 25922 (1.0 mL) were used to evaluate the antimicrobial ability of Fe@Cu core-shell nanoparticles. Firstly, both strains were resuscitated by inoculation into the freshly prepared and autoclaved nutrient broth and was incubated overnight at 37 ºC. After which, the absorbance of the organisms was adjusted using spectrophotometer at 600 nm according to McFarlan standard (0.5). To determine both the Minimum Inhibitory Concentration (MIC) and Minimum Bactericidal Concentration (MBC) 96 microplate well method was adopted and ciprofloxacin 40 % and distilled water were used

as a positive and negative control respectively. Firstly, all wells were flooded with 50 µL of sterile nutrient broth and followed by the addition of 50 µL inoculum of *Bacillus subtilis* and *Escherichia coli*. Subsequently 50 µL of Fe@Cu core-shell nanoparticles with 0.2 mg/mL was added in the first rows of 96 well micro plates and followed by a series of dilutions from the highest concentration to the lowest to ensure that all wells had 50 µL remaining. *P-iodonitrotetrazolium* (INT) was used as an indicator (Eloff, 1998). Muller Hilton agar was used to evaluate the MBC where the wells that did not indicate colour change were streak on a sterile agar and incubated at 37 °C for 12 hrs. The lowest concentration of nanoparticles that exhibited the complete killing of the trial organisms were considered as the MBC.

9.2.6 In-vitro cytotoxicity of Fe@Cu core-shell nanoparticles

The description according to Daniels and Singh (2019) was followed to achieve *in-vitro cytotoxicity* of Fe@Cu core-shell. Cell lines HEK 293 and MCF-7 were used to ascertain the cytotoxicity of the as-synthesized nanoparticles. To plate the cells with cell suspensions of 1×10^5 cells/mL concentrations 96-well plates were employed. Using tenfold dilution method, cells were seeded with different concentration of 25-100 µg/µL of nanoparticles after 48 hours of incubation. To administrate the nanoparticles a medium containing 1% of foetal bovine serum (FBS) was used and plates were incubated for 48 hrs. Cell viability was ascertained with the use of tetrazolium salt (Sigma) as an indicator. 15 µL of MTT (5 mg/mL) in phosphate buffered saline (PBS) was added to each well and incubated at 37 °C for 4 hrs. The medium with MTT and formed formazan crystals were dissolved in 100 µL of dimethyl sulfoxide (DMSO) after sucking off the wells. After which, micro plate reader was used for reading the solution, its optical density was measured at 570 nm (Daniels and Singh, 2019). The following formula was used for determining cell viability:

$$\text{Cell viability}(\%) = \frac{F1}{F0}\ X\ 100 \qquad (3)$$

Where F_1 and F_0 are the final values obtained after and before treatment with the nanoparticles, respectively.

9.2.6 Software and statistical analysis

All the experimentations were conducted in triplicates and the error bars in the figures shows the standard deviations of the data. Data were subjected to one-way analysis of variance using Graph Pad Prism ™ 6.1. *P* values ≤0.05 were regarded as significant. Values with different alphabets along the same row are significantly different.

9.3 Results and discussion

9.3.1 The dosage effect on the flocculation activity of Fe@Cu core-shell nanoparticles.

Figure 9.1 represents the results obtained during the evaluation of nanoparticles Fe@Cu core-shell effect of dosage concentration on the flocculation activity. The highest flocculation activity of above 90% was observed for all the dosage concentrations.

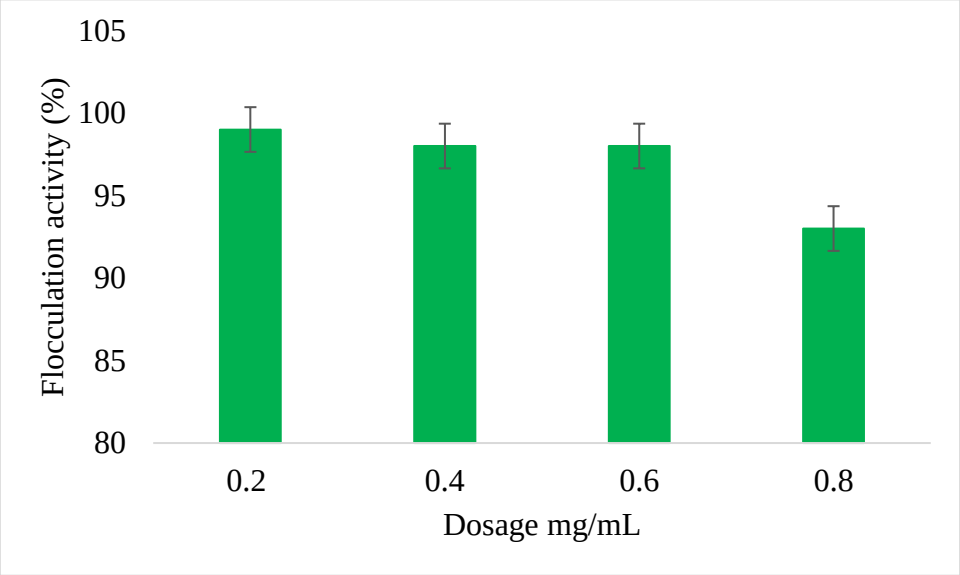

Figure 9.1: Dosage effect on the flocculation activity of Fe@Cu core-shell. (Refer to index data Table 9.1).

A flocculant with a high efficacy at the lowest dosage concentration is a necessity in wastewater treatment. From Figure 9.1, Fe@Cu core-shell nanoparticles revealed some interesting capabilities when tested against kaolin clay as the flocculation activity was observed to be highest at 0.2 mg/mL with 99% flocculation activity. With the increase in dosage, slight decrease in flocculation activity between 0.4-0.6 mg/mL and the lowest flocculation activity was observed at the highest concentration of 0.8 mg/mL. Contrary to this, the increase in polymer dosage concentration resulted in aggregation between colliding particles and larger flocs formation. However, further increase in dosage concentration is likely to result in limited floc formation as the results of fluid shear (Guibai and Gregory, 1991). From Figure 1 it can be deduced that the as-synthesized Fe@Cu core-shell nanoparticles are commercially viable as they are effective at lowest concentration.

9.3.2 Effect of cation presence in flocculation process

Table 9.1 below shows the results of cations presence effect on flocculation activity. The as synthesized Fe@Cu core-shell nanoparticles flocculate well in the absence of cation with the flocculation activity above 90%.

Table 9.1: Effect of cations on the flocculation activity of Fe@Cu core-shell.

Cations	Flocculation Activity (%) ± SD
Control	95 ± 0.3^{a}
Fe^{3+}	97 ± 0.0^{a}
Ca^{2+}	99 ± 0.2^{a}
Na^{+}	97 ± 0.2^{a}

Values represent mean ± deviation of replicate readings. Percentage flocculating activities with different letters (a) are significantly ($p<0.05$) different. (Refer to index data Table 9.2).

The presence of cation is significant in a flocculation process. The cation neutralizes charge of both the kaolin suspension and the flocculant, which in turn facilitate the formation of flocs (Manivasagan et al., 2015). In Table 9.1, all the evaluated cations i.e. trivalent, divalent and monovalent facilitated the flocculation process with the Ca^{2+} having the highest of 99%. However, the nanoparticles could flocculate well even in the absence of cations as the control had 95% flocculation activity. As shown in the Table 9.1, the statistical significance of the flocculation activity not that noteworthy as indicated in the parenthesis. This makes the synthesized nanoparticles to be a possible alternative to some chemical flocculants, which have been found to be neurotoxic, carcinogenic and environmentally unfriendly (Shevah, 2016). Similar results have been documented in a study conducted by Dlamini et al. (2019), where it was demonstrated that copper nanoparticles contributed a flocculation activity up to 96% in the absence of cation.

9.3.3 The pH effect on the flocculation activity of Fe@Cu core-shell nanoparticles

The results displayed in Figure 9.2 shows the effect of pH on flocculation process. The optimum pH was 7 with 99% flocculation activity.

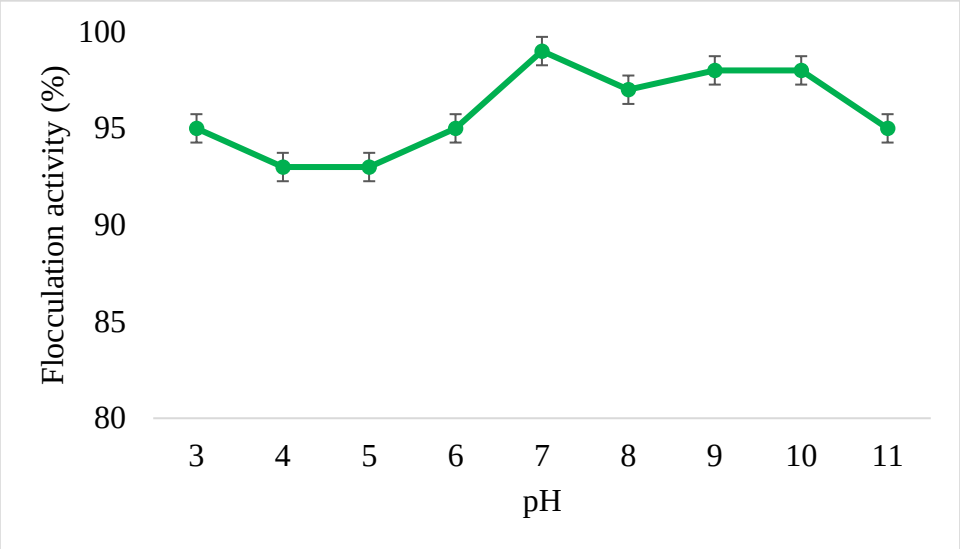

Figure 9.2: Effect of pH on flocculation activity of Fe@Cu core-shell. (Refer to index data Table 9.3).

The as-synthesized nanoparticles are pH stable and are suitable for application of both in acidic and alkaline wastewater. From Figure 9.2 it is evident that the flocculation activity of the as-synthesize nanoparticles fluctuated at pH 3 with flocculation activity of 95%. Slight change in pH (between 4-6) resulted in constant flocculation activity of 93% can be observed and at neutral pH 7 the optimum activity of 99% was witnessed. These current findings suggest that the as-synthesized Fe@Cu core-shell nanoparticles have potential applications in both acid mine wastewater and alkaline water. Also shows the ability of CSNs to withstand extreme acidic and alkaline conditions.

9.3.4 Thermostability of Fe@Cu core-shell nanoparticles

Figure 9.3 reflects the findings of heat effect on the flocculation of Fe@Cu core-shell nanoparticles. The results indicate that the nanoparticles are thermostable as the flocculation activity was above 90% at 100 ºC.

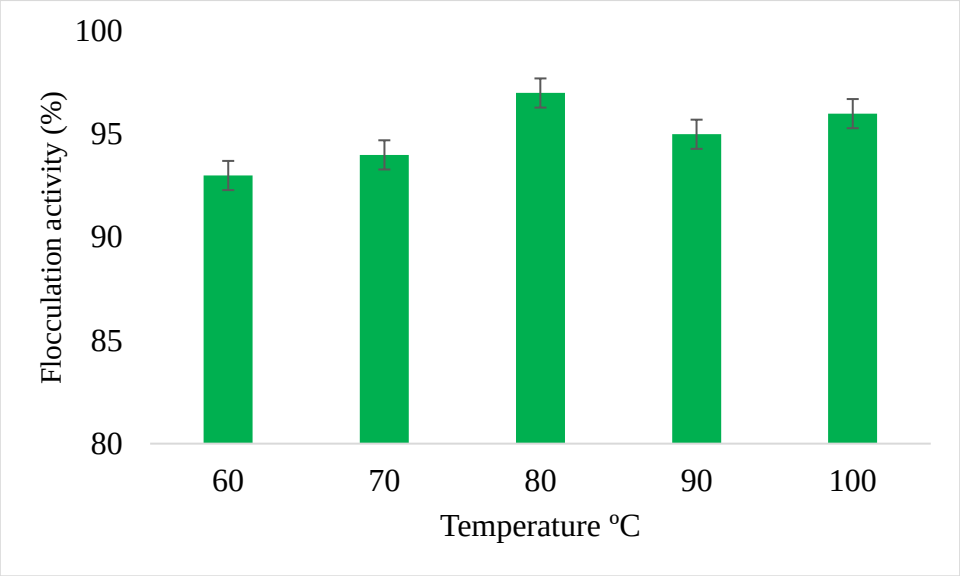

Figure 9.3: Effect of heat on flocculation activity of Fe@Cu core-shell. (Refer to index data Table 9.4).

Thermostability of nanoparticles was assessed, where the synthesized nanoparticles were exposed in water bath for 30 min at different temperatures (Figure 9.3). The flocculation activity was above 90% at all the temperatures with 80 ºC having the highest flocculation activity of 97%. Thermostability of the nanoparticles can be attributed to the temperature resistant nature of the bioflocculant that is polysaccharide in nature, from which the nanoparticles were synthesized (Dlamini et al., 2019b). Moreover, both iron and copper have a high boiling point, this may also contribute to heat resistant nature of the as-synthesized Fe@Cu core-shell nanoparticles. Furthermore, composite/core-shell material are said to be able to with stand extremely high temperatures (Yu and Dutta, 2011).

9.3.5 Application of Fe@Cu core-shell nanoparticles on dye removal

Figure 9.4 represents the results of dye removal by Fe@Cu core-shell nanoparticles. The as-synthesised nanoparticles showed the removal efficiency of above 90% for all dyes. With 95% as the highest for malachite green, safranin and methylene orange dyes and the lowest removal with 93% for methylene blue.

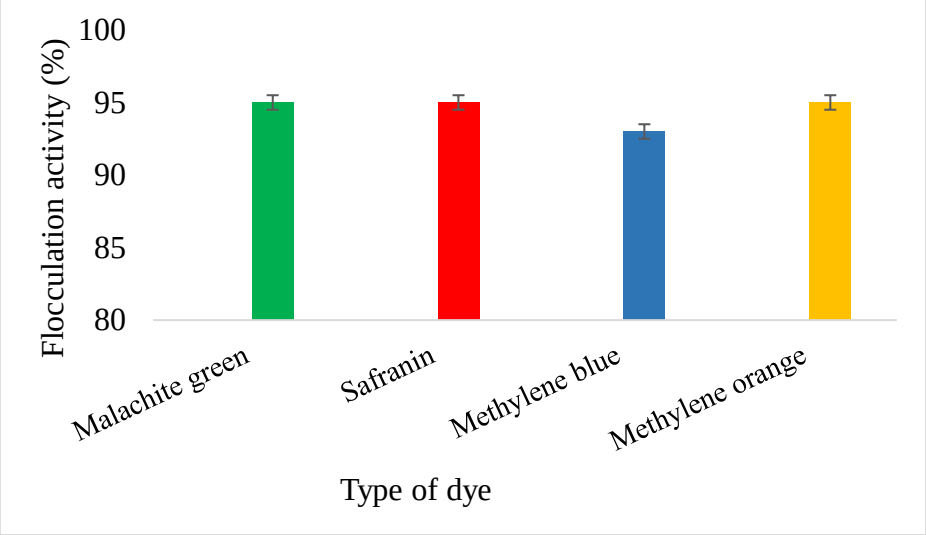

Figure 9.4: Removal of dyes by Fe@Cu core-shell. (Refer to index data Table 9.5).

Textile industries are one of the main sources for producing huge amounts of effluents. Invariably, this end up reaching water bodies when untreated. Most pigmenting material used during processing are not only toxic to the environment, but also are not degradable. The released textile wastewater causes adverse effects to the environment due to its toxicity, pigmentation and non-degradability. Moreover, the ecosystem is disturbed by these colouring agents from textile effluents, as the light cannot penetrate through the aquatic plants for photosynthesis (Merzouk et al., 2010). The highest dye removal efficiency of 95% was observed in malachite green, safranin and methylene orange. The lowest dye removal efficiency of 93% was detected for methylene blue.

9.3.6 In-vitro cytotoxicity test of Fe@Cu core-shell nanoparticles on HEK 293 and MCF7

Figure 9.5 represents in-vitro cytotoxicity of Fe@Cu core-shell nanoparticles. The as-synthesized nanoparticles are nontoxic at low concentration.

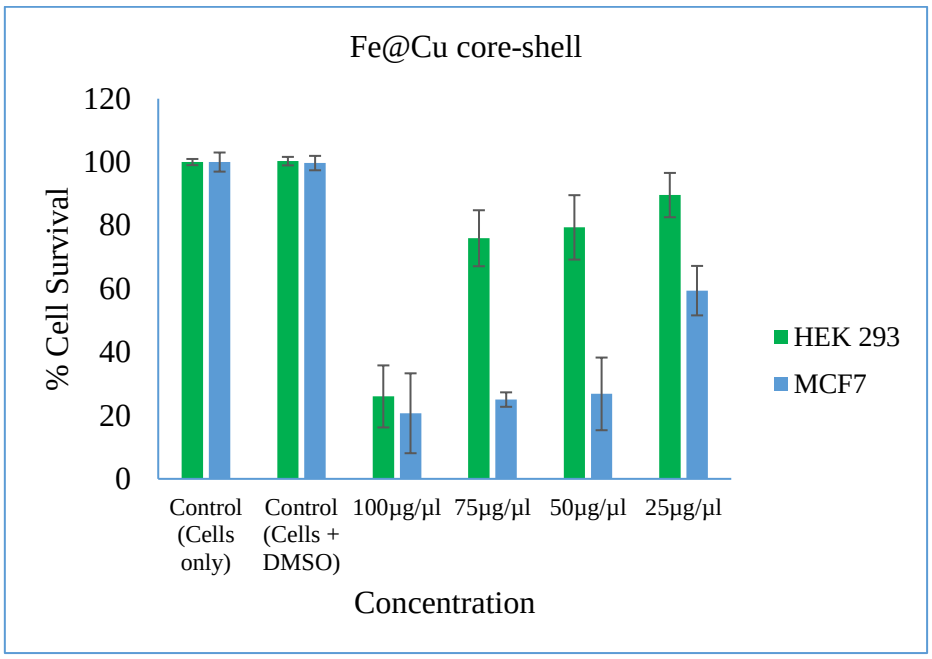

Figure 9.5: *In-vitro* cytotoxicity of Fe@Cu core-shell nanoparticles on HEK 293 and MCF7.

MTT assay was used to investigate the cytotoxicity of Fe@Cu core-shell nanoparticles on MCF7 and HEK 293 cell lines (Moodley and Singh, 2019). From Figure 9.5 the cell viability of normal cells (HEK 293) is 89% at 25 µg/µL and with the increased in concentration of the Fe@Cu core-shell nanoparticles the viability decreased to 75% at 75 µg/µL which indicates that the nanoparticles are safer to use. However, at the highest concentration 100 µg/µL the cell viability was below 50%. This, suggests that at higher concentration the nanoparticles are not safe. Contrary to this, the nanoparticles were found to be toxic against canceral cells (MCF7) as the viability was below 50% at the second lowest concentration of 50 µg/µL.

9.3.7 Antimicrobial test of Fe@Cu core-shell nanoparticles

Table 2 shows the results of Minimal Inhibitory Concentration (MIC) and Minimal Bactericidal Concentration (MBC) of the nanoparticles. The as-synthesized nanoparticles have the MIC and MCB for both the Gram-positive and Gram-negative.

Table 9.2: The antimicrobial effect of Fe@Cu core-shell.

Antimicrobial agent	Bacterial strain	MIC (mg/mL)	MBC (mg/mL)
Fe@Cu Core-shell	*E. coli*	1.563	1.563
	B. subtilis	1.563	1.563
Ciprofloxacin	*E. coli*	12.5	12.5
	B. subtilis	6.25	6.25

Antimicrobial activity of Fe@Cu core-shell nanoparticles was assessed against a Gram-positive and Gram-negative microorganisms. Here 40% ciprofloxacin was used as a positive control while 0.2 mg/mL of Fe@Cu core-shell nanoparticles were present. The as-synthesized nanoparticles proved to be more effective as both the MIC and MBC was achieved at low concentration of 1.563 mg/mL for both *E. coli and B. subtilus*. Contrary to this, when ciprofloxacin was used, the results revealed that the MIC and MBC for *E. coli and B. subtilus* are 12.5 and 6.25 mg/mL respectively.

9.3.8 Application of Fe@Cu core-shell in wastewater treatment

Table 9.3 showed the removal of pollutants in wastewater. The Fe@Cu core-shell nanoparticles are effective in COD and BOD removal.

Table 9.3: Wastewater treatment using Fe@Cu core-shell.

Flocculant	Type of wastewater	Pollutant type	Water quality before treatment (mg/mL)	Water quality after treatment (mg/mL)	Removal efficiency (%)
Fe@Cu core-shell	Coal mine water	COD	842	71	92
		BOD	123.2	3.1413	97
	Mzingazi River water	COD	3.300	0.793	76
		BOD	136	70	94
		Phosphate	85.7	0.109	99
		Total nitrogen	0.223	0.014	94
	Domestic wastewater	Phosphate	3.38	0.127	97
		Total nitrogen	0.137	0.09	84

For easy disposal of waste and convenient water access, most industries are situated along riverbanks. Wide range of contaminants such as heavy metals, hydrocarbons, alkalis, chlorinated hydrocarbons and other chemicals which often greatly change the water pH (Lokhande et al., 2011). There is high concentration of chemical oxygen demand (COD) and biochemical oxygen demand (BOD) in the coalmine wastewater as shown in Table 9.3 and the as-synthesized Fe@Cu core-shell nanoparticles were able to remove up to 92% and 97% respectively. In Mzingazi River water, the high concentration of BOD can be attributed due to crop and animal wastes, industrial effluent discharge as there are farms and industries near the Mzingazi River. The core-shell nanoparticles removed up to 95% of BOD while COD removal efficiency was 76%. Total nitrogen and phosphate removal for domestic wastewater was 84% and 97% respectively, while total nitrogen and phosphate removal efficacy for Mzingazi river water was 94% and 99%.

9.4 Conclusion

The as-synthesized Fe@Cu core-shell nanoparticles are effective to flocculate at low concentration of 0.2 mg/mL, cation independent, pH stable and thermostable. Possesses antimicrobial effect for both Gram-positive and Gram-negative bacteria and the MIC and MBC was found at the lowest concentration of 1,563 mg/mL and are not toxic against normal cells at low concentration. Also, showed some remarkable properties in removing dyes at a concentration of 4 g/L with 0.2 mg/mL dosage size. High removal efficacy for wastewater and river water was also observed.

Authors' contributions

Author Contributions: Conceptualization, A.K.B. and V.S.R.P.; formal analysis, N.G.D. and V.S.R.P.; investigation, N.G.D.; supervision, A.K.B and V.S.R.P.; writing—original draft, N.G.D.; writing—review and editing, V.S.R.P; cytotoxicity experiments, M.S.

Funding: National Research Foundation (NRF, South Arica) for the financial support in the form of the Incentive Fund Grant (Grant No: 103691).

Acknowledgments: Nkosinathi Dlamini would like to acknowledge the Council for Scientific and Industrial Research (CSIR, South Africa) for the financial assistance in the form of the Ph.D. bursary. Rajasekhar Pullabhotla would like to acknowledge the National Research Foundation (NRF, South Arica) for the financial support in the form of the Incentive Fund Grant and Research Developmental Grants for Rated Researchers (Grant No: 103691 and 116363).

9.5 References

ABDULLAH, M., ROSLAN, A., KAMARULZAMAN, M. & ERAT, M. Colloids removal from water resources using natural coagulant: Acacia auriculiformis. AIP Conference Proceedings, 2017. AIP Publishing, 020243.

BAMPOLE, D. L. & BAFUBIANDI, M. 2018. Removal Performance of Silica and Solid Colloidal Particles from Chalcopyrite Bioleaching Solution: Effect of Coagulant (Magnafloc Set# 1597) for Predicting an Effective Solvent Extraction. *Engineering Journal,* 22**,** 123-139.

CORCORAN, E. 2010. *Sick water?: the central role of wastewater management in sustainable development: a rapid response assessment*, UNEP/Earthprint.

DANIELS, A. N. & SINGH, M. 2019. Sterically stabilized siRNA: gold nanocomplexes enhance c-MYC silencing in a breast cancer cell model. *Nanomedicine*.

DLAMINI, N. G., BASSON, A. K. & PULLABHOTLA, V. S. R. 2019. Optimization and Application of Bioflocculant Passivated Copper Nanoparticles in the Wastewater Treatment. *International Journal of Environmental Research and Public Health,* 16**,** 2185.

ELOFF, J. N. 1998. A sensitive and quick microplate method to determine the minimal inhibitory concentration of plant extracts for bacteria. *Planta medica,* 64**,** 711-713.

GAWANDE, M. B., GOSWAMI, A., ASEFA, T., GUO, H., BIRADAR, A. V., PENG, D.-L., ZBORIL, R. & VARMA, R. S. 2015. Core–shell nanoparticles: synthesis and applications in catalysis and electrocatalysis. *Chemical Society Reviews,* 44**,** 7540-7590.

GUIBAI, L. & GREGORY, J. 1991. Flocculation and sedimentation of high-turbidity waters. *Water Research,* 25**,** 1137-1143.

GUO, J. & YU, J. 2014. Sorption characteristics and mechanisms of Pb (II) from aqueous solution by using bioflocculant MBFR10543. *Applied microbiology and biotechnology,* 98**,** 6431-6441.

LOKHANDE, R. S., SINGARE, P. U. & PIMPLE, D. S. 2011. Pollution in water of Kasardi River flowing along Taloja industrial area of Mumbai, India. *World Environment,* 1**,** 6-13.

MANIVASAGAN, P., KANG, K.-H., KIM, D. G. & KIM, S.-K. 2015. Production of polysaccharide-based bioflocculant for the synthesis of silver nanoparticles by Streptomyces sp. *International journal of biological macromolecules,* 77**,** 159-167.

MERZOUK, B., MADANI, K. & SEKKI, A. 2010. Using electrocoagulation–electroflotation technology to treat synthetic solution and textile wastewater, two case studies. *Desalination,* 250**,** 573-577.

MOODLEY, T. & SINGH, M. 2019. Polymeric Mesoporous Silica Nanoparticles for Enhanced Delivery of 5-Fluorouracil In Vitro. *Pharmaceutics,* 11**,** 288.

OKAIYETO, K., NWODO, U. U., OKOLI, S. A., MABINYA, L. V. & OKOH, A. I. 2016. Implications for public health demands alternatives to inorganic and synthetic flocculants: bioflocculants as important candidates. *MicrobiologyOpen,* 5**,** 177-211.

SANTSCHI, P. H. 2018. Marine colloids, agents of the self-cleansing capacity of aquatic systems: Historical perspective and new discoveries. *Marine Chemistry,* 207**,** 124-135.

SHEVAH, Y. 2016. Substitution of Chloride Chemicals with Degradable Bioflocculants for Sedimentation of Suspended Particles in Water. *Chemistry Beyond Chlorine.* Springer.

TCHOBANOGLOUS, G., BURTON, F. L. & STENSEL, H. 1991. Wastewater engineering. *Management,* 7**,** 1-4.

TIWARI, D. K., BEHARI, J. & SEN, P. 2008. Application of nanoparticles in waste water treatment 1.

WANG, H., CHEN, L., FENG, Y. & CHEN, H. 2013. Exploiting core–shell synergy for nanosynthesis and mechanistic investigation. *Accounts of chemical research,* 46**,** 1636-1646.

YU, X., LI, J., SHI, T., CHENG, C., LIAO, G., FAN, J., LI, T. & TANG, Z. 2017. A green approach of synthesizing of Cu-Ag core-shell nanoparticles and their sintering behavior for printed electronics. *Journal of Alloys and Compounds,* 724**,** 365-372.

YU, Y.-T. & DUTTA, P. 2011. Examination of Au/SnO2 core-shell architecture nanoparticle for low temperature gas sensing applications. *Sensors and Actuators B: Chemical,* 157**,** 444-449.

Chapter 10 : ARTICLE 8: Synthesis optimization of Fe@Cu core-shell nanoparticles, characterization and application

Dlamini N.G [a]*, Basson A.K [a], Shandu J.S.E[a], Rajasekhar Pullabhotla V.S.R [b]*

[a] Department of Biochemistry and Microbiology, University of Zululand, Private Bag X1001, KwaDlangezwa, 3886, South Africa

[b] Department of Chemistry, University of Zululand

*****Author to whom correspondence should be addressed; E-Mail: nathidlamini03@gmail.com; PullabhotlaV@unizulu.ac.za

Tel. +27-73 0985921/ +27-79 6828 444

Abstract: Green synthesis of core-shell nanoparticles is gaining importance nowadays as it is viewed as being environmental friendly and cost effective. The present study aimed at synthesizing iron@copper core-shell nanoparticles using a polysaccharide-based bioflocculant from *Alcalegenis faecalis* and to evaluate its efficiency in dye removal, river water and domestic wastewater treatment. The synthesized samples were characterized by Fourier transform infrared (FT-IR) spectroscopy, X-ray diffraction and scanning electron microscopy (SEM). To optimize best concentration for core-shell formation, different ratios of iron to copper were prepared: sample 1 (S1) contained 1:3 iron to copper (Fe 25% - Cu 75%), sample 2 (S2) contained 1:1 iron to copper (Fe 50% - Cu 50%) and third sample (S3) contained 3:1 iron to copper (Fe 75% - Cu 25%). The flocculation activity (FA) was above 98% at 0.2 mg/mL for all the samples and flocculate well at acidic, alkaline and neutral pH conditions. Sample 3 showed to be thermostable with flocculation activity above 90% and both sample 2 & 1 were also thermostable, but the flocculation decreased to 87 at 100 °C. All three samples revealed some remarkable properties for staining dye removal as the removal efficiency was above 89% for all dyes tested. The synthesized core-shell nanoparticles could remove nutrients such as total nitrogen and phosphate in both domestic wastewater and Mzingazi river water. Furthermore, high removal efficiency for COD and BOD was also observed.

Keywords: core-shell nanoparticles, removal efficiency, optimization, synthesis

10.1 Introduction

Drinking water scarcity i.e. water free of pathogens and toxic chemical substances is a worldwide problem due to population growth, extended droughts, competing demands from different users, and more health based regulations. However, the conditions are very severe in developing countries (Tiwari et al., 2008). Chemical flocculants have been widely used in nowadays owing to their low cost, effective flocculation performance. However, their application has been found to cause environmental and health hazards such as Alzheimer's disease (Exley et al., 2006).

Use of bioflocculants has gained interest in recent years due to the biodegradability properties they possess and negligible environmental hazards. Nonetheless, higher production cost, low flocculation yields are the limitations to the industrial application of bioflocculants (Yang et al., 2009). Consequently, in recent years, the study is mainly focussed on the synthesis of nanoparticles from bioflocculants and their application in industrial effluents and wastewater treatment. Alternatively, composite flocculants serve as a way to reduce cost as they can flocculate well even at low dosages and reduces the risk of adverse effects that comes with synthetic flocculants, since their dosage is reduced to smallest (Yang et al., 2009).

Textile industries discharge tons of effluents to the environment which contain pollutants and dyes that are carcinogenic in nature and non-degradable (Sankar et al., 2014). Furthermore, most of the paper and textile industries use dyes and discharge the effluents to water resources. Technologies such as hydrogen peroxide and UV radiation are not effective to these dyes as they are chemically stable. Recent findings suggest that nanomaterial are successful used in dye degradation which make nanoparticles to be more profitable compared to chemical and physical methods (Sankar et al., 2014).

In present study, iron@copper core-shell nanoparticles were synthesized using a bioflocculant from marine species *Alcalegenis faecalis*. Copper sulphate ($CuSO_4$) and iron chloride ($FeCl_3$) were used as the precursors for the iron@copper nanoparticles. Different ratios of iron to copper (1:3, 1:1, and 3:1) were prepared to optimize the most effective combination. Various parameters such as dosage, pH, temperature and cations were varied to optimize the effectiveness of synthesized iron@copper core-shell nanoparticles in flocculation efficiency and tested against kaolin clay as a standard test material.

10.2 Methodology

10.2.1 Synthesis of iron@copper core-shell nanoparticles

The synthesis of core-shell nanoparticles was achieved using the description by Yu et al. (2017) where 10 mL of 0.02 M $FeCl_3$ aqueous solution was prepared in a flask, after which 0.5 g of bioflocculant was added. A 10 mL of 5.0 M (NaOH) was added to the solution of $FeCl_3$ at room temperature. This mixture was added into 10 mL solution of glucose (1.0 M). Colour change indicated the formation of iron nanoparticles. To obtain different ratios of iron to copper, different volumes were prepared. The first ratio of 1:3 was prepared by mixing 25 mL (0.003 M) $FeCl_3$ with 75 mL (0.003 M) of $CuCl_2$ and the 1:1 ratio was achieved by mixing 50 mL of each sample as indicated, consequently the final ratio 3:1 was obtained by mixing 75 mL of (0.003 M) of $FeCl_3$ and 25 mL (0.003 M) of $CuCl_2$. The reaction was allowed to continue for 20 min, resulting precipitate was collected through centrifugation at 15 000 rmp, 4 °C for 30 min (Yu et al., 2017).

10.2.2 Test for flocculation activity of S1, S2 and S3

Flocculation activity was evaluated using a method developed by Kurane et al. (1986) with a slight modification, where 4 g of kaolin clay was dissolved in a litre of distilled water. 100 mL of the prepared kaolin solution was mixed with 2 mL of nanoparticles solution in a concentration of 2 mg/mL and 3 mL of $CaCl_2$ (1 g/L) solution was also added after which the mixture was shaken for a minute and transferred to 100 mL graduated measuring cylinder. To observe the flocculation ability of the synthesized core-shell nanoparticles the mixture was left to stand for 5 min at room temperature and only the upper part was taken for analysis using UV-Vis Pharo 100 Spectrophotometer® (Kurane et al., 1986). Flocculating activity was calculated according the following equation:

$$Flocculation\ activity\ (FA)\% = \frac{[A-B]}{A} X\ 100 \qquad (1)$$

A = Optical density of Control at 550 nm and B = Optical density of Sample at 550 nm.

10.2.3 Optimization of S1, S2 and S3 in flocculation activity

Optimization of core-shell nanoparticles was achieved by varying various parameters such as dosage, temperature, pH and cations against kaolin clay solution. To evaluate dosage effect 0.2-0.8 mg/mL concentrations were prepared. The dosage that resulted in the highest

flocculation activity was used for subsequent experiments. Trivalent, divalent and monovalent cations were evaluated for their effect on flocculation activity. Thermostability of the material was verified by varying the temperature (60, 80 and 100 °C). Finally, the effect of pH was conducted by changing pH (3, 7 and 11) which represented acidic, neutral and alkaline conditions respectively. All these parameters were varied in order to establish conditions that favours the optimal flocculation activity (Agunbiade et al., 2018).

10.2.4 Dyes removal by core-shell nanoparticles

Dyes such as safranin, methylene blue, methylene orange and malachite green were used to evaluate the removal efficiency of core-shell nanoparticles. Core-shell nanoparticles of 0.2 mg were dissolved in 50 mL distilled water after which 2 mL of nanoparticles solution was mixed with dye solution (4 g/L) and the mixture was shaken for a minute and allowed to stand at room temperature for 5 min. Each dye solution was measured at maximum wavelength and all the experiments were conducted in triplicates. The supernatant was analysed using Pharo 100 Spectrophotometer®. The formula below was used for calculating the removal efficiency (RE):

$$RE = \frac{Ci - Cf}{Ci} \; X \; 100 \qquad (2)$$

Where: C_i is the initial value before addition of nanoparticles and C_f is the value after the treatment with core-nanoparticles.

10.2.5 Characterization of S1, S2 and S3

10.2.5.1 Morphological surface and elementary analysis of S1, S2, S3

Scanning Electron Microscope (JEOL JSM-6100) equipped with energy-dispersive X-ray analyser (EDX) techniques were used for the morphological and compositional information of the samples S1, S2 and S3. SEM images were taken using a tungsten (W) filament operated at an emission current and accelerator voltage of 100 µA and 10 kV. SEM samples were prepared by placing a small quantity of the material on double-sided carbon tape stuck on copper stub and coated with carbon (using JEOL vacuum evaporator).

10.2.5.2 FT-IR and X-ray diffraction of S1, S2 and S3

Fourier Transform-Infrared (FT-IR) spectroscopy was used to identify and confirm the functional groups present in the bioflocculant using Tensor 27, Bruker FT-IR

spectrophotometer. The FT-IR spectra were recorded for the dry powder samples with a resolution of 4 cm^{-1} in the range of 4000–200 cm^{-1}.

The crystallinity of the synthesised samples was studied using a Bruker D8 Advance diffractometer equipped with Cu-Kα radiation (λ=1.5406 Å) at 40 kV, 40 mA at room temperature. The dry samples were placed on a sample holder and the diffraction patterns were recorded between 5 to 90°.

10.2.5.3 Thermogravimetric analysis of S1, S2 and S3

Thermogravimetric analysis were performed on the synthesised samples using (Perkin-Elmer Thermal Analysis Pyris 6 TGA) high temperatures with range 22 to 900 °C was used to heat the bioflocculant, at a constant rate of ramping, 10 °C min^{-1} and under constant under constant flow of nitrogen gas (Dlamini et al., 2019a).

10.3 Results and discussion

10.3.1 X-ray diffractions of S1, S2 and S3

The x-ray diffraction patterns of the samples S1, S2 and S3 are shown in Figure 10.1. Strong and characteristic crystalline peaks are observed between of 30 and 50° 2θ.

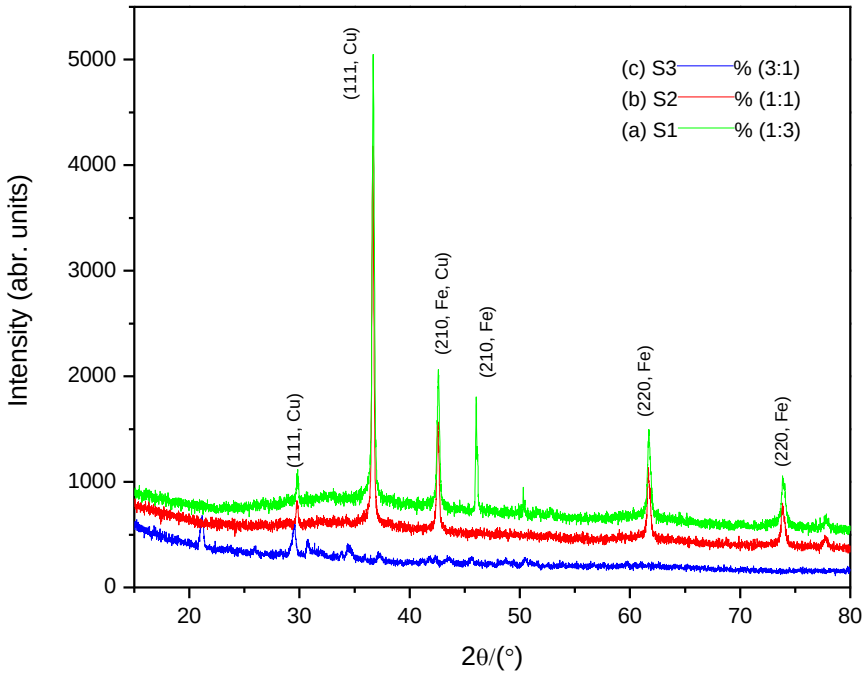

Figure 10.1: X-ray diffractograms of samples (a) S1, (b) S2 and (c) S3.

From Figure 10.1 the strong peaks were observed at 2θ ~ 35°, 40° and 65° in S1. Contrary to this, it was noted that the strongest peak was at 2θ ~ 35°, 45°, 65° and 77 ° for S2. While in S3, the strong is observed at 2θ ~ 22° and 30°. However, the peaks are not as strong as it is seen in S2. Strong peaks normally represent the crystallinity and the smaller particles. It could be deduced that when the proportion of iron to copper is 1:3, the size of as-synthesized Fe@Cu core-shell nanoparticles become smaller.

10.3.2 FT-IR spectra of S1, S2 and S3 nanoparticles

Figure 10.2 shows the functional groups that are present in S1, S2 and S3. This showed the presence of hydroxyl (OH) group and amine (NH_2) group in the samples. The weak band at 2244 cm^{-1} in all samples can be designated to the presence of aliphatic bonds.

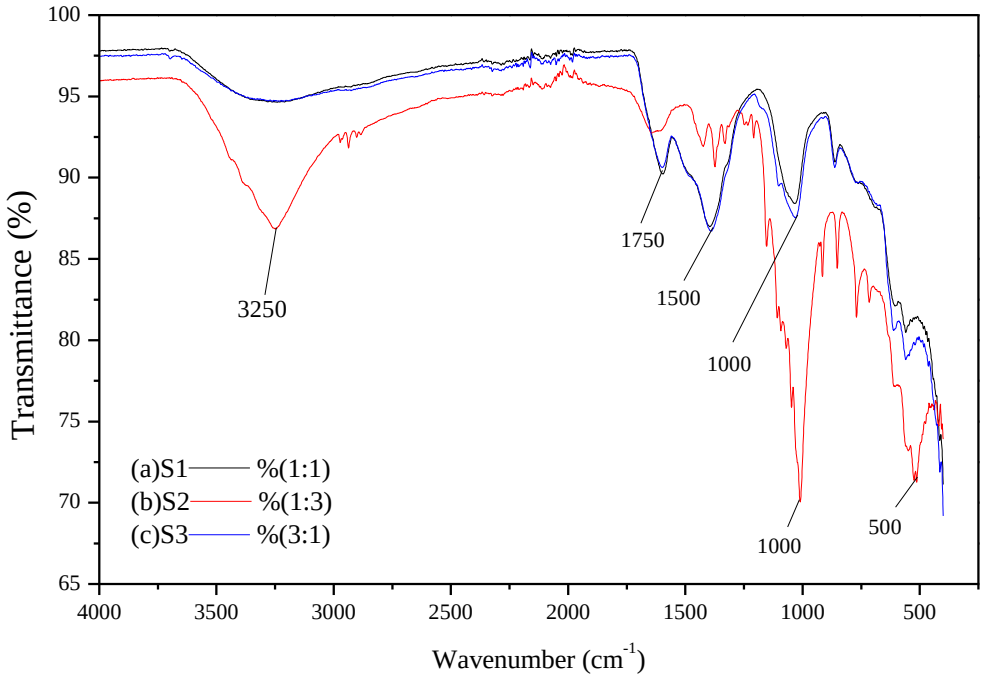

Figure 10.2: FT-IR spectra of samples (a) S1, (b) S2 and (c) S3.

Different functional groups serve as the binding sites for flocculants during flocculation process. Higher flocculation ability of the samples can be attributed to the presence of different functional groups as observed from Figure 10.2. Different functional groups were revealed by Fourier transform infrared (FT-IR) spectroscopy analysis. Hydroxyl group (-OH) and amine (NH_2) group was observed in the same plane for samples S1 and S2 respectively. The peaks at 1700 – 1500 cm^{-1} wavelengths signifies the presence of C=O amide group and the deep peak around 1200 cm^{-1} region is typical of C-OH stretching. C-O-C stretching was observed at 1250 – 1050 cm^{-1} as depicted in Figure 2. The strong peak in samples S2 at 500 cm^{-1} is typical of C-Cl this was also confirmed by the presence of Cl in the SEM-EDX analysis.

10.3.3 Morphology of S1, S2 and S3 observed using SEM EDX

From figure 10.3, a granular like morphology is observed for all 3 samples.

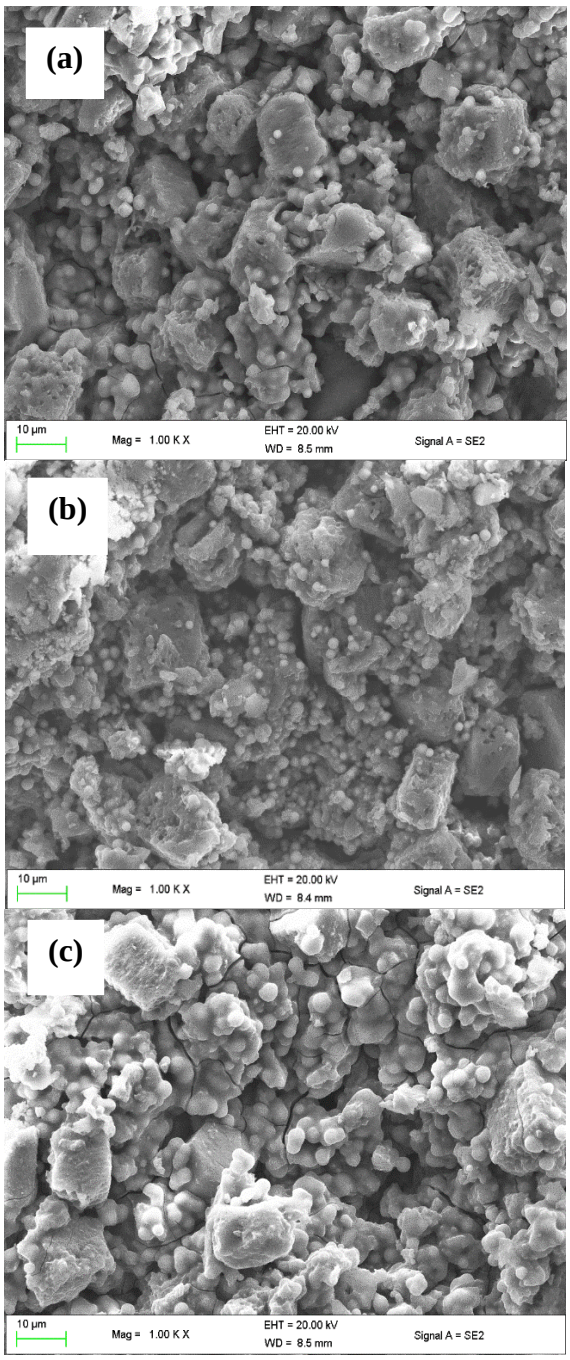

Figure 10.3: SEM images of samples (a) S1, (b) S2 and (c) S3.

The morphology of S1, S2 and S3 as observed under Scanning electron microscope (SEM) are shown in Figure 10.3. Change in morphology was observed and the proportion of iron to copper also changed. S1 showed rough amorphous like structure with granules and in S2 the structure

was similar to S1 but with much smaller granules. Contrary to this, S3 revealed a smooth amorphous structure with big granules, which signifies the structural transition as the ratio of iron to copper was varied.

10.3.4 Elementary analysis of S1, S2 and S3

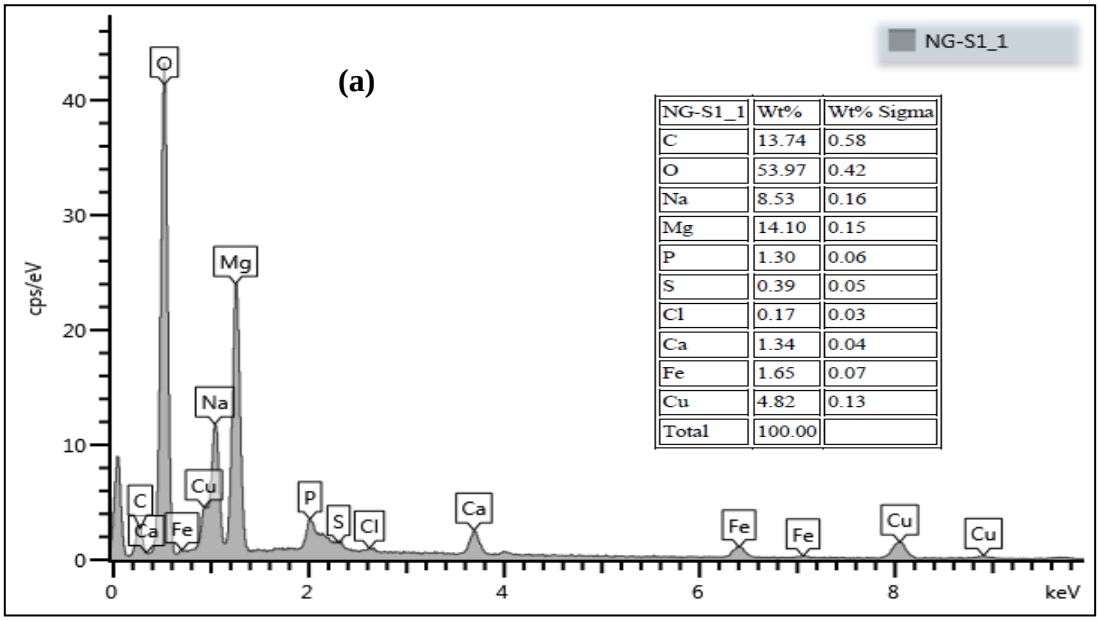

NG-S1_1	Wt%	Wt% Sigma
C	13.74	0.58
O	53.97	0.42
Na	8.53	0.16
Mg	14.10	0.15
P	1.30	0.06
S	0.39	0.05
Cl	0.17	0.03
Ca	1.34	0.04
Fe	1.65	0.07
Cu	4.82	0.13
Total	100.00	

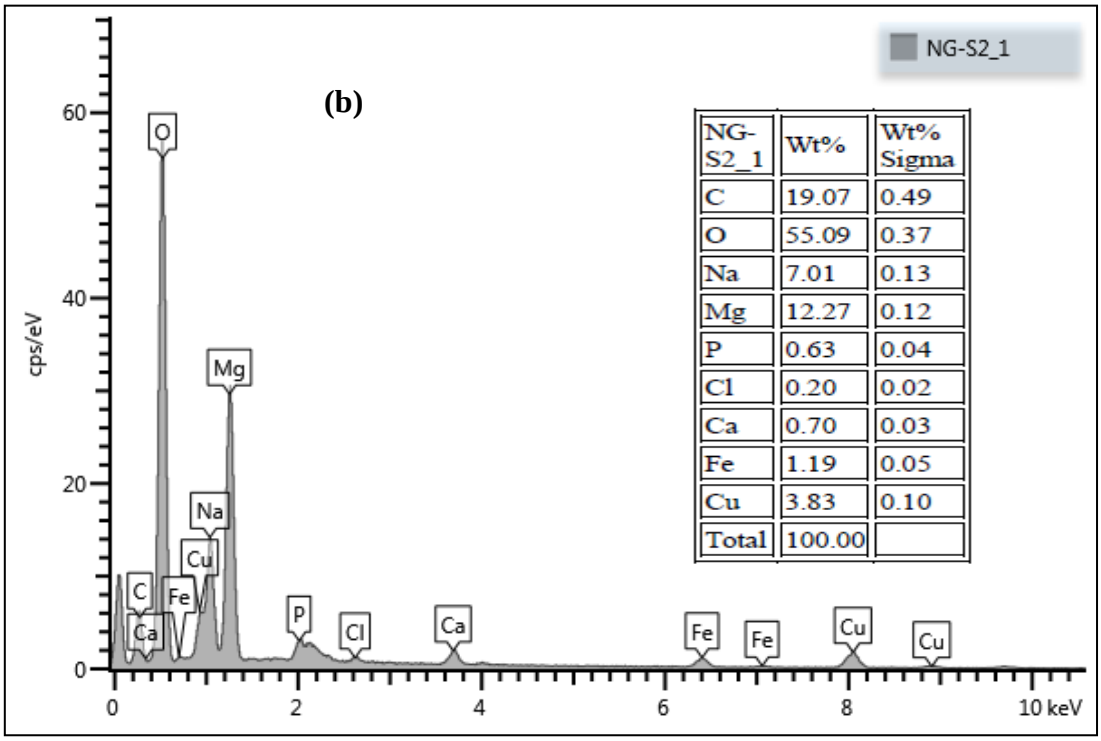

NG-S2_1	Wt%	Wt% Sigma
C	19.07	0.49
O	55.09	0.37
Na	7.01	0.13
Mg	12.27	0.12
P	0.63	0.04
Cl	0.20	0.02
Ca	0.70	0.03
Fe	1.19	0.05
Cu	3.83	0.10
Total	100.00	

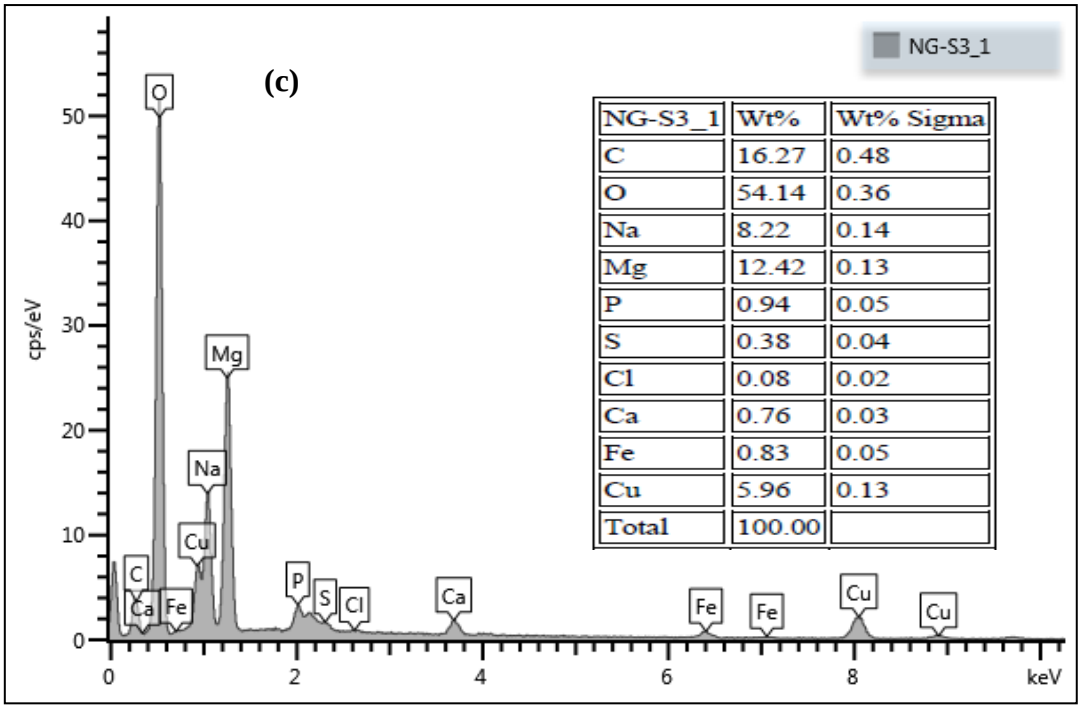

NG-S3_1	Wt%	Wt% Sigma
C	16.27	0.48
O	54.14	0.36
Na	8.22	0.14
Mg	12.42	0.13
P	0.94	0.05
S	0.38	0.04
Cl	0.08	0.02
Ca	0.76	0.03
Fe	0.83	0.05
Cu	5.96	0.13
Total	100.00	

Figure 10.4: Energy dispersive X-ray spectrum of samples (a) S1, (b) S2 and (c) S3.

SEM-EDX analysis of samples S1, S2 and S3 showed different elements present. From Figure 10.3(a) elements such as O, Mg, Na are abundant in huge percentage with oxygen having 53.97 Wt%, magnesium 14.10 Wt% and Na with 8.53 Wt%. Cu was the fourth highest elements with over 4 Wt% while Fe was 1.65 Wt%. The first three elements, which are present in abundance, could be as the results of the culture medium. This was used to grow the microorganism for bioflocculant production. From Figure 10.3(b) elements such as O, Mg, Na, Cu and Fe were most dominant in the sample S2, with oxygen, magnesium and sodium taking 74.37 Wt% combined. This is due to fact that, these elements form part of the structure of the biomolecule (bioflocculant) which was used during synthesis and the medium which was used for bioflocculant production consist of these elements. Lastly, in sample S3 the significant increase in Cu was observed as compared to the other two samples. However, O, Mg, Na were still present in high proportion just like in the rest of the samples.

10.3.5 The effect of different metal proportion in the flocculation process

Figure 10.5 shows the effect of various samples with different proportions of iron to copper on the flocculation activity. These samples were prepared where the first sample contained 1:3 iron to copper S1 (Fe 25%-Cu 75%), sample 2 contained 1:1 iron to copper S2 (Fe 50%-Cu 50%) and third sample contained 3:1 iron to copper (Fe 75%-Cu 25%). All the samples (S1, S2 and S3) were found to flocculate best at lowest concentration of 0.2 mg/mL.

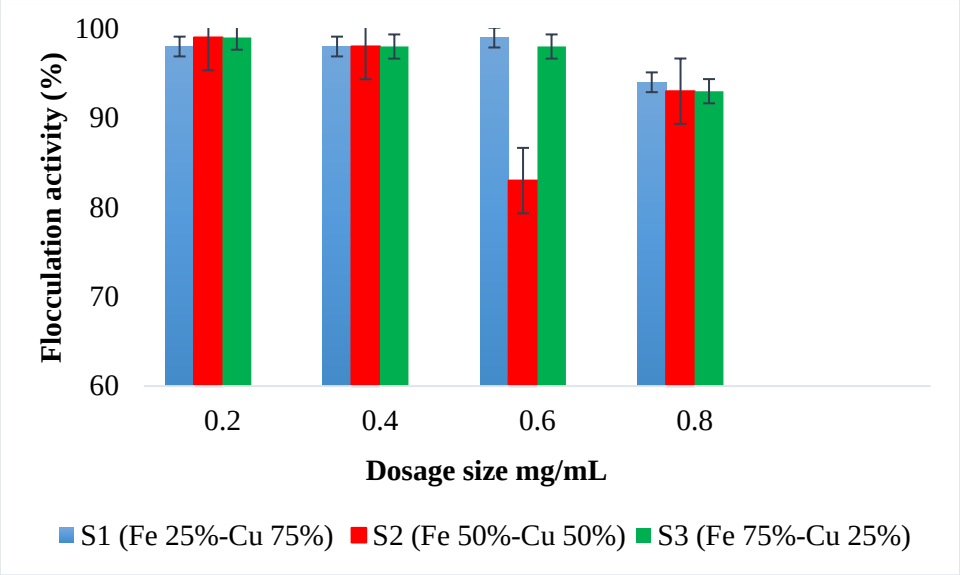

Figure 10.5: Dosage effect on flocculation activity of nanoparticles (S1, S2 & S3). (Refer to index data Table 10.5).

Sworska et al. (2000) posited that there are various flocculation mechanisms but flocculation by bridging is the most important. Consequence adsorption of the flocculant segments onto the surface of more than one particles is described as bridging. In sample S1 it was found that flocculation activity of remained almost constant with 98% between (0.2-0.6 mg/mL) suggesting that the optimum dosage for bridging to occur should be below 0.8 mg/mL. Best flocculation is observed at flocculant dosages corresponding to a particle coverage that is significantly less than complete (Sworska et al., 2000). In S2, the flocculation activity was fluctuating as it is observed between 0.4-0.8 mg/mL in Figure 10.5 this could be due to synergetic effect between iron and copper metal ions. A similar trend as in S1 was also witnessed in S3 the flocculating activity remained almost the same from (0.2-0.6 mg/mL) and it started to decrease at 0.8 mg/mL.

10.3.6 Effect of pH in the flocculation process

Figure 10.6 shows the effect of pH on the flocculation activity of different samples with different proportions of iron to copper S1 (Fe 25%-Cu 75%), S2 (Fe 50%-Cu 50%) and S3 (Fe 75%-Cu 25%). All samples indicated that they are able flocculate at extreme acidic and extreme basic pH with the flocculation activity above 95%.

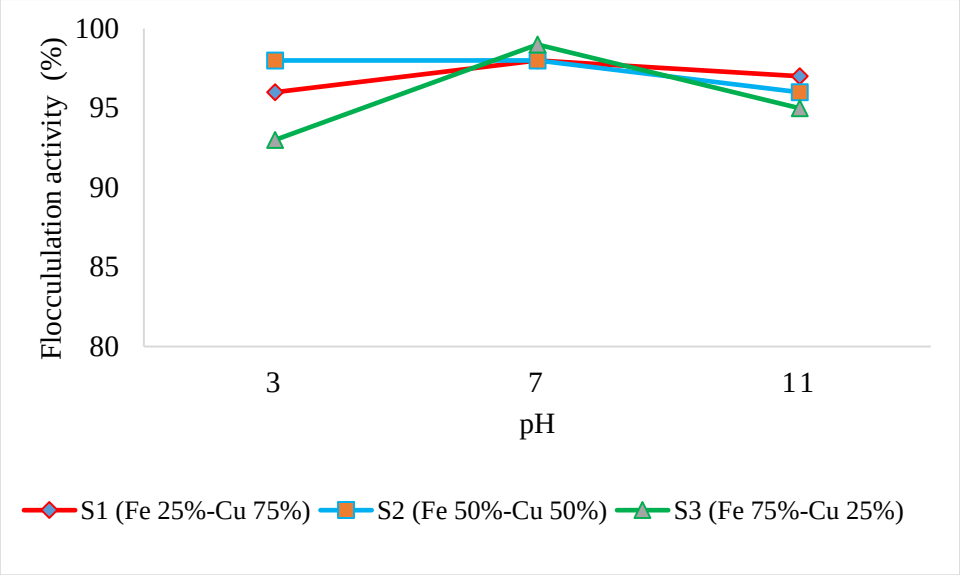

Figure 10.6: pH effect on the flocculating activity of nanoparticles (S1, S2 & S3). (Refer to index data Table 10.6).

The effect of pH on flocculation activity was evaluated in accordance to a description by Zaki et al. (2013) where 1.0 M HCl and 1.0 M NaOH was used for pH adjustment whenever necessary. All the samples (S1, S2 and S3) could flocculate best at all pH conditions (acidic, neutral and alkaline) with above 90% flocculation. As presented in Figure 10.6 the optimal flocculation activity was achieved at neutral pH, however, the flocculation activity was still above 90% for both at acidic and alkaline condition suggesting that the nanoparticles are pH stable. The absorption of H^+ ions tend to weaken the nanoparticles-kaolin complex formation at acidic and alkaline pH (Zaki et al., 2013). This remarkable properties of iron@copper core-shell nanoparticles to withstand acidic and alkaline pH could be contributed by the ability of core-shell nanomaterial to withstand harsh conditions which are brought by the relationship between a core and a shell (Gao et al., 2011). These nanoparticles are of commercial value as they can flocculate acidic and alkaline water.

10.3.7 The effect of different metal ions presence in the flocculation process

Table 10.1 represents the effect of cations on samples (S1, S2 & S3) flocculation activity. All the samples were found to be able to flocculate effectively in the absence of cations with the flocculation activity above 95%.

Table 10.1: Cations effect on nanoparticles flocculation activity.

Type of flocculant	Cations FA(%)±SD			
	Control	Na^{+}	Ca^{2+}	Fe^{3+}
S3	95±0,031[a]	97±0,012[a]	99±0,025[a]	97±0,037[a]
S2	96±0,003[a]	95±0,063[a]	98±0,007[a]	87±0,023[b]
S1	96±0,039[a]	95±0,051[a]	98±0,012[a]	97±0,014[a]

Values represent mean ± deviation of replicate readings. Percentage flocculating activities with different letters (a & b) are significantly ($p<0.05$) different. (Refer to index data Table 10.7).

Cations enhanced the flocculation activity by balancing the negatively charged kaolin suspension and that of the functional group of the flocculants (Zheng et al., 2008). Equally, the monovalent, divalent and trivalent could enhance the flocculation process. However, the synthesized nanoparticles proved to be independent of cations as the flocculation was above 95% when there was no cation added. The limitation with bioflocculants is high production cost and low flocculation efficiency as opposed to counterpart synthetic flocculants, some of the bioflocculants require cations to work effectively. These findings suggest that the synthesized Fe@Cu core-shell nanoparticles could be cost-effective as they the flocculation activity is above 95% in the absence of cations. As depicted in Table 1 above, both sample 1 and 2 flocculate best with Fe^{3+} however, the results showed that the difference between the control and Fe^{3+} is not significant. Sample 3 showed a decreased flocculation activity when Fe^{3+} was added, suggesting that the sample worked better in the absence of cation.

10.3.8 Thermostability test for samples (S1, S2 & S3)

Figure 10.7 represents the effect of temperature on the flocculation activity. All the samples showed to be thermostable with the flocculation above 80% at 100 ℃. Sample 3 was the most stable with flocculation activity of 93%.

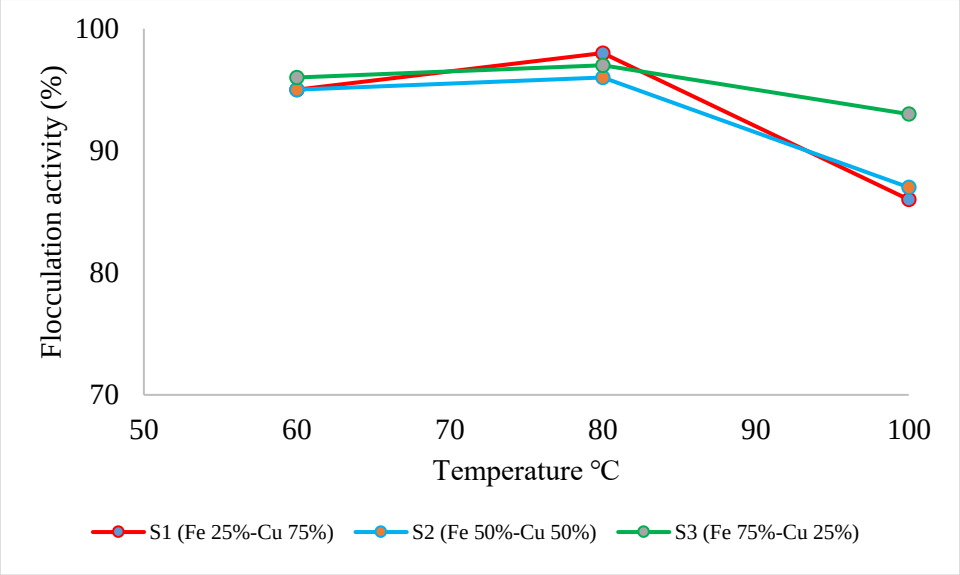

Figure 10.7: Effect of temperatures on flocculation process of samples (S1, S2 & S3). . (Refer to index data Table 10.8).

The effectiveness of samples (S1, S2 & S3) when heated at high temperatures was examined in temperature range between (60-100 °C). The samples were subjected to high temperatures in a water bath for 30 min before the flocculation activity was measured. Flocculation activity of all the samples remained almost the same between (60-80 °C) and it started to decrease when the temperature was increased to 100 °C. Sample 3 was found to be the most stable of the three samples, the flocculation activity remained above 90% even when the sample was subjected to higher temperature 100 °C. Contrarily, sample 1 and 2 revealed a slight decrease in flocculation activity when the sample were exposed to high temperature of 100 °C the flocculation activity decreased from 97 to 87%. Giri et al. (2015) reported a thermostable bioflocculant which maintained the up to 89% flocculation activity at high temperature of 100 °C. Most bioflocculant which composed mainly of carbohydrates and less proteins are able to withstand high temperature (Giri et al., 2015). The bioflocculant which was used for synthesis composed mainly of carbohydrates as the main component which could be the reason for high thermostability for this nanoparticles and literature suggests that such bioflocculants are thermally stable (Zaki et al., 2013). Moreover, the core-shell nanoparticles are said to be able to with stand extreme conditions due to the synergistic effect between the core and the shell (Zaimy et al., 2016).

10.3.9 The removal efficiency of dyes by nanoparticles samples (S1, S2 & S3).

Figure 8 represents the removal efficiency of staining dyes by nanoparticles sample (S1, S2 and S3). All the samples showed the excellent ability to remove staining dyes. Sample 3 had an efficiency above 90% for the four dyes (safranin, methylene blue, methylene orange and malachite green) which were examined.

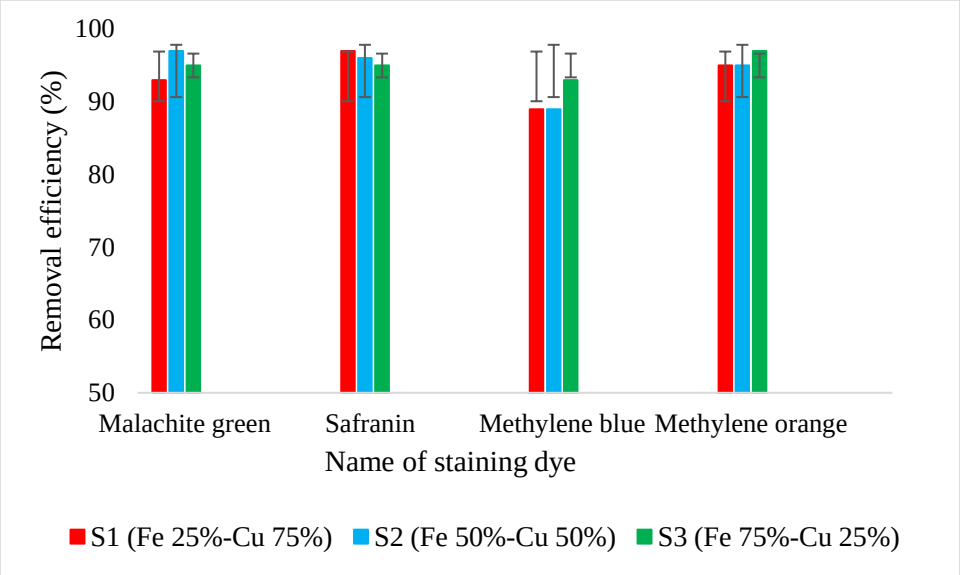

Figure 10.8: Removal efficiency of dyes by nanoparticles samples (S1, S2 & S3). (Refer to index data Table 10.9).

Treatment of some discharged effluents from some industries is still a serious issues as some of these discharges contain colourful dyes (Ali, 2010). Pharmaceuticals, leather, paper, textile, sugar, cosmetic, food, and printing are the most common discharging industries. These colourful dyes have serious impact on the ecosystem, the colour prevent light penetration at the rivers, bottom lakes and ponds, hindering photosynthesis in plants. Moreover, it may also lead to anaerobic conditions that can be fatal to aquatic life. As presented in Figure 10.8 above, the sample were prepared by mixing 4 g of dye in 1 litre of distilled water and 100 mL of the dye solution was mixed with 2 mL of 0.2 mg/mL of nanoparticles solution (S1, S2 and S3). The mixture was agitated for a minute, and transferred to a graduated measuring cylinder, and left to stand for 5 min before it was analysed using spectrophotometer. The nanoparticles were very effective in staining dye removal and the efficiency was above 89% for all with just 5 min contact time.

10.3.10 Removal efficiency of nutrients in wastewater by nanoparticles (S1, S2 & S3)

Table10.2 represents the removal of COD, BOD, phosphate and total nitrogen in Vulindlela wastewater and Mzingazi River water by nanoparticles (S1, S2 & S3). S3 was observed to be the most effective in removing both phosphate and total nitrogen in removal efficiency above 97%.

Table 10.2: Removal of pollutants in Vulindlela wastewater and Mzingazi River by nanoparticles samples (S1, S2 & S3).

Flocculants type	Type of wastewater	Types of pollutants								Removal Efficiency (%)			
		Water quality before				Water quality after treatment							
		COB mg/mL	BOD mg/mL	P mg/mL	Total nitrogen mg/mL	COD mg/mL	BOD mg/mL	P mg/mL	Total mg/mL	COD	BOD	P	N
S1	Domestic	2.313	123	3.38	0.223	1.151	17	2.55	0.017	50	86	37	88
	Mzingazi river	3.300	146	85.7	0.127	1.074	15	0.120	0.020	67	87	99	84
S2	Domestic	2.313	123	3.38	0.223	1.152	13	0.69	0.124	50	89	80	44
	Mzingazi river	3.300	146	85.7	0.127	1.900	21	0.121	0.025	42	86	99	80
S3	Domestic	2.313	123	3.38	0.223	0.464	19	0.09	0.014	85	91	97	98
	Mzingazi river	3.300	146	85.7	0.127	0.793	31	0.109	0.023	79	72	99	82

Vulindlela is a domestic wastewater treatment plant and is located within the locality of the University of Zululand, South Africa. The plant treats water before it is discharged to the surrounding streams. It is of utmost importance to treat water before it is discharged as some of the surrounding community uses the streams water for domestic crop farming purposes. As shown in Table 2, sample 3 was the most effective in removing both phosphate and total nitrogen while samples S1 and S2 could only remove total nitrogen and phosphate respectively. For the removal of COD (chemical oxygen demand) in the wastewater, both samples S1 and S2 were not so effective with just 50% removal efficiency. Contrary to this, sample 3 was most effective with 80% COD removal.

Mzingazi River is geographically located around the city of Richards's bay. It has high activity of industrialization and sugarcane farming. This accounts for high phosphate content in the water as some is washed by rain from the farming fertilizers and industries into to the river. Excess accumulation in water has the adverse impact in aquatic life, it may cause "brown blood diseases" in fish or it may result to eutrophication (Davis et al., 2006). Table 2 shows the results of the samples that were able to remove up to 99% phosphate when it was left to sand for one week and over 80% total nitrogen was removed when the samples were prepared following the manufacturers instruction on the test kit. Therefore, it can be deduced that for nanoparticles to give optimum removal efficiency for phosphate the samples should be allowed longer contact time. In COD removal both sample S1 and S3 were able to remove 67 and 79 respectively while sample S2 could only remove 42% COD in the water. In Table 2, all the samples i.e. S1, S2 and S3 showed some remarkable properties in BOD removal for both domestic wastewater and river water. Removal efficiency was over 80% for all the tested water, except for S3 in Mzingazi river water it was just 79%.

10.4 Conclusion

The synthesized samples were characterized by Fourier transform infrared (FT-IR), X-ray diffractometer and scanning electron microscope (SEM). Hydroxyl, amine and amide groups were some of the groups present in the samples, deep peaks of x-ray diffraction patterns were observed between peaks were observed at $2\theta \sim 35°$, 40° and 65° in S1. Contrary to this, it was observed that the strongest peak was at $2\theta \sim 35°$, 45°, 65° and 77 ° for S2. While in S3, the strong is observed at $2\theta \sim 22°$, 30°, and the morphological studies revealed the amorphous like structure. The synthesized samples (S1, S2 and S3) were effective at low dosage concentration of 2 mg/mL, thermostable and could flocculate at all pH. Cations are not necessary in the

flocculation process while using these samples. All three samples revealed some remarkable properties for staining dye removal as the removal efficiency was above 89% for all dyes tested. The synthesized core-shell nanoparticles could remove nutrients such as total nitrogen and phosphate in both domestic wastewater and Mzingazi river water. Furthermore, high removal efficiency for COD and BOD was also observed with S3 being the most effective samples followed by S2 while S1 was the least effective.

10.5 References

AGUNBIADE, M., POHL, C. & ASHAFA, O. 2018. Bioflocculant production from Streptomyces platensis and its potential for river and waste water treatment. *Brazilian Journal of Microbiology*.

ALI, H. 2010. Biodegradation of Synthetic Dyes—A Review. *Water, Air, & Soil Pollution,* 213**,** 251-273.

DAVIS, A. P., SHOKOUHIAN, M., SHARMA, H. & MINAMI, C. 2006. Water quality improvement through bioretention media: Nitrogen and phosphorus removal. *Water Environment Research,* 78**,** 284-293.

DLAMINI, N. G., BASSON, A. K. & PULLABHOTLA, V. S. R. 2019. Biosynthesis and Characterization of Copper Nanoparticles Using a Bioflocculant Extracted from *Alcaligenis faecalis* HCB2. *Advanced Science Engineering and Medicine,* 11**,** 1-7.

EXLEY, C., KORCHAZHKINA, O., JOB, D., STREKOPYTOV, S., POLWART, A. & CROME, P. 2006. Non-invasive therapy to reduce the body burden of aluminium in Alzheimer's disease. *Journal of Alzheimer's Disease,* 10**,** 17-24.

GAO, X., WEI, L., YAN, H. & XU, B. 2011. Green synthesis and characteristic of core-shell structure silver/starch nanoparticles. *Materials Letters,* 65**,** 2963-2965.

GIRI, S. S., HARSHINY, M., SEN, S. S., SUKUMARAN, V. & PARK, S. C. 2015. Production and characterization of a thermostable bioflocculant from Bacillus subtilis F9, isolated from wastewater sludge. *Ecotoxicology and environmental safety,* 121**,** 45-50.

KURANE, R., TOEDA, K., TAKEDA, K. & SUZUKI, T. 1986. Culture conditions for production of microbial flocculant by Rhodococcus erythropolis. *Agricultural and biological chemistry,* 50**,** 2309-2313.

SANKAR, R., MANIKANDAN, P., MALARVIZHI, V., FATHIMA, T., SHIVASHANGARI, K. S. & RAVIKUMAR, V. 2014. Green synthesis of colloidal copper oxide nanoparticles using Carica papaya and its application in photocatalytic dye degradation. *Spectrochimica Acta Part A: Molecular and Biomolecular Spectroscopy,* 121**,** 746-750.

SWORSKA, A., LASKOWSKI, J. & CYMERMAN, G. 2000. Flocculation of the Syncrude fine tailings: Part I. Effect of pH, polymer dosage and Mg2+ and Ca2+ cations. *International journal of mineral processing,* 60**,** 143-152.

TIWARI, D. K., BEHARI, J. & SEN, P. 2008. Application of nanoparticles in waste water treatment 1.

YANG, Z.-H., HUANG, J., ZENG, G.-M., RUAN, M., ZHOU, C.-S., LI, L. & RONG, Z.-G. 2009. Optimization of flocculation conditions for kaolin suspension using the composite flocculant of MBFGA1 and PAC by response surface methodology. *Bioresource technology,* 100**,** 4233-4239.

YU, X., LI, J., SHI, T., CHENG, C., LIAO, G., FAN, J., LI, T. & TANG, Z. 2017. A green approach of synthesizing of Cu-Ag core-shell nanoparticles and their sintering behavior for printed electronics. *Journal of Alloys and Compounds,* 724**,** 365-372.

ZAIMY, M., JEBALI, A., BAZRAFSHAN, B., MEHRTASHFAR, S., SHABANI, S., TAVAKOLI, A., HEKMATIMOGHADDAM, S., SARLI, A., AZIZI, H. & IZADI, P. 2016. Coinhibition of overexpressed genes in acute myeloid leukemia subtype M2 by gold nanoparticles functionalized with five antisense oligonucleotides and one anti-CD33 (+)/CD34 (+) aptamer. *Cancer gene therapy,* 23**,** 315.

ZAKI, S. A., ELKADY, M. F., FARAG, S. & ABD-EL-HALEEM, D. 2013. Characterization and flocculation properties of a carbohydrate bioflocculant from a newly isolated Bacillus velezensis 40B. *Journal of environmental biology,* 34**,** 51.

ZHENG, Y., YE, Z.-L., FANG, X.-L., LI, Y.-H. & CAI, W.-M. 2008. Production and characteristics of a bioflocculant produced by Bacillus sp. F19. *Bioresource Technology,* 99**,** 7686-7691.

Chapter 11 : ARTICLE 9: Green synthesis of Fe@Cu nanoparticles by a polysaccharide bioflocculant and characterization

Dlamini Nkosinathi G[a]*, Basson Albertus K[a], Rajasekhar Pullabhotla VSR [b]*,

[a] Department of Biochemistry and Microbiology, University of Zululand, Private Bag X1001, KwaDlangezwa, 3886, South Africa

[b] Department of Chemistry, University of Zululand

***** Author to whom correspondence should be addressed; E-Mail: nathidlamini03@gmail.com; PullabhotlaV@unizulu.ac.za

Tel. +27-73 0985921/ +27-359026155

Abstract: The aim of the study was to synthesized iron copper core-shell nanoparticles in a green approach technique whereby the extract from bacteria (bioflocculant) was used as the reducing agent. To characterize the present work, a combination of XRD (X-ray powder diffractometer), SEM (scanning electron microscope), TEM (transmission electron microscopy), FTIR (Fourier-Transform Infrared), TGA (thermogravimetric analysis) and UV–visible absorption spectroscopy were employed to characterize the morphology, structure, composition and magnetic properties of the products. The synthesized nanoparticles were found to be agglomerated and exhibited smooth granular morphology. Hydroxyl and amine groups were also found in a sample. The size range of the synthesized nanoparticles was 32 nm in average.

Keywords: Bioflocculant, Characterization, Core-shell, Synthesis.

11.1 Introduction

Nanomaterials are defined as materials which operate at the same size as cellular structures. Such materials are manipulatable and applicable in biological systems. Over the years researchers pursued to produce a single nanoparticles with multiple physical properties incorporated, highly multiple functional and versatile (Pasquale, 2017). Greater flexibility and enhanced properties is offered by bimetallic nanoparticles with a core/shell morphology as compared to monometallic nanoparticles (Vasireddi et al., 2013). Optical and catalytic properties of core/shell nanoparticles can be tuned which makes this class of nanomaterial most interesting (Vasireddi et al., 2013).

Core-shell nanoparticle have wide range of application. Therefore, to get stability and reduce agglomeration, nanoparticles are coated with different organic materials (Ghosh Chaudhuri and Paria, 2011). Hydrophilic polymers are some of the coating materials which are being use (Balakrishnan et al., 2009) and polysaccharides such as bioflocculants are very common (Babes et al., 1999, Galperin and Margel, 2007, Dlamini et al., 2019b). Due to biological functionalization nanosized organic and inorganic particles are finding increase attention in medical applications as the results of their amenability to biological functionalization (Farokhzad and Langer, 2006). Nanoparticles are of polymers, metals or ceramics and can be used as new drugs to fight human pathogens like bacteria and combat cancer (Stoimenov et al., 2002, Sondi and Salopek-Sondi, 2004).

Biological approach in metal nanoparticles synthesis might be good option due to reduced environmental impacts (Kumar et al., 2013). In this work, we demonstrated the bioflocculant facilitated synthesis of iron copper core-shell nanoparticles. Here, the bioflocculant is the reducing and capping agent for the as-synthesized nanoparticles. The synthesize core-shell nanoparticles were characterized by XRD, SEM, TEM, UV, TGA and FTIR.

11.2 Material and Methods

11.2.1 Source of bioflocculant

A marine isolate which was previously isolated and identified as *Alcalegenis faecalis* by sRNA sequencing through Inqaba Biotech, South Africa was used for bioflocculant production. A culture medium which consist of glucose (20 g), KH_2PO_4 (2.0 g), $(NH_4)_2SO_4$ (0.20 g), $MgSO_4 \cdot 7H_2O$ (0.20 g), yeast extract (0.50 g), urea (0.50 g) and K_2HPO_4 (5.0 g), the medium was prepared using 1 litre of filter sea water at pH (8) and the optimum pH was adjusted using NaOH and HCl (He et al., 2009). The medium was sterilized by autoclave at 121 °C for 15 min. After which, the medium was let cool at room temperature before it was inoculated with 1 % freshly resuscitated inoculum. It was then incubated shaking at 165 rpm for 72 hrs at 30 °C (Manivasagan et al., 2015).

11.2.2 Extraction and purification of the bioflocculant

Bioflocculant extraction was achieved in accordance to a description by (Zhu et al., 2012) with some minor modification. A broth culture, after 72 hrs incubation was then centrifuged at 4,000 rpm at 4 °C for 30 min to separate cells from the supernatant. A litre of distilled water was added onto the supernatant and was further centrifuged for 15 min under same conditions previously described. Two litres of absolute ethanol were added and the mixture was left for 12 hrs at 4 °C to allow for precipitate formation. The crude bioflocculant was purify using 100 mL distilled water and the mixture of chloroform and *n*-butyl (5:2 v/v*)*. Mixture was stirred and was left to stand at room temperature for further 12 hrs before it was vacuum dried to obtain pure bioflocculant (Cosa et al., 2011).

11.2.3 Synthesis of iron copper core-shell nanoparticles

The method used for core-shell nanoparticles synthesis was similar to that of (Vasireddi et al., 2013) with some minor modification. 0.5 g of purified bioflocculant was added into a solution containing $FeCl_3$ (10 mL, 0.2 M) in a flask. After which NaOH (10 mL, 5.0 M) was added to prevent agglomeration of synthesized nanoparticles, the mixture was left to stand at room temperature until colour changed was observed which indicated nanoparticles formation. Different volumes of synthesized iron nanoparticles (FeNPs) 10 mL, 20 m and 30 mL was mixed with a solution of copper sulphate (0.003 M) the reaction was left for 15 min and the

resulted precipitate was centrifuged at 4,000 rpm, 4 °C for 15 min. synthesized nanoparticles were washed by absolute ethanol and characterized.

11.2.4 Characterization of copper nanoparticles

Morphology and elementary analysis of the synthesized nanoparticles was determined using scanning electron microscope equipped with elementary detector (SEM-Sipma-VP-03-67). BRUKER D8 Advance X-Ray Diffractometer operated at 40 kV, 40 mA, equipped with copper monochromator CuKα radiation with wavelength λ=1.5406 Å was used to investigate the phase composition and crystallinity of the copper nanoparticles. X-ray diffractogram was recorded in the 2θ range from 20° to 80° at scanning steps of 0.03°.

Perkin-Elmer UV-Vis spectrophotometer was used to investigate UV-Vis spectrum of the synthesized copper nanoparticles. 0.1 mL of the sample was taken and diluted with 2 mL of deionized water. As a function of time of reaction the investigation was conducted in the wavelength region 300 to 700 nm operated at a resolution of 1 nm. Fourier Transform-Infrared (FT-IR) spectroscopy was used to identify and confirm the functional groups present in the bioflocculant (Tensor 27, Bruker FT-IR spectrophotometer).

TEM images for the copper nanoparticles were obtained using a JEOL 1010 transmission electron microscope. The specimens were prepared by using a micropipette to place a diluted drop of suspension in toluene on a copper grid (150 mesh). The samples were allowed to dry completely at room temperature. Samples were viewed at 100 kV as the accelerating voltage. The images were captured digitally using a Megaview III camera, stored and measured using Soft Imaging System iTEM software. The as-synthesized bioflocculant passivated copper nanoparticles decomposition was studied using a thermo-gravimetric instrument in accordance to Cosa et al. (2013). High temperatures with range 22 to 900 °C was used to heat the bioflocculant passivated copper nanoparticles, at a constant rate of 10 °C min^{-1} under constant flow of nitrogen gas.

11.3. Results and discussion

11.3.1 X-ray diffraction pattern of Fe@Cu core-shell nanoparticles

The X-ray diffraction pattern recorded for the iron copper core-shell nanoparticles is shown in Figure 11.1. The deep peaks were observed at $2\theta \approx 36°$.

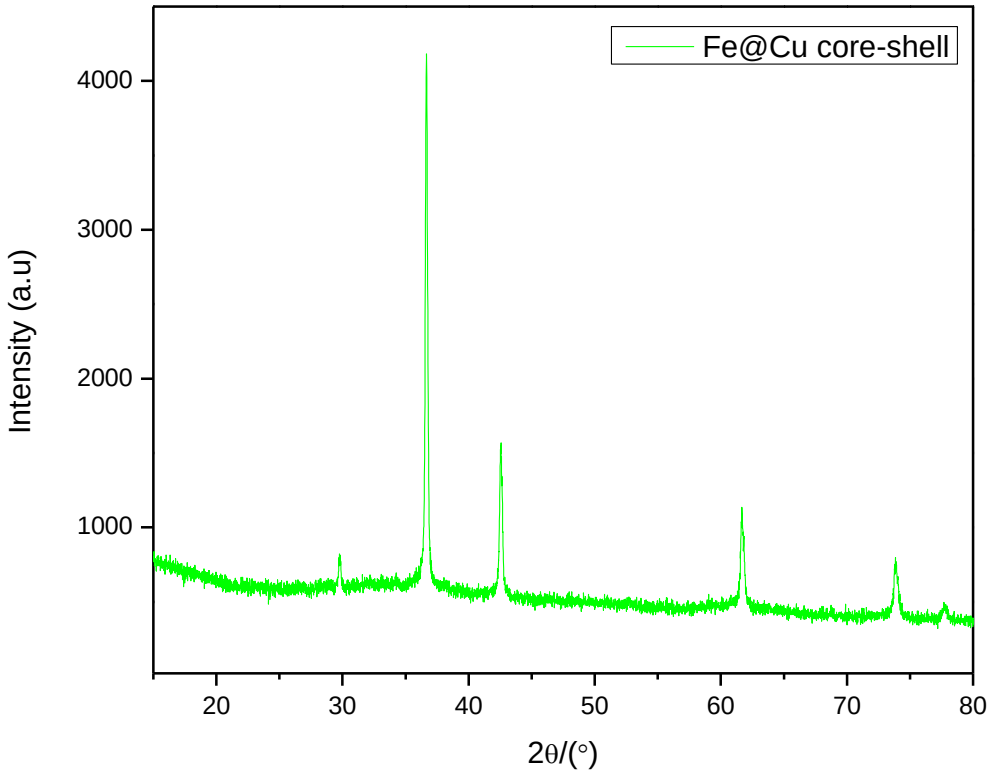

Figure 11.1: XRD diffraction of Fe@Cu core-shell nanoparticles.

From Figure 1, diffraction peaks centred at $2\theta \approx 30°$, 38°,43°, 63° and 75° corresponding to the Miller indices (110), (111), (112), (132) and (200) reflections of copper and iron (Bish and Post, 2018, Lu et al., 2013). The pattern of a-iron 44.8° is hidden under the pattern of copper due to the overlap of their peaks (Ban et al., 2005). As shown above (Figure 1), the data indicate both iron and copper. This again confirms the iron copper core-shell synthesis was a success.

11.3.2 Functional groups found in Fe@Cu core-shell nanoparticles

Figure 11.2 shows the band at 3442 cm^{-1}, 1980 cm^{-1}, which indicates the hydroxyl (OH) group and amine (NH_2) group in the sample. The weak band at 1980 cm^{-1} in both the samples can be designated to the presence of aliphatic bonds.

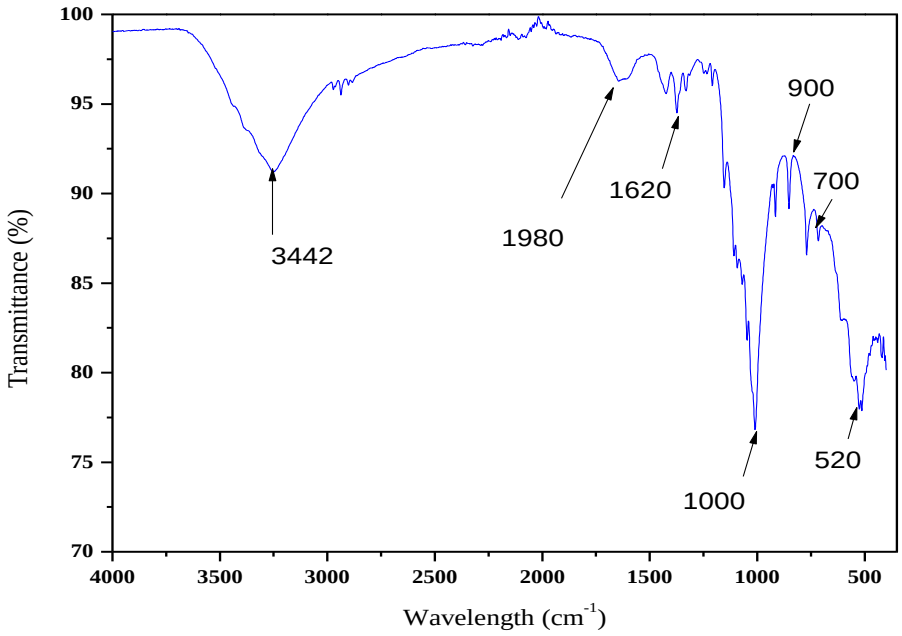

Figure 11.2: FT-IR spectrum of Fe@Cu core-shell nanoparticles.

Different functional groups present in the molecule were revealed by the Fourier-transform infrared (FTIR) spectroscope analysis. The peak located at 1620 cm^{-1} indicates the presence of an amide group. The vibrational peaks at 700 cm^{-1} are analogous to the C-O stretching in alcohols, which confirms the OH group presence. The peaks between 1,000–1,100 cm^{-1} suggests the presence of saccharide derivatives. 520 cm^{-1} Br-Cl halogen bonded to halogen. The presence of hydroxyl and amine groups in the samples indicates that Fe@Cu core-shell nanoparticles synthesized from the bioflocculant that is a polysaccharide.

11.3.3 TEM image of Fe@Cu core-shell nanoparticles

Below is Figures 3 TEM image of iron copper core-shell nanoparticles. It shows the approximation of size range of nanoparticles. A spherical morphology is observed at 200 nm scale.

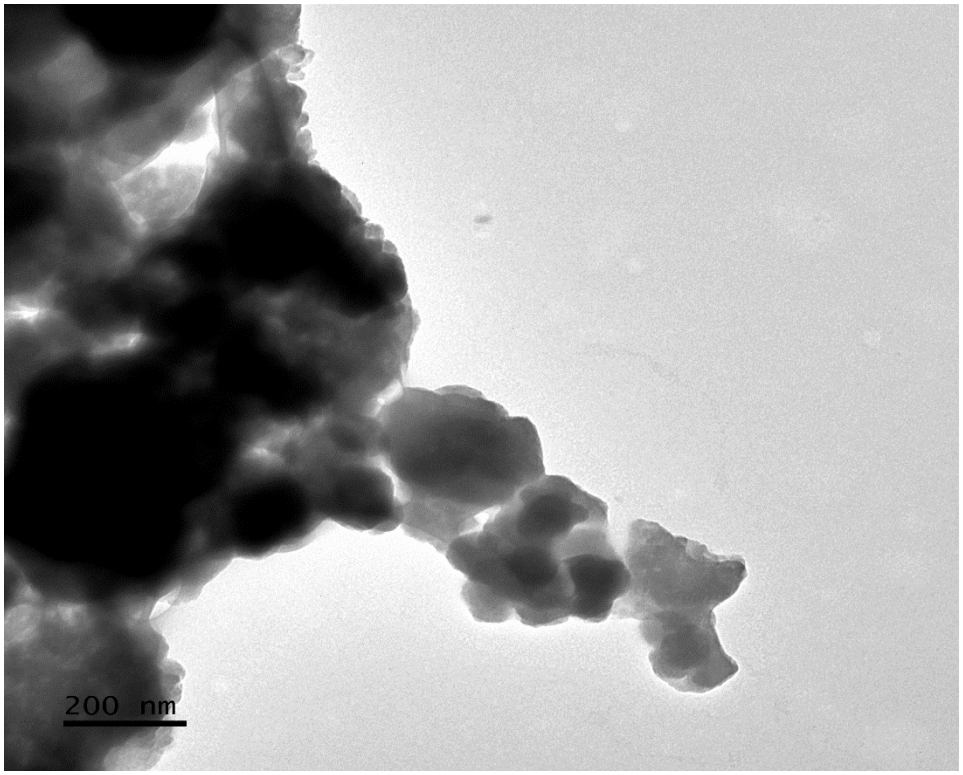

Figure 11.3: TEM micrograph of Fe@Cu core-shell nanoparticles at 200 nm.

From Figure 3, the TEM images of the sample revealed that the Fe@Cu core-shell -particles are composed of particle approximately 32 nm or less in size. The TEM images revealed that the nanoparticles are highly aggregated. This could be due to the magnetic property of those compounds (Lu et al., 2013). Agglomeration maybe attributed to the interaction of the electron of the interconnected particles (Lazarides and Schatz, 2000).

11.3.4 SEM morphology of Fe@Cu core-shell nanoparticles

Figures 11.4 illustrates the surface morphology of Fe@Cu core-shell nanoparticles. This analysis was conducted using the SEM. The morphological surface of the as-synthesize nanoparticles is smooth granulated.

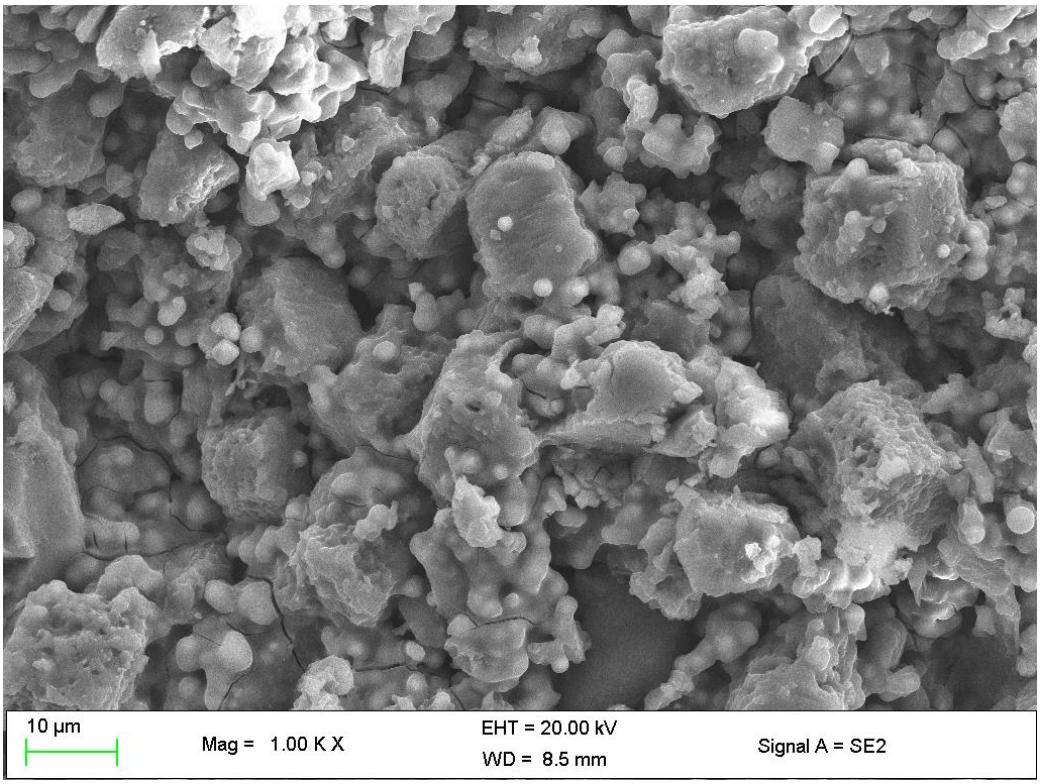

Figure 11.4: SEM morphology of Fe@Cu core-shell nanoparticles.

The morphology of Fe@Cu core-shell nanoparticles was evaluated as shown in Figure 4. SEM microstructure of the bioflocculant passivated Fe@Cu core-shell nanoparticles reveals the presence of dense agglomerations. These particles have a smooth granular like shape and their distribution is not uniform. This could be as the results of the solvent (absolute ethanol) which was used to wash the as-synthesized nanoparticles. Both in air and in water the nanoparticles were observed to be stable, as they did not convert into any other associated compounds.

11.3.5 Elementary analysis of Fe@Cu core-shell nanoparticles

These results from the SEM-EDX showed the different elements present in the purified bioflocculant in Figure 5 The bioflocculant is composed of elements such as: O, C, Na, Mg, P, S, Cl, Ca, Fe and Cu. The element with the highest weight percentage was oxygen with 53. 97 Wt% while iron was the least with just Cl 0.17 Wt%.

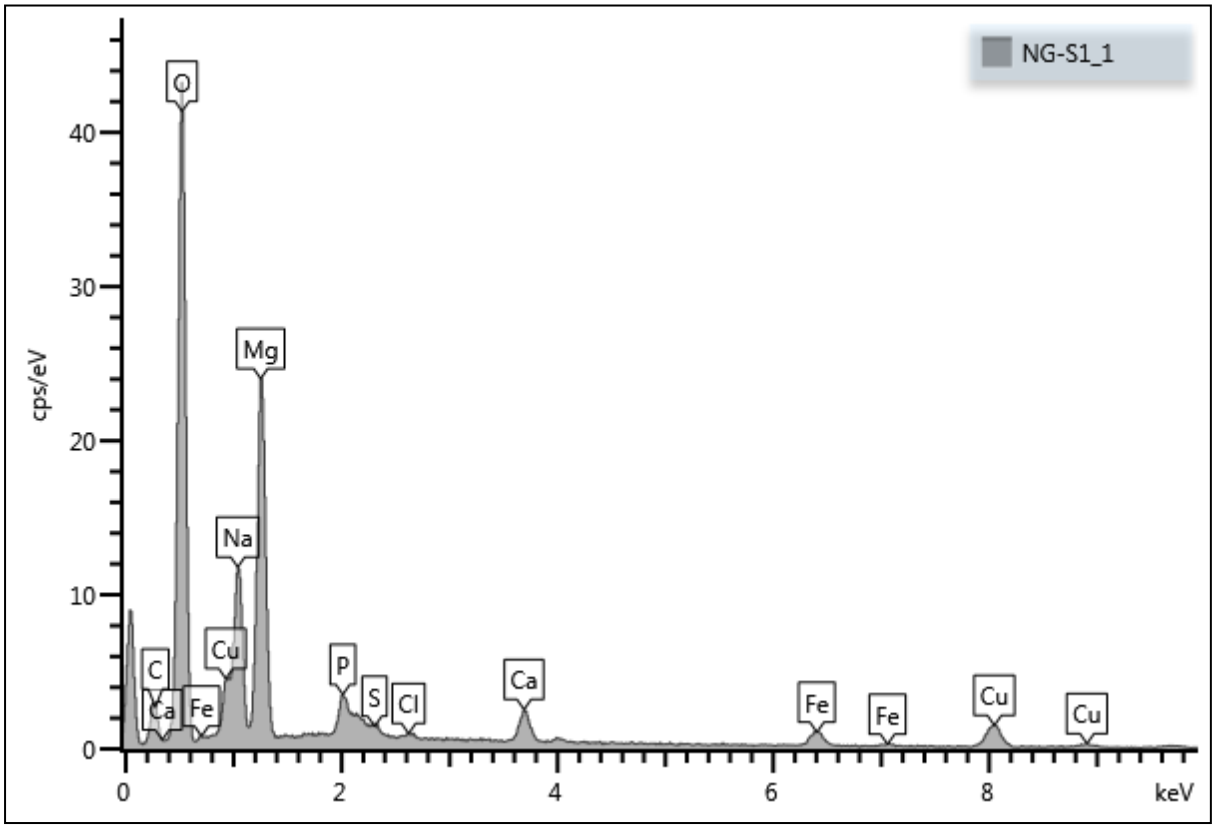

Figure 11.5: SEM-EDX of Fe@Cu core-shell nanoparticles.

The elemental composition of the bioflocculant plays a vital role in bioflocculant structure and various elements bring about the flexibility and stability of the bioflocculant (Maliehe et al., 2019). As depicted in Figure 5, oxygen accounts for 53.97 Wt% followed by carbon with 13.74 Wt%. While elements such as Mg, Na accounts for about 20 Wt% combined. These elements originated from the bioflocculant, which was used for the synthesis of as-synthesized core-shell nanoparticles. Cu and Fe were also found in the sample, which further indicated the success of the experiment.

11.3.6 Thermogravimetric analysis of Fe@Cu core-shell nanoparticles.

Thermogravimetric analysis was performed on the Fe@Cu core-shell nanoparticles to reveal the behaviour under the heat. Pyrolytic property information of the material when exposed to high temperatures is obtained using this technique. About 35% weight loss is observed when the temperature was increased to 300 °C.

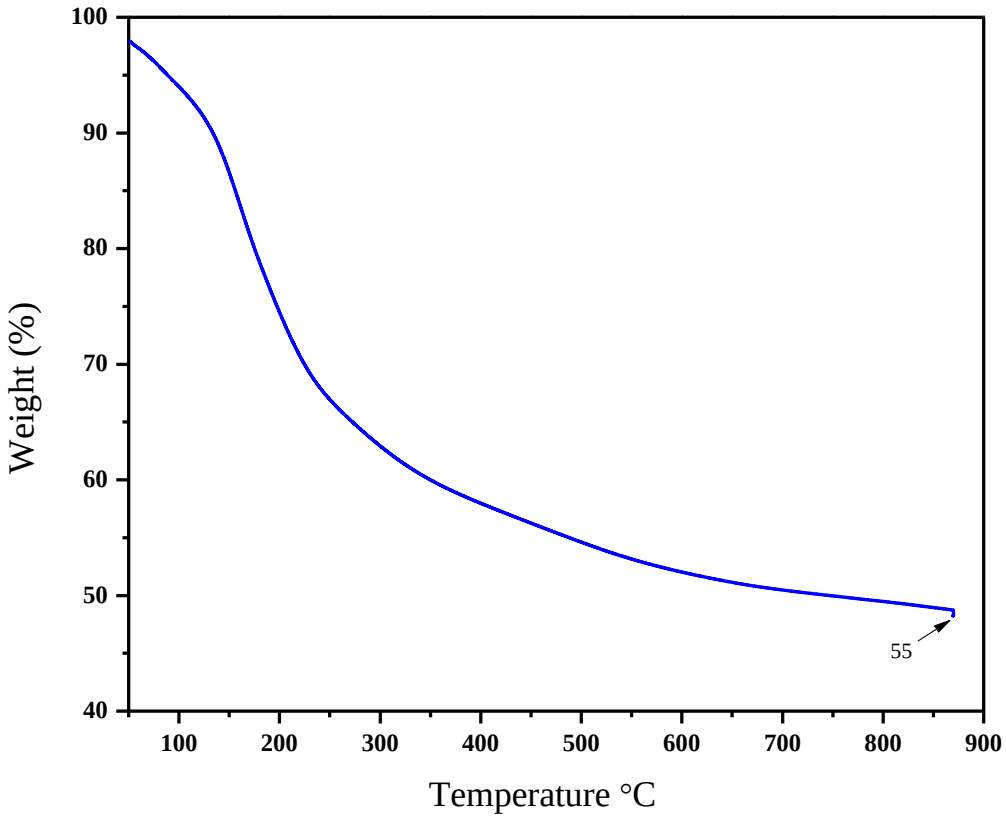

Figure 11.6: Thermogravimetric analysis of Fe@Cu core-shell nanoparticles.

From Figure 11.6, the lost is moisture content in the sample is observed between 150 and 200 °C. With the increase in temperature up to 300 °C, the second phase in pyrolytic of the Fe@Cu core-shell was observed. The first phase observed in weight loss could be attributed to moisture loss in the sample. The second phase could be related to decomposition of polymer which in turn resulted in weight loss. Moreover, further increase in temperature resulted in more weight loss in the synthesized Fe@Cu core-shell nanoparticles. At temperatures above 800 °C the weight of the sample slightly above 50% suggesting that the material is thermostable.

11.3.7 UV–vis spectrum of Fe@Cu core-shell nanoparticles

Figure 11.7 represents the UV-visible spectrum of Fe@Cu core-shell nanoparticles at a wavelength of 400 nm. The findings revealed no straight peaks, which could be due to some impurities in the samples.

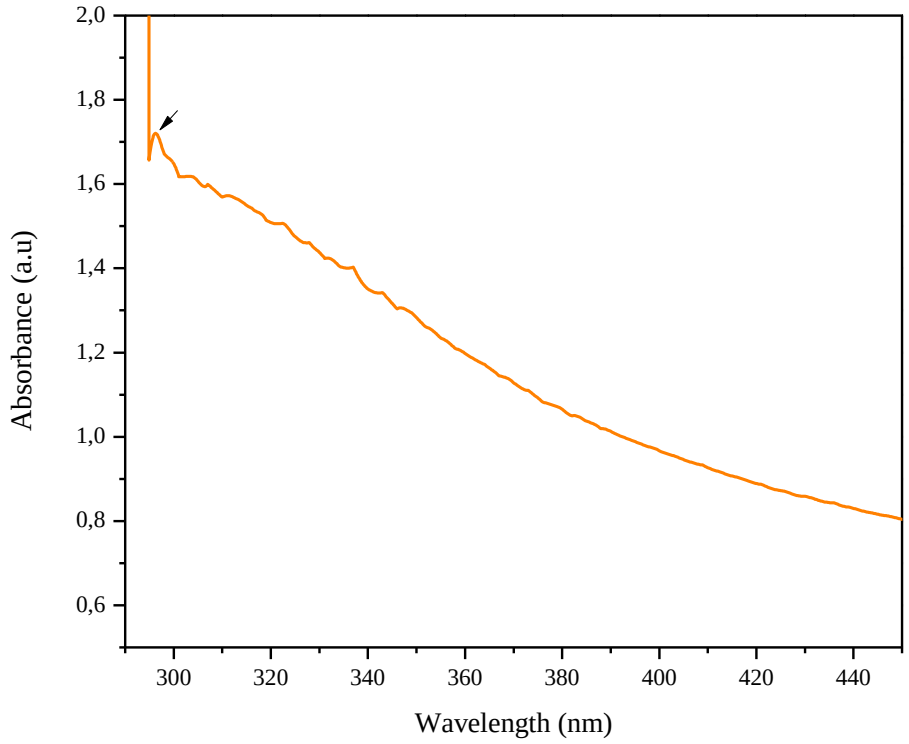

Figure 11.7: UV-visible spectrum of Fe@Cu core-shell nanoparticles.

This showed the plasmon resonance (SPR) spectra with absorbance 300-400 nm and the pic maxima for the synthesized nanoparticles was observed at around 300 nm. The peak at around 300 nm arises due to longitudinal surface plasmon resonance, which indicates the formation of Fe@Cu core-shell nanoparticles. The peak maxima for iron nanoparticles is at high wavelength usually above 400mn the shift in peak maxima could be attributed to the formation of core-shell (Kumar et al., 2013).

11.4 Conclusion

X-ray diffraction revealed $2\theta \approx 13.2°$, 17.4°, 21 and the synthesized nanoparticles exhibited hydroxyl and amine group suggesting the polysaccharide nature of the bioflocculant. SEM indicated that the synthesized nanoparticles are agglomerated and exhibited smooth granular morphology. Significant increase in Fe and Cu in SEM was observed. TGA showed that about 50% weight was remaining at temperatures above 800 ℃ indicating the thermostability of the sample. UV-visible spectrum revealed the pic maxima at 300 nm.

11.5 References

BABES, L., DENIZOT, B., TANGUY, G., LE JEUNE, J. J. & JALLET, P. 1999. Synthesis of iron oxide nanoparticles used as MRI contrast agents: a parametric study. *Journal of colloid and interface science,* 212**,** 474-482.

BALAKRISHNAN, S., BONDER, M. J. & HADJIPANAYIS, G. C. 2009. Particle size effect on phase and magnetic properties of polymer-coated magnetic nanoparticles. *Journal of magnetism and magnetic materials,* 321**,** 117-122.

BAN, Z., BARNAKOV, Y. A., LI, F., GOLUB, V. O. & O'CONNOR, C. J. 2005. The synthesis of core–shell iron@ gold nanoparticles and their characterization. *Journal of Materials Chemistry,* 15**,** 4660-4662.

BISH, D. L. & POST, J. E. 2018. *Modern powder diffraction,* Walter de Gruyter GmbH & Co KG.

COSA, S., MABINYA, L. V., OLANIRAN, A. O., OKOH, O. O., BERNARD, K., DEYZEL, S. & OKOH, A. I. 2011. Bioflocculant production by Virgibacillus sp. Rob isolated from the bottom sediment of Algoa Bay in the Eastern Cape, South Africa. *Molecules,* 16**,** 2431-2442.

DLAMINI, N. G., BASSON, A. K. & PULLABHOTLA, V. S. R. 2019. Optimization and Application of Bioflocculant Passivated Copper Nanoparticles in the Wastewater Treatment. *International Journal of Environmental Research and Public Health,* 16**,** 2185.

FAROKHZAD, O. C. & LANGER, R. 2006. Nanomedicine: developing smarter therapeutic and diagnostic modalities. *Advanced drug delivery reviews,* 58**,** 1456-1459.

GALPERIN, A. & MARGEL, S. 2007. Synthesis and characterization of radiopaque magnetic core-shell nanoparticles for X-ray imaging applications. *Journal of Biomedical Materials Research Part B: Applied Biomaterials: An Official Journal of The Society for Biomaterials, The Japanese Society for Biomaterials, and The Australian Society for Biomaterials and the Korean Society for Biomaterials,* 83**,** 490-498.

GHOSH CHAUDHURI, R. & PARIA, S. 2011. Core/shell nanoparticles: classes, properties, synthesis mechanisms, characterization, and applications. *Chemical reviews,* 112**,** 2373-2433.

HE, J., ZHEN, Q., QIU, N., LIU, Z., WANG, B., SHAO, Z. & YU, Z. 2009. Medium optimization for the production of a novel bioflocculant from Halomonas sp. V3a′ using response surface methodology. *Bioresource technology,* 100**,** 5922-5927.

KUMAR, K. M., MANDAL, B. K., KUMAR, K. S., REDDY, P. S. & SREEDHAR, B. 2013. Biobased green method to synthesise palladium and iron nanoparticles using Terminalia chebula aqueous extract. *Spectrochimica Acta Part A: Molecular and Biomolecular Spectroscopy,* 102**,** 128-133.

LAZARIDES, A. A. & SCHATZ, G. C. 2000. DNA-linked metal nanosphere materials: Structural basis for the optical properties. *The Journal of Physical Chemistry B,* 104**,** 460-467.

LU, Z.-H., LI, J., ZHU, A., YAO, Q., HUANG, W., ZHOU, R., ZHOU, R. & CHEN, X. 2013. Catalytic hydrolysis of ammonia borane via magnetically recyclable copper iron nanoparticles for chemical hydrogen storage. *International journal of hydrogen energy,* 38**,** 5330-5337.

MALIEHE, T. S., BASSON, A. K. & DLAMINI, N. G. 2019. Removal of Pollutants in Mine Wastewater by a Non-Cytotoxic Polymeric Bioflocculant from Alcaligenes faecalis HCB2. *International journal of environmental research and public health,* 16**,** 4001.

MANIVASAGAN, P., KANG, K.-H., KIM, D. G. & KIM, S.-K. 2015. Production of polysaccharide-based bioflocculant for the synthesis of silver nanoparticles by Streptomyces sp. *International journal of biological macromolecules,* 77**,** 159-167.

PASQUALE, N. 2017. *The design and synthesis of heterogeneous core shell nanomaterials for biological applications.* Rutgers University-Graduate School-New Brunswick.

SONDI, I. & SALOPEK-SONDI, B. 2004. Silver nanoparticles as antimicrobial agent: a case study on E. coli as a model for Gram-negative bacteria. *Journal of colloid and interface science,* 275**,** 177-182.

STOIMENOV, P. K., KLINGER, R. L., MARCHIN, G. L. & KLABUNDE, K. J. 2002. Metal oxide nanoparticles as bactericidal agents. *Langmuir,* 18**,** 6679-6686.

VASIREDDI, R., PAUL, R. & MITRA, A. K. 2013. Green Synthesis of AgcoreCushell Nanoparticles: Structural and Optical Characterization. *Journal of Green Science and Technology,* 1**,** 85-90.

ZHU, C., CHEN, C., ZHAO, L., ZHANG, Y., YANG, J., SONG, L. & YANG, S. 2012. Bioflocculant produced by Chlamydomonas reinhardtii. *Journal of applied phycology,* 24**,** 1245-1251.

Chapter 12 Wastewater treatment by a polymeric bioflocculant and iron nanoparticles synthesized from a bioflocculant

Nkosinathi Goodman Dlamini [1,*], Albertus Kotze Basson [1] and Rajasekhar VSR Pullabhotla [2,*]

[1] Department of Biochemistry and Microbiology, University of Zululand, Private Bag X1001, KwaDlangezwa, 3886, South Africa; BassonA@unizulu.ac.za (A.K.B.)

[2] Department of Chemistry, University of Zululand

* Correspondence: PullabhotlaV@unizulu.ac.za (R.V.S.R.P); Tel. +27- 35 9026155 (R.V.SR.P.); nathidlamini03@gmail.com (N.G.D.)

Abstract: Wastewater remains the global challenge. Various methods have been used in wastewater treatment, including flocculation. The aim of this study was to synthesize iron nanoparticles (FeNPs) using a polymeric bioflocculant and to evaluate its efficacy in the removal of pollutants in wastewater. Comparison between the efficiencies of bioflocculant and commercial flocculant ferric chloride ($FeCl_3$) was investigated. Scanning Electron Microscope (SEM) equipped with energy-dispersive X-ray analyzer (EDX) and Fourier Transform-Infrared (FT-IR) spectroscopy were used to characterize the material. SEM-EDX analysis revealed the presence of elements such as O and C that are abundant in both samples, while FT-IR studies shown the presence of functional groups such as hydroxyl (-OH) and amine ($-NH_2$). Fe nanoparticles showed best flocculation activity (FA) at 0.4 mg/mL dosage as opposed to that of bioflocculant which displayed the highest flocculation activity at 0.8 mg/mL and both samples were found to be cation dependent. When evaluated for heat stability and pH stability, FeNPs were found thermostable with 86% FA at 100 °C, while alkaline pH 11 favored FA with 93%. Bioflocculant flocculated poorly at high temperature and found effective mostly at pH 7 with over 90% FA. FeNPs effectively removed BOD (biochemical oxygen demand) and COD (chemical oxygen demand) in all two wastewater samples from Coal Mine water and Mzingazi river water. Cytotoxicity results showed both FeNPs and bioflocculant as nontoxic at concentrations up to 50 µL.

Keywords: Biosafety, Flocculation, Removal efficiency, Wastewater.

12.1 Introduction

Organic and inorganic pollutants in water are a major important concern of this era. Both organic and inorganic hazardous pollutants, including derivatives of phenols and dyes released from different industries have turn out to be a global problem [1,2]. Textile industries is one of the largest source that is contributing to pollution of water, this is due to the application of different chemicals throughout the Textile processing [3,4]. Untreated effluent discharge from the textile processing results into highly toxic wastewater [5]. This effluent contains high levels of chemical oxygen demand (COD) and biochemical oxygen demand (BOD) and is highly turbid. The release of this untreated effluent to sea, lakes or river affects the environment badly [6]. In developing countries, close to 10% of population die due to waterborne infections as well as cancer caused by untreated industrial effluents in water [7]. Hence, treatment and removal of the pollutants that are present in water bodies is necessary, though it is never an easy task.

Several techniques have been employed to treat the effluents and to remove toxic compounds from the water [7,8]. The methods include constructed wetlands, membrane filtration, hybrid ion exchange materials and electrocoagulation, etc. All these water treatment technologies play a substantial role in the treatment of effluents from industries. However, the major downside of these techniques are either very expensive or produce immense amount of sludge [9]. On the other hand, flocculants have gained interest in recent years; synthetic flocculants are mostly used due to their effectiveness. However, the monomers of this flocculants have been reported to be toxic to human [8]. Furthermore, natural flocculants are viewed as the alternative as they are said to be degradable, nontoxic and friendly to the environment, but are less effective when compared to synthetic flocculants.

Therefore, in the present study we report the synthesis of iron nanoparticles using a polymeric bioflocculant, its application in wastewater treatment in comparison to a bioflocculant and biosafety evaluation.

12.2 Materials and Methods

12.2.1 Production Medium chemicals

All reagents for production media used were obtained from Sigma-Aldrich (St Louis, MO, USA). The standard production medium as described by Zhang, *et al.* [10] was followed. A litre of the filtered sea water was used together with the following reagents: glucose (20.0 g),

KH_2PO_4 (2.0 g), K_2HPO_4 (5.0 g), $(NH_4)_2SO_4$ (0.2 g), NaCl (0.1 g), CH_4N_2O (0.5 g), $MgSO_4$ (0.2 g), and yeast extract (0.5 g).

12.2.2 Extraction and purification of the bioflocculant

The bacteria used was previously isolated from the sediment sample from Sodwana Bay in the Province of KwaZulu-Natal in South Africa (28°450' S 31°540' E) and identified as *Alcaligenes faecalis* HCB2 [8]. Bioflocculant extraction was achieved following a method as described by Dlamini, *et al.* [11]. Firstly, 1 liter of the production medium was prepared and autoclaved at 121 °C for 15 min. Subsequently, 1% in (50 mL) inoculum was added and the media incubated in a shaker at 165 rpm for 72 hours at 30 °C, after incubation the media was centrifuged at 8,000 rpm at 4 °C for 30 min. This was done in order to remove cells and insoluble substances. The supernatant was transferred into a clean container and 1 liter of distilled water and 2 liters of ethanol were added to the supernatant, agitated and the solution was stored at 4 °C for 12 hours. Later, the precipitate formed was vacuum-dried and 100 mL of distilled water was added. A mixture of chloroform and *n*-butyl (5:2 v/v*)* was also added, the mixture was left to stand for 12 hour at room temperature [11].

12.2.3 Synthesis of the iron nanoparticles (FeNPs)

To synthesize iron nanoparticles, a green approach method was adopted [12]. A metal precursor for the synthesis of iron nanoparticles (FeNPs) used is iron sulphate ($FeSO_4$). Briefly, 0.5 g of pure bioflocculant was dissolved in 0.2 M ($FeSO_4$) and to prevent agglomeration of nanoparticles 10 mL of 5.0 M sodium hydroxide (NaOH) solution was added. The mixture was left overnight at room temperature, nanoparticles formation was confirmed by physical observation i.e. color change and characterization. Subsequently, the mixture was centrifuged at 5000 rpm at 4 °C for 15 min to harvest the synthesized nanoparticles and resulting precipitate was vacuum dried at 25 °C for 24 hours [12].

12.2.4 Characterization of the bioflocculant and iron nanoparticles

12.2.4.1 Morphology and element analysis

Scanning Electron Microscope (SEM), Energy Dispersive X-ray Spectroscopy (EDX) was used to evaluate morphology and elements in FeNPs and bioflocculant.

12.2.4.2 Functional groups analysis

Fourier Transform-Infrared (FT-IR) spectroscopy was used to identify and confirm the functional groups present in FeNPs and bioflocculant (Tensor 27, Bruker FT-IR spectrophotometer).

12.2.5 Determination of flocculation activity

Kaolin clay was used as the test material in this study; 4.0 g in 1 litre distilled water was prepared. 50 mL kaolin clay solution was added into a 250 mL conical flask, thereafter 2.0 mL (0.2 mg/mL) solution of the bioflocculant or iron nanoparticles was added and 3.0 mL $CaCl_2$ (1.0 g/L) solution was also added. The mixtures were shaken for 1 min and transferred to 100 mL graduated measuring cylinders. The mixture was left to stand for 5 min before the supernatant was taken for analysis [13]. The following equation was used to calculate the flocculation activity:

Flocculation activity $\mathbf{FA}\ \% = \frac{[A-B]}{A}\ \mathbf{X\ 100}$ $(\mathbf{1})$

Where A is the optical density of a control at 550 nm and B is the optical density of a sample at 550 nm.

12.2.6 Optimization of the flocculation efficiency of bioflocculant and FeNPs

12.2.6.1 Evaluation of Flocculation activity of bioflocculant and FeNPs

To evaluate the most effective dosage, different concentrations were prepared (0.2, 0.4, 0.6 and 0.8 mg/mL) by dissolving bioflocculant and FeNPs in distilled water to obtain respective concentration. A liter of kaolin solution was prepared using distilled water 4 g/L. After which, 100 mL of kaolin solution, 2 mL of bioflocculant or FeNPs and 3 mL of 1% $CaCl_2$ was transferred into a 300 mL conical flask. The mixture was vigorously shaken for 1 min before transferring into a measuring cylinder (100 mL) and allowed to settle for 5 min at room temperature. This procedure was also followed for the control, where 2 mL of nanoparticles were replaced by 2 mL distilled water. The clear top layer of the supernatant was pipetted into a cuvette to determine the flocculation activity. The UV-Visible spectrophotometer was used to measure the optical density (OD_{550nm}). All experiments were conducted in triplicates. Equation (1) above was used to calculate the flocculation activity.

12.2.6.2 Effect of cations on flocculating activity

Different salts were used to ascertain cation effect on flocculation activity, solutions were used to replace 1% $CaCl_2$, the salts used comprises of monovalent (LiCl & NaCl), divalent ($MgCl_2$ & $CaCl_2$) and trivalent ($FeCl_3$) at the same concentration. The control was maintained without

cations. To measure the flocculating activity, the above procedure was used to evaluate cation effect on flocculation activity.

12.2.6.3 Effect of pH and temperature on flocculating activity

A solution of NaOH (1.0 M) or HCl (1.0 M) was used whenever necessary to adjust pH in a range (3 to 11). The flocculation activity was assessed using previously described method. Both the bioflocculant and FeNPs were subjected to high temperatures (50-100 °C) in a water bath for 30 min to determine thermostability. After which a flocculation activity was calculated using a method described above.

12.2.7 Wastewater treatment

To assess removal efficiency (RE), Coal Mine wastewater and Mzingazi River water sample were collected and autoclaved at 121 °C for 15 min to ensure that no microorganisms present to interfere with experimentation. The samples were collected from Tendele Coal Mine and Mzingazi River in KwaZulu Natal, RSA. Following the method described by Maliehe, Basson and Dlamini [8], COD and BOD removal was evaluated. UV-Vis spectrophotometer Pharo 300 Spectroquant® was used at 680 nm for RE measure. The removal efficiency (RE) of the pollutants was calculated by the following equation:

$$\boldsymbol{RE}\ (\%) = \frac{\boldsymbol{Ci - Cf}}{\boldsymbol{Ci}}\ \boldsymbol{X}\ \mathbf{100} \qquad (\mathbf{2})$$

Where: C_i is the initial value before treatment with bioflocculant and nanoparticles and C_f is the value after treatment.

12.2.8 Cytotoxicity of the bioflocculant and iron nanoparticles

A method described by Daniels and Singh [14] was adopted to evaluate cytotoxicity of bioflocculant and nanoparticles using human embryonic kidney (HEK 293) and breast cancer cells (MCF-7). Cells with cell suspensions of 1×10^5 cells/mL concentrations were platted on 96-well-plate. Using a tenfold serial dilution method, the cells were seeded with different concentrations of nanoparticles (25-100 µg/µL). After 48 hours of incubation, media containing 1 % of foetal bovine serum (FBS) were used for the administration of nanoparticles and the plates were returned to the incubator for 48 hours. To ascertain cell viability tetrazolium salt (Sigma) was added as an indicator after 48 hours of incubation. 15 µL of MTT (5 mg/mL) in phosphate buffered saline (PBS) was added to each well and incubated at 37 °C for 4 hours. After sucking off from the wells, the medium with MTT and the formed formazan crystals were dissolved in 100 µL of dimethyl sulfoxide (DMSO). The optical density of the solutions was measured at 570 nm using a micro plate reader [14].

The % cell inhibition was determined using following formula:

Cell viability (%) $= \frac{F1}{F0} \boldsymbol{X\ 100}$, Where F_1 and F_0 are the final values obtained after and before treatment with the bioflocculant and nanoparticles, respectively.

12.2.9 Experimental, software and statistical analysis

All data was collected in triplicates and the error bars in the Figures show the standard deviations of the data. Data was subjected to One-way analysis of variances (ANOVA) using Graph Pad Prism™ 6.1. A significant level of $p<0.05$ was used.

12.3 Results

12.3.1 FT-IT spectra of the bioflocculant and iron nanoparticles

Figure 1 below represents the functional groups present in the bioflocculant and iron nanoparticles. The peak at 3245 cm^{-1} (bioflocculant) and 3250 cm^{-1} (iron nanoparticles) indicates the presence of hydroxyl (-OH) and amine ($-NH_2$) functional groups in the sample.

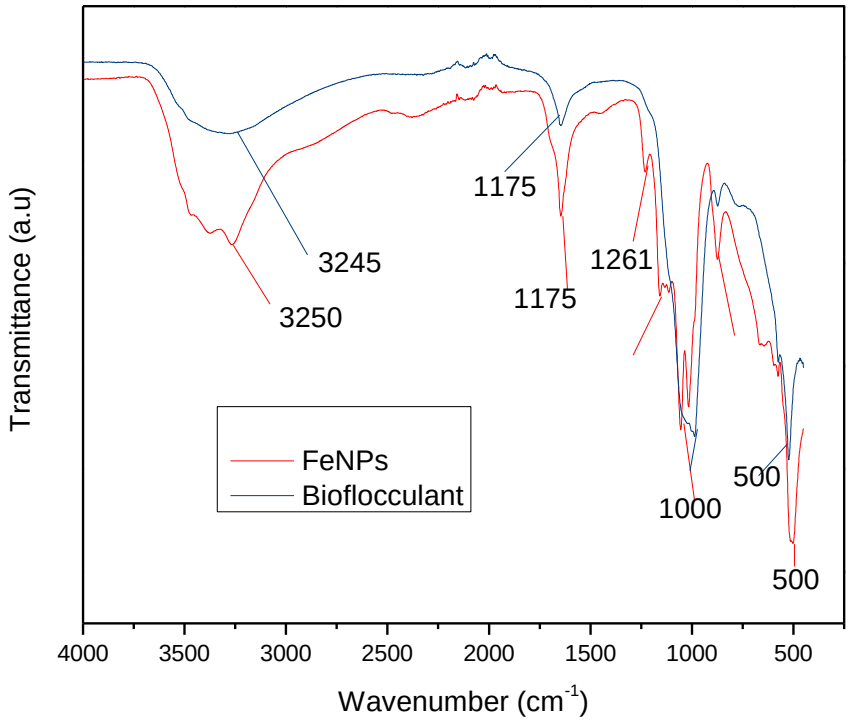

Figure 12.1: FT-IR spectra of the bioflocculant and iron nanoparticles.

12.3.2 The SEM morphology of the bioflocculant and iron nanoparticles.

Figure 2 and 3 below represent the surface morphology of bioflocculant and iron nanoparticles respectively. The bioflocculant have the crystal like morphology while the nanoparticles seem to have granular like shape.

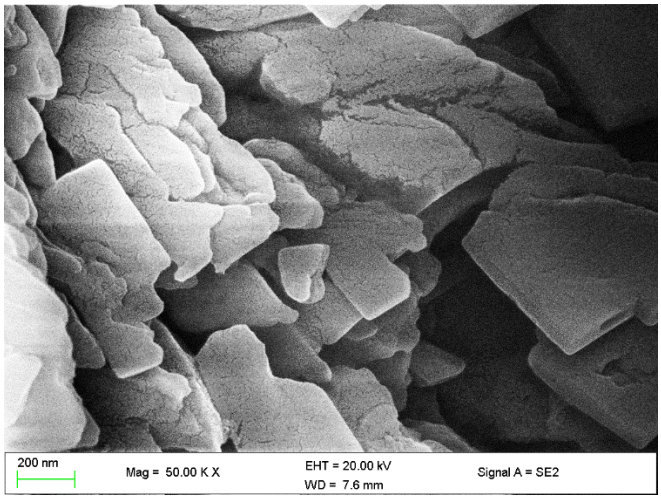

Figure 12.2: SEM surface morphology of the bioflocculant.

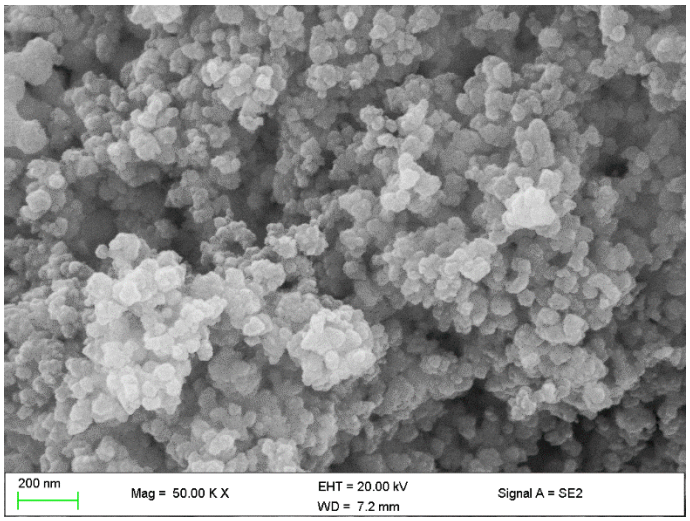

Figure 12.3: SEM surface morphology of the iron nanoparticles.

12.3.3 Elemental composition of the bioflocculant and iron nanoparticles

From table 1 below, elements such as O, C, Mg, P, K, Ca, Fe, and Cu are present in the bioflocculant and iron nanoparticles samples. From both samples, oxygen and carbon account for over 50%, while iron and copper were only found to be present in the iron nanoparticles alone and absent in the bioflocculant.

Table 12.1: Energy-dispersive X-ray analysis (EDX) of bioflocculant and iron nanoparticles.

Elements	Sample	
	Bioflocculant (wt.%)	FeNPs (wt.%)
C	13.21	12.39
O	55.25	47.94
Mg	13.35	1.12
P	16.00	13.43
K	0.14	0.24
Ca	2.04	7.33
Fe	-	17.31
Cu	-	0.30
Total	100.00	100.00

12.3.4 Dosage concentration effect on flocculation

The adequate dosage is required for the efficient flocculation process. Fe nanoparticles showed the optimum flocculation activity (FA) at 0.4 mg/mL dosage as opposed to that of bioflocculant which displayed the highest flocculation activity at 0.8 mg/mL.

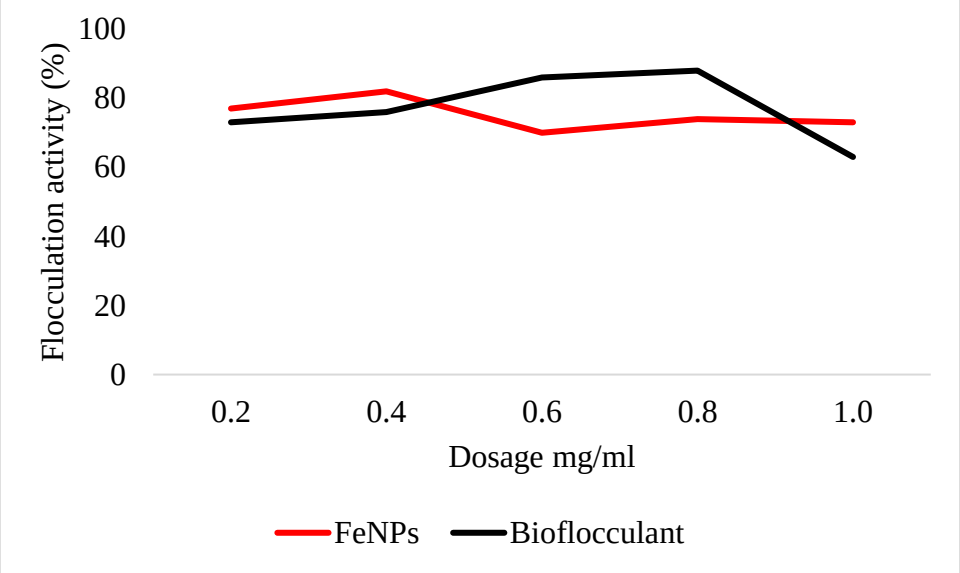

Figure 12.4: Dosage effect on flocculation activity.

12.3.5 Temperature effect on flocculation activity

The FeNPs are more thermostable compare to the bioflocculant as the flocculation activity was above 86% at 100 °C. While the significant drop in flocculation activity is observed with the increased temperature in bioflocculant.

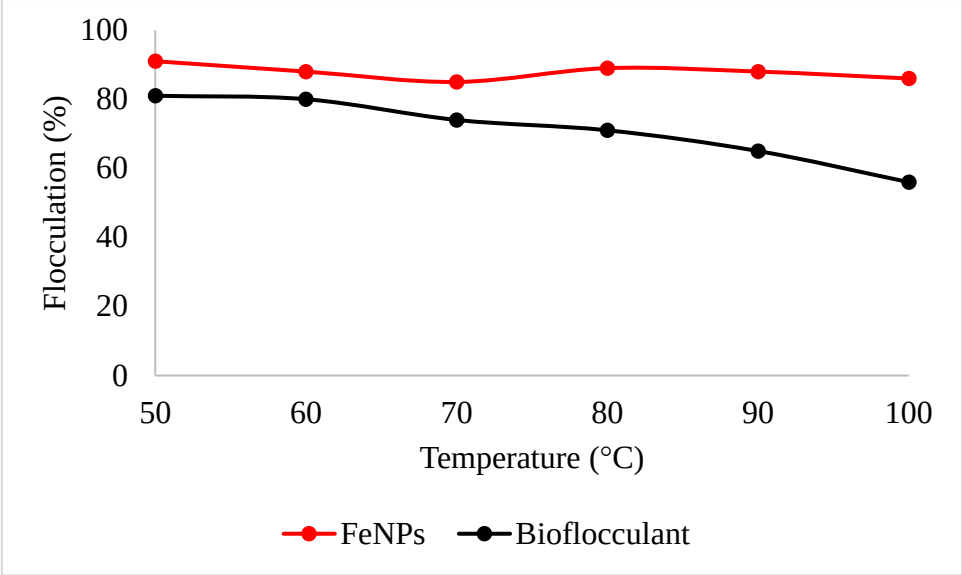

Figure 12.5: Temperature effect on flocculation activity.

3.6 Effect of pH on flocculation activity

Both the FeNPs and bioflocculant flocculate well in alkaline condition, with FeNPs having the optimum flocculation activity at pH 12, while that of the bioflocculant is at pH 7.

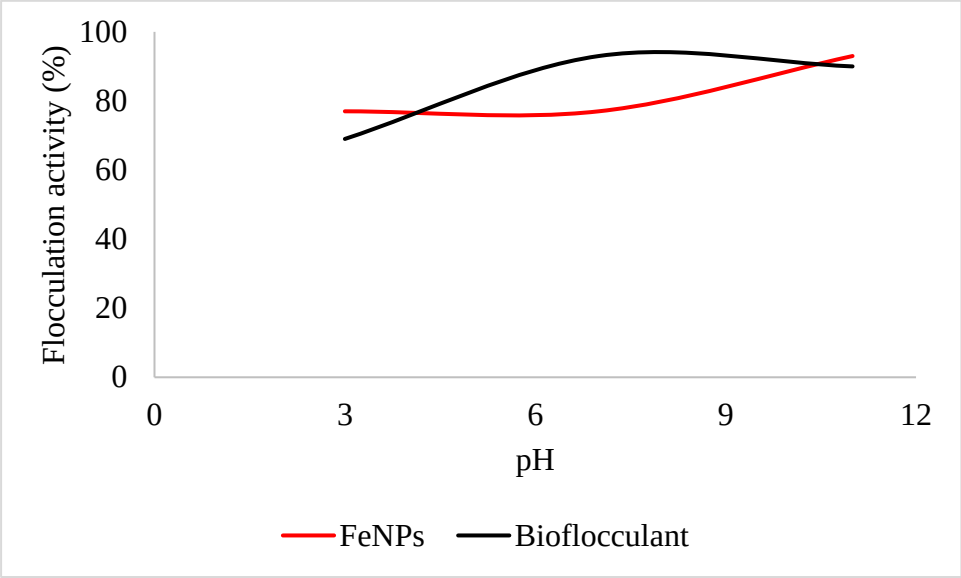

Figure 12.6: pH effect on flocculation activity.

3.7 Effect of metal irons on flocculation activity

The nanoparticles and bioflocculant flocculated poorly when the cation was not added, with 49% and 46% flocculation activity respectively.

Table 12.2: Cation effect on flocculation activity.

Cations	**Flocculation Activity (%)**	
	Bioflocculant	**FeNPs**
Control	49±3.35	46±2.03[b]
Fe^{3+}	31±3.15	85±2.72[a]
Mg^{2+}	63±6.78	82±1.53[a]
Ca^{2+}	71±5.42	82±3.64[a]
Li^{+}	75±2.31	72±1.15[a]
Na^{+}	62±7.28	72±1.15[a]

12.3.8 The removal of COD and BOD

Table 3 represents removal efficiency by $FeCl_3$, FeNPs and bioflocculant; Fe nanoparticles were the most effective in reducing both COD and BOD compare to the other two flocculants.

Table 12.3: COD and BOD removal in wastewater by bioflocculant and iron nanoparticles.

Flocculant	Types of waste water	Types of pollutants in water	Water quality before treatment (mg/L)	Water quality after treatment (mg/L)	Removal efficiency (%)
$FeCl_3$	Coal Mine water	COD	842	437.84	52
		BOD	123.2	66.5	54
	Mzingazi river water	COD	3.300	1.65	50
		BOD	136	63.92	47
FeNPs	Coal Mine water	COD	842	204	76
		BOD	123.2	23	81
	Mzingazi river water	COD	3.300	1.700	48
		BOD	136	24	82
Bioflocculant	Coal Mine water	COD	842	208	72
		BOD	123.2	77.88	59
	Mzingazi river water	COD	3.300	1.68	51
		BOD	136	72.08	53

3.9 Evaluation of cytotoxicity of the FeNPs and bioflocculant

In-vitro cytotoxicity of both FeNPs and bioflocculant were evaluated and FeNPs were found nontoxic at low concentration and the bioflocculant was nontoxic at all concentrations.

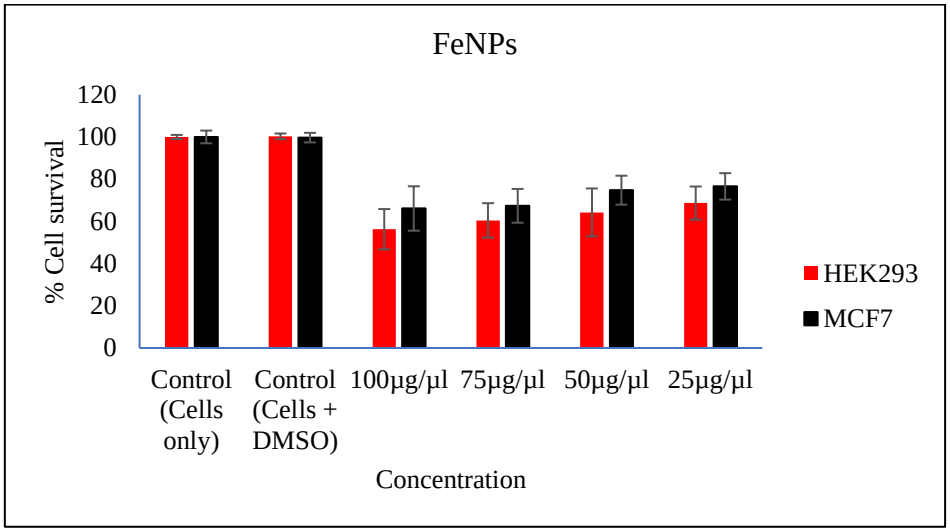

Figure 12.7: In-vitro cytotoxicity effect of FeNPs nanoparticles on HEK293 & MCF7 cells.

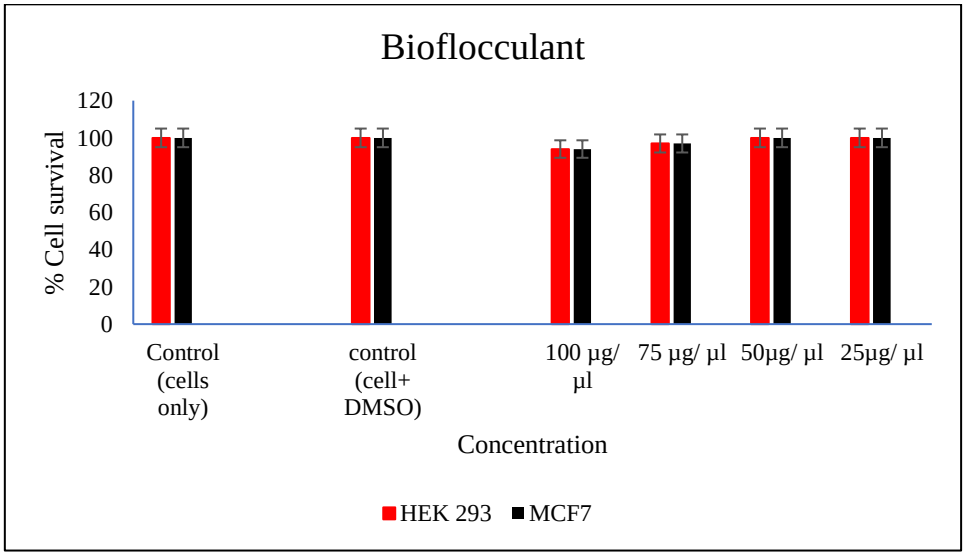

Figure 12.8: In-vitro cytotoxicity effect of bioflocculant nanoparticles on HEK293 & MCF7 cells.

12.4 Discussion

The functional groups present in the molecular chains of the bioflocculant facilitate the binding capability of the bioflocculants [15]. The presence of –OH group plays the significant role in reducing and stabilizing nanoparticles during synthesis [16]. Thermostability of the nanoparticles when subjected in heat further confirm the presence of hydroxyl group. Flocculation process is influenced by the surface morphology of the flocculant, it accounts for the effectiveness or poor efficiency of the flocculant [10]. From Figure 3, the crystal like and granular morphology is observed. The change in bioflocculant structure is the indication of the formation of nanoparticles in the synthesis. Furthermore, it can be noted that the nanoparticles have more surface area for pollutants absorption. Therefore, it can be deduced that the synthesis of nanoparticles does not only modify the surface structure but it also increases the surface area on nanoparticles for particles flocculation and pollutants removal in water. Flexibility and stability of flocculants is brought about by the different elements present in the sample. From Table 1, elements such as O and C were found in the bioflocculant sample and accounts for major percentage, these elements form backbone structure of the biomolecule. Furthermore, Mg, P, K and Ca accounts for the production media which was used for the bioflocculant production. Similarly, the as-synthesized iron nanoparticles also had O and C, which accounts for 60.33% and Fe was found to be the second highest present element with 17.31%, which indicates that the nanoparticles synthesis was successful. The copper grid, which was used during analysis, could account for 0.30% Cu present in the sample.

To effectively neutralize some of the negative charges on colloidal particles, the adequate dosage is required, if the dosage is insufficient, poor flocculation results [17]. Contrary to this, excess dosage may increase the viscosity, which results to poor flocculation activity [18]. As illustrated in Figure 4, the optimum flocculation activity was achieved at 0.4 mg/mL and 0.8 mg/mL for nanoparticles and bioflocculant respectively. Increase in flocculation activity was observed between 02-04 mg/mL for FeNPs, however, with the increase in dosage concentration to 0.6-1.0 mg/mL, the flocculation activity dropped a little and it remained consistent throughout. This could be due to competition and repulsion of negatively charged kaolin particles, which in turn blocks binding sites. The low flocculation activity for the bioflocculant at 0.2-0.6 mg/mL may be due to the fact that low dosage did not permit bridging phenomena to occur effectively [8]. Both the bioflocculant and the FeNPs were subjected to different temperatures (50-100 °C) for 30 minutes in a water bath. As depicted from Figure 5, higher

flocculation activity was observed at 50 °C with 91 and 81% for nanoparticles and bioflocculant respectively. The increase in temperature did not affect the flocculation process of the as-synthesized nanoparticles. The flocculation activity remained above 86% suggesting that the nanoparticles are thermostable. This could be attributed to the presence of -OH group as indicated in Figure 1 above. Contrary, the bioflocculant showed the decrease in flocculation activity with the increase in temperature.

Key factors that influence the flocculation process include pH. Flocculation activity may be affected by pH; it may alter flocculant status charge and surface characteristics of colloidal particles in suspension [17]. From Figure 6, the highest flocculation activity of 90% was achieved with FeNPs at strong alkaline pH of 11. Nonetheless, the flocculation activity was still above 77% at strong acidic pH 3, suggesting that FeNPs can be applied in both acidic and alkaline conditions, but most effective using alkaline conditions. Contradictory to this, the flocculation activity of the bioflocculant was poor at acidic conditions with the optimum of 93% at pH 7. The poor performance at strong acidic conditions may be attributed to protein denaturation in the bioflocculant. These findings suggest that the nanoparticles can be suitable flocculant in Coal Mine waste as the pH is mostly alkaline.

Residual negative net surface charge of the bioflocculant functional group is neutralized by cations which in turn enhance the flocculation activity [19]. Various metal ions effect was evaluated on as-synthesized nanoparticle and bioflocculant as shown in Table 2. The highest flocculation activity of 85% was observed when a trivalent cation (Fe^{3+}) was used as an enhancing metal ion. However, both the monovalent and divalent cations could still have enhanced the flocculation activity with the flocculation activity above 70%. Contrary to this, the nanoparticles flocculate poorly without the presence of cation, suggesting that they are cation dependent. In the bioflocculant, both monovalent and divalent were found to be most effective with Li^{+} being the highest flocculation activity of 75%. The least flocculation activity was observed when trivalent cation (Fe^{3+}) was used. Conflicting the findings that suggest monovalent cations reduce the strength of the bonds and results to loose flocs, thus producing poor flocculation activity [20].

The higher amount of both COD and BOD is not good for aquatic ecosystem. This condition results in decrease in the amount of dissolved oxygen (DO), which in turn results to anaerobic

conditions that is detrimental to higher aquatic life. Furthermore, high amount of BOD in water signifies high amount of nutrients, which may result into alga boom. From Table 3, different wastewaters were used to evaluate effectiveness of FeNPs and bioflocculant in comparison to a commercial flocculant ferric chloride. Samples were analysed using UV-Vis spectrophotometer Spectroquant® at 620 nm wavelength. The nanoparticles proved to be most effective when compared to both the bioflocculant and ferric chloride with BOD over 80%, while the COD was 76% for Coal Mine waste water and least effective on river water with just 48%. Both the ferric chloride and bioflocculant remained consistently poor in all the samples for BOD removal with just 50% efficacy. However, a remarkable improvement was observed in COD removal for Coal Mine wastewater by the bioflocculant with 72%, but it remained poor in the river water sample. Ferric chloride remained poor for all samples; this could be due to the dosage concentration used. Therefore, it can be deduced that FeNPs are a better flocculant compared to the bioflocculant and ferric chloride. Bioflocculants are generally nontoxic but they still need to be tested for biosafety reasons [21]. From Figure 7, nanoparticles were evaluated against human normal cells (HEK 293) and cancer cells (MCF7). As-synthesized nanoparticles are found to be nontoxic al low concentration as the cell survival was above 76% for both cell at 25-50 µL, with the increase in concentration cell survival rate decrease, however, cell survival was still above 56%. It is therefore, recommended that FeNPs should not be used at high concentrations as may result in cell toxicity. Contrarily, bioflocculant proved to be nontoxic against both cells at highest concentration of 100 µL with the cell survival over 90%.

12.5 Conclusions

The samples as-synthesized nanoparticles and bioflocculant revealed the presence of functinal groups -OH and -NH_2 repectively. SEM-EDX indicated huge percentage of O and C wt.% in both samples. FeNPs most effective at low concentration while bioflcculant works best when the dosage is increased to 0.8 mg/mL. FeNPs are effective at all pH conditions and temperature ranges, while the bioflocculant was only effective at lower temperatures and nuetral to weak alkaline conditions. Nanoparticles could remove effectively both COD and BOD in all water samples, while biflocculant and ferric chloride were seen to be less effective. FeNPs are nontoxic only at lower concentration, while bioflocccculant is nontoxic even at higher concentrations. Therefore, FeNPs can be reccomanded as an alternative flocculant provided the concentration is maintained lower.

Author Contributions: Conceptualization, A.K.B. and V.S.R.P.; formal analysis, N.G.D. and V.S.R.P.; investigation, N.G.D.; supervision, A.K.B. and V.S.R.P.; writing—original draft, N.G.D.; writing—review and editing, V.S.R.P.

Acknowledgments: Nkosinathi Dlamini would like to acknowledge the Council for Scientific and Industrial Research (CSIR, South Africa) for the financial assistance in the form of the Ph.D. bursary. The authors would like to acknowledge the Electron Microscopy Unit at the University of KwaZulu-Natal,Westville campus, for providing support by letting us use the SEM-EDX facilities for the characterization of nanomaterials. The authors would like to acknowledge Dr Singh and her team for assisting with cytotoxicity test. Rajasekhar Pullabhotla would like to acknowledge the National Research Foundation (NRF, South Arica) for the financial support in the form of the Incentive Fund Grant (Grant No: 103691).

Conflicts of Interest: The authors declare no conflict of interest

12.6 References

1. Ali, I.; Asim, M.; Khan, T.A. Low cost adsorbents for the removal of organic pollutants from wastewater. *Journal of environmental management* **2012**, *113*, 170-183.

2. Qu, X.; Alvarez, P.J.; Li, Q. Applications of nanotechnology in water and wastewater treatment. *Water research* **2013**, *47*, 3931-3946.

3. Verma, Y. Acute toxicity assessment of textile dyes and textile and dye industrial effluents using Daphnia magna bioassay. *Toxicology and industrial health* **2008**, *24*, 491-500.

4. Samanta, A.K.; Agarwal, P. Application of natural dyes on textiles. **2009**.

5. Merzouk, B.; Madani, K.; Sekki, A. Using electrocoagulation–electroflotation technology to treat synthetic solution and textile wastewater, two case studies. *Desalination* **2010**, *250*, 573-577.

6. Verma, A.K.; Dash, R.R.; Bhunia, P. A review on chemical coagulation/flocculation technologies for removal of colour from textile wastewaters. *Journal of environmental management* **2012**, *93*, 154-168.

7. Tiwari, D.K.; Behari, J.; Sen, P. Application of nanoparticles in waste water treatment 1. **2008**.

8. Maliehe, T.S.; Basson, A.K.; Dlamini, N.G. Removal of Pollutants in Mine Wastewater by a Non-Cytotoxic Polymeric Bioflocculant from Alcaligenes faecalis HCB2. *International journal of environmental research and public health* **2019**, *16*, 4001.

9. Lu, H.; Wang, J.; Wang, T.; Wang, N.; Bao, Y.; Hao, H. Crystallization techniques in wastewater treatment: An overview of applications. *Chemosphere* **2017**, *173*, 474-484, doi:https://doi.org/10.1016/j.chemosphere.2017.01.070.

10. Zhang, Z.-q.; Bo, L.; XIA, S.-q.; WANG, X.-j.; YANG, A.-m. Production and application of a novel bioflocculant by multiple-microorganism consortia using brewery wastewater as carbon source. *Journal of Environmental Sciences* **2007**, *19*, 667-673.

11. Dlamini, N.G.; Basson, A.K.; Pullabhotla, V.S.R. Optimization and Application of Bioflocculant Passivated Copper Nanoparticles in the Wastewater Treatment. *International Journal of Environmental Research and Public Health* **2019**, *16*, 2185.

12. Dlamini, N.G.; Basson, A.K.; Shandu, J.S.E.; Mavuso, S.S.; Pullabhotla, V.S.R. Biosynthesis, Characterization, and Application of Iron Nanoparticles: in Dye Removal and as Antimicrobial Agent. *Water, Air, & Soil Pollution* **2020**, *231*, 1-10, doi:https://doi.org/10.1007/s11270-020-04498-x.

13. Xia, X.; Lan, S.; Li, X.; Xie, Y.; Liang, Y.; Yan, P.; Chen, Z.; Xing, Y. Characterization and coagulation-flocculation performance of a composite flocculant in high-turbidity drinking water treatment. *Chemosphere* **2018**, *206*, 701-708, doi:https://doi.org/10.1016/j.chemosphere.2018.04.159.

14. Daniels, A.N.; Singh, M. Sterically stabilized siRNA: gold nanocomplexes enhance c-MYC silencing in a breast cancer cell model. *Nanomedicine* **2019**.

15. Xiong, Y.; Wang, Y.; Yu, Y.; Li, Q.; Wang, H.; Chen, R.; He, N. Production and characterization of a novel bioflocculant from Bacillus licheniformis. *Appl. Environ. Microbiol.* **2010**, *76*, 2778-2782.

16. Mata, Y.; Torres, E.; Blazquez, M.; Ballester, A.; González, F.; Munoz, J. Gold (III) biosorption and bioreduction with the brown alga Fucus vesiculosus. *Journal of hazardous materials* **2009**, *166*, 612-618.

17. Li, X.-M.; Yang, Q.; Huang, K.; Zeng, G.-M.; Liao, D.-X.; Liu, J.-J.; Long, W.-F. Screening and characterization of a bioflocculant produced by Aeromonas sp. *Biomedical and environmental sciences: BES* **2007**, *20*, 274-278.

18. Wang, L.; Ma, F.; Qu, Y.; Sun, D.; Li, A.; Guo, J.; Yu, B. Characterization of a compound bioflocculant produced by mixed culture of Rhizobium radiobacter F2 and Bacillus sphaeicus F6. *World Journal of Microbiology and Biotechnology* **2011**, *27*, 2559-2565.

19. Manivasagan, P.; Kang, K.-H.; Kim, D.G.; Kim, S.-K. Production of polysaccharide-based bioflocculant for the synthesis of silver nanoparticles by Streptomyces sp. *International journal of biological macromolecules* **2015**, *77*, 159-167.

20. Wu, J.-Y.; Ye, H.-F. Characterization and flocculating properties of an extracellular biopolymer produced from a Bacillus subtilis DYU1 isolate. *Process Biochemistry* **2007**, *42*, 1114-1123.

21. Pathak, M.; Devi, A.; Bhattacharyya, K.; Sarma, H.; Subudhi, S.; Lal, B. Production of a non-cytotoxic bioflocculant by a bacterium utilizing a petroleum hydrocarbon source and its application in heavy metal removal. *Rsc Advances* **2015**, *5*, 66037-66046.

Chapter 13 General Conclusion and recommendations

The synthesized nanoparticles were characterized with analytical techniques such as FT-IR, XRD, TEM, TGA, SEM-EDX and UV-Vis. For copper nanoparticles, TEM images revealed close to spherical shaped particles with an average particle size of ~53 nm, which is in good agreement with that of the calculated using the Scherrer equation from XRD results. Powder X-ray diffraction peaks revealed the crystalline nature of the synthesised material with no impurities and are in correlation with the JCPDS card no: 04-0836. The characteristic diffraction peaks of copper were observed at around 33° and 47° 2θ, corresponding to the (111) and (220) planes of the fcc structure. Synthesized copper nanoparticles were applied in wastewater treatment, dye removal and its antimicrobial effect was evaluated. The elemental composition of CuNPs compared to that of bioflocculant revealed that, there was a significant increase in copper with 37.8 Wt.%, while there was no copper present in the bioflocculant. Thermogravimetric analysis of both the bioflocculant and CuNPs showed that the synthesized nanoparticles are more thermally stable compared to bioflocculant. The synthesized copper nanoparticles showed an excellent flocculation property at a low dosage with a concentration of 0.2 mg/mL. They flocculate independent of cation, are thermostable, and work at weak acidic, neutral, and alkaline pH. Agitation (shaking speed) is not required for the effectiveness of the synthesized nanoparticles in flocculation. They possess great properties for pollutants removal in coal mine water, domestic wastewater, and river water. Over 89% of COD and BOD removal efficiency was observed for both the coal mine and river water. Furthermore, they are able to remove staining dyes at a low concentration of 0.2 mg/mL and for 10 min contact time. The removal efficiencies were determined using different water samples, one from coalmine water the other from domestic and industrial wastewater respectively. In the treatment of wastewater, the synthesized nanoparticles worked better compared to both the iron chloride and bioflocculant. The CuNPs possess some good properties in terms of dye affinity as it had above 80% removal efficiency in tested dyes. The synthesized particles possessed some antimicrobial properties, to all selected test strain positive results were obtained. The bioflocculant alone did not give any positive results, suggesting that the antimicrobial property was due to the presence of copper.

The synthesized iron nanoparticles revealed the presence of hydroxyl group (-OH) and amine group ($-NH_2$) in the sample through FT-IR studies. In comparison to a bioflocculant, there was no iron present in the pure bioflocculant and 17.31 Wt.% iron was observed in the iron

nanoparticles. This suggests the incorporation of iron onto the bioflocculant. Furthermore, SEM-EDX results reveal the presence of the elements such as O, P, C, Ca, Cu and K in the sample, which can be attributed to the medium which was used for bioflocculant production. The X-ray diffraction analysis reveals the crystallite size of ~53 nm, which indicates a higher surface area and surface to volume ratio of the nanoparticles. The TGA analysis shows that the synthesized nanoparticles are thermostable as they are able to maintain weight above 60% even at temperatures above 700 °C. UV-Vis spectrum illustrated the plasmon resonance (SPR) spectra with absorbance 300-350 nm and the peak maxima for the synthesized particles was observed at around 300 nm.

Both CuNPs and Fe@Cu core-shell nanoparticles had the highest flocculation activity of 96 and 99 % respectively at a low dosage with a concentration of 0.2 mg/mL, while the optimum flocculation activity for FeNPs was achieved at 0.4 mg/mL with 82 %. Iron nanoparticles are cation dependent with 85% flocculation activity when Fe^{3+} was used as opposed to 46% flocculation activity when there was no cation present. Contrary to this, CuNPs and Fe@Cu core-shell nanoparticles flocculate well without the addition of cations and are pH stable. Both CuNPs and Fe@Cu core-shell nanoparticles have remarkable ability to remove dyes, while FeNPs needs the addition of cation to yield RE above 50%. The synthesized nanoparticles work well in removing both the COD and BOD in river water and coal mine wastewater. When evaluated for antimicrobial activity, CuNPs were able to inhibit and kill the Gram-positive and Gram-negative microorganisms, while FeNPs did not show any antimicrobial activity. In the cytotoxicity study, all the nanoparticles showed to be safer when used at a low concentration 25 µg/µL, as the cell viability was above 70 % again HEK 293 and MCF7. After 7 weeks, all the nanoparticles were biodegraded by microorganisms. The as-synthesized Fe@Cu core-shell nanoparticles are effective to flocculate at low concentration of 0.2 mg/mL, cation independent, pH stable and thermostable. Possesses antimicrobial effect for both Gram-positive and Gram-negative and the MIC and MBC was found at the lowest concentration of 1.563 mg/mL and are not toxic against normal cells at low concentration. These core-shell nanoparticles also showed some remarkable properties in removing dyes at of 4 g/L concentration with just 0.2 mg/mL dosage size. High removal efficacy for wastewater and river water was also observed.

CuNPs and Fe@Cu core-shell nanoparticles are the most effective compared to FeNPs in wastewater treatment, MIC and MBC, dye removal and in flocculation process. Therefore, for

application purposes copper nanoparticles are most suitable and also the combination of iron and copper can be preferred over iron nanoparticles alone.

13.1 Recommendations

The iron nanoparticles did not perform well in dye and wastewater treatment. More optimization is required on this material and also the antimicrobial activity maybe further evaluated against more strains or the dosage concentration be increased. Both the Fe@Cu core-shell and copper nanoparticles were found to be effective in wastewater treatment but they can also be tested against heavy metals removals in water. Furthermore, mechanisms of action for all the synthesis materials maybe evaluated in the future studies.

Indices

Publications cover pages

Copyright © 2019 American Scientific Publishers
All rights reserved
Printed in the United States of America

Article

Advanced Science, Engineering and Medicine
Vol. 11, 1–7, 2019
www.aspbs.com/asem

Biosynthesis and Characterization of Copper Nanoparticles Using a Bioflocculant Extracted from *Alcaligenis faecalis* HCB2

Nkosinathi G. Dlamini[1], Albertus K. Basso[1], and V. S. R. Rajasekhar Pullabhotla[2,*]

[1] *Bioflocculation Research Group, Department of Biochemistry and Microbiology*
[2] *Department of Chemistry, University of Zululand, Private Bag X1001, Kwa-Dlangezwa, 3886, South Africa*

Bioflocculant from Alcaligenis faecalis HCB2 was used in the eco-friendly synthesis of the copper nanoparticles. Nanoparticles were characterized using a scanning electron microscope (SEM), transmission electron microscopy (TEM), UV-visible spectroscopy, thermo gravimetric analysis (TGA) and Fourier Transform Infrared Spectroscopy (FT-IR). The transmission electron microscopy images showed close to spherical shapes with an average particle size of ~53 nm. Energy-dispersive X-ray spectroscopy analysis confirmed the presence of the Cu nanopartilces and also the other elements such as O, C, P, Ca, Cl, Na, K, Mg, and S originated from the bioflocculant. FT-IR results showed the presence of the –OH and $–NH_2$ groups, aliphatic bonds, amide and Cu–O bonds. Powder X-ray diffraction peaks confirmed the presence of (111) and (220) planes of fcc structure at 2θ of 33° and 47° respectively with no other impurity peaks.

Keywords: Bioflocculant, Copper Nanoparticles, Electron Microscopy, Biosynthesis.

International Journal of
Environmental Research and Public Health

MDPI

Article

Optimization and Application of Bioflocculant Passivated Copper Nanoparticles in the Wastewater Treatment

Nkosinathi Goodman Dlamini [1,*], Albertus Kotze Basson [1] and Viswanadha Srirama Rajasekhar Pullabhotla [2,*]

[1] Department of Biochemistry and Microbiology, University of Zululand, Private Bag X1001, KwaDlangezwa 3886, South Africa; BassonA@unizulu.ac.za
[2] Department of Chemistry, University of Zululand, Private Bag X1001, KwaDlangezwa 3886, South Africa
* Correspondence: nathidlamini03@gmail.com (N.G.D.); PullabhotlaV@unizulu.ac.za (V.S.R.P.); Tel.: +27-35-902-6155 (V.S.R.P.)

Received: 23 May 2019; Accepted: 13 June 2019; Published: 20 June 2019

check for updates

Abstract: Nanotechnology offers a great opportunity for efficient removal of pollutants and pathogenic microorganisms in water. Copper nanoparticles were synthesized using a polysaccharide bioflocculant and its flocculation, removal efficiency, and antimicrobial properties were evaluated. The synthesized nanoparticles were characterized using thermogravimetry, UV-Visible spectroscopy, Fourier-transform infrared spectroscopy (FT-IR), powder X-ray diffraction, scanning electron microscope (SEM), and transmission electron microscope (TEM). The highest flocculation activity (FA) was achieved with the lowest concentration of copper nanoparticles (0.2 mg/mL) with 96% (FA) and the least flocculation activity was 80% at 1 mg/mL. The copper nanoparticles (CuNPs) work well without the addition of the cation as the flocculation activity was 96% and worked best at weak acidic, neutral, and alkaline pH with the optimal FA of 96% at pH 7. Furthermore, the nanoparticles were found to be thermostable with 91% FA at 100 °C. The synthesized copper nanoparticles are also high in removal efficiency of staining dyes, such as safranin (92%), carbol fuchsine (94%), malachite green (97%), and methylene blue (85%). The high removal efficiency of nutrients such as phosphate and total nitrogen in both domestic wastewater and Mzingazi river water was observed. In comparison to ciprofloxacin, CuNPs revealed some remarkable properties as they are able to kill both the Gram-positive and Gram-negative microorganisms.

Keywords: copper nanoparticles; flocculation activity; removal efficiency; wastewater treatment

Water Air Soil Pollut _###################_
https://doi.org/10.1007/s11270-020-04498-x

Biosynthesis, Characterization, and Application of Iron Nanoparticles: in Dye Removal and as Antimicrobial Agent

Dlamini G. Nkosinathi · Basson K. Albertus · Shandu S. E. Jabulani · Mavuso Siboniso · Rajasekhar VSR Pullabhotla

Received: 29 November 2019 / Accepted: 26 February 2020
© Springer Nature Switzerland AG 2020

Abstract Green protocols for synthesizing nanoparticles have demonstrated numerous benefits and advantages, which include environmental friendliness, good efficacy and possess less threat to human. The aim of this study was to biosynthesize, characterize and evaluate the effectiveness of biosynthesized iron nanoparticles. The bioflocculant was extracted using a solvent extraction method and purified by 100 mL distilled water and a mixture of chloroform and butanol (5:2 v/v). Iron nanoparticles (FeNPs) were successfully synthesized through the chemical reduction method. Where 0.5 g of bioflocculant was mixed with 3 mM iron sulphate ($FeSO_4$) solution and left to stand at room temperature for 24 h. Characterization of the as-synthesized nanoparticles was achieved with a Scanning Electron Microscope (SEM), Energy Dispersive X-ray Spectroscopy (EDX) and Fourier-Transform Infrared spectroscopy (FT-IR). The various parameters that effect on flocculation activity were evaluated, with optimum flocculation activity at a dosage size of 0.4 mg/mL (88%). The FeNPs were found to be cation-dependent Mg^{2+} (82%) and flocculate both in acidic pH 3 and in alkaline pH 11 with (93%) flocculation activity. The synthesized FeNPs are thermostable as they maintain flocculation activity above 80% at 100 °C temperatures.

Keywords Dye removal · Flocculation activity · Iron nanoparticles · Optimization

1 Introduction

Freshwater is a major source of water for human and animals. Industrialization, population growth and changes in climate have resulted in water scarcity in most countries, especially developing countries (Vörösmarty et al. 2004). There are general methods that are applied in water purification, which include, boiling, filtration, sedimentation and salting-in method (Buthelezi et al. 2012). Chemicals used are of viewed as the better water treatment tools, as they are highly efficient and cheaper. However, the inadequacy is that they have been found to be environmentally unfriendly and detrimental to human health (Exley et al. 2006).

Conversely, bioflocculants have recently gained a

processes

MDPI

Article

A Comparative Study between Bimetallic Iron@copper Nanoparticles with Iron and Copper Nanoparticles Synthesized Using a Bioflocculant: Their Applications and Biosafety

Nkosinathi Goodman Dlamini [1,*], Albertus Kotze Basson [1] and Viswanadha Srirama Rajasekhar Pullabhotla [2,*]

[1] Department of Biochemistry and Microbiology, University of Zululand, Private Bag X1001, KwaDlangezwa 3886, South Africa; BassonA@unizulu.ac.za

[2] Department of Chemistry, University of Zululand, Private Bag X1001, KwaDlangezwa 3886, South Africa

* Correspondence: nathidlamini03@gmail.com (N.G.D.); PullabhotlaV@unizulu.ac.za (V.S.R.P.); Tel.: +27-35-902-6155 (V.S.R.P.)

Received: 20 July 2020; Accepted: 19 August 2020; Published: date

Abstract: Nanotechnology addresses numerous environmental problems such as wastewater treatment. Ground water, surface water and wastewater that is contaminated by toxic organic, inorganic solutes and pathogenic microorganisms can now be treated through the application of nanotechnology. The study reports iron@copper (Fe@Cu) nanoparticles, iron nanoparticles (FeNPs) and copper nanoparticles (CuNPs) synthesized using a bioflocculant in a green approach technique. Characterization of the as-synthesized materials was achieved using analytical techniques such as Fourier transform-Infrared spectroscopy (FT-IR), Thermogravimetric analysis (TGA), Scanning Electron Microscope (SEM), Transmission Electron Microscopy (TEM), UV-Vis spectroscopy (UV-Vis) and X-Ray diffraction (XRD). The presence of hydroxyl (–OH) and amine ($–NH_2$) groups was shown by FT-IR spectroscopy studies and the as-synthesized material was shown to be thermostable. Elements such as oxygen, carbon, iron and copper were found to be abundant in Wt%. Absorption peaks were found between 200 and 390 nm wavelength and diffraction peaks at 20–29°, 33° and 35° for FeNPs, CuNPs and Fe@Cu, respectively. In their application, the effect of various parameters on the flocculation activity were evaluated. Both the CuNPs and (Fe@Cu) nanoparticles have shown the best flocculation activity at a concentration of 0.2 mg/mL with over 90% activity, while the dosage size with a concentration of 0.4 mg/mL was optimal for FeNPs. The FeNPs were found to be cation dependent, while CuNPs and Fe@Cu nanoparticles flocculate in the absence of a cation and flocculate both in acidic and alkaline pH. All the synthesized nanoparticles are thermostable and maintain flocculation activity above 80% at 100 °C. Both the Fe@Cu and CuNPs were found to be effective in removing dyes with the removal efficiency above 89% and were found to be effective in removal of chemical oxygen demand (COD) and biochemical oxygen demand (BOD) in Mzingazi river water and coal mine wastewater with over 80% removal efficiency. Moreover, the synthesized nanoparticles showed some remarkable antimicrobial properties when evaluated against Gram-positive and Gram-negative bacteria. The as-synthesized material was found to be safe to use at low concentration when verified against human embryonic cells (HEK293) and breast cancer cells (MCF7) and biodegradable.

Keywords: bioflocculant; flocculation activity; wastewater treatment; dye removal; iron nanoparticle; copper nanoparticles

catalysts

MDPI

Article

Optimization of Fe@Cu Core–Shell Nanoparticle Synthesis, Characterization, and Application in Dye Removal and Wastewater Treatment

Nkosinathi Goodman Dlamini [1], Albertus Kotze Basson [1], Shandu Jabulani Siyabonga Emmanuel [1] and Viswanadha Srirama Rajasekhar Pullabhotla [2,*]

[1] Department of Biochemistry and Microbiology, University of Zululand, Private Bag X1001, KwaDlangezwa 3886, South Africa; nathidlamini03@gmail.com (N.G.D.); Bassona@unizulu.ac.za (A.K.B.); ShanduJ@unizulu.ac.za (S.J.S.E.)

[2] Department of Chemistry, University of Zululand, Private Bag X1001, KwaDlangezwa 3886, South Africa

* Correspondence: PullabhotlaV@unizulu.ac.za; Tel.: +27-35-902 6155

Received: 27 November 2019; Accepted: 8 January 2020; Published: 7 July 2020

check for updates

Abstract: Green synthesis of core–shell nanoparticles is gaining importance nowadays as it is viewed as being environmental friendly and cost effective. The present study aimed to synthesize iron@copper core–shell nanoparticles using a polysaccharide-based bioflocculant from *Alcaligenis faecalis* and to evaluate its efficiency in dye removal and river water and domestic wastewater treatment. The synthesized samples were characterized by Fourier-transform infrared spectroscopy, X-ray diffraction, scanning electron microscopy, thermogravimetric analysis, transmission electron microscopy, and UV-Vis spectroscopy analysis. To optimize the best concentration for core–shell formation, different ratios of iron to copper were prepared. Sample 1 (S1) contained 1:3 iron to copper (Fe 25%–Cu 75%), sample 2 (S2) contained 1:1 iron to copper (Fe 50%–Cu 50%), and the third sample (S3) contained 3:1 iron to copper (Fe 75%–Cu 25%). The flocculation activity (FA) was above 98% at 0.2 mg/mL for all the samples and the samples flocculated well under acidic, alkaline, and neutral pH conditions. Sample 3 was shown to be thermostable, with flocculation activity above 90%, and samples 2 and 1 were also thermostable, but the flocculation decreased to 87 at 100 °C. All three samples revealed some remarkable properties for staining dye removal as the removal efficiency was above 89% for all dyes tested. The synthesized core–shell nanoparticles could remove nutrients such as total nitrogen and phosphate in both domestic wastewater and Mzingazi river water. Furthermore, high removal efficiency for chemical oxygen demand (COD) and biological oxygen demand (BOD) was also observed.

Keywords: core–shell nanoparticles; removal efficiency; optimization; synthesis

Copyright © 2020 American Scientific Publishers
All rights reserved
Printed in the United States of America

Article

Advanced Science, Engineering and Medicine
Vol. 12, 1–6, 2020
www.aspbs.com/asem

Green Synthesis of Iron Nanoparticles by a Polysaccharide Bioflocculant from Marine *Alcaligenes faecalis sp.* and Characterization

Nkosinathi G. Dlamini[1], Albertus K. Basson[1], and Rajasekhar V. S. R. Pullabhotla[2,*]

[1] *Bioflocculation Research Group, Department of Biochemistry and Microbiology*
[2] *Department of Chemistry, University of Zululand, Private Bag X1001, Kwa-Dlangezwa, 3886, South Africa*

Iron, the most ubiquitous of the transition metals and the fourth most plentiful metal in the Earth's crust, is the structural backbone of our modern infrastructure. It is therefore ironic that as a nanoparticle, iron has been somewhat neglected in favour of its own oxides as well as other metals such as cobalt, nickel, gold, and platinum. This study reports the green synthesis of iron nanoparticles using a bioflocculant and their characterization. The as-synthesised materials were characterized using Scanning Electron Microscopy (SEM), Transmission Electron Microscopy (TEM), X-ray diffraction (XRD), Fourier Transform Infrared Spectroscopy (FT-IR), Thermogravimetric analysis (TGA) and UV-Vis absorption spectroscopy. Spherical morphology was observed for the as-synthesised iron nanoparticles (FeNPs) and elemental analysis indicated iron with 17.31%. XRD studies revealed the broader peaks at 24°, 29°, 30°, and 35° 2θ for the as-synthesised iron nanoparticles indicating the nano sized particles. FT-IR spectra showed the bands at 3154 cm^{-1} (bioflocculant) and 3244 cm^{-1} (iron nanoparticles) representing the presence of hydroxyl (–OH) and amine ($–NH_2$) functional groups.

Keywords: Bioflocculant, Iron Nanoparticles, Characterization, Electron Microscopy, Green Synthesis.

polymers

MDPI

Article

Wastewater Treatment by a Polymeric Bioflocculant and Iron Nanoparticles Synthesized from a Bioflocculant

Nkosinathi Goodman Dlamini [1,*], Albertus Kotze Basson [1] and Rajasekhar VSR Pullabhotla [2,*]

[1] Department of Biochemistry and Microbiology, University of Zululand, Private Bag X1001, KwaDlangezwa 3886, South Africa; BassonA@unizulu.ac.za

[2] Department of Chemistry, University of Zululand, Private Bag X1001, KwaDlangezwa 3886, South Africa

* Correspondence: nathidlamini03@gmail.com (N.G.D.); PullabhotlaV@unizulu.ac.za (R.V.S.R.P.); Tel.: +27-359-026-155 (R.V.S.R.P.)

Received: 22 June 2020; Accepted: 14 July 2020; Published: 21 July 2020

check for updates

Abstract: Wastewater remains a global challenge. Various methods have been used in wastewater treatment, including flocculation. The aim of this study was to synthesize iron nanoparticles (FeNPs) using a polymeric bioflocculant and to evaluate its efficacy in the removal of pollutants in wastewater. A comparison between the efficiencies of the bioflocculant and iron nanoparticles was investigated. A scanning electron microscope (SEM) equipped with an energy-dispersive X-ray analyzer (EDX) and Fourier transform-infrared (FT-IR) spectroscopy were used to characterize the material. SEM-EDX analysis revealed the presence of elements such as O and C that were abundant in both samples, while FT-IR studies showed the presence of functional groups such as hydroxyl (–OH) and amine ($–NH_2$). Fe nanoparticles showed the best flocculation activity (FA) at 0.4 mg/mL dosage as opposed to that of the bioflocculant, which displayed the highest flocculation activity at 0.8 mg/mL, and both samples were found to be cation-dependent. When evaluated for heat stability and pH stability, FeNPs were found thermostable with 86% FA at 100 °C, while an alkaline pH of 11 favored FA with 93%. The bioflocculant flocculated poorly at high temperature and was found effective mostly at a pH of 7 with over 90% FA. FeNPs effectively removed BOD (biochemical oxygen demand) and COD (chemical oxygen demand) in all two wastewater samples from coal mine water and Mzingazi River water. Cytotoxicity results showed both FeNPs and the bioflocculant as nontoxic at concentrations up to 50 µL.

Keywords: biosafety; flocculation; removal efficiency; wastewater

Contents lists available at ScienceDirect

Physics and Chemistry of the Earth

journal homepage: http://www.elsevier.com/locate/pce

Biosynthesis of bioflocculant passivated copper nanoparticles, characterization and application

Nkosinathi Goodman Dlamini, PhD (Microbiology) [a,*], Albertus Kotze Basson, PhD [a], Viswanadha Srirama Rajasekhar Pullabhotla, PhD [c,**]

[a] Department of Biochemistry and Microbiology, University of Zululand, Private Bag X1001, KwaDlangezwa, 3886, South Africa
[c] Department of Chemistry, University of Zululand, South Africa

ARTICLE INFO

Keywords:
Bioflocculant
Synthesis
Characterization
Antimicrobial activity
Removal efficiency

ABSTRACT

There has been great progress in the 'green' chemistry approach for the synthesis of nanoparticles in recent years. Nanoparticles have gained special significance due to their unique properties. Herein we report a bioflocculant facilitated eco-friendly synthesis of copper nanoparticles (CuNPs). The copper nanoparticles were successfully synthesized through the reduction of copper sulphate (3 mM) solution by the bioflocculant (0.5 g). The synthesized nanoparticles were characterized by Scanning electron microscope equipped with elementary detector (SEM), X-ray diffractometer (XRD), Fourier Transform Infrared Spectrophotometer (FT-IR), Transmission electron microscopy (TEM), and UV spectroscope. CuNPs were applied in the treatment of both the domestic and industrial wastewater, removal of dyes and were confirmed for the antimicrobial effect against both Gram-negative and Gram-positive microorganisms. The synthesized nanoparticles showed great potential for industrial application when compared to the chemical flocculant. In comparison to $FeCl_3$ and bioflocculant, the nanoparticles were found to be effective in BOD and COD removal in coalmine wastewater samples. The highest flocculating activity and removal efficiency was observed at the lowest dosage of 0.2 mg/mL. Moreover, both the Minimal inhibitory concentration (MIC) and Minimal bactericidal concentration (MBC) were observed at the concertation of 12.5 µL.

Raw Data

Table 4.3: Copper nanoparticles dosage size, Optical density OD: 550 nm

Dosage (mg/mL)	1st reading	2nd reading	3rd reading	Average
0.2	0.172	0.139	0.152	**0.154**
0.4	0.794	0.123	0.031	**0.316**
0.6	0.171	0.230	0.760	**0.387**
0.8	0.311	0.472	0.748	**0.510**

Table 4.4: pH stability of CuNPs, OD: 550 nm

pH	1st reading	2nd reading	3rd reading	Average
3	0.116	0.877	0.891	**0.628**
4	0.727	0.905	0.915	**0.849**
5	0.826	0.914	0.783	**0.841**
6	0.162	0.364	0.170	**0.232**
7	0.070	0.131	0.074	**0.092**
8	0.159	0.155	0.158	**0.157**
9	0.043	0.628	0.652	**0.441**
10	0.509	0.709	0.682	**0.633**
11	0.476	0.657	0.702	**0.611**
12	0.699	0.693	0.492	**0.628**

Table 4.5: Effect of cations on flocculating activity of CuNPs, OD: 550 nm

Cations	1st reading	2nd reading	3rd reading	Average
Na^{+}	0.330	0.301	0.355	**0.328**
Li^{+}	0.059	0.052	0.084	**0.065**
K^{+}	0.031	0.077	0.134	**0.080**
Ca^{2+}	0.172	0.139	0.152	**0.154**
Mn^{2+}	0.065	0.042	0.121	**0.076**
Ba^{2+}	0.156	0.033	0.114	**0.067**
Fe^{3+}	0.223	0.457	0.393	**0.357**
Control	0.073	0.135	0.050	**0.086**

Table 4.6: Thermostability of CuNPs, OD: 550 nm

Temperature °C	1st reading	2nd reading	3rd reading	Average
50	0.194	0.137	0.168	**0.166**
60	0.143	0.211	0.094	**0.149**
70	0.131	0.072	0.143	**0.115**
80	0.208	0.108	0.146	**0.154**
90	0.226	0.066	0.156	**0.149**
100	0.300	0.164	0.200	**0.221**

Table 4.7: Effect of speed on flocculating activity of CuNPs, OD: 550 nm

Speed (rpm)	1st reading	2nd reading	3rd reading	Average
0	0.240	0.100	0.491	**0.277**
60	0.085	0.442	0.165	**0.231**
90	0.098	0.027	0.410	**0.178**
120	0.128	0.154	0.061	**0.114**
165	0.042	0.320	0.073	**0.145**
220	0.092	0.261	0.019	**0.124**

Table 4.8: Dyes removal efficiency by CuNPs, OD: 550 nm

Name of staining dye	1st reading	2nd reading	3rd reading	Average
Safranin	0.089	0.256	0.230	**0.192**
Carbol Fuchsine	0.268	0.077	0.184	**0.176**
Malachite green	0.072	0.048	0.161	**0.094**
Methylene blue	0.370	0.148	0.934	**0.484**

Table 5.7: Dosage size CuNPs, Optical density OD: 550 nm

Dosage (mg/mL)	1st reading	2nd reading	3rd reading	Average
0.2	0.173	0.139	0.153	**0.154**
0.4	0.792	0.125	0.031	**0.316**
0.6	0.171	0.232	0.758	**0.387**
0.8	0.311	0.472	0.748	**0.510**

Table 5.8: Flocculating efficiency of CuNPs compare to iron chloride and bioflocculant, OD: 550nm

Type of suspension		1st reading	2nd reading	3rd reading	Average
Kaolin clay	CuNPs	0.172	0.139	0.152	**0.154**
	$FeCl_3$	1.247	0.223	2.132	**1.201**
	Bioflocculant	0.468	0.210	0.265	**0.314**
Industrial	CuNPs	0.175	0.129	0.069	**0.124**
	$FeCl_3$	0.337	0.050	0.865	**0.417**
	Bioflocculant	0.191	0.796	0.733	**0.573**
Domestic	CuNPs	0.254	0.100	0.218	**0.190**
	$FeCl_3$	0.321	0.495	0.790	**0.535**
	Bioflocculant	1.761	0.156	0.967	**0.961**
Mine waste	CuNPs	0.112	0.047	0.031	**0.063**
	$FeCl_3$	0.195	2.598	0.645	**1.146**
	Bioflocculant	0.284	0.044	0.034	**0.121**

Table 5.9: Dyes removal by CuNPs, OD: 550 nm

Name of staining dye	1st reading	2nd reading	3rd reading	Average
Safranin	0.089	0.256	0.230	**0.192**
Carbol Fuchsine	0.268	0.077	0.184	**0.176**
Malachite green	0.072	0.048	0.161	**0.094**
Methylene blue	0.370	0.148	0.934	**0.484**

Table 7.4: Dosage size of FeNPs, OD: 550 nm

Dosage size (mg/mL)	1st reading	2nd reading	3rd reading	Average
0.2	0.550	0.373	0.809	**0.577**
0.4	0.440	0.180	0.698	**0.439**
0.6	0.956	0.739	0.314	**0.734**
0.8	0.718	0.559	0.705	**0.660**

Table 7.5: Cations effect for FeNPs, OD: 550 nm

Cations	1st reading	2nd reading	3rd reading	Average
Na^{+}	0.248	0.629	0.983	**0.620**
Li^{+}	0.859	0.889	0.337	**0.695**
K^{+}	0.950	0.962	0.867	**0.499**
Ca^{2+}	0.440	0.180	0.698	**0.439**
Mg^{2+}	0.357	0.783	0.357	**0.499**
Br^{2+}	0.954	0.794	0.104	**0.950**
Fe^{3+}	0.262	0.601	0.903	**0.588**
Control	0.073	0.135	0.050	**0.086**

Table 7.6: pH stability of FeNPs, OD: 550 nm

pH	1st reading	2nd reading	3rd reading	Average
3	0.116	0.877	0.891	**0.628**
4	0.727	0.905	0.915	**0.849**
5	0.826	0.914	0.783	**0.841**
6	0.162	0.364	0.170	**0.232**
7	0.070	0.131	0.074	**0.092**
8	0.159	0.155	0.158	**0.157**
9	0.043	0.628	0.652	**0.441**
10	0.509	0.709	0.682	**0.633**
11	0.476	0.657	0.702	**0.611**
12	0.699	0.693	0.492	**0.628**

Table 7.7: Thermostability of FeNPs, OD: 550 nm

Temperature °C	1st reading	2nd reading	3rd reading	Average
50	0.194	0.137	0.168	**0.166**
60	0.143	0.211	0.094	**0.149**
70	0.131	0.072	0.143	**0.115**
80	0.208	0.108	0.146	**0.154**
90	0.226	0.066	0.156	**0.149**
100	0.300	0.164	0.200	**0.221**

Table 8.1: Dosage effect of CuNPs, FeNPs and Fe@Cu core-shell, OD: 550 nm

Dosage (mg/mL)	**1st reading**	**2nd reading**	**3rd reading**	**Average**
0.2	0.172	0.139	0.152	**0.154**
0.4	0.794	0.123	0.031	**0.316**
0.6	0.171	0.230	0.760	**0.387**
0.8	0.311	0.472	0.748	**0.510**
Dosage size (mg/mL)	**1st reading**	**2nd reading**	**3rd reading**	**Average**
0.2	0.550	0.373	0.809	**0.577**
0.4	0.440	0.180	0.698	**0.439**
0.6	0.956	0.739	0.314	**0.734**
0.8	0.718	0.559	0.705	**0.660**
Dosage size (mg/mL)	**1st reading**	**2nd reading**	**3rd reading**	**Average**
0.2	0.058	0.070	0.045	**0.057**
0.4	0.061	0.051	0.072	**0.061**
0.6	0.067	0.061	0.106	**0.078**
0.8	0.153	0.126	0.141	**0.140**

Table 8.2: Cation effect of CuNPs, FeNPs and Fe@Cu core-shell, OD: 550 nm

Cations	**1st reading**	**2nd reading**	**3rd reading**	**Average**
Na^+	0.330	0.301	0.355	**0.328**
Ca^{2+}	0.172	0.139	0.152	**0.154**
Fe^{3+}	0.223	0.457	0.393	**0.357**
Control	0.073	0.135	0.050	**0.086**
Cations	**1st reading**	**2nd reading**	**3rd reading**	**Average**
Na^+	0.248	0.629	0.983	**0.620**
Ca^{2+}	0.440	0.180	0.698	**0.439**
Fe^{3+}	0.262	0.601	0.903	**0.588**
Control	0.073	0.135	0.050	**0.086**
Cations (S_3)	**1st reading**	**2nd reading**	**3rd reading**	**Average**

Na^{+}	0.112	0.194	0.100	**0.135**
Ca^{2+}	0.058	0.070	0.045	**0.043**
Fe^{3+}	0.083	0.082	0.057	**0.074**
Control	0.071	0.123	0.149	**0.114**

Table 8.3: pH effect of CuNPs, FeNPs and Fe@Cu core-shell, OD: 550 nm

pH	**1st reading**	**2nd reading**	**3rd reading**	**Average**
3	0.116	0.877	0.891	**0.628**
7	0.070	0.131	0.074	**0.092**
11	0.476	0.657	0.702	**0.611**
pH	**1st reading**	**2nd reading**	**3rd reading**	**Average**
3	0.116	0.877	0.891	**0.628**
7	0.070	0.131	0.074	**0.092**
11	0.476	0.657	0.702	**0.611**
pH	**1st reading**	**2nd reading**	**3rd reading**	**Average**
3	0.160	0.106	0.108	**0.124**
7	0.058	0.070	0.045	**0.057**
11	0.061	0.188	0.098	**0.116**

Table 8.4: Thermostability effect of CuNPs, FeNPs and Fe@Cu core-shell, OD: 550 nm

Temperature ℃	**1st reading**	**2nd reading**	**3rd reading**	**Average**
60	0.143	0.211	0.094	**0.149**
80	0.208	0.108	0.146	**0.154**
100	0.300	0.164	0.200	**0.221**
Temperature ℃	**1st reading**	**2nd reading**	**3rd reading**	**Average**
60	0.143	0.211	0.094	**0.149**
80	0.208	0.108	0.146	**0.154**
100	0.300	0.164	0.200	**0.221**
Temperature ℃	**1st reading**	**2nd reading**	**3rd reading**	**Average**
60	0.101	0.103	0.158	**0.257**
80	0.047	0.051	0.061	**0.053**
100	0.167	0.451	0.342	**0.320**

Table 8.5: Removal of dyes by CuNPs, FeNPs and Fe@Cu core-shell, OD: 550 nm

Name of staining dye (CuNPs)	**1st reading**	**2nd reading**	**3rd reading**	**Average**
Safranin	0.089	0.256	0.230	**0.192**
Carbol Fuchsine	0.268	0.077	0.184	**0.176**
Malachite green	0.072	0.048	0.161	**0.094**
Methylene blue	0.370	0.148	0.934	**0.484**
Name of staining dye (FeNPs)	**1st reading**	**2nd reading**	**3rd reading**	**Average**
Safranin	0.112	0.120	0.107	**0.113**
Methylene orange	0.148	0.181	0.125	**0.151**
Malachite green	0.409	0.142	0.112	**0.221**
Methylene blue	0.408	0.315	0.386	**0.369**
Name of staining dye Fe@Cu core-shell	**1st reading**	**2nd reading**	**3rd reading**	**Average**
Safranin	0.143	0.161	0.236	**0.329**
Methylene orange	0.117	0.102	0.104	**0.107**
Malachite green	0.157	0.075	0.230	**0.154**
Methylene blue	0.163	0.229	0.287	**0.226**

Table 8.6: Flocculating efficiency of CuNPs, FeNPs and Fe@Cu core-shell OD: 550nm

Type of suspension		**1st reading**	**2nd reading**	**3rd reading**	**Average**
Kaolin clay	CuNPs	0.172	0.139	0.152	**0.154**
	FeNPs	1.247	0.223	2.132	**1.201**
	Fe@Cu core-shell	0.468	0.210	0.265	**0.314**
Industrial	CuNPs	0.175	0.129	0.069	**0.124**
	FeNPs	0.337	0.050	0.865	**0.417**
	Fe@Cu core-shell	0.191	0.796	0.733	**0.573**
Domestic	CuNPs	0.254	0.100	0.218	**0.190**
	FeNPs	0.321	0.495	0.790	**0.535**
	Fe@Cu core-shell	1.761	0.156	0.967	**0.961**

Mine waste	CuNPs	0.112	0.047	0.031	**0.063**
	FeNPs	0.195	2.598	0.645	**1.146**
	Fe@Cu core-shell	0.284	0.044	0.034	**0.121**

Table 9.1: Fe@Cu core-shell nanoparticles dosage size on flocculation activity, Optical density OD: 550 nm

Dosage size (mg/mL)	**1st reading**	**2nd reading**	**3rd reading**	**Average**
0.2	0.049	0.059	0.010	**0.039**
0.4	0.043	0.010	0.122	**0.058**
0.6	0.188	0.008	0.003	**0.066**
0.8	0.082	0.067	0.091	**0.080**

Table 9.2: Cations Fe@Cu core-shell nanoparticles effect, Optical density OD: 550 nm

Cations (S_3)	**1st reading**	**2nd reading**	**3rd reading**	**Average**
Na^+	0.112	0.194	0.100	**0.135**
Ca^{2+}	0.058	0.070	0.045	**0.043**
Fe^{3+}	0.083	0.082	0.057	**0.074**
Control	0.071	0.123	0.149	**0.114**

Table 9.3: pH effect on Fe@Cu core-shell nanoparticles, Optical density OD: 550 nm

pH	**1st reading**	**2nd reading**	**3rd reading**	**Average**
3	0.160	0.106	0.108	**0.124**
7	0.058	0.070	0.045	**0.057**
11	0.061	0.188	0.098	**0.116**

Table 9.4: Fe@Cu core-shell nanoparticles thermostability, Optical density OD: 550 nm

Temperature °C	**1st reading**	**2nd reading**	**3rd reading**	**Average**
60	0.101	0.103	0.158	**0.257**
80	0.047	0.051	0.061	**0.053**
100	0.167	0.451	0.342	**0.320**

Table 9.5: Dye removal efficiency by Fe@Cu core-shell nanoparticles, OD: 550 nm

Name of staining dye	**1st reading**	**2nd reading**	**3rd reading**	**Average**
Safranin	0.112	0.120	0.107	**0.113**
Methylene orange	0.148	0.181	0.125	**0.151**
Malachite green	0.409	0.142	0.112	**0.221**
Methylene blue	0.408	0.315	0.386	**0.369**

Table 10.5: Dosage effect on flocculation activity of (S1, S2 and S3), Optical density OD: 550 nm

Dosage size (mg/mL) (S3)	**1st reading**	**2nd reading**	**3rd reading**	**Average**
0.2	0.049	0.059	0.010	**0.039**
0.4	0.043	0.010	0.122	**0.058**
0.6	0.188	0.008	0.003	**0.066**
0.8	0.082	0.067	0.091	**0.080**
Dosage size (mg/mL) (S2)	**1st reading**	**2nd reading**	**3rd reading**	**Average**
0.2	0.054	0.069	0.064	**0.062**
0.4	0.017	0.053	0.064	**0.045**
0.6	0.092	0.173	0.230	**0.165**
0.8	0.177	0.203	0.189	**0.443**
Dosage size (mg/mL) (S1)	**1st reading**	**2nd reading**	**3rd reading**	**Average**
0.2	0.058	0.070	0.045	**0.057**
0.4	0.061	0.051	0.072	**0.061**
0.6	0.067	0.061	0.106	**0.078**
0.8	0.153	0.126	0.141	**0.140**

Table 10.6: pH effect on flocculation activity of (S1, S2 and S3), Optical density OD: 550 nm

pH (S3)	**1st reading**	**2nd reading**	**3rd reading**	**Average**
3	0.092	0.164	0.245	**0.167**
7	0.049	0.059	0.010	**0.069**
11	0.068	0.273	0.133	**0.158**
pH (S2)	**1st reading**	**2nd reading**	**3rd reading**	**Average**
3	0.018	0.047	0.065	**0.043**
7	0.054	0.069	0.064	**0.062**
11	0.080	0.106	0.175	**0.120**
pH (S1)	**1st reading**	**2nd reading**	**3rd reading**	**Average**
3	0.160	0.106	0.108	**0.124**
7	0.058	0.070	0.045	**0.057**
11	0.061	0.188	0.098	**0.116**

Table 10.7: Cation effect on flocculation activity of (S1, S2 and S3), Optical density OD: 550 nm

Cations (S_3)	**1st reading**	**2nd reading**	**3rd reading**	**Average**
Na^+	0.090	0.081	0.106	**0.092**
Ca^{2+}	0.049	0.059	0.010	**0.039**
Fe^{3+}	0.125	0.050	0.084	**0.086**
Control	0.141	0.164	0.101	**0.135**
Cations (S_3)	**1st reading**	**2nd reading**	**3rd reading**	**Average**
Na^+	0.201	0.140	0.074	**0.138**
Ca^{2+}	0.054	0.069	0.064	**0.062**
Fe^{3+}	0.170	0.123	0.152	**0.148**
Control	0.113	0.115	0.120	**0.116**
Cations (S_1)	**1st reading**	**2nd reading**	**3rd reading**	**Average**
Na^+	0.112	0.194	0.100	**0.135**
Ca^{2+}	0.058	0.070	0.045	**0.043**
Fe^{3+}	0.083	0.082	0.057	**0.074**
Control	0.071	0.123	0.149	**0.114**

Table 10.8: Heat effect on flocculation activity of (S1, S2 and S3), Optical density OD: 550 nm

Temperature ℃ (S3)	**1st reading**	**2nd reading**	**3rd reading**	**Average**
60	0.127	0.003	0.140	**0.090**
80	0.079	0.104	0.057	**0.080**
100	0.254	0.202	0.052	**0.169**
Temperature ℃ (S2)	**1st reading**	**2nd reading**	**3rd reading**	**Average**
60	0.096	0.117	0.156	**0.123**
80	0.191	0.047	0.158	**0.132**
100	0.189	0.049	0.001	**0.079**
Temperature ℃ (S1)	**1st reading**	**2nd reading**	**3rd reading**	**Average**
60	0.101	0.103	0.158	**0.257**
80	0.047	0.051	0.061	**0.053**
100	0.167	0.451	0.342	**0.320**

Table 10.9: Dye removal efficiency by (S1, S2 and S3), Optical density OD: 550 nm

Name of staining dye (S3)	**1st reading**	**2nd reading**	**3rd reading**	**Average**
Safranin	0.143	0.161	0.236	**0.329**
Methylene orange	0.117	0.102	0.104	**0.107**
Malachite green	0.157	0.075	0.230	**0.154**
Methylene blue	0.163	0.229	0.287	**0.226**
Name of staining dye (S2)	**1st reading**	**2nd reading**	**3rd reading**	**Average**
Safranin	0.120	0.150	0.143	**0.137**
Methylene orange	0.186	0.217	0.114	**0.172**
Malachite green	0.103	0.090	0.139	**0.110**
Methylene blue	0.342	0.355	0.403	**0.366**
Name of staining dye	**1st reading**	**2nd reading**	**3rd reading**	**Average**

(S1)				
Safranin	0.112	0.120	0.107	**0.113**
Methylene orange	0.148	0.181	0.125	**0.151**
Malachite green	0.409	0.142	0.112	**0.221**
Methylene blue	0.408	0.315	0.386	**0.369**

Chapter 14 All References

ABD EL-SALAM, A. E., ABD-EL-HALEEM, D., YOUSSEF, A. S., ZAKI, S., ABU-ELREESH, G. & EL-ASSAR, S. A. 2017. Isolation, characterization, optimization, immobilization and batch fermentation of bioflocculant produced by Bacillus aryabhattai strain PSK1. *Journal of Genetic Engineering and Biotechnology*, 15**,** 335-344.

ABDEL-HALIM, E. & AL-DEYAB, S. S. 2011. Removal of heavy metals from their aqueous solutions through adsorption onto natural polymers. *Carbohydrate Polymers*, 84**,** 454-458.

AGUNBIADE, M., POHL, C. & ASHAFA, O. 2018. Bioflocculant production from Streptomyces platensis and its potential for river and waste water treatment. *Brazilian Journal of Microbiology*.

BAN, Z., BARNAKOV, Y. A., LI, F., GOLUB, V. O. & O'CONNOR, C. J. 2005. The synthesis of core–shell iron@ gold nanoparticles and their characterization. *Journal of Materials Chemistry,* 15**,** 4660-4662.

BISH, D. L. & POST, J. E. 2018. *Modern powder diffraction*, Walter de Gruyter GmbH & Co KG.

CRINI, G. 2005. Recent developments in polysaccharide-based materials used as adsorbents in wastewater treatment. *Progress in polymer science,* 30**,** 38-70.

DANIELS, A. N. & SINGH, M. 2019. Sterically stabilized siRNA: gold nanocomplexes enhance c-MYC silencing in a breast cancer cell model. *Nanomedicine*.

DAVIS, A. P., SHOKOUHIAN, M., SHARMA, H. & MINAMI, C. 2006. Water quality improvement through bioretention media: Nitrogen and phosphorus removal. *Water Environment Research,* 78**,** 284-293.

DLAMINI, N. G., BASSON, A. K. & PULLABHOTLA, V. S. R. 2019a. Biosynthesis and Characterization of Copper Nanoparticles Using a Bioflocculant Extracted from *Alcaligenis faecalis* HCB2. *Advanced Science Engineering and Medicine,* 11**,** 1-7.

DLAMINI, N. G., BASSON, A. K. & PULLABHOTLA, V. S. R. 2019b. Optimization and Application of Bioflocculant Passivated Copper Nanoparticles in the Wastewater Treatment. *International Journal of Environmental Research and Public Health,* 16**,** 2185.

DLAMINI, N. G., BASSON, A. K., SHANDU, J. S. E., MAVUSO, S. S. & PULLABHOTLA, V. S. R. 2020. Biosynthesis, Characterization, and Application of Iron Nanoparticles: in Dye Removal and as Antimicrobial Agent. *Water, Air, & Soil Pollution,* 231**,** 1-10.

ELOFF, J. N. 1998. A sensitive and quick microplate method to determine the minimal inhibitory concentration of plant extracts for bacteria. *Planta medica,* 64**,** 711-713.

EXLEY, C., KORCHAZHKINA, O., JOB, D., STREKOPYTOV, S., POLWART, A. & CROME, P. 2006. Non-invasive therapy to reduce the body burden of aluminium in Alzheimer's disease. *Journal of Alzheimer's Disease,* 10**,** 17-24.

GONG, W.-X., WANG, S.-G., SUN, X.-F., LIU, X.-W., YUE, Q.-Y. & GAO, B.-Y. 2008. Bioflocculant production by culture of Serratia ficaria and its application in wastewater treatment. *Bioresource technology,* 99**,** 4668-4674.

KALE, G., AURAS, R., SINGH, S. P. & NARAYAN, R. 2007. Biodegradability of polylactide bottles in real and simulated composting conditions. *Polymer Testing,* 26**,** 1049-1061.

KARTHIGA DEVI, K. & NATARAJAN, K. A. 2015. Production and characterization of bioflocculants for mineral processing applications. *International Journal of Mineral Processing,* 137**,** 15-25.

KOLÁŘ, M., URBÁNEK, K. & LÁTAL, T. 2001. Antibiotic selective pressure and development of bacterial resistance. *International journal of antimicrobial agents,* 17**,** 357-363.

KUMAR, M. & PURI, A. 2012. A review of permissible limits of drinking water. *Indian journal of occupational and environmental medicine,* 16**,** 40.

LI, O., LU, C., LIU, A., ZHU, L., WANG, P.-M., QIAN, C.-D., JIANG, X.-H. & WU, X.-C. 2013. Optimization and characterization of polysaccharide-based bioflocculant produced by Paenibacillus elgii B69 and its application in wastewater treatment. *Bioresource technology,* 134**,** 87-93.

LIN, Z.-Z., HUANG, C.-L., HUANG, Z. & ZHEN, W.-K. 2017. Surface/interface influence on specific heat capacity of solid, shell and core-shell nanoparticles. *Applied Thermal Engineering,* 127**,** 884-888.

LU, H., WANG, J., WANG, T., WANG, N., BAO, Y. & HAO, H. 2017. Crystallization techniques in wastewater treatment: An overview of applications. *Chemosphere,* 173**,** 474-484.

LU, Z.-H., LI, J., ZHU, A., YAO, Q., HUANG, W., ZHOU, R., ZHOU, R. & CHEN, X. 2013. Catalytic hydrolysis of ammonia borane via magnetically recyclable copper iron

nanoparticles for chemical hydrogen storage. *International journal of hydrogen energy,* 38**,** 5330-5337.

MALIEHE, S., SHANDU, S. J. & BASSON, K. A. 2015. The antibacterial and antidiarreal activities of the crude methanolic Syzygium cordatum [S. Ncik, 48 (UZ)] fruit pulp and seed extracts. *Journal of Medicinal Plants Research,* 9**,** 884-891.

MALIEHE, T. S., BASSON, A. K. & DLAMINI, N. G. 2019. Removal of Pollutants in Mine Wastewater by a Non-Cytotoxic Polymeric Bioflocculant from Alcaligenes faecalis HCB2. *International journal of environmental research and public health,* 16**,** 4001.

MITTAL, H., MISHRA, S. B., MISHRA, A., KAITH, B., JINDAL, R. & KALIA, S. 2013. Preparation of poly (acrylamide-co-acrylic acid)-grafted gum and its flocculation and biodegradation studies. *Carbohydrate polymers,* 98**,** 397-404.

MOUSSAVI, G. & MAHMOUDI, M. 2009. Removal of azo and anthraquinone reactive dyes from industrial wastewaters using MgO nanoparticles. *Journal of hazardous materials,* 168**,** 806-812.

PATIL, S. V., PATIL, C. D., SALUNKE, B. K., SALUNKHE, R. B., BATHE, G. & PATIL, D. M. 2011. Studies on characterization of bioflocculant exopolysaccharide of Azotobacter indicus and its potential for wastewater treatment. *Applied biochemistry and biotechnology,* 163**,** 463-472.

QU, X., ALVAREZ, P. J. & LI, Q. 2013. Applications of nanotechnology in water and wastewater treatment. *Water research,* 47**,** 3931-3946.

RUPARELIA, J. P., CHATTERJEE, A. K., DUTTAGUPTA, S. P. & MUKHERJI, S. 2008. Strain specificity in antimicrobial activity of silver and copper nanoparticles. *Acta biomaterialia,* 4**,** 707-716.

SALEHIZADEH, H. & SHOJAOSADATI, S. 2001. Extracellular biopolymeric flocculants: recent trends and biotechnological importance. *Biotechnology advances,* 19**,** 371-385.

SHAHWAN, T., SIRRIAH, S. A., NAIRAT, M., BOYACı, E., EROĞLU, A. E., SCOTT, T. B. & HALLAM, K. R. 2011. Green synthesis of iron nanoparticles and their application as a Fenton-like catalyst for the degradation of aqueous cationic and anionic dyes. *Chemical Engineering Journal,* 172**,** 258-266.

SHIH, I., VAN, Y., YEH, L., LIN, H. & CHANG, Y. 2001. Production of a biopolymer flocculant from Bacillus licheniformis and its flocculation properties. *Bioresource technology,* 78**,** 267-272.

SINGH, R. P., KARMAKAR, G., RATH, S., KARMAKAR, N., PANDEY, S., TRIPATHY, T., PANDA, J., KANAN, K., JAIN, S. & LAN, N. 2000. Biodegradable drag reducing agents and flocculants based on polysaccharides: materials and applications. *Polymer Engineering & Science,* 40**,** 46-60.

SONDI, I. & SALOPEK-SONDI, B. 2004. Silver nanoparticles as antimicrobial agent: a case study on E. coli as a model for Gram-negative bacteria. *Journal of colloid and interface science,* 275**,** 177-182.

SUN, J., ZHANG, X., MIAO, X. & ZHOU, J. 2012. Preparation and characteristics of bioflocculants from excess biological sludge. *Bioresource Technology,* 126**,** 362-366.

XIA, S., ZHANG, Z., WANG, X., YANG, A., CHEN, L., ZHAO, J., LEONARD, D. & JAFFREZIC-RENAULT, N. 2008. Production and characterization of a bioflocculant by Proteus mirabilis TJ-1. *Bioresource technology,* 99**,** 6520-6527.

XIA, X., LAN, S., LI, X., XIE, Y., LIANG, Y., YAN, P., CHEN, Z. & XING, Y. 2018. Characterization and coagulation-flocculation performance of a composite flocculant in high-turbidity drinking water treatment. *Chemosphere,* 206**,** 701-708.

YU, X., LI, J., SHI, T., CHENG, C., LIAO, G., FAN, J., LI, T. & TANG, Z. 2017. A green approach of synthesizing of Cu-Ag core-shell nanoparticles and their sintering behavior for printed electronics. *Journal of Alloys and Compounds,* 724**,** 365-372.

ZAKI, S. A., ELKADY, M. F., FARAG, S. & ABD-EL-HALEEM, D. 2013. Characterization and flocculation properties of a carbohydrate bioflocculant from a newly isolated Bacillus velezensis 40B. *Journal of environmental biology,* 34**,** 51.

ZHU, C., CHEN, C., ZHAO, L., ZHANG, Y., YANG, J., SONG, L. & YANG, S. 2012. Bioflocculant produced by Chlamydomonas reinhardtii. *Journal of applied phycology,* 24**,** 1245-1251.

ABD EL-SALAM, A. E., ABD-EL-HALEEM, D., YOUSSEF, A. S., ZAKI, S., ABU-ELREESH, G. & EL-ASSAR, S. A. 2017. Isolation, characterization, optimization, immobilization and batch fermentation of bioflocculant produced by Bacillus aryabhattai strain PSK1. *Journal of Genetic Engineering and Biotechnology,* 15**,** 335-344.

ABDEL-HALIM, E. & AL-DEYAB, S. S. 2011. Removal of heavy metals from their aqueous solutions through adsorption onto natural polymers. *Carbohydrate Polymers,* 84**,** 454-458.

AGUNBIADE, M., POHL, C. & ASHAFA, O. 2018. Bioflocculant production from Streptomyces platensis and its potential for river and waste water treatment. *Brazilian Journal of Microbiology*.

BAN, Z., BARNAKOV, Y. A., LI, F., GOLUB, V. O. & O'CONNOR, C. J. 2005. The synthesis of core–shell iron@ gold nanoparticles and their characterization. *Journal of Materials Chemistry,* 15**,** 4660-4662.

BHAUMIK, A., HAQUE, A., KARNATI, P., TAUFIQUE, M. F. N., PATEL, R. & GHOSH, K. 2014. Copper oxide based nanostructures for improved solar cell efficiency. *Thin Solid Films,* 572**,** 126–133.

BISH, D. L. & POST, J. E. 2018. *Modern powder diffraction*, Walter de Gruyter GmbH & Co KG.

CRINI, G. 2005. Recent developments in polysaccharide-based materials used as adsorbents in wastewater treatment. *Progress in polymer science,* 30**,** 38-70.

DANIELS, A. N. & SINGH, M. 2019. Sterically stabilized siRNA: gold nanocomplexes enhance c-MYC silencing in a breast cancer cell model. *Nanomedicine*.

DAVIS, A. P., SHOKOUHIAN, M., SHARMA, H. & MINAMI, C. 2006. Water quality improvement through bioretention media: Nitrogen and phosphorus removal. *Water Environment Research,* 78**,** 284-293.

DLAMINI, N. G., BASSON, A. K. & PULLABHOTLA, V. 2020a. Optimization of Fe@Cu Core–Shell Nanoparticle Synthesis, Characterization, and Application in Dye Removal andWastewater Treatment. *Catalysts,* 10.

DLAMINI, N. G., BASSON, A. K. & PULLABHOTLA, V. S. R. 2019a. Biosynthesis and Characterization of Copper Nanoparticles Using a Bioflocculant Extracted from *Alcaligenis faecalis* HCB2. *Advanced Science Engineering and Medicine,* 11**,** 1-7.

DLAMINI, N. G., BASSON, A. K. & PULLABHOTLA, V. S. R. 2019b. Optimization and Application of Bioflocculant Passivated Copper Nanoparticles in the Wastewater Treatment. *International Journal of Environmental Research and Public Health,* 16**,** 2185.

DLAMINI, N. G., BASSON, A. K., SHANDU, J. S. E., MAVUSO, S. S. & PULLABHOTLA, V. S. R. 2020b. Biosynthesis, Characterization, and Application of Iron Nanoparticles: in Dye Removal and as Antimicrobial Agent. *Water, Air, & Soil Pollution,* 231**,** 1-10.

ELOFF, J. N. 1998. A sensitive and quick microplate method to determine the minimal inhibitory concentration of plant extracts for bacteria. *Planta medica,* 64**,** 711-713.

EXLEY, C., KORCHAZHKINA, O., JOB, D., STREKOPYTOV, S., POLWART, A. & CROME, P. 2006. Non-invasive therapy to reduce the body burden of aluminium in Alzheimer's disease. *Journal of Alzheimer's Disease,* 10**,** 17-24.

GONG, W.-X., WANG, S.-G., SUN, X.-F., LIU, X.-W., YUE, Q.-Y. & GAO, B.-Y. 2008. Bioflocculant production by culture of Serratia ficaria and its application in wastewater treatment. *Bioresource technology,* 99**,** 4668-4674.

IRAVANI, S., KORBEKANDI, H., MIRMOHAMMADI, S. V. & ZOLFAGHARI, B. 2014. Synthesis of silver nanoparticles: chemical, physical and biological methods. *Research in Pharmacetutical Science,* 9**,** 385-406.

KALE, G., AURAS, R., SINGH, S. P. & NARAYAN, R. 2007. Biodegradability of polylactide bottles in real and simulated composting conditions. *Polymer Testing,* 26**,** 1049-1061.

KARTHIGA DEVI, K. & NATARAJAN, K. A. 2015. Production and characterization of bioflocculants for mineral processing applications. *International Journal of Mineral Processing,* 137**,** 15-25.

KAUR, P., THAKUR, R., MALWAL, H., MANUJA, A. & CHAUDHURY, A. 2018. Biosynthesis of biocompatible and recyclable silver/iron and gold/iron core-shell nanoparticles for water purification technology. *Biocatalysis and Agricultural Biotechnology,* 14**,** 189-197.

KHATAMI, M., ALIJANI, H., NEJAD, M. & VARMA, R. 2018. Core@shell Nanoparticles: Greener Synthesis Using Natural Plant Products. *Applied Sciences,* 8**,** 411.

KOLÁŘ, M., URBÁNEK, K. & LÁTAL, T. 2001. Antibiotic selective pressure and development of bacterial resistance. *International journal of antimicrobial agents,* 17**,** 357-363.

KUMAR, M. & PURI, A. 2012. A review of permissible limits of drinking water. *Indian journal of occupational and environmental medicine,* 16**,** 40.

LI, O., LU, C., LIU, A., ZHU, L., WANG, P.-M., QIAN, C.-D., JIANG, X.-H. & WU, X.-C. 2013. Optimization and characterization of polysaccharide-based bioflocculant

produced by Paenibacillus elgii B69 and its application in wastewater treatment. *Bioresource technology,* 134**,** 87-93.

LIN, Z.-Z., HUANG, C.-L., HUANG, Z. & ZHEN, W.-K. 2017. Surface/interface influence on specific heat capacity of solid, shell and core-shell nanoparticles. *Applied Thermal Engineering,* 127**,** 884-888.

LU, H., WANG, J., WANG, T., WANG, N., BAO, Y. & HAO, H. 2017. Crystallization techniques in wastewater treatment: An overview of applications. *Chemosphere,* 173**,** 474-484.

LU, Z.-H., LI, J., ZHU, A., YAO, Q., HUANG, W., ZHOU, R., ZHOU, R. & CHEN, X. 2013. Catalytic hydrolysis of ammonia borane via magnetically recyclable copper iron nanoparticles for chemical hydrogen storage. *International journal of hydrogen energy,* 38**,** 5330-5337.

MALIEHE, S., SHANDU, S. J. & BASSON, K. A. 2015. The antibacterial and antidiarreal activities of the crude methanolic Syzygium cordatum [S. Ncik, 48 (UZ)] fruit pulp and seed extracts. *Journal of Medicinal Plants Research,* 9**,** 884-891.

MALIEHE, T. S., BASSON, A. K. & DLAMINI, N. G. 2019. Removal of Pollutants in Mine Wastewater by a Non-Cytotoxic Polymeric Bioflocculant from Alcaligenes faecalis HCB2. *International journal of environmental research and public health,* 16**,** 4001.

MITTAL, H., MISHRA, S. B., MISHRA, A., KAITH, B., JINDAL, R. & KALIA, S. 2013. Preparation of poly (acrylamide-co-acrylic acid)-grafted gum and its flocculation and biodegradation studies. *Carbohydrate polymers,* 98**,** 397-404.

MOUSSAVI, G. & MAHMOUDI, M. 2009. Removal of azo and anthraquinone reactive dyes from industrial wastewaters using MgO nanoparticles. *Journal of hazardous materials,* 168**,** 806-812.

NOMOEV, A. V., BARDAKHANOV, S., P, SCHREIBER, M., BAZAROVA, D. G., ROMANOV, N. A., BALDANOV, B. B., RADNAEV, B. R. & SYZRANTSEV, V. V. 2015. Structure and mechanism of the formation of core–shell nanoparticles obtained through a one-step gas-phase synthesis by electron beam evaporation. *BEILSTEIN JOURNAL OF NANOTECHNOLOGY,* 6**,** 874–880.

PATIL, S. V., PATIL, C. D., SALUNKE, B. K., SALUNKHE, R. B., BATHE, G. & PATIL, D. M. 2011. Studies on characterization of bioflocculant exopolysaccharide of Azotobacter indicus and its potential for wastewater treatment. *Applied biochemistry and biotechnology,* 163**,** 463-472.

QU, X., ALVAREZ, P. J. & LI, Q. 2013. Applications of nanotechnology in water and wastewater treatment. *Water research,* 47**,** 3931-3946.

RUPARELIA, J. P., CHATTERJEE, A. K., DUTTAGUPTA, S. P. & MUKHERJI, S. 2008. Strain specificity in antimicrobial activity of silver and copper nanoparticles. *Acta biomaterialia,* 4**,** 707-716.

SALEHIZADEH, H. & SHOJAOSADATI, S. 2001. Extracellular biopolymeric flocculants: recent trends and biotechnological importance. *Biotechnology advances,* 19**,** 371-385.

SHAHWAN, T., SIRRIAH, S. A., NAIRAT, M., BOYACı, E., EROĞLU, A. E., SCOTT, T. B. & HALLAM, K. R. 2011. Green synthesis of iron nanoparticles and their application as a Fenton-like catalyst for the degradation of aqueous cationic and anionic dyes. *Chemical Engineering Journal,* 172**,** 258-266.

SHIH, I., VAN, Y., YEH, L., LIN, H. & CHANG, Y. 2001. Production of a biopolymer flocculant from Bacillus licheniformis and its flocculation properties. *Bioresource technology,* 78**,** 267-272.

SINGH, R. P., KARMAKAR, G., RATH, S., KARMAKAR, N., PANDEY, S., TRIPATHY, T., PANDA, J., KANAN, K., JAIN, S. & LAN, N. 2000. Biodegradable drag reducing agents and flocculants based on polysaccharides: materials and applications. *Polymer Engineering & Science,* 40**,** 46-60.

SONDI, I. & SALOPEK-SONDI, B. 2004. Silver nanoparticles as antimicrobial agent: a case study on E. coli as a model for Gram-negative bacteria. *Journal of colloid and interface science,* 275**,** 177-182.

SUN, J., ZHANG, X., MIAO, X. & ZHOU, J. 2012. Preparation and characteristics of bioflocculants from excess biological sludge. *Bioresource Technology,* 126**,** 362-366.

VASIREDDI, R., PAUL, R. & MITRA, A. K. 2013. Green Synthesis of AgcoreCushell Nanoparticles: Structural and Optical Characterization. *Journal of Green Science and Technology,* 1**,** 85-90.

VLASOVA, I. I., KAPRALOV, A. A., MICHAEL, Z. P., BURKERT, S. C., SHURIN, M. R., STAR, A., SHVEDOVA, A. A. & KAGAN, V. E. 2016. Enzymatic Oxidative Biodegradation of Nanoparticles: Mechanisms, Significance and Applications. *Toxicology and Applied Pharmocology,* 299**,** 58-69.

XIA, S., ZHANG, Z., WANG, X., YANG, A., CHEN, L., ZHAO, J., LEONARD, D. & JAFFREZIC-RENAULT, N. 2008. Production and characterization of a bioflocculant by Proteus mirabilis TJ-1. *Bioresource technology,* 99**,** 6520-6527.

XIA, X., LAN, S., LI, X., XIE, Y., LIANG, Y., YAN, P., CHEN, Z. & XING, Y. 2018. Characterization and coagulation-flocculation performance of a composite flocculant in high-turbidity drinking water treatment. *Chemosphere,* 206**,** 701-708.

YU, X., LI, J., SHI, T., CHENG, C., LIAO, G., FAN, J., LI, T. & TANG, Z. 2017. A green approach of synthesizing of Cu-Ag core-shell nanoparticles and their sintering behavior for printed electronics. *Journal of Alloys and Compounds,* 724**,** 365-372.

ZAKI, S. A., ELKADY, M. F., FARAG, S. & ABD-EL-HALEEM, D. 2013. Characterization and flocculation properties of a carbohydrate bioflocculant from a newly isolated Bacillus velezensis 40B. *Journal of environmental biology,* 34**,** 51.

ZHANG, L., PETERSEN, E. J., HABTESELASSIE, M. Y., MAO, L. & HUANG, Q. 2013. Degradation of multiwall carbon nanotubes by bacteria. *Environ. Pollut,* 181**,** 335-339.

ZHU, C., CHEN, C., ZHAO, L., ZHANG, Y., YANG, J., SONG, L. & YANG, S. 2012. Bioflocculant produced by Chlamydomonas reinhardtii. *Journal of applied phycology,* 24**,** 1245-1251.

ABD EL-SALAM, A. E., ABD-EL-HALEEM, D., YOUSSEF, A. S., ZAKI, S., ABU-ELREESH, G. & EL-ASSAR, S. A. 2017. Isolation, characterization, optimization, immobilization and batch fermentation of bioflocculant produced by Bacillus aryabhattai strain PSK1. *Journal of Genetic Engineering and Biotechnology,* 15**,** 335-344.

ABDEL-HALIM, E. & AL-DEYAB, S. S. 2011. Removal of heavy metals from their aqueous solutions through adsorption onto natural polymers. *Carbohydrate Polymers,* 84**,** 454-458.

ABDULLAH, M., ROSLAN, A., KAMARULZAMAN, M. & ERAT, M. Colloids removal from water resources using natural coagulant: Acacia auriculiformis. AIP Conference Proceedings, 2017. AIP Publishing, 020243.

ADEBAYO-TAYO, B. C. & ADEBAMI, G. E. 2017. Production, Characterization and Effect of Cultural Condition on Bioflocculant Produced by Alcaligenes aquatilis AP4. *Journal of Applied Life Sciences International,* 14**,** 1-12.

AGUIRRE, M. E., RODRÍGUEZ, H. B., SAN ROMÁN, E., FELDHOFF, A. & GRELA, M. A. 2011. Ag@ ZnO core–shell nanoparticles formed by the timely reduction of Ag+ ions and zinc acetate hydrolysis in N, N-dimethylformamide: mechanism of growth and photocatalytic properties. *The Journal of Physical Chemistry C,* 115**,** 24967-24974.

AGUNBIADE, M., POHL, C. & ASHAFA, O. 2018. Bioflocculant production from Streptomyces platensis and its potential for river and waste water treatment. *Brazilian Journal of Microbiology*.

ALI, H. 2010. Biodegradation of Synthetic Dyes—A Review. *Water, Air, & Soil Pollution,* 213**,** 251-273.

ALJUBOORI, A. H. R., IDRIS, A., AL-JOUBORY, H. H. R., UEMURA, Y. & ABUBAKAR, B. I. 2015. Flocculation behavior and mechanism of bioflocculant produced by Aspergillus flavus. *Journal of environmental management,* 150**,** 466-471.

ALLAFCHIAN, A., JALALI, S. A. H., BAHRAMIAN, H. & AHMADVAND, H. 2016. Preparation, characterization, and antibacterial activity of NiFe2O4/PAMA/Ag–TiO2 nanocomposite. *Journal of Magnetism and Magnetic Materials,* 404**,** 14-20.

AMOURI, H., DESMARETS, C. & MOUSSA, J. 2012. Confined nanospaces in metallocages: guest molecules, weakly encapsulated anions, and catalyst sequestration. *Chemical reviews,* 112**,** 2015-2041.

ANLIKER, R. 1977. Color chemistry and the environment. *Ecotoxicology and environmental safety,* 1**,** 211-237.

ASHAJYOTHI, C., HARISH, K. H., DUBEY, N. & CHANDRAKANTH, R. K. 2016. Antibiofilm activity of biogenic copper and zinc oxide nanoparticles-antimicrobials collegiate against multiple drug resistant bacteria: a nanoscale approach. *Journal of Nanostructure in Chemistry,* 6**,** 329-341.

ASTEFANEI, A., NÚÑEZ, O. & GALCERAN, M. T. 2015. Characterisation and determination of fullerenes: a critical review. *Analytica chimica acta,* 882**,** 1-21.

BABES, L., DENIZOT, B., TANGUY, G., LE JEUNE, J. J. & JALLET, P. 1999. Synthesis of iron oxide nanoparticles used as MRI contrast agents: a parametric study. *Journal of colloid and interface science,* 212**,** 474-482.

BAE, J.-S. & FREEMAN, H. S. 2007. Aquatic toxicity evaluation of new direct dyes to the Daphnia magna. *Dyes and Pigments,* 73**,** 81-85.

BAHADAR, H., MAQBOOL, F., NIAZ, K. & ABDOLLAHI, M. 2016. Toxicity of nanoparticles and an overview of current experimental models. *Iranian biomedical journal,* 20**,** 1.

BALAKRISHNAN, S., BONDER, M. J. & HADJIPANAYIS, G. C. 2009. Particle size effect on phase and magnetic properties of polymer-coated magnetic nanoparticles. *Journal of magnetism and magnetic materials,* 321**,** 117-122.

BAMPOLE, D. L. & BAFUBIANDI, M. 2018. Removal Performance of Silica and Solid Colloidal Particles from Chalcopyrite Bioleaching Solution: Effect of Coagulant (Magnafloc Set# 1597) for Predicting an Effective Solvent Extraction. *Engineering Journal,* 22**,** 123-139.

BAN, Z., BARNAKOV, Y. A., LI, F., GOLUB, V. O. & O'CONNOR, C. J. 2005. The synthesis of core–shell iron@ gold nanoparticles and their characterization. *Journal of Materials Chemistry,* 15**,** 4660-4662.

BAUGHMAN, G. L. & PERENICH, T. A. 1988. Fate of dyes in aquatic systems: I. Solubility and partitioning of some hydrophobic dyes and related compounds. *Environmental Toxicology and Chemistry: An International Journal,* 7**,** 183-199.

BEIK, J., ABED, Z., GHOREISHI, F. S., HOSSEINI-NAMI, S., MEHRZADI, S., SHAKERI-ZADEH, A. & KAMRAVA, S. K. 2016. Nanotechnology in hyperthermia cancer therapy: From fundamental principles to advanced applications. *Journal of Controlled Release,* 235**,** 205-221.

BISH, D. L. & POST, J. E. 2018. *Modern powder diffraction,* Walter de Gruyter GmbH & Co KG.

BO, X., GAO, B., PENG, N., WANG, Y., YUE, Q. & ZHAO, Y. 2012. Effect of dosing sequence and solution pH on floc properties of the compound bioflocculant–aluminum sulfate dual-coagulant in kaolin–humic acid solution treatment. *Bioresource technology,* 113**,** 89-96.

BUTHELEZI, S. P., OLANIRAN, A. O. & PILLAY, B. 2012. Textile dye removal from wastewater effluents using bioflocculants produced by indigenous bacterial isolates. *Molecules,* 17**,** 14260-14274.

CHEN, M., HE, Y., WANG, X. & HU, Y. 2018. Complementary enhanced solar thermal conversion performance of core-shell nanoparticles. *Applied Energy,* 211**,** 735-742.

CORCORAN, E. 2010. *Sick water?: the central role of wastewater management in sustainable development: a rapid response assessment,* UNEP/Earthprint.

COSA, S., MABINYA, L. V., OLANIRAN, A. O., OKOH, O. O., BERNARD, K., DEYZEL, S. & OKOH, A. I. 2011. Bioflocculant production by Virgibacillus sp. Rob isolated from the bottom sediment of Algoa Bay in the Eastern Cape, South Africa. *Molecules,* 16**,** 2431-2442.

COSA, S., UGBENYEN, A. M., MABINYA, L. V., RUMBOLD, K. & OKOH, A. I. 2013. Characterization and flocculation efficiency of a bioflocculant produced by a marine Halobacillus. *Environmental technology,* 34**,** 2671-2679.

CRINI, G. 2005. Recent developments in polysaccharide-based materials used as adsorbents in wastewater treatment. *Progress in polymer science,* 30**,** 38-70.

DANIELS, A. N. & SINGH, M. 2019. Sterically stabilized siRNA: gold nanocomplexes enhance c-MYC silencing in a breast cancer cell model. *Nanomedicine*.

DAVIS, A. P., SHOKOUHIAN, M., SHARMA, H. & MINAMI, C. 2006. Water quality improvement through bioretention media: Nitrogen and phosphorus removal. *Water Environment Research,* 78**,** 284-293.

DENG, S., YU, G. & TING, Y. P. 2005. Production of a bioflocculant by Aspergillus parasiticus and its application in dye removal. *Colloids and surfaces B: Biointerfaces,* 44**,** 179-186.

DEVATHA, C. P., THALLA, A. K. & KATTE, S. Y. 2016. Green synthesis of iron nanoparticles using different leaf extracts for treatment of domestic waste water. *Journal of Cleaner Production,* 139**,** 1425-1435.

DLAMINI, N. G., BASSON, A. K. & PULLABHOTLA, V. S. R. 2019a. Biosynthesis and Characterization of Copper Nanoparticles Using a Bioflocculant Extracted from *Alcaligenis faecalis* HCB2. *Advanced Science Engineering and Medicine,* 11**,** 1-7.

DLAMINI, N. G., BASSON, A. K. & PULLABHOTLA, V. S. R. 2019b. Optimization and Application of Bioflocculant Passivated Copper Nanoparticles in the Wastewater Treatment. *International Journal of Environmental Research and Public Health,* 16**,** 2185.

DREADEN, E. C., ALKILANY, A. M., HUANG, X., MURPHY, C. J. & EL-SAYED, M. A. 2012. The golden age: gold nanoparticles for biomedicine. *Chemical Society Reviews,* 41**,** 2740-2779.

DURÁN, N., MARCATO, P. D., CONTI, R. D., ALVES, O. L., COSTA, F. & BROCCHI, M. 2010. Potential use of silver nanoparticles on pathogenic bacteria, their toxicity and possible mechanisms of action. *Journal of the Brazilian Chemical Society,* 21**,** 949-959.

ELOFF, J. N. 1998. A sensitive and quick microplate method to determine the minimal inhibitory concentration of plant extracts for bacteria. *Planta medica,* 64**,** 711-713.

EROKHIN, A., LOKTEVA, E., YERMAKOV, A. Y., BOUKHVALOV, D., MASLAKOV, K., GOLUBINA, E. & UIMIN, M. 2014. Phenylacetylene hydrogenation on Fe@ C

and Ni@ C core–shell nanoparticles: about intrinsic activity of graphene-like carbon layer in H2 activation. *Carbon,* 74**,** 291-301.

EXLEY, C., KORCHAZHKINA, O., JOB, D., STREKOPYTOV, S., POLWART, A. & CROME, P. 2006. Non-invasive therapy to reduce the body burden of aluminium in Alzheimer's disease. *Journal of Alzheimer's Disease,* 10**,** 17-24.

FAN, J., GUO, Y., WANG, J. & FAN, M. 2009. Rapid decolorization of azo dye methyl orange in aqueous solution by nanoscale zerovalent iron particles. *Journal of Hazardous Materials,* 166**,** 904-910.

FAROKHZAD, O. C. & LANGER, R. 2006. Nanomedicine: developing smarter therapeutic and diagnostic modalities. *Advanced drug delivery reviews,* 58**,** 1456-1459.

FARROW, J. & SWIFT, J. 1996. A new procedure for assessing the performance of flocculants. *International Journal of Mineral Processing,* 46**,** 263-275.

FONOVICH, T. M. 2013. Sudan dyes: are they dangerous for human health? *Drug and chemical toxicology,* 36**,** 343-352.

FUJITA, M., IKE, M., TACHIBANA, S., KITADA, G., KIM, S. M. & INOUE, Z. 2000. Characterization of a bioflocculant produced by Citrobacter sp. TKF04 from acetic and propionic acids. *Journal of Bioscience and Bioengineering,* 89**,** 40-46.

GALPERIN, A. & MARGEL, S. 2007. Synthesis and characterization of radiopaque magnetic core-shell nanoparticles for X-ray imaging applications. *Journal of Biomedical Materials Research Part B: Applied Biomaterials: An Official Journal of The Society for Biomaterials, The Japanese Society for Biomaterials, and The Australian Society for Biomaterials and the Korean Society for Biomaterials,* 83**,** 490-498.

GAO, J., BAO, H.-Y., XIN, M.-X., LIU, Y.-X., LI, Q. & ZHANG, Y.-F. 2006. Characterization of a bioflocculant from a newly isolated Vagococcus sp. W31. *Journal of Zhejiang University Science B,* 7**,** 186-192.

GAO, X., WEI, L., YAN, H. & XU, B. 2011. Green synthesis and characteristic of core-shell structure silver/starch nanoparticles. *Materials Letters,* 65**,** 2963-2965.

GAWANDE, M. B., GOSWAMI, A., ASEFA, T., GUO, H., BIRADAR, A. V., PENG, D.-L., ZBORIL, R. & VARMA, R. S. 2015. Core–shell nanoparticles: synthesis and applications in catalysis and electrocatalysis. *Chemical Society Reviews,* 44**,** 7540-7590.

GHOSH CHAUDHURI, R. & PARIA, S. 2011. Core/shell nanoparticles: classes, properties, synthesis mechanisms, characterization, and applications. *Chemical reviews,* 112**,** 2373-2433.

GIRI, S. S., HARSHINY, M., SEN, S. S., SUKUMARAN, V. & PARK, S. C. 2015. Production and characterization of a thermostable bioflocculant from Bacillus subtilis F9, isolated from wastewater sludge. *Ecotoxicology and environmental safety,* 121**,** 45-50.

GONG, W.-X., WANG, S.-G., SUN, X.-F., LIU, X.-W., YUE, Q.-Y. & GAO, B.-Y. 2008. Bioflocculant production by culture of Serratia ficaria and its application in wastewater treatment. *Bioresource technology,* 99**,** 4668-4674.

GUDIKSEN, M. S., LAUHON, L. J., WANG, J., SMITH, D. C. & LIEBER, C. M. 2002. Growth of nanowire superlattice structures for nanoscale photonics and electronics. *Nature,* 415**,** 617.

GUIBAI, L. & GREGORY, J. 1991. Flocculation and sedimentation of high-turbidity waters. *Water Research,* 25**,** 1137-1143.

GUNDERSON, J. G., KOLB, J. E. & AUSTIN, V. 1981. The diagnostic interview for borderline patients. *The American Journal of Psychiatry*.

GUO, H., HONG, C., ZHANG, C., ZHENG, B., JIANG, D. & QIN, W. 2018. Bioflocculants' production from a cellulase-free xylanase-producing Pseudomonas boreopolis G22 by degrading biomass and its application in cost-effective harvest of microalgae. *Bioresource Technology,* 255**,** 171-179.

GUO, J. & CHEN, C. 2017. Sludge conditioning using the composite of a bioflocculant and PAC for enhancement in dewaterability. *Chemosphere,* 185**,** 277-283.

GUO, J. & YU, J. 2014. Sorption characteristics and mechanisms of Pb (II) from aqueous solution by using bioflocculant MBFR10543. *Applied microbiology and biotechnology,* 98**,** 6431-6441.

GUO, S.-L., ZHAO, X.-Q., WAN, C., HUANG, Z.-Y., YANG, Y.-L., ALAM, M. A., HO, S.-H., BAI, F.-W. & CHANG, J.-S. 2013. Characterization of flocculating agent from the self-flocculating microalga Scenedesmus obliquus AS-6-1 for efficient biomass harvest. *Bioresource technology,* 145**,** 285-289.

HANDY, R. D., VON DER KAMMER, F., LEAD, J. R., HASSELLÖV, M., OWEN, R. & CRANE, M. 2008. The ecotoxicology and chemistry of manufactured nanoparticles. *Ecotoxicology,* 17**,** 287-314.

HE, J., ZHEN, Q., QIU, N., LIU, Z., WANG, B., SHAO, Z. & YU, Z. 2009. Medium optimization for the production of a novel bioflocculant from Halomonas sp. V3a′ using response surface methodology. *Bioresource technology,* 100**,** 5922-5927.

HE, J., ZOU, J., SHAO, Z., ZHANG, J., LIU, Z. & YU, Z. 2010. Characteristics and flocculating mechanism of a novel bioflocculant HBF-3 produced by deep-sea bacterium mutant Halomonas sp. V3a'. *World Journal of Microbiology and Biotechnology,* 26**,** 1135-1141.

HISATOMI, T., KUBOTA, J. & DOMEN, K. 2014. Recent advances in semiconductors for photocatalytic and photoelectrochemical water splitting. *Chemical Society Reviews,* 43**,** 7520-7535.

HUANG, J., LIU, Y., HOU, H. & YOU, T. 2008. Simultaneous electrochemical determination of dopamine, uric acid and ascorbic acid using palladium nanoparticle-loaded carbon nanofibers modified electrode. *Biosensors and Bioelectronics,* 24**,** 632-637.

HUBER, D. L. 2005. Synthesis, properties, and applications of iron nanoparticles. *Small,* 1**,** 482-501.

IŞIK, M. & SPONZA, D. T. 2003. Effect of oxygen on decolorization of azo dyes by Escherichia coli and Pseudomonas sp. and fate of aromatic amines. *Process Biochemistry,* 38**,** 1183-1192.

JAIS, N. M., MOHAMED, R., AL-GHEETHI, A. & HASHIM, M. A. 2017. The dual roles of phycoremediation of wet market wastewater for nutrients and heavy metals removal and microalgae biomass production. *Clean Technologies and Environmental Policy,* 19**,** 37-52.

KALE, G., AURAS, R., SINGH, S. P. & NARAYAN, R. 2007. Biodegradability of polylactide bottles in real and simulated composting conditions. *Polymer Testing,* 26**,** 1049-1061.

KARLSSON, H. L., CRONHOLM, P., HEDBERG, Y., TORNBERG, M., DE BATTICE, L., SVEDHEM, S. & WALLINDER, I. O. 2013. Cell membrane damage and protein interaction induced by copper containing nanoparticles—Importance of the metal release process. *Toxicology,* 313**,** 59-69.

KARTHIGA DEVI, K. & NATARAJAN, K. A. 2015. Production and characterization of bioflocculants for mineral processing applications. *International Journal of Mineral Processing,* 137**,** 15-25.

KAUR, P., THAKUR, R., BARNELA, M., CHOPRA, M., MANUJA, A. & CHAUDHURY, A. 2015. Synthesis, characterization and in vitro evaluation of cytotoxicity and

antimicrobial activity of chitosan–metal nanocomposites. *Journal of Chemical Technology & Biotechnology,* 90**,** 867-873.

KAUR, P., THAKUR, R., MALWAL, H., MANUJA, A. & CHAUDHURY, A. 2018. Biosynthesis of biocompatible and recyclable silver/iron and gold/iron core-shell nanoparticles for water purification technology. *Biocatalysis and Agricultural Biotechnology,* 14**,** 189-197.

KHAN, B. & GOYAL, D. G. 2007. *Microbial decolorization of triphenylmethane dyes.*

KHAN, I., SAEED, K. & KHAN, I. 2017. Nanoparticles: Properties, applications and toxicities. *Arabian Journal of Chemistry*.

KIRUBHA, E. & PALANISAMY, P. 2014. Green synthesis, characterization of Au–Ag core–shell nanoparticles using gripe water and their applications in nonlinear optics and surface enhanced Raman studies. *Advances in Natural Sciences: Nanoscience and Nanotechnology,* 5**,** 045006.

KOENKER, R. & HALLOCK, K. F. 2001. Quantile regression. *Journal of economic perspectives,* 15**,** 143-156.

KOLÁŘ, M., URBÁNEK, K. & LÁTAL, T. 2001. Antibiotic selective pressure and development of bacterial resistance. *International journal of antimicrobial agents,* 17**,** 357-363.

KUMAR, C. G. & ANAND, S. 1998. Significance of microbial biofilms in food industry: a review. *International journal of food microbiology,* 42**,** 9-27.

KUMAR, K. M., MANDAL, B. K., KUMAR, K. S., REDDY, P. S. & SREEDHAR, B. 2013. Biobased green method to synthesise palladium and iron nanoparticles using Terminalia chebula aqueous extract. *Spectrochimica Acta Part A: Molecular and Biomolecular Spectroscopy,* 102**,** 128-133.

KUMAR, M. & PURI, A. 2012. A review of permissible limits of drinking water. *Indian journal of occupational and environmental medicine,* 16**,** 40.

KURANE, R. & MATSUYAMA, H. 1994. Production of a bioflocculant by mixed culture. *Bioscience, biotechnology, and biochemistry,* 58**,** 1589-1594.

KURANE, R., TOEDA, K., TAKEDA, K. & SUZUKI, T. 1986. Culture conditions for production of microbial flocculant by Rhodococcus erythropolis. *Agricultural and biological chemistry,* 50**,** 2309-2313.

LAUHON, L. J., GUDIKSEN, M. S., WANG, D. & LIEBER, C. M. 2002. Epitaxial core–shell and core–multishell nanowire heterostructures. *Nature,* 420**,** 57.

LAZARIDES, A. A. & SCHATZ, G. C. 2000. DNA-linked metal nanosphere materials: Structural basis for the optical properties. *The Journal of Physical Chemistry B,* 104**,** 460-467.

LEE, D.-J. & CHANG, Y.-R. 2018. Bioflocculants from isolated stains: A research update. *Journal of the Taiwan Institute of Chemical Engineers,* 87**,** 211-215.

LEONG, K. H., CHU, H. Y., IBRAHIM, S. & SARAVANAN, P. 2015. Palladium nanoparticles anchored to anatase TiO2 for enhanced surface plasmon resonance-stimulated, visible-light-driven photocatalytic activity. *Beilstein journal of nanotechnology,* 6**,** 428.

LEVY, S. B. & MARSHALL, B. 2004. Antibacterial resistance worldwide: causes, challenges and responses. *Nature medicine,* 10**,** S122.

LI-FAN, L. & CHENG, W. 2010. Characteristics and culture conditions of a bioflocculant produced by Penicillium sp. *Biomedical and environmental sciences,* 23**,** 213-218.

LI, O., LU, C., LIU, A., ZHU, L., WANG, P.-M., QIAN, C.-D., JIANG, X.-H. & WU, X.-C. 2013. Optimization and characterization of polysaccharide-based bioflocculant produced by Paenibacillus elgii B69 and its application in wastewater treatment. *Bioresource technology,* 134**,** 87-93.

LI, Q., MAHENDRA, S., LYON, D. Y., BRUNET, L., LIGA, M. V., LI, D. & ALVAREZ, P. J. 2008. Antimicrobial nanomaterials for water disinfection and microbial control: potential applications and implications. *Water research,* 42**,** 4591-4602.

LI, Y., XU, Y., LIU, L., JIANG, X., ZHANG, K., ZHENG, T. & WANG, H. 2016. First evidence of bioflocculant from Shinella albus with flocculation activity on harvesting of Chlorella vulgaris biomass. *Bioresource Technology,* 218**,** 807-815.

LIN, J. M., LIN, H. Y., CHENG, C. L. & CHEN, Y. F. 2006. Giant enhancement of bandgap emission of ZnO nanorods by platinum nanoparticles. *Nanotechnology,* 17**,** 4391.

LIN, Z.-Z., HUANG, C.-L., HUANG, Z. & ZHEN, W.-K. 2017. Surface/interface influence on specific heat capacity of solid, shell and core-shell nanoparticles. *Applied Thermal Engineering,* 127**,** 884-888.

LIU, H., WANG, H. & QIN, H. 2016. Characteristics of hydrogen and bioflocculant production by a transposon-mutagenized strain of Pantoea agglomerans BH18. *International Journal of Hydrogen Energy,* 41**,** 22786-22792.

LOKHANDE, R. S., SINGARE, P. U. & PIMPLE, D. S. 2011. Pollution in water of Kasardi River flowing along Taloja industrial area of Mumbai, India. *World Environment,* 1**,** 6-13.

LU, H., WANG, J., WANG, T., WANG, N., BAO, Y. & HAO, H. 2017. Crystallization techniques in wastewater treatment: An overview of applications. *Chemosphere,* 173**,** 474-484.

LU, Z.-H., LI, J., ZHU, A., YAO, Q., HUANG, W., ZHOU, R., ZHOU, R. & CHEN, X. 2013. Catalytic hydrolysis of ammonia borane via magnetically recyclable copper iron nanoparticles for chemical hydrogen storage. *International journal of hydrogen energy,* 38**,** 5330-5337.

LUVUYO, N., NWODO, U. U., MABINYA, L. V. & OKOH, A. I. 2013. Studies on bioflocculant production by a mixed culture of Methylobacterium sp. Obi and Actinobacterium sp. Mayor. *BMC biotechnology,* 13**,** 62.

MABINYA, L. V., COSA, S., NWODO, U. & OKOH, A. I. 2012. Studies on bioflocculant production by Arthrobacter sp. Raats, a freshwater bacteria isolated from Tyume River, South Africa. *International journal of molecular sciences,* 13**,** 1054-1065.

MAHDY, S. A., RAHEED, Q. J. & KALAICHELVAN, P. 2012. Antimicrobial activity of zero-valent iron nanoparticles. *International Journal of Modern Engineering Research,* 2**,** 578-581.

MAJDALAWIEH, A., KANAN, M. C., EL-KADRI, O. & KANAN, S. M. 2014. Recent advances in gold and silver nanoparticles: synthesis and applications. *Journal of nanoscience and nanotechnology,* 14**,** 4757-4780.

MALIEHE, S., SHANDU, S. J. & BASSON, K. A. 2015. The antibacterial and antidiarreal activities of the crude methanolic Syzygium cordatum [S. Ncik, 48 (UZ)] fruit pulp and seed extracts. *Journal of Medicinal Plants Research,* 9**,** 884-891.

MALIEHE, T., SIMONIS, J., BASSON, A., REVE, M., NGEMA, S. & XABA, P. 2016. Production, characterisation and flocculation mechanism of bioflocculant TMT-1 from marine Bacillus pumilus JX860616. *African Journal of Biotechnology,* 15**,** 2352-2367.

MALIEHE, T. S., BASSON, A. K. & DLAMINI, N. G. 2019. Removal of Pollutants in Mine Wastewater by a Non-Cytotoxic Polymeric Bioflocculant from Alcaligenes faecalis HCB2. *International journal of environmental research and public health,* 16**,** 4001.

MANIVASAGAN, P., KANG, K.-H., KIM, D. G. & KIM, S.-K. 2015. Production of polysaccharide-based bioflocculant for the synthesis of silver nanoparticles by Streptomyces sp. *International journal of biological macromolecules,* 77**,** 159-167.

MANZ, W., AMANN, R., SZEWZYK, R., SZEWZYK, U., STENSTRÖM, T.-A., HUTZLER, P. & SCHLEIFER, K.-H. 1995. In situ identification of Legionellaceae using 16S rRNA-targeted oligonucleotide probes and confocal laser scanning microscopy. *Microbiology,* 141**,** 29-39.

MATA, Y., TORRES, E., BLAZQUEZ, M., BALLESTER, A., GONZÁLEZ, F. & MUNOZ, J. 2009. Gold (III) biosorption and bioreduction with the brown alga Fucus vesiculosus. *Journal of hazardous materials,* 166**,** 612-618.

MERZOUK, B., MADANI, K. & SEKKI, A. 2010. Using electrocoagulation–electroflotation technology to treat synthetic solution and textile wastewater, two case studies. *Desalination,* 250**,** 573-577.

MITTAL, H., MISHRA, S. B., MISHRA, A., KAITH, B., JINDAL, R. & KALIA, S. 2013. Preparation of poly (acrylamide-co-acrylic acid)-grafted gum and its flocculation and biodegradation studies. *Carbohydrate polymers,* 98**,** 397-404.

MONTALESCOT, G., SECHTEM, U., ACHENBACH, S., ANDREOTTI, F., ARDEN, C., BUDAJ, A., BUGIARDINI, R., CREA, F., CUISSET, T. & DI MARIO, C. 2013. 2013 ESC guidelines on the management of stable coronary artery disease: the Task Force on the management of stable coronary artery disease of the European Society of Cardiology. *Eur Heart J,* 34**,** 2949-3003.

MOODLEY, T. & SINGH, M. 2019. Polymeric Mesoporous Silica Nanoparticles for Enhanced Delivery of 5-Fluorouracil In Vitro. *Pharmaceutics,* 11**,** 288.

MORROW, C., MOORE, D. E. & LOCKNER, D. 2000. The effect of mineral bond strength and adsorbed water on fault gouge frictional strength. *Geophysical research letters,* 27**,** 815-818.

MOUSSAVI, G. & MAHMOUDI, M. 2009. Removal of azo and anthraquinone reactive dyes from industrial wastewaters using MgO nanoparticles. *Journal of hazardous materials,* 168**,** 806-812.

MUKHERJEE, R., KUMAR, R., SINHA, A., LAMA, Y. & SAHA, A. K. 2016. A review on synthesis, characterization, and applications of nano zero valent iron (nZVI) for environmental remediation. *Critical Reviews in Environmental Science and Technology,* 46**,** 443-466.

MUTHULAKSHMI, L., RAJINI, N., VARADA RAJALU, A., SIENGCHIN, S. & KATHIRESAN, T. 2017. Synthesis and characterization of cellulose/silver nanocomposites from bioflocculant reducing agent. *International Journal of Biological Macromolecules,* 103**,** 1113-1120.

NAICKER, K., CUKROWSKA, E. & MCCARTHY, T. 2003. Acid mine drainage arising from gold mining activity in Johannesburg, South Africa and environs. *Environmental pollution,* 122**,** 29-40.

NAVARRO, E., BAUN, A., BEHRA, R., HARTMANN, N. B., FILSER, J., MIAO, A.-J., QUIGG, A., SANTSCHI, P. H. & SIGG, L. 2008. Environmental behavior and ecotoxicity of engineered nanoparticles to algae, plants, and fungi. *Ecotoxicology,* 17**,** 372-386.

NONTEMBISO, P., SEKELWA, C., LEONARD, M. V. & ANTHONY, O. I. 2011. Assessment of bioflocculant production by Bacillus sp. Gilbert, a marine bacterium isolated from the bottom sediment of Algoa Bay. *Marine drugs,* 9**,** 1232-1242.

NWODO, U. U., AGUNBIADE, M. O., GREEN, E., MABINYA, L. V. & OKOH, A. I. 2012. A freshwater Streptomyces, isolated from Tyume river, produces a predominantly extracellular glycoprotein bioflocculant. *International journal of molecular sciences,* 13**,** 8679-8695.

OKAIYETO, K., NWODO, U., MABINYA, L. & OKOH, A. 2013. Characterization of a bioflocculant produced by a consortium of Halomonas sp. Okoh and Micrococcus sp. Leo. *International journal of environmental research and public health,* 10**,** 5097-5110.

OKAIYETO, K., NWODO, U. U., MABINYA, L. V. & OKOH, A. I. 2015a. Bacillus toyonensis Strain AEMREG6, a Bacterium Isolated from South African Marine Environment Sediment Samples Produces a Glycoprotein Bioflocculant. *Molecules,* 20**,** 5239.

OKAIYETO, K., NWODO, U. U., MABINYA, L. V., OKOLI, A. S. & OKOH, A. I. 2015b. Characterization of a Bioflocculant (MBF-UFH) Produced by Bacillus sp. AEMREG7. *International journal of molecular sciences,* 16**,** 12986-13003.

OKAIYETO, K., NWODO, U. U., OKOLI, S. A., MABINYA, L. V. & OKOH, A. I. 2016. Implications for public health demands alternatives to inorganic and synthetic flocculants: bioflocculants as important candidates. *MicrobiologyOpen,* 5**,** 177-211.

OLSEN, K. N., LARSEN, M. H., GAHAN, C. G., KALLIPOLITIS, B., WOLF, X. A., REA, R., HILL, C. & INGMER, H. 2005. The Dps-like protein Fri of Listeria monocytogenes

promotes stress tolerance and intracellular multiplication in macrophage-like cells. *Microbiology,* 151**,** 925-933.

OWEN, A., FAWELL, P., SWIFT, J. & FARROW, J. 2002. The impact of polyacrylamide flocculant solution age on flocculation performance. *International journal of mineral processing,* 67**,** 123-144.

PADMAVATHY, N. & VIJAYARAGHAVAN, R. 2008. Enhanced bioactivity of ZnO nanoparticles—an antimicrobial study. *Science and technology of advanced materials,* 9**,** 035004.

PASQUALE, N. 2017. *The design and synthesis of heterogeneous core shell nanomaterials for biological applications.* Rutgers University-Graduate School-New Brunswick.

PATHAK, M., DEVI, A., BHATTACHARYYA, K., SARMA, H., SUBUDHI, S. & LAL, B. 2015. Production of a non-cytotoxic bioflocculant by a bacterium utilizing a petroleum hydrocarbon source and its application in heavy metal removal. *Rsc Advances,* 5**,** 66037-66046.

PATIL, S. V., PATIL, C. D., SALUNKE, B. K., SALUNKHE, R. B., BATHE, G. & PATIL, D. M. 2011. Studies on characterization of bioflocculant exopolysaccharide of Azotobacter indicus and its potential for wastewater treatment. *Applied biochemistry and biotechnology,* 163**,** 463-472.

PINHEIRO, H. M., TOURAUD, E. & THOMAS, O. 2004. Aromatic amines from azo dye reduction: status review with emphasis on direct UV spectrophotometric detection in textile industry wastewaters. *Dyes and pigments,* 61**,** 121-139.

POFF, N. L. & ZIMMERMAN, J. K. 2010. Ecological responses to altered flow regimes: a literature review to inform the science and management of environmental flows. *Freshwater Biology,* 55**,** 194-205.

PRASERTSAN, P., DERMLIM, W., DOELLE, H. & KENNEDY, J. 2006. Screening, characterization and flocculating property of carbohydrate polymer from newly isolated Enterobacter cloacae WD7. *Carbohydrate polymers,* 66**,** 289-297.

QU, X., ALVAREZ, P. J. & LI, Q. 2013. Applications of nanotechnology in water and wastewater treatment. *Water research,* 47**,** 3931-3946.

REBAH, F. B. & SIDDEEG, S. 2017. Cactus an eco-friendly material for wastewater treatment: a review. *Journal of Materials and Environmental Sciences,* 8**,** 1770-1782.

RIETER, W. J., TAYLOR, K. M., AN, H., LIN, W. & LIN, W. 2006. Nanoscale metal−organic frameworks as potential multimodal contrast enhancing agents. *Journal of the American Chemical Society,* 128**,** 9024-9025.

ROBINSON, T., MCMULLAN, G., MARCHANT, R. & NIGAM, P. 2001. Remediation of dyes in textile effluent: a critical review on current treatment technologies with a proposed alternative. *Bioresource technology,* 77**,** 247-255.

RUDÉN, C. 2004. Acrylamide and cancer risk—expert risk assessments and the public debate. *Food and Chemical Toxicology,* 42**,** 335-349.

RUPARELIA, J. P., CHATTERJEE, A. K., DUTTAGUPTA, S. P. & MUKHERJI, S. 2008. Strain specificity in antimicrobial activity of silver and copper nanoparticles. *Acta biomaterialia,* 4**,** 707-716.

SAJAYAN, A., SEGHAL KIRAN, G., PRIYADHARSHINI, S., POULOSE, N. & SELVIN, J. 2017. Revealing the ability of a novel polysaccharide bioflocculant in bioremediation of heavy metals sensed in a Vibrio bioluminescence reporter assay. *Environmental Pollution,* 228**,** 118-127.

SALEHIZADEH, H. & SHOJAOSADATI, S. 2001. Extracellular biopolymeric flocculants: recent trends and biotechnological importance. *Biotechnology advances,* 19**,** 371-385.

SANKAR, R., MANIKANDAN, P., MALARVIZHI, V., FATHIMA, T., SHIVASHANGARI, K. S. & RAVIKUMAR, V. 2014. Green synthesis of colloidal copper oxide nanoparticles using Carica papaya and its application in photocatalytic dye degradation. *Spectrochimica Acta Part A: Molecular and Biomolecular Spectroscopy,* 121**,** 746-750.

SANPUI, P., MURUGADOSS, A., PRASAD, P. D., GHOSH, S. S. & CHATTOPADHYAY, A. 2008. The antibacterial properties of a novel chitosan–Ag-nanoparticle composite. *International journal of food microbiology,* 124**,** 142-146.

SANTSCHI, P. H. 2018. Marine colloids, agents of the self-cleansing capacity of aquatic systems: Historical perspective and new discoveries. *Marine Chemistry,* 207**,** 124-135.

SARAVANAN, R., GUPTA, V., PRAKASH, T., NARAYANAN, V. & STEPHEN, A. 2013. Synthesis, characterization and photocatalytic activity of novel Hg doped ZnO nanorods prepared by thermal decomposition method. *Journal of Molecular Liquids,* 178**,** 88-93.

SATHIYANARAYANAN, G., KIRAN, G. S. & SELVIN, J. 2013. Synthesis of silver nanoparticles by polysaccharide bioflocculant produced from marine Bacillus subtilis MSBN17. *Colloids and Surfaces B: Biointerfaces,* 102**,** 13-20.

SEKELWA, C., ANTHONY, U. M., VUYANI, M. L. & ANTHONY, O. I. 2013. Characterization of a thermostable polysaccharide bioflocculant produced by Virgibacillus species isolated from Algoa bay. *African Journal of Microbiology Research,* 7**,** 2925-2938.

SHAHADAT, M., TENG, T. T., RAFATULLAH, M., SHAIKH, Z. A., SREEKRISHNAN, T. R. & ALI, S. W. 2017. Bacterial bioflocculants: A review of recent advances and perspectives. *Chemical Engineering Journal,* 328**,** 1139-1152.

SHAHWAN, T., SIRRIAH, S. A., NAIRAT, M., BOYACı, E., EROĞLU, A. E., SCOTT, T. B. & HALLAM, K. R. 2011. Green synthesis of iron nanoparticles and their application as a Fenton-like catalyst for the degradation of aqueous cationic and anionic dyes. *Chemical Engineering Journal,* 172**,** 258-266.

SHEVAH, Y. 2016. Substitution of Chloride Chemicals with Degradable Bioflocculants for Sedimentation of Suspended Particles in Water. *Chemistry Beyond Chlorine.* Springer.

SHIH, I., VAN, Y., YEH, L., LIN, H. & CHANG, Y. 2001. Production of a biopolymer flocculant from Bacillus licheniformis and its flocculation properties. *Bioresource technology,* 78**,** 267-272.

SHINDE, A. J. & MORE, H. N. 2009. Nanoparticles: As Carriers for Drug Delivery System. *Research Journal of Pharmaceutical Dosage Forms and Technology,* 1**,** 80-86.

SHU, Z., CHEN, Y., ZHOU, J., LI, T., YU, D. & WANG, Y. 2015. Nanoporous-walled silica and alumina nanotubes derived from halloysite: controllable preparation and their dye adsorption applications. *Applied Clay Science,* 112**,** 17-24.

SINGH, R., TRIPATHY, T., KARMAKAR, G., RATH, S., KARMAKAR, N., PANDEY, S., KANNAN, K., JAIN, S. & LAN, N. 2000a. Novel biodegradable flocculants based on polysaccharides. *CURRENT SCIENCE-BANGALORE-,* 78**,** 798-803.

SINGH, R. P., KARMAKAR, G., RATH, S., KARMAKAR, N., PANDEY, S., TRIPATHY, T., PANDA, J., KANAN, K., JAIN, S. & LAN, N. 2000b. Biodegradable drag reducing agents and flocculants based on polysaccharides: materials and applications. *Polymer Engineering & Science,* 40**,** 46-60.

SINGHAL, G., BHAVESH, R., KASARIYA, K., SHARMA, A. R. & SINGH, R. P. 2011. Biosynthesis of silver nanoparticles using Ocimum sanctum (Tulsi) leaf extract and screening its antimicrobial activity. *Journal of Nanoparticle Research,* 13**,** 2981-2988.

SONDI, I. & SALOPEK-SONDI, B. 2004. Silver nanoparticles as antimicrobial agent: a case study on E. coli as a model for Gram-negative bacteria. *Journal of colloid and interface science,* 275**,** 177-182.

SPONZA, D. T. 2003. Investigation of extracellular polymer substances (EPS) and physicochemical properties of different activated sludge flocs under steady-state conditions. *Enzyme and Microbial Technology,* 32**,** 375-385.

STOIMENOV, P. K., KLINGER, R. L., MARCHIN, G. L. & KLABUNDE, K. J. 2002. Metal oxide nanoparticles as bactericidal agents. *Langmuir,* 18**,** 6679-6686.

SUBUDHI, S., BISHT, V., BATTA, N., PATHAK, M., DEVI, A. & LAL, B. 2016. Purification and characterization of exopolysaccharide bioflocculant produced by heavy metal resistant Achromobacter xylosoxidans. *Carbohydrate polymers,* 137**,** 441-451.

SUN, J., ZHANG, X., MIAO, X. & ZHOU, J. 2012. Preparation and characteristics of bioflocculants from excess biological sludge. *Bioresource Technology,* 126**,** 362-366.

SUN, Y.-P., LI, X.-Q., CAO, J., ZHANG, W.-X. & WANG, H. P. 2006. Characterization of zero-valent iron nanoparticles. *Advances in colloid and interface science,* 120**,** 47-56.

SWIERCZEWSKA, M., HAN, H., KIM, K., PARK, J. & LEE, S. 2016. Polysaccharide-based nanoparticles for theranostic nanomedicine. *Advanced drug delivery reviews,* 99**,** 70-84.

SWORSKA, A., LASKOWSKI, J. & CYMERMAN, G. 2000. Flocculation of the Syncrude fine tailings: Part I. Effect of pH, polymer dosage and Mg2+ and Ca2+ cations. *International journal of mineral processing,* 60**,** 143-152.

TAN, K. B., VAKILI, M., HORRI, B. A., POH, P. E., ABDULLAH, A. Z. & SALAMATINIA, B. 2015. Adsorption of dyes by nanomaterials: recent developments and adsorption mechanisms. *Separation and Purification Technology,* 150**,** 229-242.

TAVASSOLI, T., MOUSAVI, S., SHOJAOSADATI, S. & SALEHIZADEH, H. 2012. Asphaltene biodegradation using microorganisms isolated from oil samples. *Fuel,* 93**,** 142-148.

TCHOBANOGLOUS, G., BURTON, F. L. & STENSEL, H. 1991. Wastewater engineering. *Management,* 7**,** 1-4.

THOMAS, J. R., SILVERMAN, S. & NELSON, J. 2015. *Research methods in physical activity, 7E,* Human kinetics.

TIWARI, D. K., BEHARI, J. & SEN, P. 2008. Application of nanoparticles in waste water treatment 1.

TOEDA, K. & KURANE, R. 1991. Microbial flocculant from Alcaligenes cupidus KT201. *Agricultural and Biological Chemistry,* 55**,** 2793-2799.

UGBENYEN, A., COSA, S., MABINYA, L., BABALOLA, O. O., AGHDASI, F. & OKOH, A. 2012. Thermostable bacterial bioflocculant produced by Cobetia spp. isolated from Algoa Bay (South Africa). *International journal of environmental research and public health,* 9**,** 2108-2120.

UGBENYEN, A. & OKOH, A. 2014. Characteristics of a bioflocculant produced by a consortium of Cobetia and Bacillus species and its application in the treatment of wastewaters. *Water SA,* 40**,** 140-144.

VASIREDDI, R., PAUL, R. & MITRA, A. K. 2013. Green Synthesis of AgcoreCushell Nanoparticles: Structural and Optical Characterization. *Journal of Green Science and Technology,* 1**,** 85-90.

VERMA, Y. 2008. Acute toxicity assessment of textile dyes and textile and dye industrial effluents using Daphnia magna bioassay. *Toxicology and industrial health,* 24**,** 491-500.

VÖRÖSMARTY, C., LETTENMAIER, D., LEVEQUE, C., MEYBECK, M., PAHL-WOSTL, C., ALCAMO, J., COSGROVE, W., GRASSL, H., HOFF, H. & KABAT, P. 2004. Humans transforming the global water system. *Eos, Transactions American Geophysical Union,* 85**,** 509-514.

WANG, H., CHEN, L., FENG, Y. & CHEN, H. 2013. Exploiting core–shell synergy for nanosynthesis and mechanistic investigation. *Accounts of chemical research,* 46**,** 1636-1646.

WANG, Z., QUAN, X., ZHANG, Z. & CHENG, P. 2018. Optical absorption of carbon-gold core-shell nanoparticles. *Journal of Quantitative Spectroscopy and Radiative Transfer,* 205**,** 291-298.

WU, J.-Y. & YE, H.-F. 2007. Characterization and flocculating properties of an extracellular biopolymer produced from a Bacillus subtilis DYU1 isolate. *Process Biochemistry,* 42**,** 1114-1123.

XIA, S., ZHANG, Z., WANG, X., YANG, A., CHEN, L., ZHAO, J., LEONARD, D. & JAFFREZIC-RENAULT, N. 2008. Production and characterization of a bioflocculant by Proteus mirabilis TJ-1. *Bioresource technology,* 99**,** 6520-6527.

XIA, X., LAN, S., LI, X., XIE, Y., LIANG, Y., YAN, P., CHEN, Z. & XING, Y. 2018. Characterization and coagulation-flocculation performance of a composite flocculant in high-turbidity drinking water treatment. *Chemosphere,* 206**,** 701-708.

XIONG, Y., WANG, Y., YU, Y., LI, Q., WANG, H., CHEN, R. & HE, N. 2010. Production and characterization of a novel bioflocculant from Bacillus licheniformis. *Appl. Environ. Microbiol.,* 76**,** 2778-2782.

YAGUB, M. T., SEN, T. K., AFROZE, S. & ANG, H. M. 2014. Dye and its removal from aqueous solution by adsorption: a review. *Advances in colloid and interface science,* 209**,** 172-184.

YANG, Z.-H., HUANG, J., ZENG, G.-M., RUAN, M., ZHOU, C.-S., LI, L. & RONG, Z.-G. 2009. Optimization of flocculation conditions for kaolin suspension using the composite flocculant of MBFGA1 and PAC by response surface methodology. *Bioresource technology,* 100**,** 4233-4239.

YIM, J. H., KIM, S. J., AHN, S. H. & LEE, H. K. 2007. Characterization of a novel bioflocculant, p-KG03, from a marine dinoflagellate, Gyrodinium impudicum KG03. *Bioresource technology,* 98**,** 361-367.

YOKOI, H., OBITA, T., HIROSE, J., HAYASHI, S. & TAKASAKI, Y. 2002. Flocculation properties of pectin in various suspensions. *Bioresource Technology,* 84**,** 287-290.

YOU, Y., HAN, J., CHIU, P. C. & JIN, Y. 2005. Removal and inactivation of waterborne viruses using zerovalent iron. *Environmental science & technology,* 39**,** 9263-9269.

YU, X., LI, J., SHI, T., CHENG, C., LIAO, G., FAN, J., LI, T. & TANG, Z. 2017. A green approach of synthesizing of Cu-Ag core-shell nanoparticles and their sintering behavior for printed electronics. *Journal of Alloys and Compounds,* 724**,** 365-372.

YU, Y.-T. & DUTTA, P. 2011. Examination of Au/SnO2 core-shell architecture nanoparticle for low temperature gas sensing applications. *Sensors and Actuators B: Chemical,* 157**,** 444-449.

ZAIMY, M., JEBALI, A., BAZRAFSHAN, B., MEHRTASHFAR, S., SHABANI, S., TAVAKOLI, A., HEKMATIMOGHADDAM, S., SARLI, A., AZIZI, H. & IZADI, P. 2016. Coinhibition of overexpressed genes in acute myeloid leukemia subtype M2 by gold nanoparticles functionalized with five antisense oligonucleotides and one anti-CD33 (+)/CD34 (+) aptamer. *Cancer gene therapy,* 23**,** 315.

ZAKI, S., ELTARAHONY, M., ELKADY, M. & ABD-EL-HALEEM, D. 2014. The use of bioflocculant and bioflocculant-producing Bacillus mojavensis strain 32A to synthesize silver nanoparticles. J Nanomater 2014: 1–7.

ZAKI, S. A., ELKADY, M. F., FARAG, S. & ABD-EL-HALEEM, D. 2013. Characterization and flocculation properties of a carbohydrate bioflocculant from a newly isolated Bacillus velezensis 40B. *Journal of environmental biology,* 34**,** 51.

ZHANG, C.-L., CUI, Y.-N. & WANG, Y. 2012. Bioflocculant produced from bacteria for decolorization, Cr removal and swine wastewater application. *Sustainable Environment Research,* 22**,** 129-134.

ZHANG, W., HE, H., FENG, Y. & DA, S. 2003. Separation and purification of phosphatidylcholine and phosphatidylethanolamine from soybean degummed oil residues by using solvent extraction and column chromatography. *Journal of Chromatography B,* 798**,** 323-331.

ZHANG, X., SUN, J., LIU, X. & ZHOU, J. 2013. Production and flocculating performance of sludge bioflocculant from biological sludge. *Bioresource Technology,* 146**,** 51-56.

ZHANG, Z.-Q., BO, L., XIA, S.-Q., WANG, X.-J. & YANG, A.-M. 2007. Production and application of a novel bioflocculant by multiple-microorganism consortia using brewery wastewater as carbon source. *Journal of Environmental Sciences,* 19**,** 667-673.

ZHENG, Y., YE, Z.-L., FANG, X.-L., LI, Y.-H. & CAI, W.-M. 2008. Production and characteristics of a bioflocculant produced by Bacillus sp. F19. *Bioresource Technology,* 99**,** 7686-7691.

ZHOU, Z., SONG, J., TIAN, R., YANG, Z., YU, G., LIN, L., ZHANG, G., FAN, W., ZHANG, F. & NIU, G. 2017. Activatable singlet oxygen generation from lipid hydroperoxide nanoparticles for cancer therapy. *Angewandte Chemie International Edition,* 56**,** 6492-6496.

ZHU, C., CHEN, C., ZHAO, L., ZHANG, Y., YANG, J., SONG, L. & YANG, S. 2012. Bioflocculant produced by Chlamydomonas reinhardtii. *Journal of applied phycology,* 24**,** 1245-1251.

ZIERVOGEL, G., NEW, M., ARCHER VAN GARDEREN, E., MIDGLEY, G., TAYLOR, A., HAMANN, R., STUART-HILL, S., MYERS, J. & WARBURTON, M. 2014. Climate change impacts and adaptation in South Africa. *Wiley Interdisciplinary Reviews: Climate Change,* 5**,** 605-620.